PYROLYSIS AND COMBUSTION OF FOAMED POLYURETHANES

by

MARK ANDREW BOULT

A thesis submitted in support of candidature for the degree of Doctor of Philosophy

Department of Chemical Engineering & Chemical Technology,
Imperial College of Science and Technology,
London SW7.

July 1975

ABSTRACT

Rigid polyurethane foams of nominal density 30 kg m^{-3} containing variously tris(chloroethyl) phosphate (TCEP), a reactive phosphorylated polyol, and the isocyanurate ring were used.

The foams were studied in order to determine how they would react when exposed to temperatures beyond their design limits and to assess the degree of hazard they presented in fire emergency situations.

Samples were subjected to thermal irradiation and heat penetration was followed with implanted thermocouples. Conditions necessary for ignition were measured. The weight loss in heated foams was analysed to find global rate constants, and the charred remains were qualitatively assessed, and their activity measured. Differential thermal analysis was employed to elucidate the reaction paths. A mass spectrographic analysis of the volatile products of pyrolysis was made.

Values of the critical surface temperature for pilot ignition were found to be 225°C for urethanes and 380°C for isocyanurate based foams.

It was confirmed that the urethane group dissociated between 250°C and 300°C. Between 300°C and 350°C there was formation of isocyanurate rings, not as previously reported degradation of the trimer.

It has been established that TCEP does not improve ignition characteristics, but it does enhance heat transfer and, by promotion of softening of the foams, the rate of combustion.

DTA allowed elucidation of the stages of degradation, and the activation energy for fracture of the urethane group was found to be in the range 125 - 460 kJ $mole^{-1}$.

Mass spectrometry provides evidence that the phosphorylated polyol released volatile matter containing phosphorus at temperatures as low as 250°C.

It was shown how an empirical model describing the behaviour of a foam when heated could be formed incorporating experimental data.

Polyurethane foams have proved useful materials within limited conditions. Further information is needed to extend the range of application, and this work has identified weaknesses and indicated directions for improvements.

ACKNOWLEDGEMENTS

Thanks are due to Dr D H Napier for his encouragement and the interest he has shown in the progress of this work. I am indebted to him for the guidance he has given.

I would also like to thank Coolag Ltd for supplying the foams studied, and Messrs J Burbridge and W J Wilson for useful discussion and the additional foams used in the DTA work.

Support for this work by British Rigid Urethane Foams Manufacturers Association is acknowledged.

INDEX

1 INTRODUCTION

1.1 Although not predominant in the materials, it is the urethane group, $-O-\overset{O}{\overset{\|}{C}}-\overset{H}{N}-$, common to all members of the class that gives polyurethanes their name. As the urethane group is formed by the reaction between the isocyanate and hydroxyl end groups of the starting materials, polyurethanes are block polymers of the general form; -R.NH.CO.O.R'.O.CO.NH.R.NH.CO.O.R'.O.CO.NH-. Polyurethanes are often referred to simply as 'urethanes' and occasionally as 'isocyanate polymers'. The identity of the groups R and R' can be varied almost limitlessly and so the nature of the resulting material spans a wide range. Urethanes can be formulated that are elastomeric fibres, thermoplastics capable of being extruded, thermosetting materials with great abrasive resistance, or light weight foams of excellent strength. A class of polymer with such a wide range of properties would be expected to have many uses, and indeed polyurethanes find application in fields extending from flooring to horseshoes, and paint additives to furniture. The foamed polyurethanes can be produced with densities ranging from 30 kg m^{-3} (2 lb ft^{-3}) upwards.

Since the work of Bayer in 1937 which led to the development of the synthetic fibre Perlon U, a linear polyurethane from hexamethylene diisocyanate and 1.4-butanediol, there has been constant research to develop the new polymers and the success is due to painstaking and systematic efforts.[1]

Up to 1957 the foamed urethanes were based on costly polyesters, but the commercial entry of polyether polyols derived from propylene oxide brought about major changes in urethane technology and market potential. The usage of foamed urethanes is still growing. In the UK in 1970, 7000 tonnes of rigid and 40 000 tonnes of non-rigid polyurethane foams were used:[2] in 1972 the corresponding figures were, rigid 17 500 tonnes, flexible and semi-flexible 48 000 tonnes.[3]

The major use of rigid foams is in insulation applications, insulating pipework, commercial and domestic refrigerators, and increasingly, internal and external walls in buildings. It also finds application as structural and minor components of furniture, and as packaging. The flexible foams are used extensively in packaging, clothing, soft furnishings, automobile and air-craft trimmings and some insulation situations.

1.2 The common reactions of isocyanates can be split into two main classes[1], viz;

a) The reaction of isocyanates with compounds containing active hydrogen to give addition products

b) The polymerisation of isocyanates.

It is the addition reactions with active hydrogen containing groups about which most is known, and which are extensively used in urethane production. The general reaction is shown in the equation,

$$RNCO + R'H \longrightarrow RNH.CO.R'$$

In detail the reactions are

$$RNCO + R'OH \longrightarrow RNH.CO.O.R' \quad \text{(urethane)}$$

$$RNCO + R'NH_2 \longrightarrow RNH.CO.NH.R' \quad \text{(urea)}$$

$$RNCO + H_2O \longrightarrow RNH.COOH \quad \text{(carbamic acid)}$$

$$\downarrow$$

$$RNH_2 + CO_2$$

$$\downarrow \text{(RNCO)}$$

$$RNH.CO.NH.R \quad \text{(urea)}$$

$$RNCO + R'COOH \longrightarrow RNH.CO.O.CO.R'$$

$$\downarrow$$

$$RNH.CO.R' + CO_2 \quad \text{(amide)}$$

Isocyanates react with hydroxyl compounds to give urethanes and with amines to give ureas. Similar reactions occur with water, to form carbamic acid, and carboxylic acids to give the mixed acid anhydride. However in both of these cases the product is unstable and carbon dioxide is eliminated to give, in the reaction with water, an amine which then reacts with isocyanate to give an urea, and in the reaction with carboxylic acid, an amide. These reactions are the backbone of urethane chemistry, and it can be seen that by incorporating the latter two reactions into the polyurethane system the production of a relatively inert gas can be made an integral part of the reaction, thus supplying the blowing agent if a foamed product is required. The products of these reactions can be seen to contain active hydrogen atoms, so further reactions with isocyanates are possible to give secondary products.

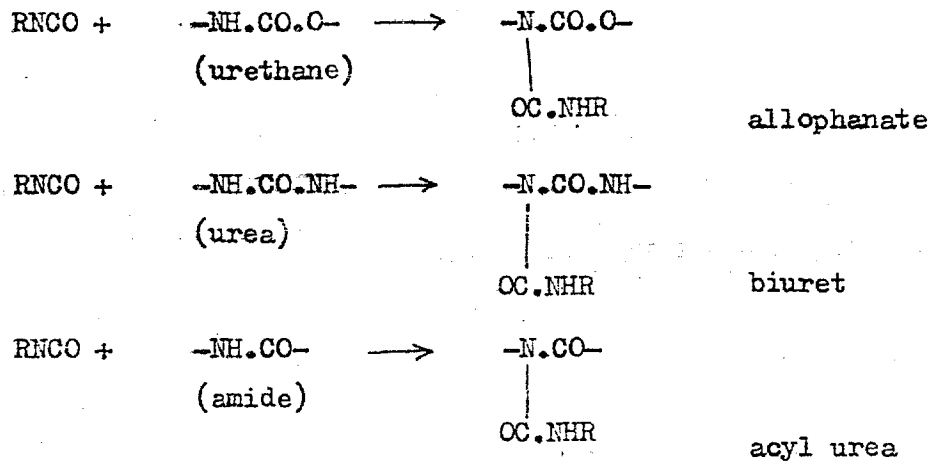

Thus isocyanates react with urethanes to give allophanates, with ureas to give biurets, and with amides to give acyl ureas. Although these secondary reactions occur to a much smaller extent than the primary reactions their importance ought not to be underestimated, for it is these reactions, especially the allophanate and biuret forming ones, that play a vital part in producing the cross-linking of the polymer chains which has a decisive effect upon the properties of the polyurethane.

The second class of isocyanate reactions comprises the polymerisation reactions. Dimerisation to uretidine dionesis an equilibrium reaction occurring at room temperature, although catalysts are needed to achieve a reasonable reaction rate.

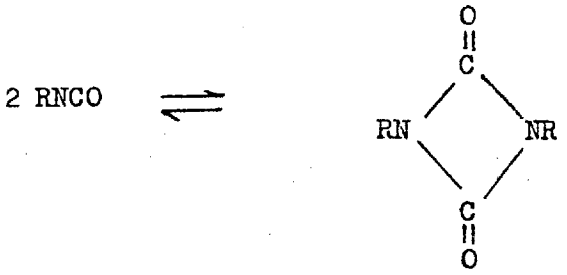

The tendency towards dimerisation is affected by the electronic and steric influences of ring substituents. For example, ortho substitution greatly retards the dimerisation of the NCO group, hence the isocyanate group in the 2 position of 2–4 tolylene diisocyanate is slower to dimerise than the group in the 4 position. 4.4' diphenyl-methane diisocyanate dimerises slowly on standing at room temperature even without any catalyst. The isocyanate dimer is dissociated at elevated temperatures. Aliphatic isocyanates have not been observed to form dimers.

In contrast to dimer formation, trimerisation is not an equilibrium reaction, and both aliphatic and aromatic isocyanates can undergo this reaction.

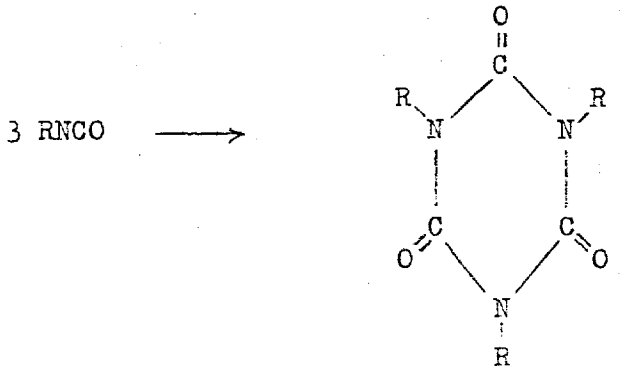

isocyanurate ring

A wide variety of catalyst have been reported for this reaction, and the resulting trimer is stable at over 300°C. The isocyanurate ring is important in polyurethanes as it leads to crosslinking and increased temperature resistance.

A third type of polymerisation reaction, resulting in the formation of substituted linear polyamides, is only brought about at low temperatures with the use of special catalysts, and is of no practical importance at present.

There is another reaction of isocyanates, a condensation polymerisation whereby two isocyanate groups react with the elimination of carbon dioxide to form a carbodiimide.

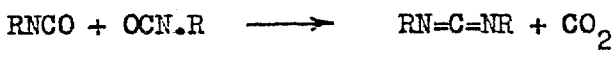

This is normally a degradation reaction of isocyanates, occuring at high temperatures.

1.3 The polyols used in production of urethane foams are generally either polyesters or polyethers. In spite of their high cost polyesters still command the major place in flexible foams because they produce foams that are inherently less flammable than polyether foams.[4] Polyesters are built up by condensation of polyalcohols and dicarboxylic acids, and the use of excess glycol affords predominantly hydroxyl endings to the chains, although some proportion of carboxyl terminations do persist.

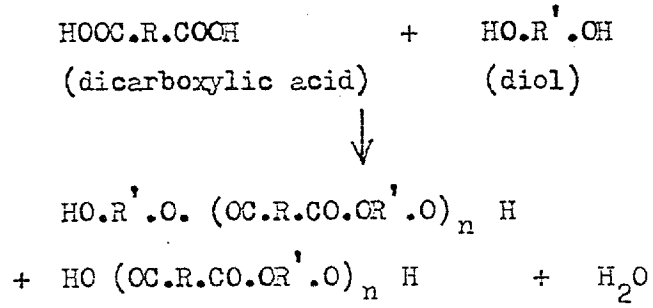

Glycols result in linear polyesters while the use of higher polyhydric alcohols leads to branched polyesters. Commonly used carboxylic acids include adipic acid, phthalic anhydride, and dimerised linoleic acid, while the simple glycols most common are ethylene, propylene, 1, 3-butylene, 1,4-butylene and diethylene glycols. Glycerol is the usual triol and pentaerythritol may sometimes be used as a source of crosslinking. The condensation reaction involves the exclusion of water that must be removed to drive the reaction at a reasonable rate. This is generally achieved by sweeping with an inert gas and the use of high temperatures, although care must be taken to avoid decarboxylation and the formation of non-reactive chain endings which is known to occur above 290°C.[1]

Under conditions of high relative humidity and temperature polyester foams degrade faster than polyether foams owing to hydrolysis of the ester groups, and the presence of unreacted starting material in commercial polyesters reduces their hydrolytic stability.[5]

1.4 Polyethers are produced by the base catalysed polymerisation of alkoxides with an initiator containing active hydrogen atoms. Propylene oxide is commonly used because of cost and the fact that the resulting polyethers are less water soluble than those based on ethylene oxide.[6] Absorption of water is detrimental as it upsets the stoichiometric balance of the formulation on which foam properties depend.

Nearly all the end groups in propylene oxide polymers are secondary hydroxyl groups which are less reactive to isocyanates than primary hydroxyl groups. This problem can be overcome by use of block copolymers which are made by reacting propylene oxide with the initiator to form a poly(oxypropylene) polymer and then reacting this with ethylene oxide to tip the block polymer with primary hydroxyl groups. The general diol of

this type can be represented by,

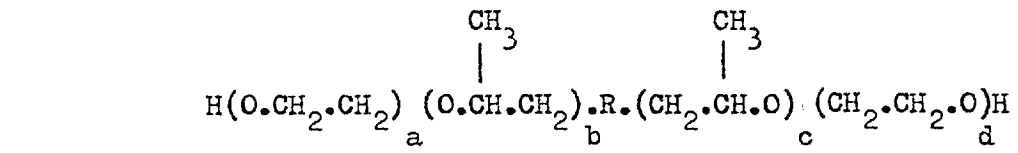

More recently though this problem has been overcome by the judicious use of a mixture of amine and tin catalysts.[6]

In addition to the simple glycols and trihydric alcohols used as initiators other polyfunctional molecules have been used including sorbitol, sucrose, pentaerithritol and 2,2,6,6-tetrakis (hydroxymethyl) cyclohexanol. Also used are some basic polyethers prepared by propoxylation of nitrogen bearing initiators among which are ethylenediamine, and toluenediamine.

1.5 Flexible foams are based on both polyesters and polyethers depending on intended use of the foam.[6] The lower resilience of polyester foams has led to an almost complete replacement by polyether foams in upholstery applications, but the higher hardness, tensile strength and elongation at break of the polyester foams has assured them of a continuing place in most other applications.

Toluene diisocyanate (TDI) is used almost exclusively in flexible foams as both the 80 : 20 and 65 : 35 mixtures of isomers, and the blowing agent to give rise to the foam is the carbon dioxide formed by reaction of isocyanate with water included in the formulation. By varying the percentage of water used the density of the foam can be adjusted at will.

1.6 Even though they were produced with ease in the laboratory, rigid foams were slower to gain a commercial foothold because the technology was more complex.[6] The high crosslinking in the polyesters originally used made for viscous systems and poor mixing. The highly exothermic reactions with TDI had to be very carefully controlled to avoid scorch in the blocks of foam, and to allow more freedom in temperature control

it was necessary to form a 'quasi-prepolymer' from the isocyanate and part of the polyol. This was then reacted with the balance of polyether and the other components to form the foam. The introduction of diphenylmethane diisocyanate (MDI) removed this need as it did not react with such a high degree of exothermicity. It also had the advantage of much lower volatility and toxicity[7] and allowed in situ filling of spaces without hazard when the low viscosity polyether resins were developed.

The difference in chemistry between flexible and rigid foams is principally in the factors governing the stiffness of the polymer network. The high crosslinking required to meet this stiffness factor is controlled by the length of the polyether extensions and the functionality of the initiator. As flexibility increases with chain length there is a limit beyond which the polyether chains become increasingly unsuitable for rigid foams: in practice the useful range of molecular weight lies approximately between 300 and 1000.

The need for extraneous catalysts for the urethane forming reactions can be reduced by choice of an initiator containing nitrogen as the resulting polyether has a degree of self catalysis. The use of an initiator with an aromatic rather than aliphatic nucleus increases the stiffness of the polymer.

Most rigid foams are now blown with low boiling halogenated alkanes, of which trichlorofluoromethane, $CFCl_3$ is most widely used. The inert low viscosity liquid plays no part in the reaction but is vaporised by the exothermic reaction between isocyanate and polyol, and remains trapped in the cells of the foam where its low thermal conductivity improves the foam as an insulant.

A surfactant is vital to control the size and stability of the cell size and those developed for rigid urethane foams are mainly polyoxalkylene-polysiloxane copolymers.[6]

1.7 Flame retardants for use in polyurethane foams can be split into two categories, inert additives and reactive molecules that are bound into the foam structure. The use of solid powder type additives is ruled out by the sensitive balance in the foaming process and the inherent instability of the bubbles before the foam has set and cured. The other additive type flame retardants are generally organic liquids containing phosphorus and halogens in varying amounts, and tris (2-chlorethyl) phosphate is a good example of the widely used halogenated phosphate esters. In 1972 approximately 90% of the retardants used in rigid foams were additives[8] even though it is recognised that these liquids can be very easily boiled off if the heat front reaches the foam before the flame front and the self extinguishing foam converted to a flammable material.[9]

The methods in which the elements phosphorus and halogens affect their flame retardant effect are completely different. Chlorine containing molecules are found to be more effective if they readily release hydrogen chloride on heating and it is found that the greater the proportion of chlorine in the foam, the more effective the protection. The halogens act by competing for the free radicals in flame reaction chains.[19,71,72] On the other hand the phosphorus compounds inhibit oxidation by retarding the carbon oxidation in the solid state. It has been hypothesised that generated phosphorus acids are reduced by carbon to free radical phosphorus species, which are then readily oxidised back to phosphorus acids.[73] In this sequence combustionable gases are starved of oxygen and an impervious char barrier from the substrate is promoted. In many cases the flame retardant is designed to contain both phosphorus and a halogen as there is a synergistic effect between these elements.[74]

Papa[75] has reviewed the reactive flame retardants for urethane foams and has considered the merits of the various polyols containing phosphorus and the drawbacks they present. Polyols containing bromine and chloride

show a tendency to produce scorch in the centre of a block of foam as it is being cured because they decompose on heating. Isocyanates containing halogens and phosphorus have also been assessed but are not widely used. Of increasing importance is the promotion of low flammability by incorporation of heat resistant groups into the polymer chains. Selection of suitable catalysts can promote the formation of isocyanurate, imide, biuret and carbodiimide groups all of which improve the flame retardancy of polyurethane foams.

Phosphorus retention does not necessarily guarantee complete retention of initial flame resistance.[9] Other less obvious factors such as loss of ability to charcoat brought about by polymer degradation, variations in the proportions of volatile materials present, or changes in the activation energy required for oxidation caused by thermally induced chemical modifications, may greatly influence flame properties even though little phosphorus has been lost.

Piechota[74] found that flammability resistance reached a maximum at 1.5% phosphorus content, both for additive type and for reactive phosphorus compounds.

1.8 Certain generalities may be made about the effects of various factors on the properties of urethane polymers.[1,82]

The molecular weight of the polymer has the effect of increasing the strength, softening temperature and glass transition temperature, and decreasing the solubility and brittleness as it increases to a value of about 10 000, but the rigid foams have large enough molecular weights not to show this effect.

Intermolecular forces, the results of hydrogen bonding, dipole moments and vander Waals attractions, tend to hold polymer chains together in

a similar fashion to primary chemical bonds, but are much weaker and are more readily affected by increased temperature. Strong intermolecular forces in conjunction with good 'fit' favour a high modulus, tensile strength, density, hardness and low swelling by solvents. Poor 'fit' in highly crosslinked polymers prevents full realisation of these effects.

Chain units having very limited rotational or configurational possibilities tend to stiffen polymer chains. Such units are typified by aromatic rings, themselves rigid units. This stiffening effect favours high melting point, hardness, strength and reduced elasticity and solubility. On the other hand highly flexible groups, such as the ether group, favour softness, flexibility, elasticity and low melting point.

Increases in the degree of crosslinking make amorphous polymers more rigid and cause them to have higher softening points and glass transition temperatures and reduce elongation and swelling by solvents.

The high crosslink density required for high thermal stability and rigidity can be provided by using polyols and polyisocyanates of high functionality or of low molecular weight. Incorporation of relatively stable chemical groups such as aromatic rings, carbodiimides, isocyanurates and imides increases the thermal stability and the amount of char formed.

The urethane group forms hydrogen bonds that stiffen the polymer chain as evidenced by the high cohesive energy of the group,[44] but the presence of the easily rotated $-CH_2-O-$ groups increase the flexibility of the chain.

1.9 The aims of the experiments in this work were to determine how the foams would react when subjected to temperatures beyond their designed

limits and to assess the degree of hazard they would present in a fire emergency situation.

By exposing the foams to thermal radiation it was intended to follow the changes in insulating ability as thermal damage increased, and to determine the conditions necessary for ignition. Spontaneous ignition of foams would appear to be relatively unimportant as in most circumstances there is a source of pilot ignition.

In order to determine at what temperatures the foams suffered degradation and to identify the effects of varying the components of the urethanes, differential thermal analyses were performed. Identification of the products of pyrolysis would greatly assist in elucidating the reactions by which degradation occurred, and the natures of the volatile products were investigated with the aid of mass spectrometry, gas-liquid chromatography and simple qualitative analysis.

From measurements of the weight lost on exposure to elevated temperatures for various times, global rate constants were evaluated and evidence of the degradation route was gained. The charred remains from the weight loss and ignition experiments were qualitatively assessed in order to ascertain the continuing protection offered when polyurethane foams have suffered thermal damage, and the activity of the chars was measured to see if they could be rekindled by a fresh supply of air.

The measured ignition conditions allowed a theory to be advanced for the ignition process, and this and the other experimental data was incorporated into a model designed to describe the behaviour of urethane foam when heated.

1.10 Many reviews of the methods of production of polyurethane foams have been made [6,41,76,77] and the foams incorporating the isocyanurate ring have also received attention. [36,42,78]

1.11 Measurements of the flammability of various foamed plastics, including polyurethanes, have been made [58,79,80,81] but development of theoretical treatment has been limited by the complex and varying nature of urethane foams. Hilado [80] describes the processes involved in the burning of cellular plastics and lists the following as flammability characteristics of a material:

ease of ignition,

fire endurance,

smoke density,

flame spread,

fuel contribution,

and products of pyrolysis and combustion.

The apparent performance of a material depends on the test being used, but the differences in performance can be attributed to basic behaviour of the tested material. [79,80] While small and medium scale tests are useful for research and screening purposes, the large scale tests simulating fire conditions should be considered more realistic. [2]

Models have been formulated for the ignition of cellulosic solids. Simms and Law [20] assumed that wet wood receiving constant radiative intensity ignited when the surface reached a fixed temperature and fitted their results to an empirical relationship. With wet wood the critical temperature for pilot ignition was 380°C and for spontaneous ignition 545°C.

Using several test methods Hilado [80] found that the ignition temperature for rigid polyurethane foam was in the range 310°C to 550°C, depending on the conditions prevailing.

Considering the piloted ignition of wood, Wesson et al [22] concluded that the time to ignition, t_i, was approximately proportional to the density

of the wood. t_i was approximately inversely proportional to the cube of the intensity of radiation, but was independent of sample thickness when greater than 2 cm.

Garg and Stewart[21] set up a model for pilot ignition of wood shavings using an energy modulus and a cooling modulus and derived a family of curves at varying Biot numbers.

The effect of surface area on the time of ignition was investigated by Simms,[29,67] and Alvares et al[63] formulated a model for the dependence of ignition time on the height of the vertical sample of cellulosic solid subjected to irradiation. They found that below a transitional intensity of 18 kW m^{-2} t_i decreased with height of sample, but above it t_i was independent. This was explained in terms of the time required to set up a steady state free convection boundary layer with position dependent heat losses.

1.12 Combustion of polyurethane foams occurs when the volatile products of pyrolysis of the foam are mixed with air, thus there are reactions in two phases - in the vapour phase where the flame reactions occur, and in the solid phase, usually in the form of a surface, in which fuel for the gas reactions is being generated. From this it can be seen that there are two ways in which flammability may be controlled, either by modification of the course of the reactions in the solid to produce less volatile matter, or by preventing burning in the gas phase. Reactions in the gas phase are usually controlled by the incorporation of a material that generates a hydrogen halide when heated, as these effectively reduce flammability by interfering with the free radical chain reactions in the flames.[19,81] Chlorine containing compounds are most widely used although it has been found that bromine has greater effectiveness[19,71,72,84] as a flame retardant. The art in designing a good fire retardant for a foam system lies in matching the temperature at which the hydrogen halide is eliminated with the temperature at which

pyrolysis occurs releasing small combustible fragments. If this is done then the flammable mixture produced will contain the species necessary to poison the flame. Care is needed to ensure that the high temperatures reached at the centre of a 'bun' of foam do not form acidic gases which then scorch the foam.[75] An alternative means of using halogens is to select a liquid additive that boils at the temperature of pyrolysis and rely on the exothermic flame processes to cause the release of the HCl or HBr. The problem with additives of this type is that the heat front may reach the foam before the fire front and boil off the additive leaving the foam unprotected.[9]

Control of the solid state reactions is usually effected by use of phosphorus containing molecules because they alter the nature of the pyrolysis products to favour production of carbon rather than small volatile fragments[75,85] and so tend to consolidate the char formation.[58]

When both phosphorus and a halogen are present together in a foam there is a synergistic effect whereby each element enhances the flame retardant effect of the other.[72,74] Papa and Proops[84] found that bromine shows synergy with phosphates and phosphonites, but not with phosphites.

1.13 The production of smoke during combustion is dependent on the fire retardant used in the foam. Einhorn et al[58] have investigated the effects of structure on smoke production and conclude that foam systems which develop char structure during combustion produce considerable quantities of dense smoke. The principle parameters which affect development of char structure, and as a consequence, smoke development are:

1 Degree of aromaticity in the polymer backbone - higher aromatic polyols produce more smoke

2 Nature and functionality of the isocyanate - higher functionality results in more rapid smoke production

3 Molecular weight per crosslink density, M_c - low values of M_c produced much smoke, and higher values gave foams that were completely consumed on combustion

4 Additives incorporated into the polymer structure to retard combustion - phosphorus additives gave rise to more smoke than chlorine additives.

Gross et al[28] found that when they underwent non-flaming combustion foams produced smoke at similar high rates whether they were fire retardant or not. With flaming combustion the foam without additive produced little smoke, but the foam with fire retardant formed smoke at a greater rate than it did in non-flaming combustion.

1.14 Qualitative relationships between thermal stability and the groups present in polyurethane foams have already been noted in section 1.8.

The effect of the nature of the groups adjacent to the urethane group has been recorded by Dombrow[86] and are shown in table 1.1.

Table 1.1; Thermal stability of urethane group

Type of urethane group	Approx. top temperature of stability (°C)
n-alkyl. NH.CO.O. n-alkyl	250
aryl. NH.CO.O. n-alkyl	200
n-alkyl. NH.CO.O. aryl	180
aryl. NH.CO.O. aryl	120

Studies of urethane foams have generally put the fracture of the urethane link in the temperature range 220°C to 285°C.[36,42,43]

Between 250 and 350°C urethane foams have been found to suffer a weight loss of some 50% and this can be attributed to the breakdown of the polyol.[87]

Foams incorporating the isocyanurate ring have been tested and interpretation of the DTA results has resulted in assignment of a temperature range 295°C - 325°C to the fracture of the isocyanurate ring.[36,42,43,52]

1.15 Many studies of the pyrolysis products of various materials have been made[7,28,53,88], and Coleman[89] concludes that plastics present no great problems of toxicity as the oxygen deficiency and the concentration of carbon monoxide far outweigh any HCN and HCl produced. From animal experiments Seader et al[90] found that there was no significant cause of death other than CO poisoning when rats were exposed to pyrolysis products of isocyanurate foams. Zapp[7] concluded that polyurethane foams are no more hazardous with respect to pyrolysis products and critical pyrolysis temperature than any other foamed plastic in common use.

Backus et al[52] studied the volatile degradation products of rigid polyurethane foams and his results are shown in table 1.2.

Foam 1 was a polyether urethane, Foam 2 a flame retardant polyether urethane with a reactive phosphonate, and Foam 3 a chlorinated polyester urethane. These results demonstrate the effect of phosphorylation in lowering reaction temperatures. The alkene probably resulted from the polyether degradation in Foams 1 and 2 and from the glycol in Foam 3.

Table 1.2 Volatile degradation products

Temperature	Foam 1	Foam 2	Foam 3
80–100°C	–	CO_2, unsaturated gas	–
150–180°C	–	$CFCl_3$, CO_2	–
Below 200°C	CO_2 $CFCl_3$ volatile alkene	–	–
Below 240°C	–	$CFCl_3$, CO_2, CO mixture with –NH, –CH, COH, CCC and H_2O IR bands	–
Below 300°C	H_2O, CO_2, CO, alkene, mixture characterised by –NH, OH, CCC, ester, aldehyde and COCH	CO_2, CO, alkene, H_2O, mixture characterised by –NH, CH, CCC and mono-substituted phenyl I R Bands. Possible phosphorus containing product	H_2O, CO_2, CO, alkene, product containing C–Cl bonds

Madorsky and Straus[91] studied degradation of polypropylene oxides and found that the major products were acetaldehyde, acetone, and propene.

In his study of flexible polyurethane foams Woolley[92] observed that the foams decomposed to release the isocyanate content of the foam as a volatile yellow smoke, stable to 750°C. High temperature degradation of the foam (> 800°C) produced nitrogenous molecules of low molecular weight, mainly hydrogen cyanide, acetonitrile, acrylonitrile, pyridene and benzonitrile.

Einhorn et al[36] found the isocyanurates produced little oxidisable gas below 500°C, but above this the products included benzene, pyridene, toluene, amiline, tolunitrile, acetonitrile and acrylonitrile.

Gross, Loftus, Lee and Gray[28] irradiated at 25 kW m^{-2} intensity, samples of approximate volume 130 cm^3 in a box of volume 0.5 m^3 with and without pilot flames. The resulting gas concentration of some toxic products are given in table 1.3.

Table 1.3; Gases produced by burning flexible urethanes

		Gas concentrations ppm		
Sample	Test	CO	HCl	HCN
15	F	50	0	2
	N	50	0	2
52	F	250	0	3
	N	250	0	2
128A	F	320	150	25
	N	160	25	2
128B	F	150	2	2
	N	190	2	2

Flexible polyether foams of approximate density 30 kg m^{-3}

52, 128A with fire retardant

15, 128B no additive

F - with pilot flame

N - without pilot flame

Work performed at Matsushita Electrical Industrial Co Ltd has been developed with air being passed through the sample bed at varying rates.[93] Analysis of the combustion products of a polyester urethane is given in table 1.4.

Table 1.4; Product gases from combustion of urethane

Air flow $l\ hr^{-1}$	Amount of combustion product, mg/g of sample					
	CO_2	CO	HCN	C_4H_4	C_2H_4	C_2H_2
100	666	173	3.3	21	14	51.4
50	625	160	1.1	17	6.4	44.5

Napier and Wong[56] showed that phosphorus was released in the volatile degradation products when it was included in the foam as either an additive or bound in as a phosphorylated polyol. Einhorn[61] has tentatively identified a bicyclic phosphate in the degradation products of rigid polyurethane foam fire retarded with Fyrol 6 (diethyl-N, N-bis (2 hydroxyethyl) aminomethyl phosphonate).

2 EXPERIMENTAL

2.1 MATERIALS

When this work was commenced five samples of polyurethane foam were made available. They were:

Foam A Polyurethane, no additives.

The formulation of this material was:

Component	Parts by Weight
Daltolac 51*	135
Glycerol	10
F11*	11
Silicone DC 193*	1
Dimethylcyclohexylamine*	0.8
Supersec DN*	201.5

Foam B Polyurethane, 20 parts TCEP

Formulation:

Component	Parts by Weight
Daltolac 51	135
Tris(2-chlorethyl)phosphate (TCEP)	20
Glycerol	10
F11	11
Silicone DC 193	1
Dimethylcyclohexylamine	0.8
Supersec DN	201.5

Foam C Polyurethane, 30 parts TCEP

Formulation:

Component	Parts by Weight
Daltolac 51	135

TCEP	30
F11	3
Silicone DC 193	1
Dimethylcyclohexylamine	0.8
Dibutyltin dilaurate*	0.05
Water	0.5
Supersec DN	134

Foam D Phosphorylated polyurethane

Formulation:

Component	Parts by Weight
Propylan RF33*	70
Propylan P450*	30
Silicone DC 193	1.5
F11	40
Dimethylaminoethanol*	2
Dabco*	0.4
Supersec DN	128

Foam E Isocyanurate based foam

Formulation:

Component	Parts by Weight
Diphenylmethyl diisocyanate (MDI)	100
F11	26
Activator G*	37.5

* Daltolac 51 comprises 35 parts of F11 and 100 parts of Daltolac 50, a polyether tertol produced b y the propoxylation of toluene diamine.

F11 is fluorotrichloromethane used as a blowing agent.

Silicone DC 193 is a surfactant used to ensure that the cell sizes and distribution meet requirements.

Dimethylcyclohexylamine, dibutyltin dilaurate, dimethylaminoethanol, and DABCO (triethyldiamine) are all catalysts.

Supersec DN is crude diphenylmethyl diisocyanate.
Activator G is a pre-formulated component including the polyol resin and all necessary catalysts.

Propylan RF33 is a polyether produced by the propoxylation of sucrose, and has a functionality of 8. Propylan P450 is a triol containing 7% of phosphorus formed by the propoxylation of phosphoric acid, H_3PO_4.

The foams B, C, D and E were supplied in sheets of size 370 x 370 mm and thickness 76 mm. Foam A was in sheets of thickness 50 mm. The nominal density of all the foams was 32 kg m^{-3}.

2.2 HEAT PENETRATION

Apparatus: Radiant Heat Source

The first radiant heat source was a 50.8 mm diameter aperture in the front of an electrically heated panel. The elements were tungsten filaments of nominal resistance 60 ohms enclosed in silica glass tubes. Four of these were mounted on a board of 9.5 mm thick Sindanyo at a centre to centre separation of 25 mm, and another board of Sindanyo fixed at a distance of approximately 70 mm in front of the elements. An aperture cut in the shielding panel provided the heat source (figure 2.1). The resistance elements were wired in parallel and the intensity of radiation adjusted by varying the mains supply voltage to the panel by means of a variable rotary autotransformer.

This source had a brief stabilization time but was discarded as the element life was short and unpredictable, owing to the susceptibility of the elements to mechanical and electrical shock. The heating panel

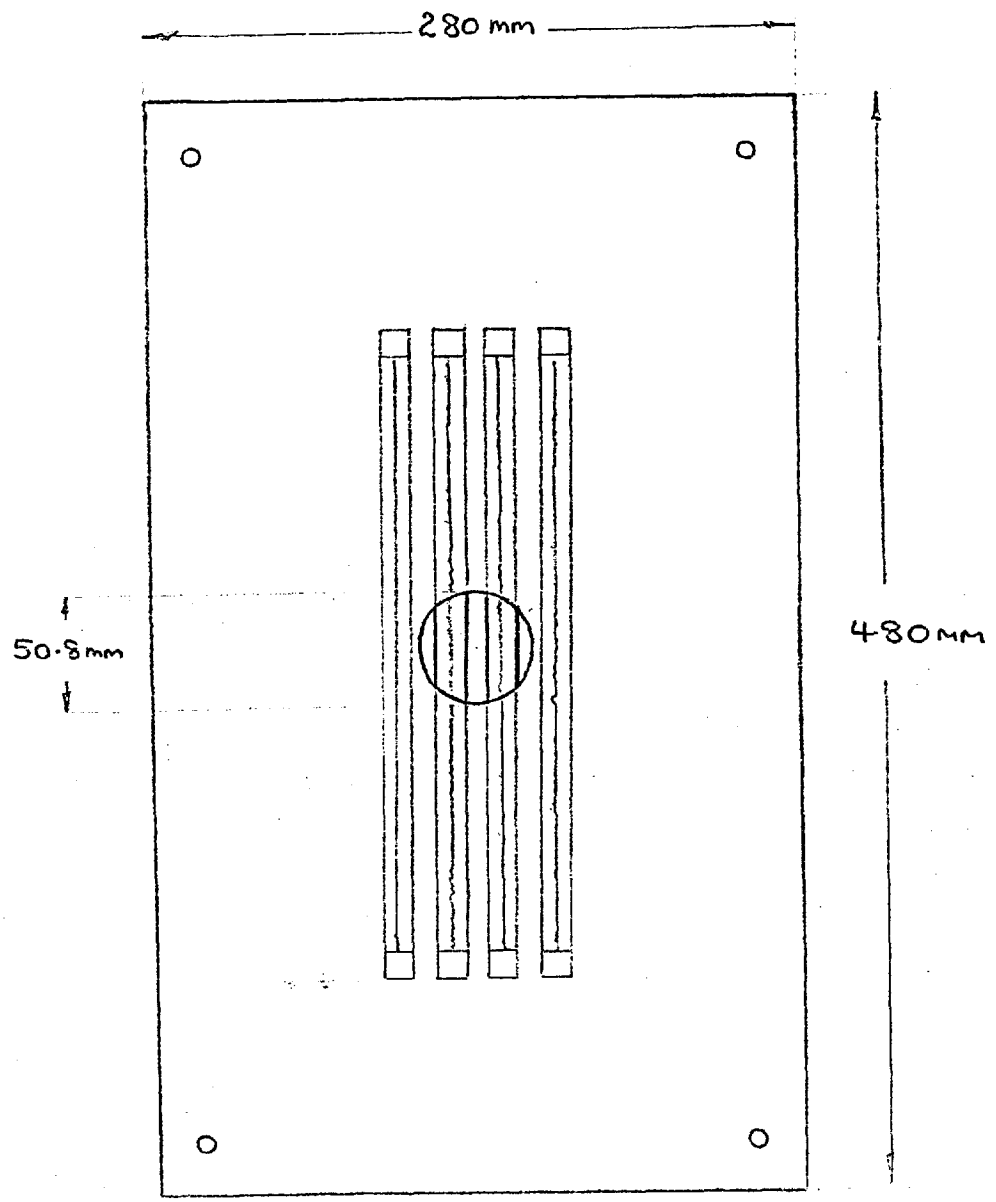

Figure 2.1 : Heating panel with tungsten/silica glass elements.

required careful handling, and the resistance of the elements changed as the length of service increased.

In view of the delicacy of tungsten elements it was necessary to construct a more substantial source of radiant heat. Again the source would be an aperture in the wall of a furnace, but the furnace was to be a sturdier piece of equipment. The heating elements chosen were Crusilite silicon carbide tubes manufactured by Morganite Electroheat Ltd. Crusilite type X elements were of diameter 18 mm and overall length 465 mm with a hot zone length of 150 mm. The hot zone is formed by a spiral cutting of the tubular element to increase locally the resistance per unit length of element. When supplied the elements had a resistance of 1.2 ohms which tended to increase but slowly with use. Four Crusilite rods were inserted into a firebrick core, as shown in figure 2.2, which was then clad in 25 mm thick lightweight asbestos board. Cladding with insulating board reduced the heat losses from the furnace and made the operation more independent of ambient conditions, thus allowing a constant heat flux to be obtained from the furnace. A hole of diameter 52 mm cut in the centre of the front panel provided the radiant source. The Crusilite rods were connected in series by means of clips and tapes of braided aluminium wire, and an A.C. voltage applied to them by a 4.4 KVA rotary variable autotransformer. The current was monitored with a 0–20 A ammeter.

Sample Holder

Cylindrical samples of foam of diameter 48 mm and length approximately 60 mm were to be used in the heat penetration experiments. A Pyrex glass holder was designed to support the samples. It consisted of a tube of internal diameter 48 mm and length 80 mm, closed at one end. To allow for the insertion of thermocouples into the sample four access ports were made in the holder as shown in figure 2.3.

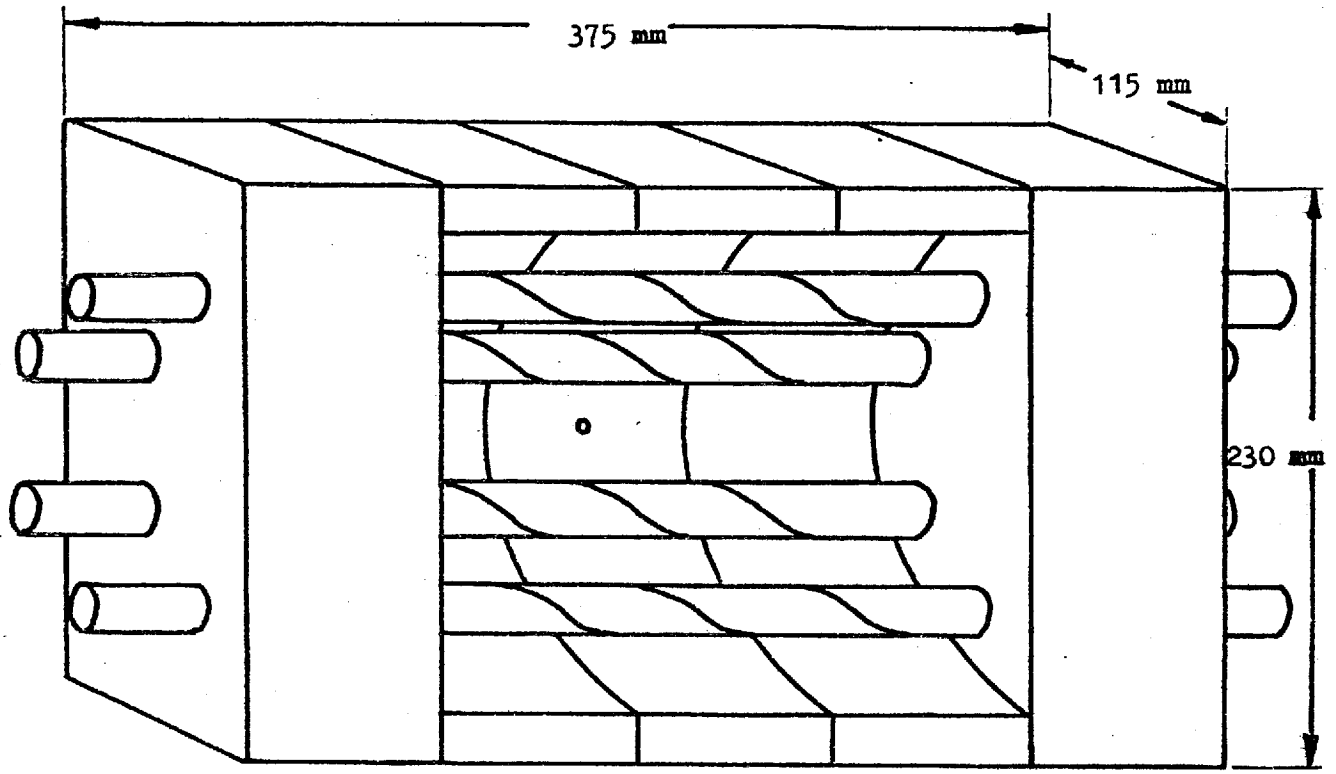

Figure 2.2 : Core of radiant heat source.

The support medium was firebrick, the heating elements were 'Crusilite' rods, and this core was clad in 25 mm thick lightweight asbestos board. A hole of diameter 52 mm cut in the centre of the front panel provided the radiant source.

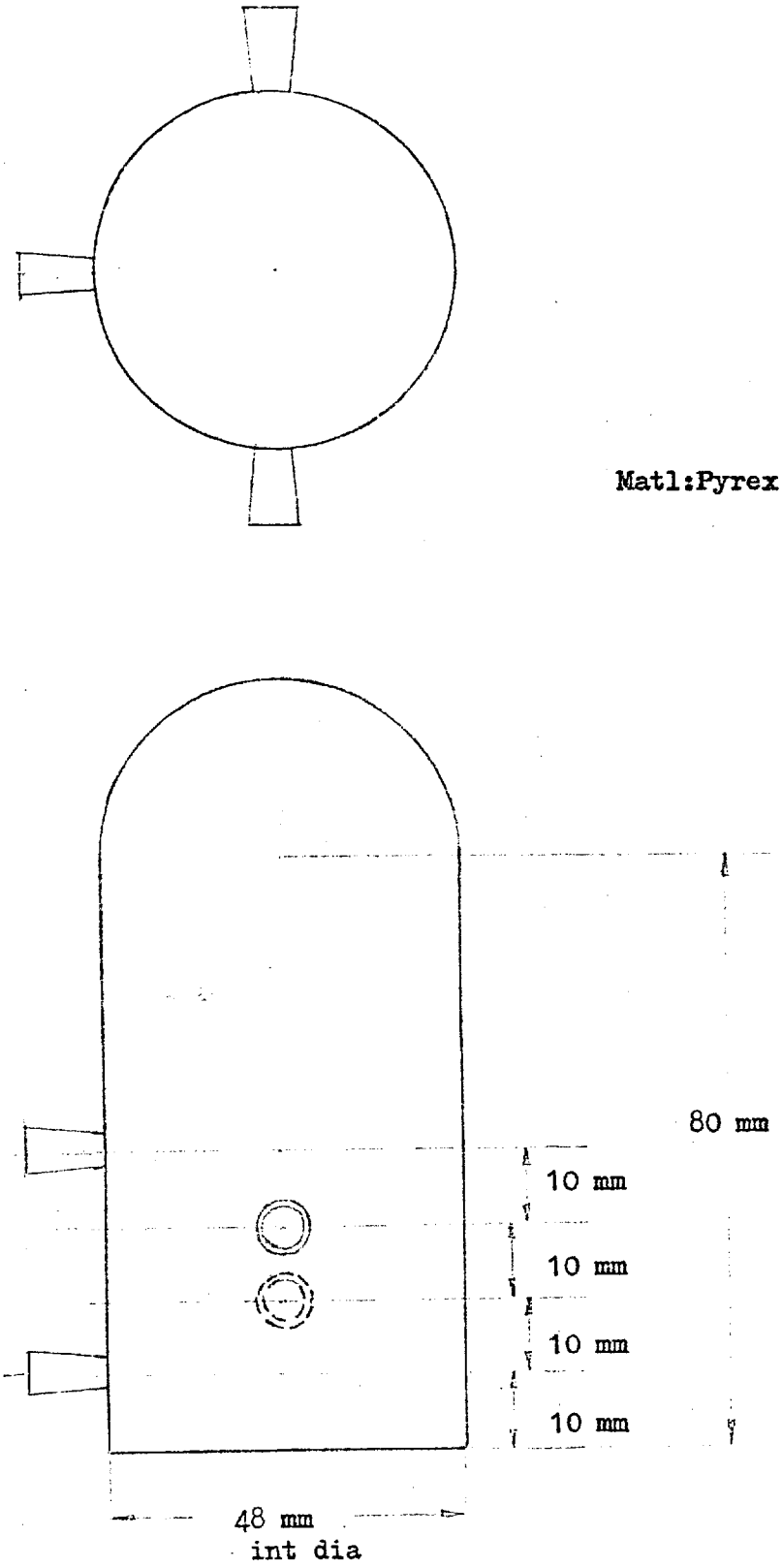

Figure 2.3 : Specimen holder for heat penetration experiments.

Temperature Measurement

The temperatures at the axis of the cylindrical sample were to be measured by means of thermocouples inserted into the polyurethane foam. Chromel/Alumel thermocouples were constructed from 0.3375 mm diameter wires by welding the junctions in a gas/oxygen flame. The junctions were washed after welding to remove the borax that was used as flux. Silica tubes were threaded over the wires before they were passed through the silicone rubber bungs that retained the thermocouples in the ports of the sample holder.

A thermocouple was positioned at the heated surface of the sample to measure the temperature of any volatile materials evolved. To prevent it receiving radiative heat from the source, this thermocouple was shielded by a strip of copper that was attached to a heat sink. The area of the shielding strip was kept to a minimum to reduce the shadowed area of sample face.

A Honeywell 16 point sequential spotting chart recorder was used to record the temperatures. The recording cycle was 96 seconds, so the input was changed and a point printed once every 6 seconds. As only five thermocouples were being used each could be connected to more than one input, and the distribution was weighted in favour of those thermocouples nearest to the heated face of the sample as at these points the temperature would be changing most rapidly.

As the full scale deflection of the recorder was 5 mv, and this represents approximately 125°C for a chromel/alumel thermocouple [10], it was necessary to insert a voltage divider to reduce the sensitivity for some of the points. Thermocouples need to be connected to a high resistance to keep the current drawn to a minimum, and the chart recorder inputs need to be a low resistance, so a compromise had to be made. An

input impedance of 200 ohms was tried and it was found that this value gave satisfactory accuracy and response. Figure 2.4 shows how the thermocouples were connected via the voltage dividing network to the chart recorder. The values of resistors used gave the following attenuation resulting in the temperature ranges shown, which were adequate to cover the measurements to be made:

Thermocouple Position	Attenuation	Temperature Range
Surface	1 : 3	0 – 375° C
10 mm	1 : 3	0 – 375° C
20 mm	1 : 3	0 – 375° C
30 mm	1 : 2	0 – 250° C
40 mm	1 : 1	0 – 125° C

The attenuation was verified by measurement of the ice and steam points which proved to be correct within accuracy of measurement

Calibration of the Source

The intensity of the radiation emitted by the radiant source was measured indirectly. A metal disc was positioned in front of the aperture of the furnace and the system allowed to come equilibrium. The temperature of the disc and its ambient temperature were measured. A smaller aperture was then interposed between the source and the disc, thus reducing the heat flux received by the disc, and when a new equilibrium had been reached the temperature of the disc and its surroundings were remeasured. The heat flux was then calculated as in Appendix I. The heat flux was calculated for several settings of the voltage supply and then by extrapolation between the measured settings it was possible to adjust the current to give a desired heat flux.

A brass disc of diameter 50.8 mm and thickness 3.18 mm was used originally for these measurements. Its temperature was measured by means of a thermocouple welded to the centre of the back face and connected to

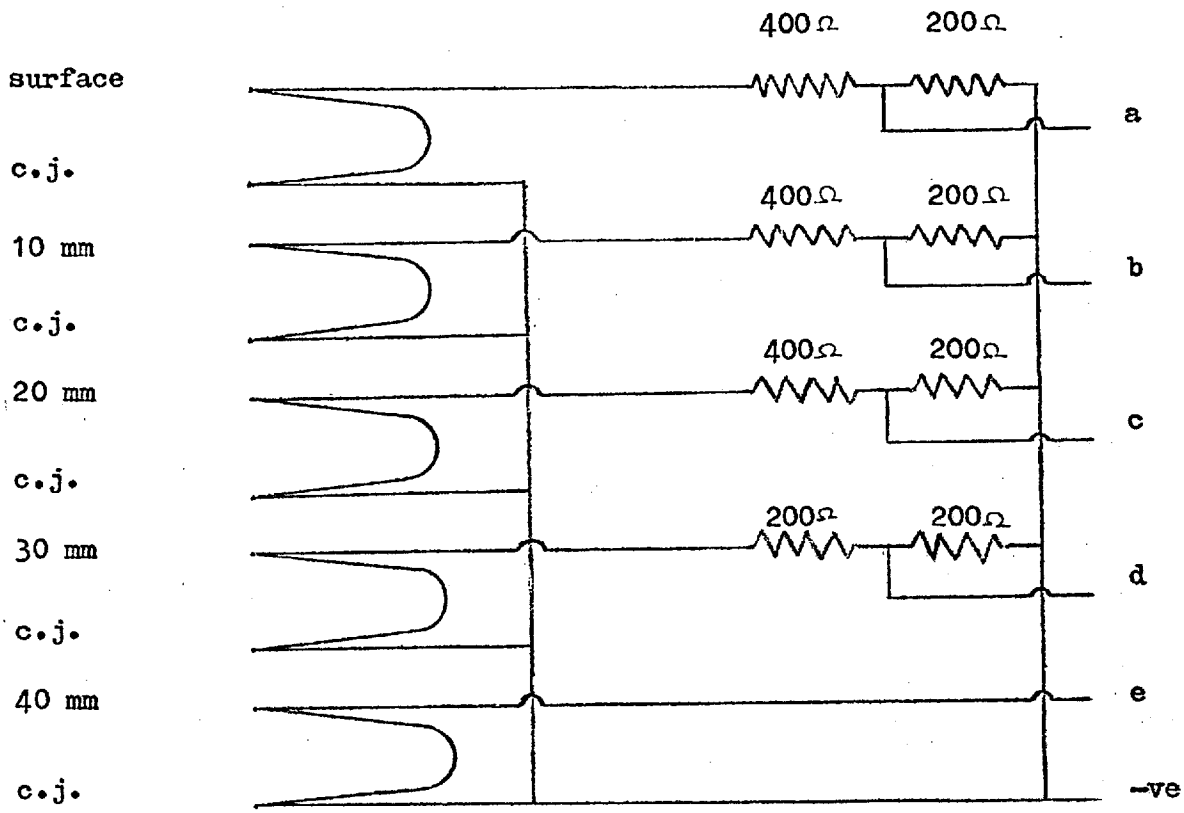

c.j. – cold junction

a was connected to inputs 1, 3, 6, 10, 13

b " " " " 4, 8, 12, 16

c " " " " 5, 11, 15

d " " " " 2, 9

e " " " " 7, 14

All the negative inputs were connected to the cold junction.

Figure 2.4:

Connection of thermocouples through voltage divider network to recorder.

a Pye direct reading galvanometer calibrated to 1000° C. The calibration of the galvanometer for a chromel/alumel thermocouple had been checked at the ice and steam points and at 420° C, the melting point of zinc. No cold junction was needed for these measurements as the instrument had an auto-compensating cold junction incorporated. Another thermocouple at a distance of 5 mm from the disc back measured the ambient temperature. This disc was satisfactory for the measurements of lower intensities of radiation, but when the temperature increased the brass oxidised and the surface of the disc blistered to such an extent that there was a large air gap between the oxide skin and the underlying metal, which made the disc quite unsuitable for the purpose of calibration.

The replacement disc was one of mild steel of the same diameter, 50.8 mm but of thickness 5 mm. As welding the thermocouple to the disc would have presented practical problems it was secured in a different position. A 2 mm diameter hole was drilled into the back of the disc at a distance of 12 mm from the edge. The thermocouple junction was inserted into this hole and secured in a good thermal contact with the disc by a 6BA bolt in a radial hole from the edge of the disc. Although not unaffected by the high temperature the mild steel disc gave satisfactory service as the oxide film formed was stable, thin and did not separate from the substrate. Once formed, the film protected the steel disc from further oxidation, even at temperatures in excess of 400° C.

The smaller aperture was a 33.4 mm diameter hole cut in a sheet of asbestos that could be hung in front of the furnace opening. It was found that the time taken for the furnace to reach steady state when the setting was changed was approximately 60 hours so the furnace was kept running constantly, which also prolonged the life of the Crusilite elements. Some fifty or so determinations of the heat flux were made and a log/lin least squares fit of flux versus current was made to get the best

relationship in order that the flux could be set to any desired value by means of the current.

Method

The current through the furnace was set to give a radiant intensity of 4.2 kW m^{-2} (0.1 cal cm^{-2} s^{-1}) and allowed to stabilize. The amplifier of the chart recorder was switched on, and the thermocouple cold junctions were packed in ice. A length of steel tubing with a sharpened end was used to cut cylindrical samples of diameter 48 mm from the sheets of foam. One of these samples was introduced into the sample holder and positioned so that its end face was level with the open end of the holder. A steel pin was pushed into the foam through the thermocouple ports to make holes for the thermocouples which were then inserted so that the beads were at the axis of the cylinder. The sample holder was mounted in a clamp and the shielded thermocouple positioned at the surface of the foam. The chart drive was switched on and the sample holder placed concentrically in front of the aperture in the furnace so that the end face of the sample was in the same position as the disc had been during the calibration. Immediately the sample was exposed a mark was made upon the chart to note commencement of the run. The exposure was continued until the temperatures reached steady values or the trend was apparent. The usual period was 15 to 20 minutes.

When the samples were removed from the source care had to be exercised on removing the thermocouple from the foam, as in some cases they were held firmly in the char by hardened lacquer-like decomposition products. The condition of the sample was noted as it was taken from the holder.

Each of the materials was in turn subjected to the radiant source, and temperature-time histories for their axial points were constructed. The intensity of radiation was raised to 8.4 kW m^{-2} and similar measurements were attempted, but several of the foams burst into flames making

any readings both erratic and unrepeatable.

2.3 SPONTANEOUS IGNITION

Apparatus

The furnace used as the radiant source in the heat penetration experiments was also utilised for investigations into the spontaneous ignition of polyurethane foams. In the earlier experiments attempts were made to measure the temperature of the evolved volatile matter by means of a shielded thermocouple similar to that used in the heat penetration experiments. The thermocouple was connected with the Pye direct reading galvanometer. Times were measured with a stopwatch.

Method

a) The intensity of radiant heat from the furnace was set to the chosen value and allowed to stabilise. The thermocouple and its shield were attached to a stand by a boss and clamp. A second clamp held the sample of foam, a slab of size approximately 90 x 90 mm and of some 25-40 mm thickness, in place behind the thermocouple. The stand was then re-positioned to bring the sample before the aperture in the furnace wall and the timing commenced. When ignition occurred the watch was stopped and the temperature indicated by the galvanometer recorded. The flame was observed until extinction and the condition of the residue of the sample was noted. This procedure was repeated for several values of the intensity of radiation.

b) It was noted in the above experiments that when volatile materials were being evolved at a high rate they were being induced into the aperture in the front face of the furnace by a convective current. Observation showed that when ignition occurred the flame emerged from the aperture and flashed back on to the face of the sample. As this did not truly represent the conditions of spontaneous ignition that were being sought, but rather a form of pilot ignition, it was deemed necessary to obviate the induction of the evolved stream. To effect this end the

furnace was rebuilt, taking care to cement all gaps between the asbestos board that formed the front face and the brickwork core. An additional safeguard was provided by maintaining the furnace interior at a slight positive pressure. This was achieved by means of a thin piece of silica glass tubing (4 mm o d) inserted through a hole in the back of the furnace. Through this tube was passed nitrogen at a rate of $\frac{1}{2}$ l min^{-1} which effectively ensured that there was a continuous stream issuing from the aperture thus preventing the ingress of any combustibles.

Further ignition experiments were then performed, but measurement of the surface temperature was not attempted. The size of the sample was 100 mm x 75 mm x 50 mm thick and it was oriented with the longest side vertical. The sample was held centrally before the aperture in a clamp for a period of five minutes during which time observations of the behaviour, including the delay before ignition and the duration of the ignition were performed. On removal the sample was inspected and a photographic record of its condition made. On occasion the sample was not clamped securely enough and as combustion occurred the sample distorted and fell from the clamp. When this happened the experiment was repeated with a fresh sample of foam.

The intensity of radiation was varied from a value at which ignition occurred for none of the foams to one at which all the materials ignited.

2.4 WEIGHT LOSS AND CHAR FORMATION

2.4.1 WEIGHT LOSS

Apparatus

Samples of foam were heated in a vertical tube furnace, the core of which consisted of a 300 mm length of moulded fireclay tubing of internal diameter 63 mm would with nichrome wire to give an element resistance of approximately 50 ohms. The heating element was cemented to the base of a box made of Sindanyo board which was then filled with expanded vermiculite to cut down heat losses, as shown in figure 2.5. Power was applied

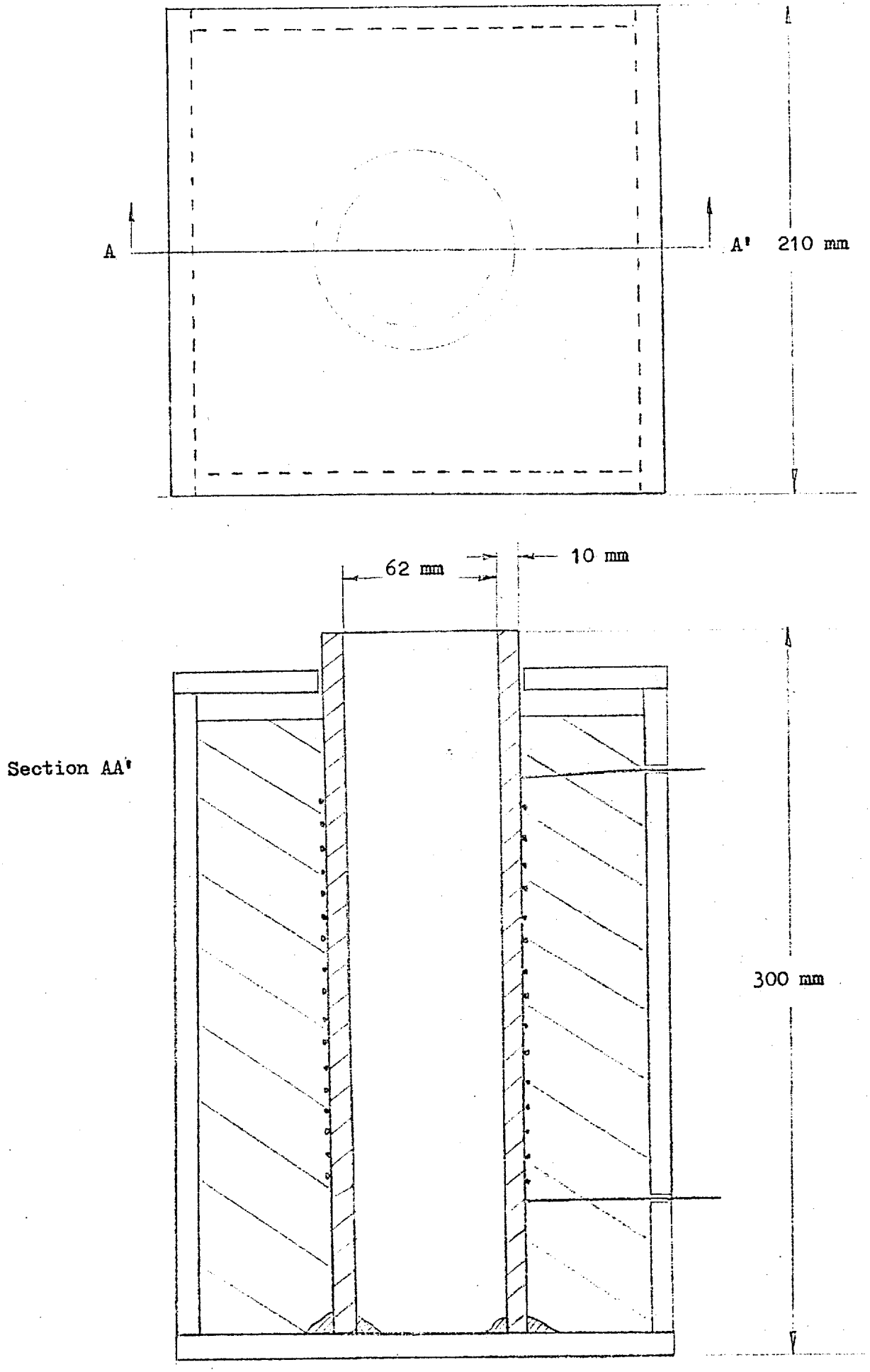

Figure 2.5 : Vertical tube furnace.

to the furnace through a variable rotary autotransformer rated at 4.4 kVA.

Calibration of Furnace

Power was applied to the furnace and several hours allowed to elapse during which time the furnace came to equilibrium. A chromel/alumel thermocouple connected with the direct reading galvanometer was used for temperature measurement. The hot zone was located by lowering the thermocouple down along the axis of the furnace and plotting the temperatures and positions of the axial points to find the plateau. A hot zone of approximately 120 mm length was found. The temperature of the furnace and the voltage across the heating elements as measured by a voltmeter were recorded. A range of voltages were applied and the associated equilibrium temperature was measured each time until a satisfactory calibration graph of hot zone temperature versus applied voltage could be drawn. The thermal capacity of the furnace was so great that introduction of a sample did not disturb the equilibrium.

Method

In the preliminary experiments cylinders of foam of diameter 47 mm were cut from the slabstock, and a sample of each of the foam types weighed. The furnace was set to the required temperature and allowed to reach steady state.

A stiff steel wire of diameter approximately 1.5 mm was used to pierce a cylinder of foam along its axis. A length of copper wire was threaded through the hole in the foam and then through the hole in the centre of a 47 mm diameter disc of 0.3mm thick aluminium foil. The end of the wire was bent to hold the disc and the sample gently pushed down to the disc. A hook was bent into the wire further along in such a position that when suspended from a clamp fixed above the furnace the sample would be in the hot zone. The sample was lowered into the hot zone of the furnace and maintained there for an hour before it was removed. When it had cooled the sample was taken from the wire and weighed.

The procedure was followed for each of the materials for exposure periods of both one hour and 3 hours, at three different temperatures.

Several facets highlighted the shortcomings of this procedure and led to the adoption of a modified system of exposure. It was found to be vital that the sample should be lowered centrally down into the furnace as the clearance was not excessive and any misalignment resulted in the exposure of the sample to temperatures in excess of that projected, or even the adhesion of the sample to the wall if contact occurred. Exposure to excessive temperatures produced misleading results as did adhesion to the furnace wall, for here there was the additional problem of the charred sample being broken apart upon attempts of manoeuvre within the furnace to rectify misplacement.

At the temperatures of the experiments some of the materials undergo a softening which leads to problems of inaccuracy and irreproducibility. Although the aluminium disc was employed to minimise the risk of pull through of the supporting wire, a similar effect was achieved when the sample shrank, at the same time adhering to both the disc and the wire. This usually resulted in a coating of charred foam extending some distance up the wire beyond the top of the foam, but often in the rupture of the top surface of the sample which allowed material to escape from the interior without passing through the charred surface layers. In some experiments the interior of the foam softened and gravitated to the aluminium disc to then flow radially and exude beyond the surface, once again by-passing the barrier produced by the charred foam.

It was also felt that the intrusion of the metallic wire into the interior of the foam was detrimental as it provided a route for the premature access of heat to the centre of the sample, which might affect the behaviour. When the interior of the foam softened the wire provided a support upon which the molten foam could collect and further react, which was an unreal situation and undesirable.

In the revised procedure the sample was reduced by using a cutter that produced cylinders of only 33 mm diameter rather than the previous 47 mm. This ensured that the sample would not, by a minor misalignment, contact the furnace tube. By virtue of the greater clearance the sample was confined to the axial volume where the temperature gradients were small compared with those near the wall.

A handling system was devised that obviated the need to pierce the sample. A flat bottomed dish of diameter approximately 45 mm and with a side of height 7 mm was fashioned from a piece of 0.3 mm thick aluminium foil to serve as a sample holder. This was in turn held on a simple carriage fabricated from brass strip of section 6.3 mm x 1.6 mm. The carriage was in the form of a cranked vertical support with a horizontal cross at the bottom, the ends of which were bent up to restrain the sample holder (figure 2.6). Two clamps above the furnace held the carriage in position and, when slackened, allowed it to be slid in or out of the furance. Before each sample was exposed the sample carrier was weighed and then with the sample on it. The carrier was then placed on the carriage and slid into the furance for the required length of time, then removed and allowed to cool. When it had reached room temperature the carrier with the charred sample was reweighed. From these measurements the original weight and the loss of weight of the foam sample were derived. The char was then carefully removed from the sample carrier to which it had occasionally become affixed by the lacquer-like degradation products and retained for later inspection and assessment.

Besides ensuring that the experimental conditions were more consistent, the introduction of the sample holder removed the causes of complaint that prevailed with the pierced sample. No longer was the integrity of the sample destroyed, and unnecessary strains were not imposed on the sometimes fragile charred skin. Any tendency to shrink

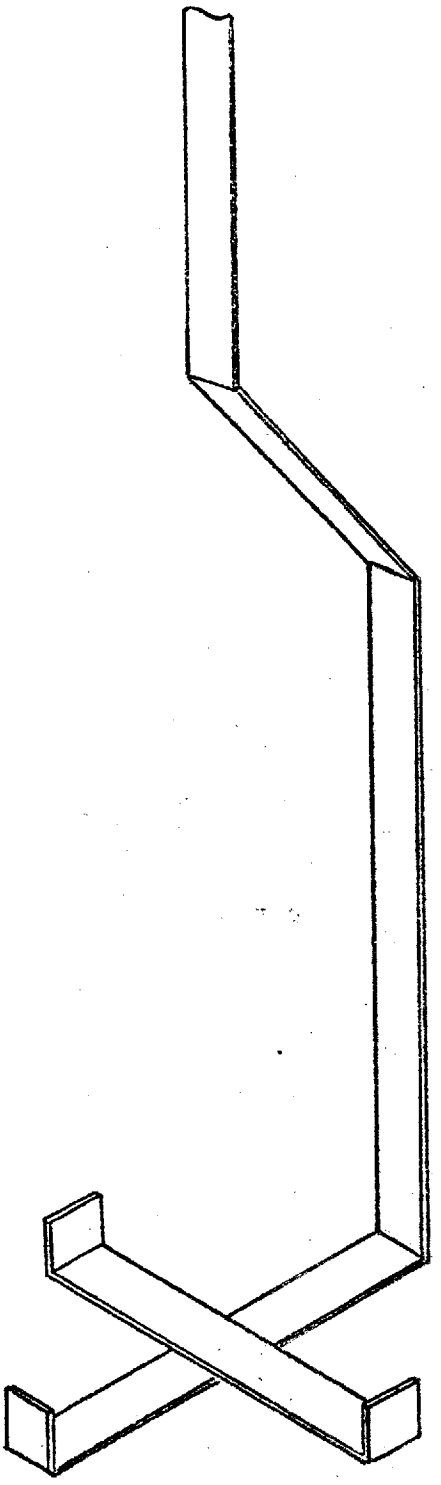

Figure 2.6 : Carriage for weight loss sample.

was unrestricted except when the sample adhered to the foil holder.

2.4.2 CHARS

When the weight loss experiments were completed the charred samples were inspected. They were cut longitudinally into halves to permit observation of the interior. Assessment was made of the strength, shrinkage, cell size and degree of melting of the char.

After manual investigation the strength was assessed on an arbitrary scale ranging from 1, very frail, through to 5, as strong as the original foam. It was the overall strength of the sample that was considered, not just the stronger skin or the insubstantial interior, but a combination of these two extremes.

The volumetric shrinkage was estimated by the cross-sectional area of the bisected sample. Three arbitrary grades were used. 'Low' shrinkage represented a volume reduction of less than 30%, 'high' shrinkage more than 75% reduction, and 'medium' any intermediate value. Assuming that contraction was symmetric in all directions the limits of the categories were represented by concentric rectangles on a card. Half of the sample was placed centrally on this chart to see which boundary it lay inside.

Cell size was an indication of the larger cells present, although if one regime did not predominate by virtue of there being two distinct zones then both major sizes were recorded. The three divisions were:- 'a', less than 1 mm, which included the original foam; 'b', 1 to 5 mm; and 'c', greater than 5 mm. If the sample was but a shell with no internal structure, then this was noted.

If there was evidence that the foam had softened or melted during exposure to the elevated temperature this fact was recorded. Enlargement of the cells and a central pillar of compact char are typical signs of melting.

Any other pertinent observations were noted and a photographic record of the samples was made.

2.4.3 ACTIVITY OF CHAR

Apparatus

The apparatus for measurement of the activity of the chars produced in previous experiments is shown in figure 2.7. The heating tube was constructed of Pyrex glass with a removable end section which carried the thermocouple that measured the temperature of the sample. It was wrapped with asbestos paper and then wound with a resistance wire element and lagged with asbestos string. A plug of glass wool diffused the incoming gas stream and facilitated its preheating.

The flow of gas through this tube was controlled by the regulator on the gas cylinder and measured by a capillary type differential pressure manometer (figure 2.8) which had been calibrated against a Rotameter variable area flowmeter. The simple bubble manometer formed by insertion of a side-leg into water both regulated the flowrate and protected the capillary monometer against damage from over-pressure. The thermocouple was connected to a Pye direct reading galvanometer and the heating element was supplied with an AC voltage from a variable rotary autotransformer.

Method

Preliminary investigation showed that the greatest temperature rises were observed with a gas flowrate of approximately 100 ml min^{-1} so this value was used throughout.

A sample of char was broken into large pieces which were loosely packed into the tube and the thermocouple inserted. Nitrogen was passed through the tube, a voltage applied to the heating element and the temperature was allowed to rise to a steady value. The gas flow was then switched to oxygen and the temperature at half minute intervals recorded for some 5 to 10 minutes.

The experiment was repeated with a fresh char sample and a different supply voltage, and hence equilibrium temperature, until sufficient runs

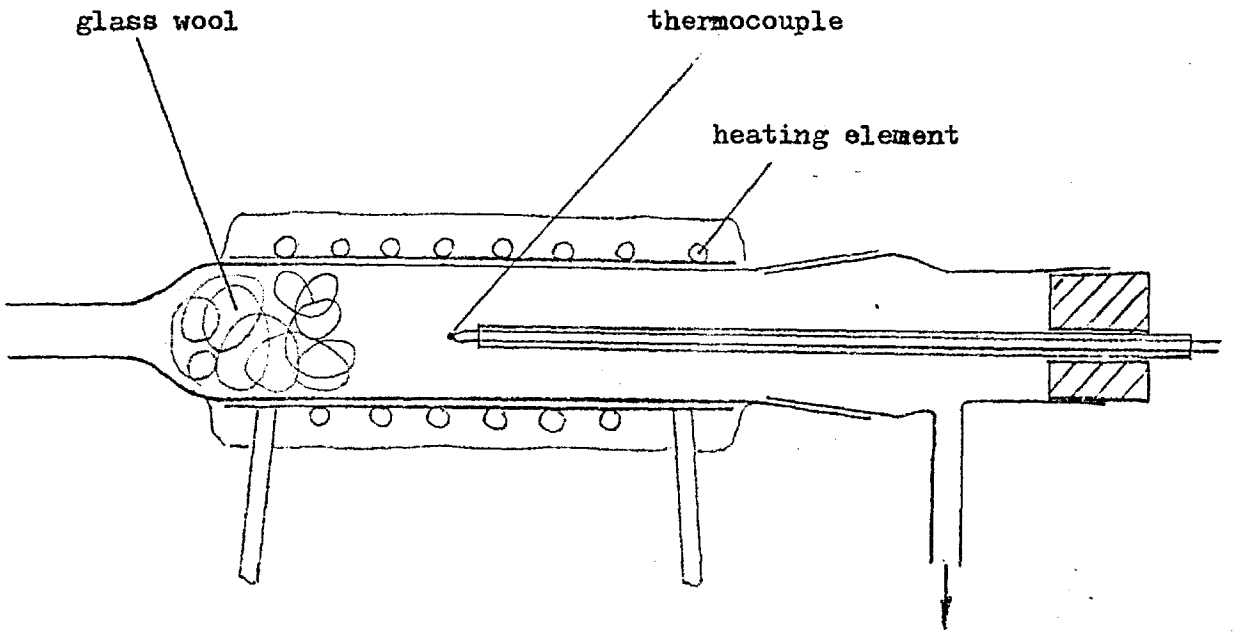

Approximately full scale

Figure 2.7 : Heating tube for char activity.

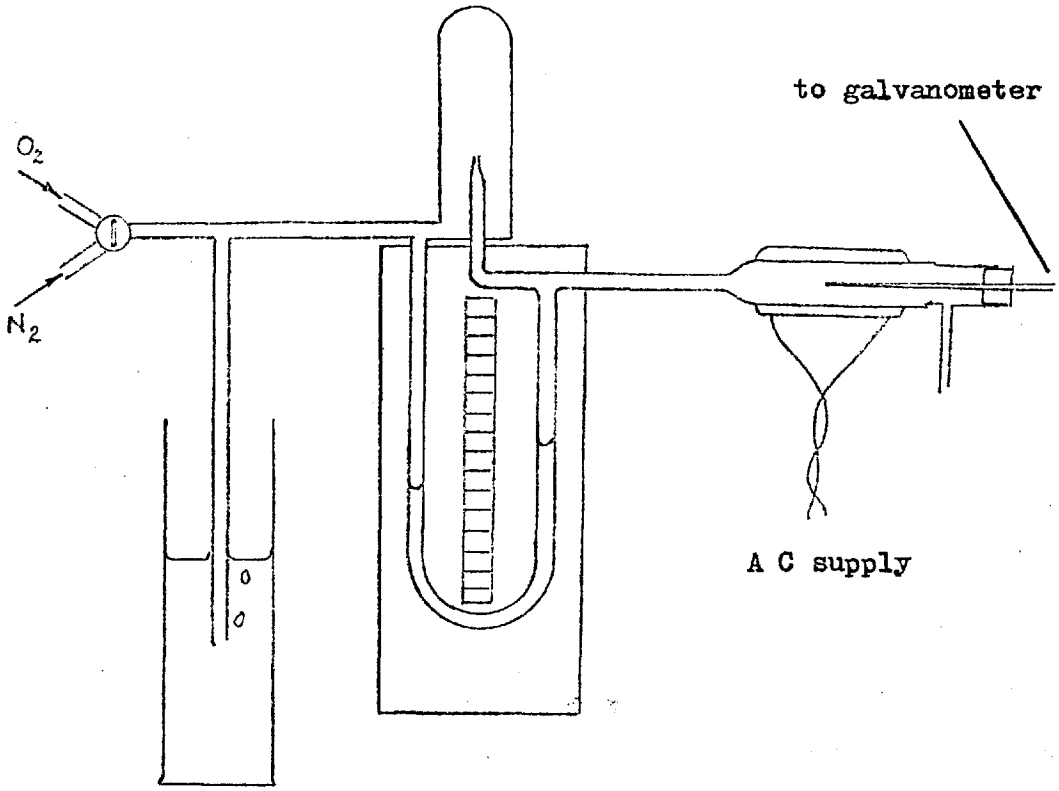

Figure 2.8 : Arrangement of apparatus for measurement of char activity.

were recorded to show a limiting case of thermal explosion.

Evaluations of activity were made for all the chars produced by combustion at the infra-red furnace, and for the char produced from the weight loss experiments for Foams, A, C and E.

2.5 DIFFERENTIAL THERMAL ANALYSIS (DTA)

Initially it was proposed to build an apparatus for making differential thermal analyses of the urethane foams. Various forms of equipment were considered and a trial heating block was constructed before it was concluded that such a construction was beyond the resources of this investigation. Fortuitously spare running capacity became available on a commercial instrument, which was used to analyse the polyurethanes. The machine was a Du Pont Differential Thermal Analyser.

A powdered sample of each of the materials was prepared by compressing a block of foam to a sheet and scraping it with a metal edge. Some powder was rammed gently into a 2 mm diameter glass sample tube and an analysis performed. The sample block was initially at room temperature and the temperature was programmed to increase linearly at a rate of 15° C per minute to a maximum of 400° C. Glass beads were used as a reference material. The temperature of the reference material and the temperature difference between the sample and the reference were plotted on an x-ray pen recorder.

Samples of the isocyanate and polyols used in the foams and of TCEP were also run on the equipment. Attempts were made to formulate polymers to determine the effect of varying the groups in the chains, but it was found that such formulations required extensive work, so trials were abandoned in favour of other approaches.

Further samples of polyurethane foams were produced and made available for the purposes of this DTA work. They were formulated as follows:-

Table 2.1 : Sample Formulation
(+ denotes that component is present in material)

Component	F1	F2	F3	F4	F5
Supersec DN	+	+	+	+	+
Daltolac 51	+	+	+		
Sorbitol polyether				+	+
TCEP		+	+	+	
Propylan P450					+
Dimethylcyclohexylamine	+	+	+	+	+
Dibutyltin Dilaurate			+		
Silicone	+	+	+	+	+
Arcton 11	+	+	+	+	+

These foams were powdered in the same manner as the foams A - E, and analyses performed similarly.

The major problem with the apparatus was that of maintaining a uniform sample as the tube was of small bore and the powder varied making it impossible to tamp it down to the same extent each time. Chromel/alumel thermocouples were used to measure the temperatures and the minor discrepancies in matching of pairs contributed towards the unpredictable nature of the base line slope. A run was made with glass beads in both the sample and reference positions to investigate the nature of the base line. When the solid samples pyrolised in the sample tubes the expanding volatile products tended to transport some of the material along the tubes and in some cases out of the tubes. This may reduce the efficiency of the thermal contact with the thermocouple and the size of the sample under investigation, both of which make for unrepresentative results. Towards the end of the experiments the temperature programmer developed fault and had to be replaced by a different unit, so the final runs were made with a heating rate of 20° C per minute and using 4 mm diameter sample tubes.

2.6 ANALYSIS OF PYROLYSIS PRODUCTS

A variety of methods was used in an attempt to obtain information about the nature of the products of decomposition of polyurethane foams. In each case the foams were heated in an oxygen deficient atmosphere in order to approximate to the pyrolytic conditions that prevail in the bulk of the material.

2.6.1 CHROMATOGRAPHY

Gas Liquid Chromatography (GLC) seemed ideally suited to the problem in hand as, with suitable operating conditions and the correct column, it is possible to separate compounds of very similar natures that could not readily be resolved otherwise. The equipment used was a Perkin-Elmer Fractometer fitted with an ionisation detector. A proprietary column of length 2 metres and diameter 8 mm filled with Carbowax 1500 was fitted in the oven. This column is designed for the separation of high boiling polar compounds and can be used at temperatures of up to 200° C.

The ionisation detector contained a tritium source emitting β radiation which ionised the gas stream. It was operated in an electron capture mode which ensured that sensitivity is as high as possible. Nitrogen was used as the carrier gas as it was compatible with the required conditions and the detector, but it needed to be first passed through a drying tube of silica gel as moisture interferes with detector operation. The apparatus was pressure tested for leaks as directed in the operating manual, and the nitrogen flowrate then adjusted to approximately 20 ml min^{-1}. The thermostat was set to give an oven temperature of 125° C, and the amplifier and recorder switched on. The equipment was allowed to reach steady state before any calibrations were made as the amplifier especially needed an extended period to settle down. By procedures laid down in the manual zeros were set and a curve of output signal versus applied voltage to the detector was plotted. It was necessary to locate the knee of this curve as the operating voltage for electron capture

detection should be just below the knee voltage to ensure maximum sensitivity. The applied voltage to the detector was set at -30 volts and the backing off current increased to give a zero output signal.

The gas samples were initially introduced to the carrier gas stream by means of a 'cross-over' sampling valve with a push-pull mode of operation (figure 2.9). Nitrogen was passed through a length of glass tubing containing a sample of foam and into the valve. After the line had been flushed of air, the glass tubing was heated with a soft bunsen flame. The evolved decomposition products were swept away by a stream of nitrogen and through the sampling valve. When it was apparent from the issue of fumes from the exit line of the valve that the stream contained a high concentration of products, the piston was pushed to the sampling position for two seconds and then pulled out. The chart drive of the recorder was started and the commencement indexed. After approximately 5 seconds the output gave a sharp narrow peak and then no further signal was produced even though the equipment was left running for some 30 minutes.

Similar runs were performed using other foams and varying the operating conditions, viz; gas flowrate, gas pressure, pyrolysis temperature, oven temperature, sample size and detector voltage, without producing any further peaks other than the narrow one after approximately 5 seconds which was attributed to the pressure fluctuations on sample introduction. As there was a possibility that water was one of the evolved products and that there was enough present to interfere with the functioning of the detector, a small drying tube of silica gel was inserted between the pyrolysis chamber and the sampling valve. There was no effect on the output.

The evolved products from heated foam were drawn into a 1 ml hyperdermio syringe and injected into the chromatograph through the silicone rubber septum of the sample port, but no peaks were obtained.

In place of the sample of polyurethane in the glass tube used initially, was placed a piece of filter paper soaked with methanol. When

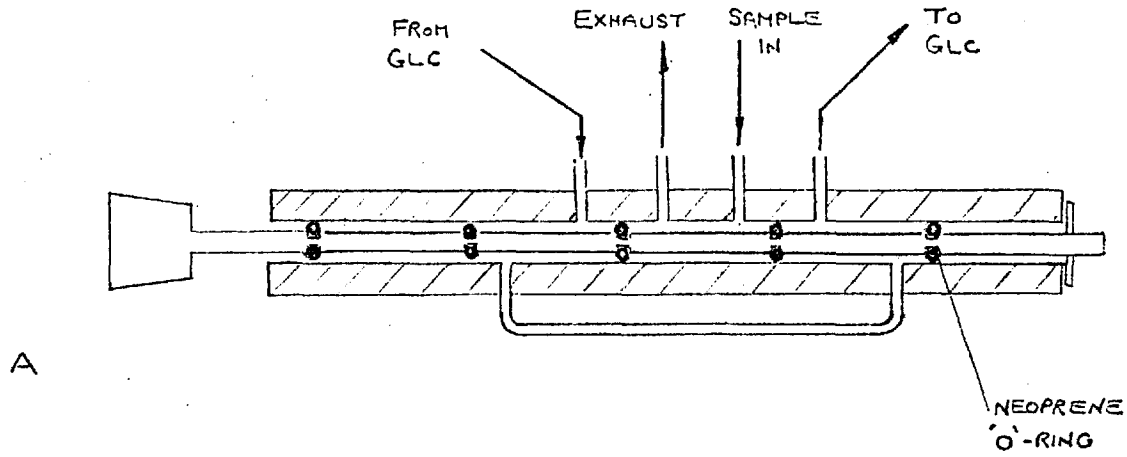

A

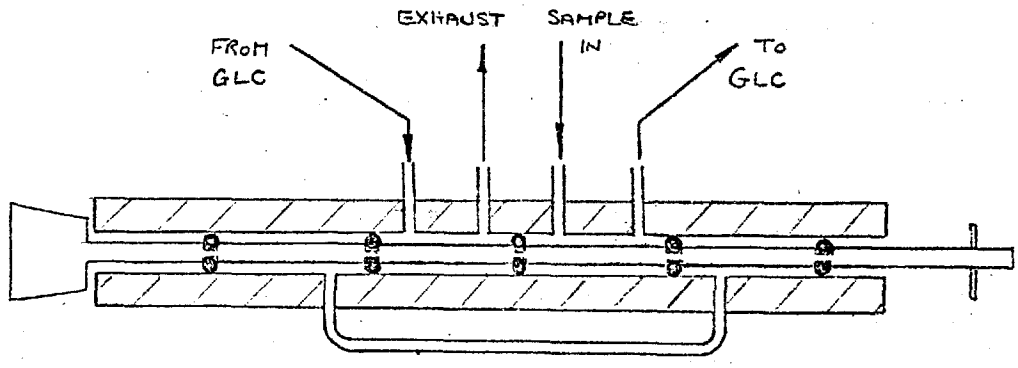

B

Figure 2.9 : 'Cross-over' gas sampling valve.

A Normal

B Sampling

the nitrogen flow had flushed the system the tube was warmed to evaporate the methanol and a sample introduced to the apparatus. This produced an output signal but the detector was overloaded so a large peak with a very slowly decaying tail was produced. By using very small samples it was possible to obtain a reasonable set of peaks for methanol. Other polar liquids such as chloroform, ohlorobromomethane, and ethanol were introduced into the chromatograph and by careful adjustment of the sample size it proved possible to avoid overloading the detector. Unfortunately the peaks produced were cramped and rather diffused so it was only feasible to discriminate between these few compounds by careful measurement.

In view of the minute quantities required to affect the detector, a hyperdermic syringe of capacity one microlitre was procured and used to inject the liquids into the chromatograph through the septum. Again the sample size was critical: 1μl caused saturation of the detector, but 0.5μl was satisfactory. When the methanol peaks were known a sample was prepared by pyrolysing a quantity of polyurethane foam under a stream of nitrogen and passing the gases through a wash bottle of methanol to extract the products of decomposition. Several grams of foam were pyrolysed to ensure that the extract was of a reasonable concentration and a sample of the liquid was injected into the apparatus. The output consisted of the methanol peaks with no other additions, even after a protracted period. Similar experiments were performed using other liquids as the extraction medium and varying the pyrolysis conditions, but no peaks were produced to suggest the decomposition products.

The ionization amplifier had been giving noisier output signals for some while, but now its isolation failed completely as the switching of the thermostat was producing an extraneous signal which could not be eliminated. The amplifier was overhauled by the manufacturers and all the valves replaced to give a more faithful response.

At this stage a new gas sampling valve was obtained to replace the

old "cross-over" type which was not gas tight and tended to stick. The new valve, manufactured by Hewlett-Packard Limited, was of the disc type and was attached to a pair of $\frac{1}{2}$ ml stainless steel loops. As shown in figure 2.10 the operation of the valve switched the two loops between the lines they were in, allowing the loop that had been in the apparatus line to be filled in preparation for the next analysis.

When the foam in the glass tube was heated with a bunsen burner it was not possible to exert much control over the temperature of pyrolysis, so a unit was assembled to provide pyrolysis by means of a heated gas stream. This was constructed as shown in figure 2.11 and was attached to a trap with a cold finger to remove the tars from the gas stream to avoid gumming up the sampling valve. A piece of foam was inserted in the unit, the stream of nitrogen was started to flush the line, and the current then increased until the heating element glowed bright red. When the foam started to show signs of charring a sample was introduced to the chromatograph. No output signal other than the injection peak was produced. The gas flowrate through the unit was varied, but even so it was not possible to achieve a situation whereby the gas stream was hot enough to ensure a high rate of decomposition of the sample. This means that the sampled gas stream was too dilute, so this pyrolyser was abandoned.

The column was washed by injection of quantities of petroleum ether and purged with nitrogen for several days to remove any residual material that might have lodged therein.

A series of known liquid compounds were then injected into the apparatus to determine retention times for them. Included were the lower ketones, phenylalkanes, alcohols and halogenated hydrocarbons, but for most of these materials a series of peaks of the same size was obtained even though they were known to be of high purity. Although a consistent trace was produced for each of the materials, the peaks were not discrete so there was extensive interference when more than one substance was present as they all had similar short retention times.

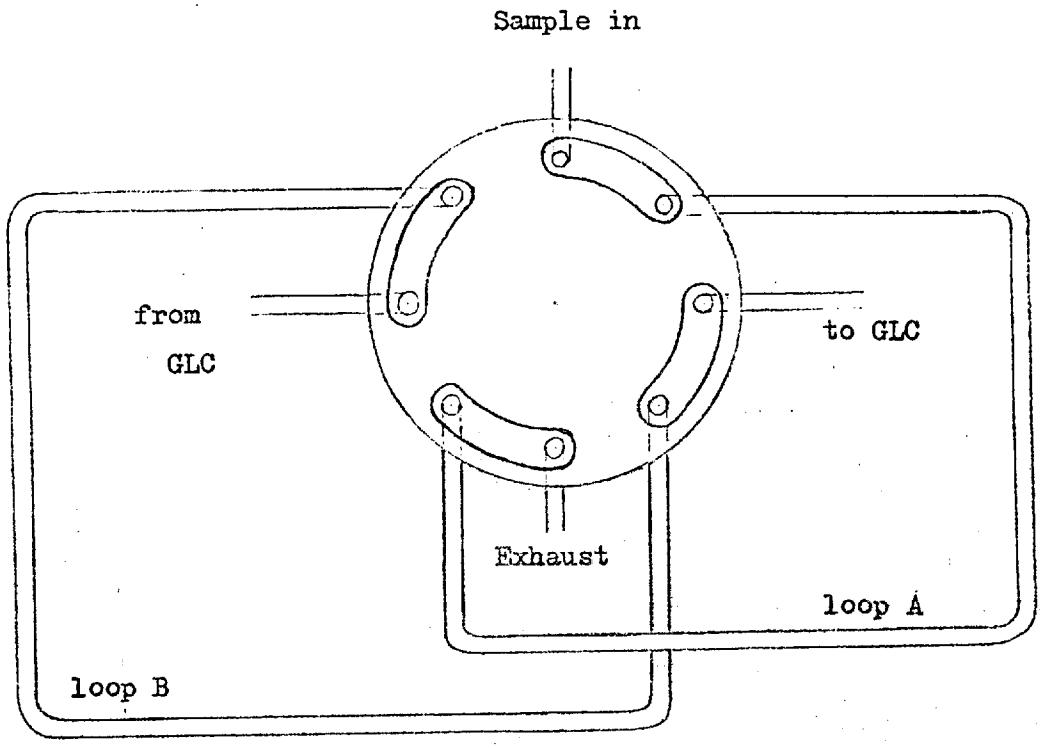

(a)

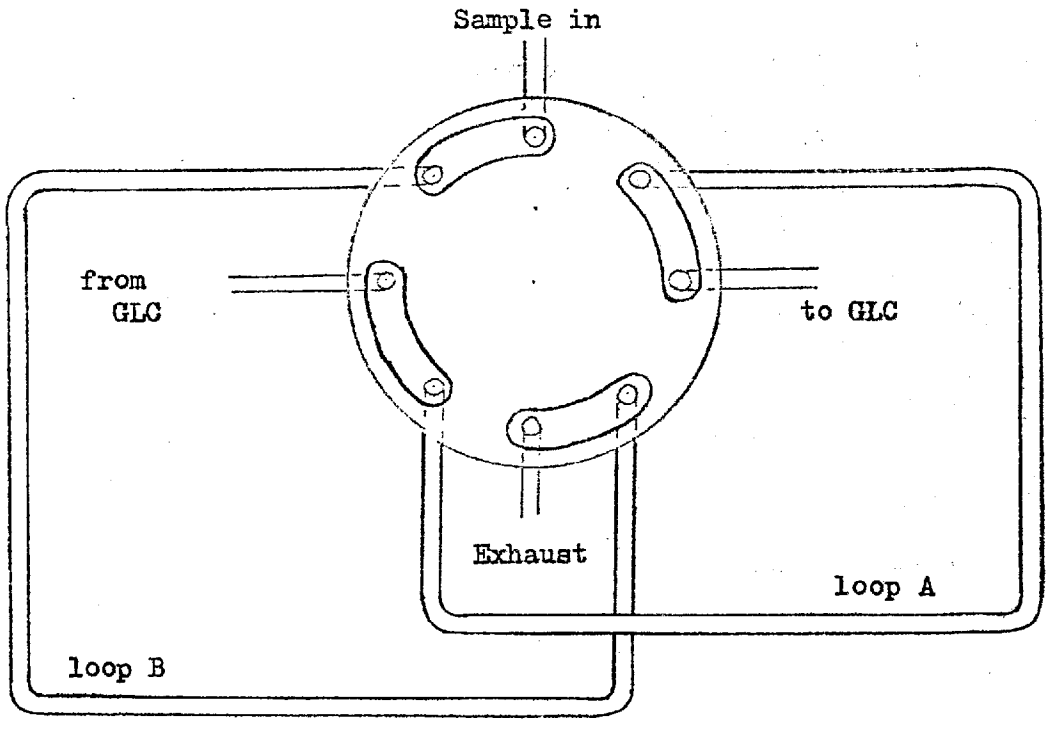

(b)

Figure 2.10 : Plan of Hewlett-Packard sampling valve.

(a) Loop A being filled with sample

(b) Contents of loop A being discharged into GLC

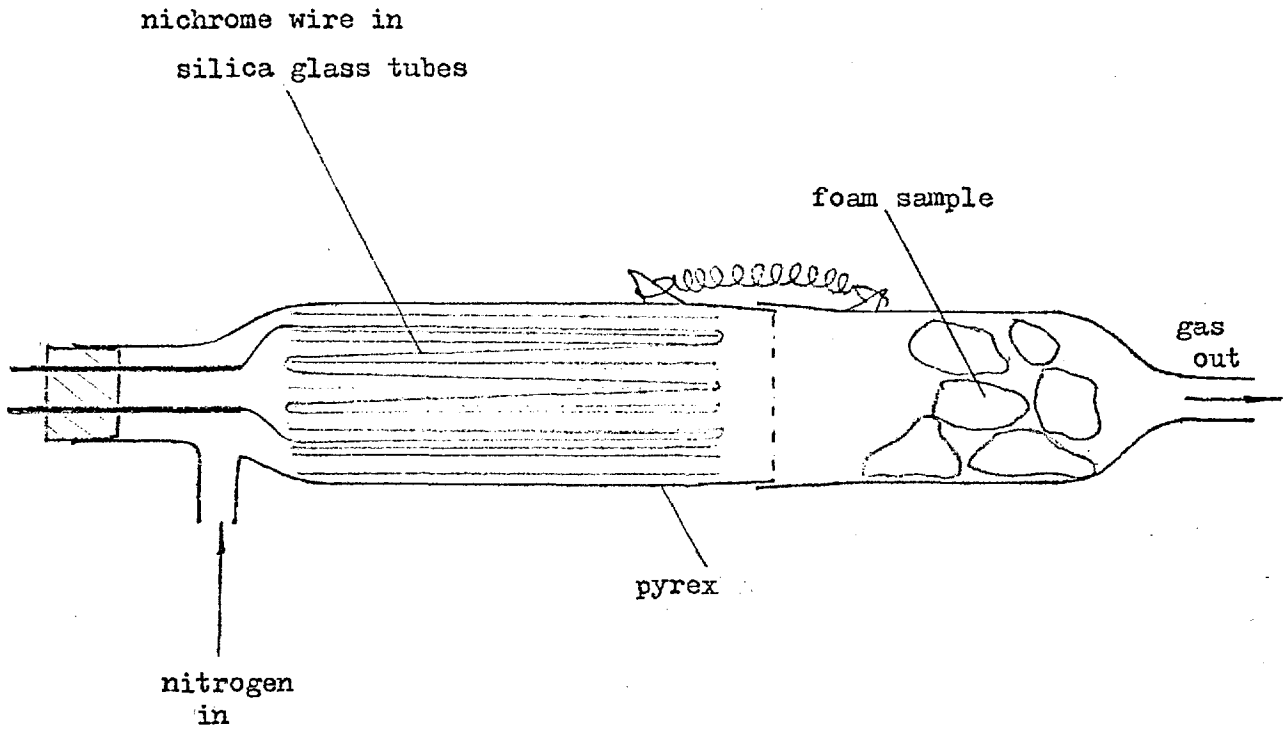

Figure 2.11 : Hot gas pyrolyser.

In an attempt to determine whether or not the pyrolysis products include any small polar molecules, samples were prepared by passing the evolved gas stream through methanol, xylene and dimethylketone. These were then injected into the chromatograph and the resulting trace compared with that of the solvent. There were no significant differences.

0.2 μl of tris (chloroethyl) phosphate was injected for analysis, but the trace had only the injection peak.

To enable the pyrolysis to be performed at a controlled temperature another pyrolyser was constructed. It consisted of a 80 mm length of 12 mm diameter brass bar, bored with a 4 mm hole for 70 mm of its length. The mouth of the hole was tapped to enable it to be screwed on to the fitting of the sampling valve. A teflon washer was fabricated to make the seal gas tight. The bar was lightly packed with foam, flushed with nitrogen and then screwed on to the valve coupling which had been flushed with nitrogen. The brass bar was plunged into a pre-heated bath of liquid paraffin and progress followed by immersing the end of the "exhaust" lead of the sample valve in water and observing the bubbles. There was a rapid stream of bubbles for some 40 seconds while the nitrogen expanded and then a slower stream as the pyrolysis proceeded. When the stream had reduced to an occasional bubble, after another 3 minutes or so, it was taken that the loop was full of decomposition products and a sample was analysed. The output consisted of a single early peak with a very slowly subsiding tail which had no features of note.

This was repeated with various sized samples for each of the foams at liquid paraffin temperatures of up to 200° C, but no peaks of significance were produced, so no further investigations were made with this apparatus.

2.6.2 CHLORIDE DETERMINATION

A $\frac{1}{2}$ gram sample of foam was rammed into a 250 mm length of 10 mm diameter glass tube. This was connected to allow a stream of nitrogen to pass through the foam and then to bubble through 15 ml of distilled water

in a test tube. The tube was heated with a bunsen flame to pyrolyse the foam and the evolved materials were swept away by the gas stream and through the water wash. If the sample was heated more violently the high boiling tar produced in the pyrolysis was also boiled over, only to collect at the bottom of the test tube of water.

The aqueous liquor, which had a yellow tint, was split into three and tested. To the first portion an equal volume of N/10 silver nitrate solution was added, and a grey or black precipitate was thrown down. A blank gave no visible reaction.

To the second portion was added a few drops of concentrated nitric acid and then an equal volume of N/10 silver nitrate solution. All the materials gave some indication of chloride, although in some cases it was only a faint turbidity. The white precipitate slowly darkened if it was left, presumably as it was reduced to silver.

The approximate pH of the final portion was determined with universal papers.

2.6.3 MASS SPECTROMETRY

Samples for analysis by mass spectrometry were prepared in the apparatus shown in figure 2.12. Stopcock B was closed and the sample bulb was evacuated through stopcock A with a rotary pump. Stopcock A was closed, and a pyrolysis tube of heat resistant glass oontaining approximately $\frac{1}{2}$ gram of polyurethane foam was affixed. The pyrolysis tube and the connecting passages were then evacuated through stopcock C for 30 seconds. This ensured that the bulk of the air was removed without rupturing too many of the cells and so removing the blowing agent. Stopcock C was closed and the pyrolysis tube was immersed in a beaker of heated liquid paraffin which was maintained at the desired pyrolysis temperature. Stopcock B was opened to admit the evolved materials to the sample tube.

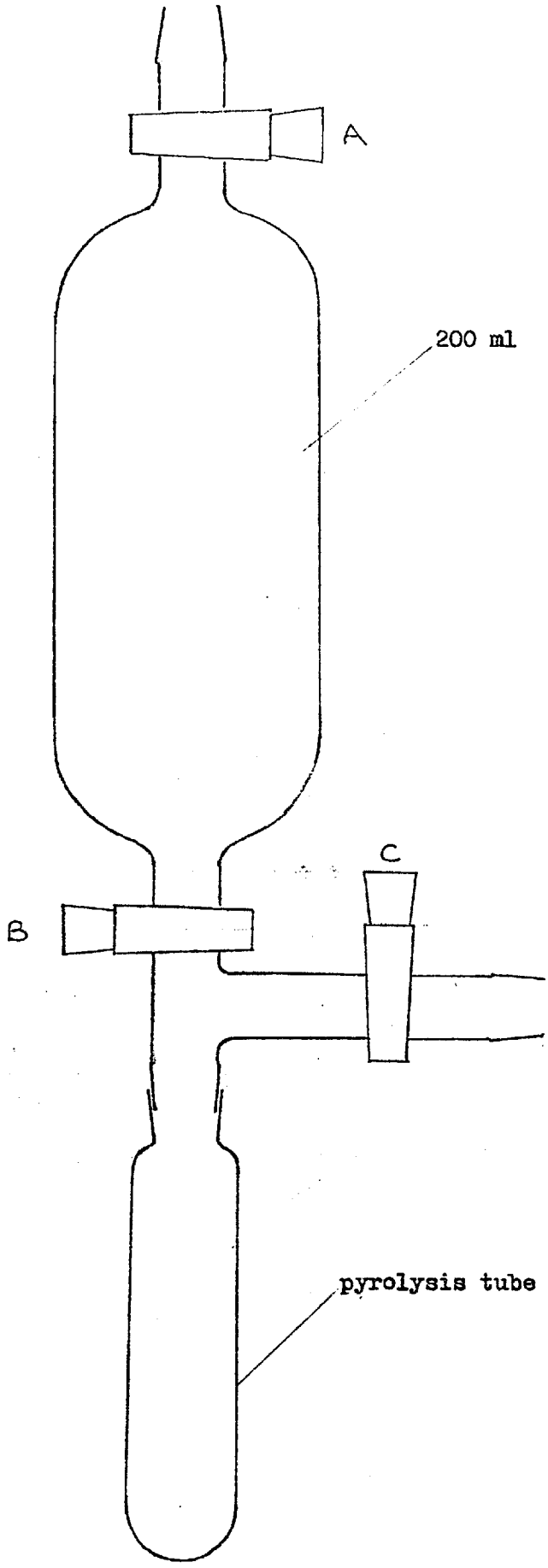

Figure 2.12 : Sample tube for mass spectrometry.

After approximately 20 minutes stopcock B was closed and the tube removed from the heating bath. By admitting air through stopcock C the pyrolysis tube could be removed for emptying and cleaning for another sample and the sample tube taken for analysis of its contents. The machine upon which these analyses were performed was an MS9 manufactured by AEI Limited.

3. RESULTS.

3.1 HEAT PENETRATION.

The temperature-time histories of the cylindrical samples at axial points various distances from the irradiated end of the samples are presented in figures 3.1- 3.5.

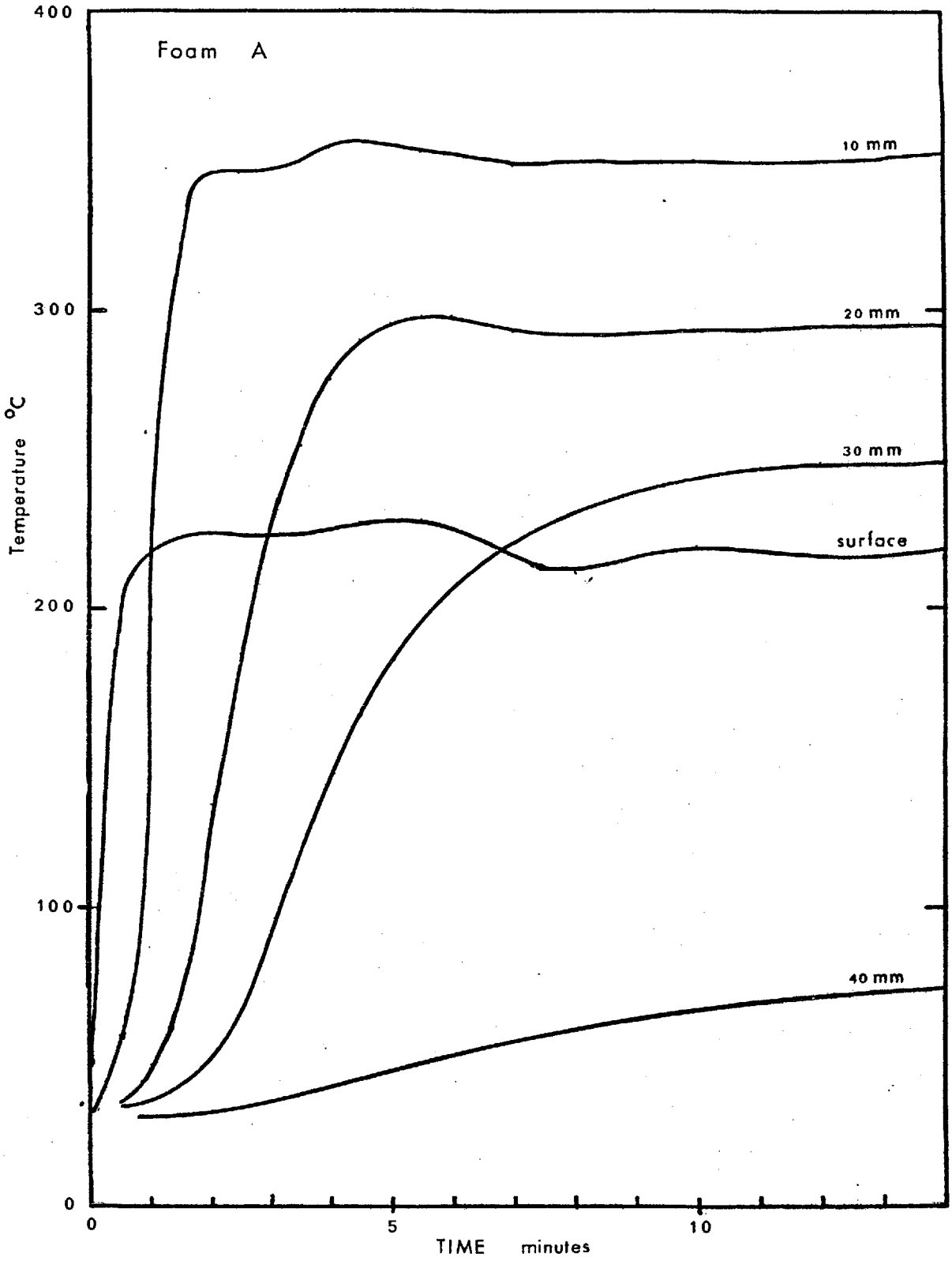

Figure 3.1 : Temperature - time history, Foam A

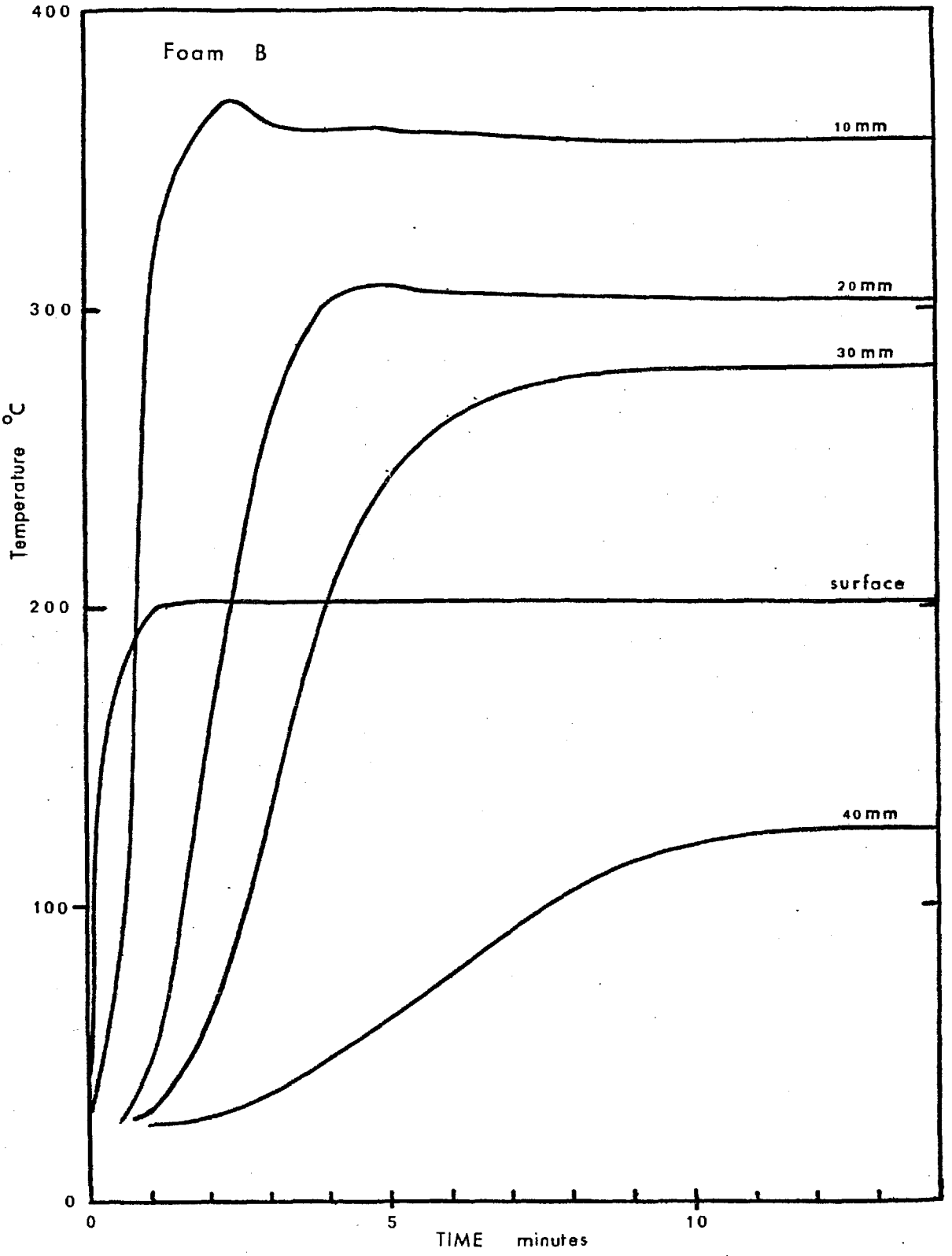

Figure 3.2 : Temperature – time history, Foam B

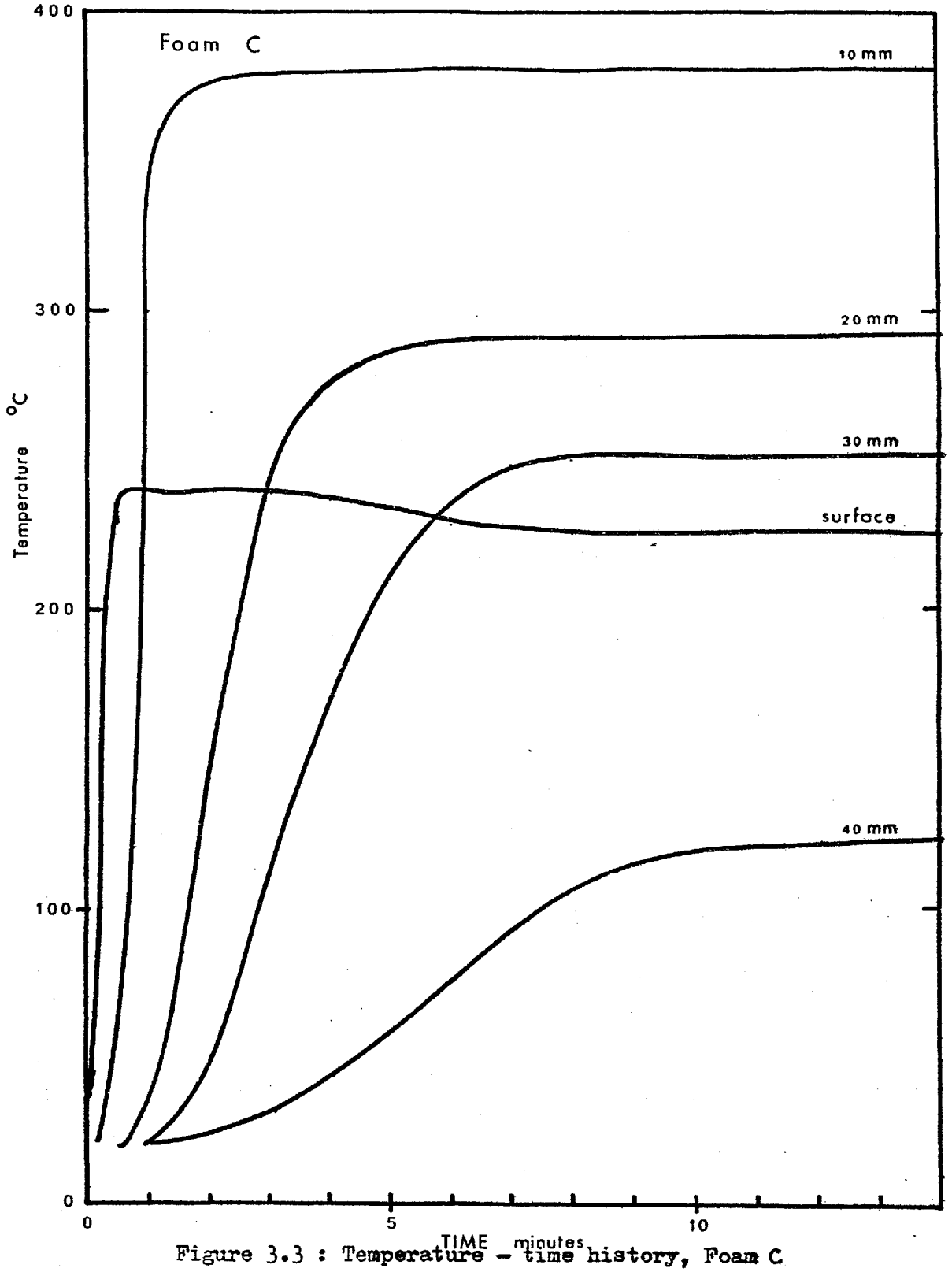

Figure 3.3 : Temperature - time history, Foam C

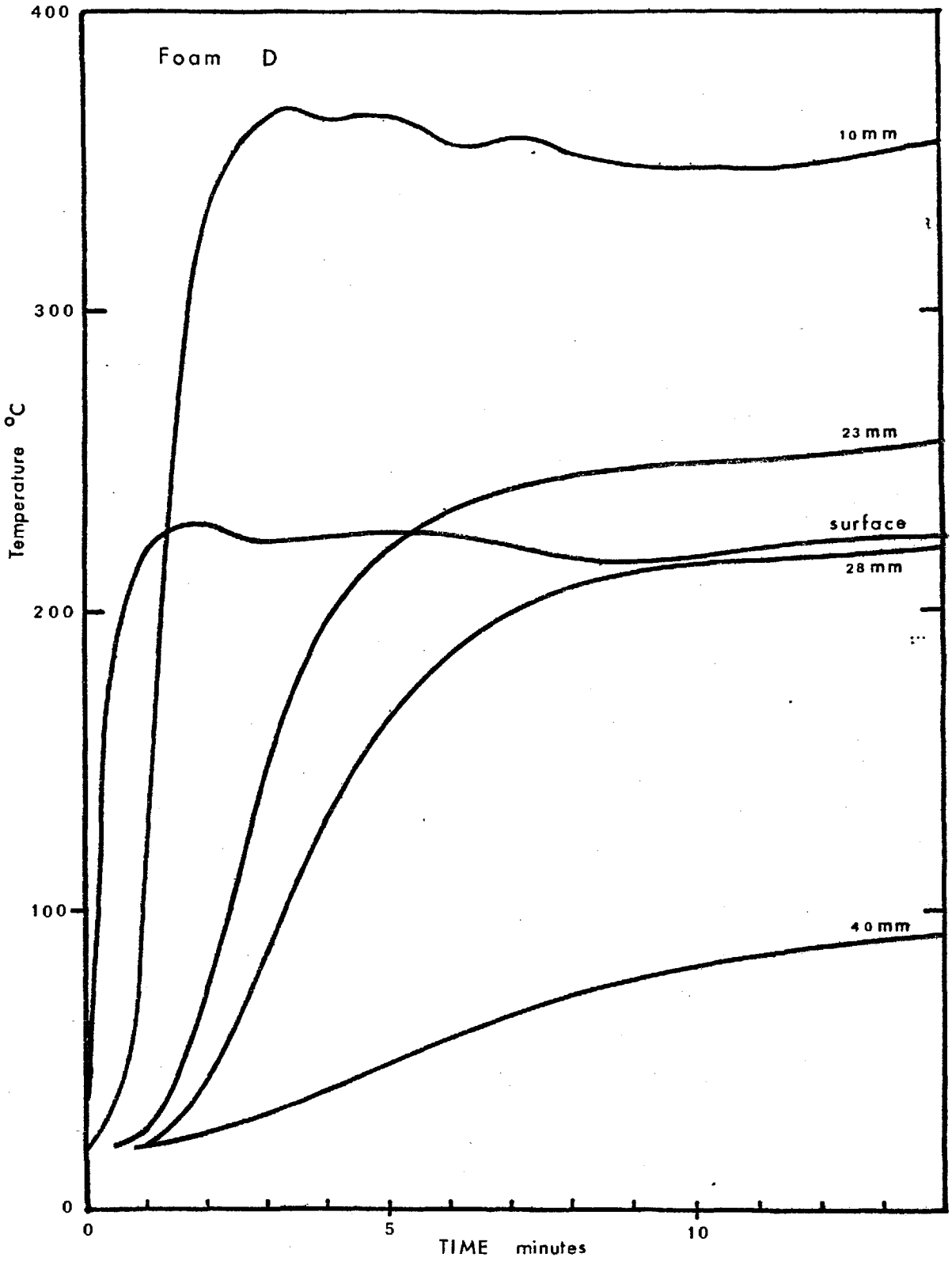

Figure 3.4 : Temperature – time history, Foam D

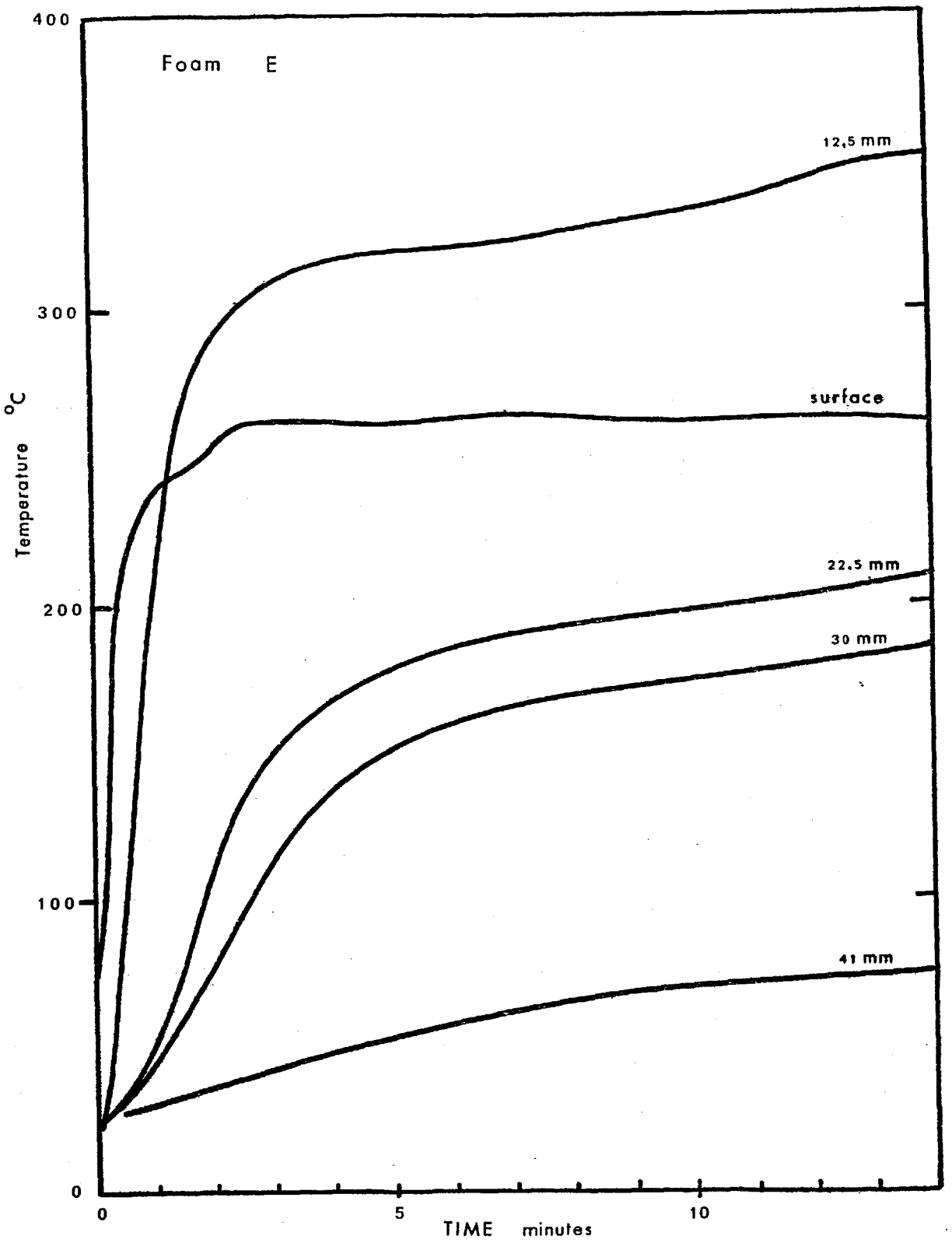

Figure 3.5 : Temperature – time history, Foam E

THERMAL DIFFUSIVITIES

These values are calculated from the temperature histories measured in the heat penetration experiments, under the assumption that the sample can be represented by a semi-infinite inert solid (vide 4.1.3)

Table 3.1 : Thermal Diffusivities

FOAM	THERMAL DIFFUSIVITY: $m^2 s^{-1} \times 10^{-6}$						
A	0.685	0.657	0.935	1.181	0.833	0.850	0.850
B	0.627	0.689	0.918	1.111	0.964	1.028	1.028
C	0.550	0.609	0.785	0.953	0.923	0.850	0.833
D	0.782	0.647	0.759	0.987	0.678	0.741	0.878
E	0.890	0.772	1.330	3.600	0.790	1.251	2.535
FROM CURVES AT DEPTH mm	10/20	10/20	10/30	20/30	10/20	10/30	20/30
AT TIME (SECS)	60	90			120		

3.2 SPONTANEOUS IGNITION

3.2.1 Preliminary Experiments

The following table contains the results of the experiments in which the furnace was not pressurised, thus allowing the ejection of the evolved volatiles into the furnace.

Table 3.2 : Preliminary results

Radiation Intensity ($kW\ m^{-2}$)	Foam	Ignition Time (s)	Ignition Temp (^{o}C)	Observations
6.3	A	NO IGNITION		Chars have large cavities.
	B			Chars have large cavities.
	C			
	D			Considerable shrinkage but even charring.
	E			Slightly scorched.
8.4	A	5	250	Black sooty smoke. Flame extinguished without irradiation.
	B	4	230	Grey sooty smoke. Combustion spread small distance beyond irradiated zone.
	C	4.5	225	Grey sooty smoke.
	D	5	225	Some spread of flame along face. Some shrinkage but remaining char of good density.
	E	NO IGNITION		Lightly charred where irradiated.
12.6	A	2.5	250	Combustion penetrated and spread.
	B	3	240	Complete combustion of irradiated area; extensive spreading.
	C	2	230	Extensive combustion; foam softened.
	D	2	240	Flame spread over whole face. Good char.
	E	7.5	400	Small flame, self extinguished after 20 seconds.
16.8	A	2.5	250	Complete combustion of irradiated area; some spread of flame.
	B	1.5	240	Almost complete combustion.
	C	1.5	240	Extensive combustion; material softened.
	D	<0.5	250	Considerable spread of combustion; good char.
	E	3.5	380	Small transient flame; some white smoke; char friable at surface, strengthens with depth.

3.2.2 Secondary experiments.

These tables record the results when a draught of nitrogen screened the aperture in the face of the furnace. No measurement of temperature was attempted.

Table 3.3 : Radiation intensity, 16.8 kW m^{-2}

Foam	Time to ignition (s)	Time to extinction (s)	Observations
A	NO IGNITION		Sample softened and receded at the surface and then charred with shrinkage. Although no burn through, the back face softened and bulged. Front face distended.
B	NO IGNITION		Generally as A. As a whole the sample retained its rigidity, but the irradiated char was weak.
C	NO IGNITION		Rapid evolution of volatiles as heated face receded from heat source. Signs of softening and bulging at rear face. Surface remained integral.
D	NO IGNITION		The surface charred and receded as the substrate shrank. Surface split open in heated area, otherwise integrity was good.
E	NO IGNITION		Very little decomposition outside irradiated area, where fissures formed in surface of char, which was soft at surface

Table 3.4 : Radiation intensity, 21.0 kW m^{-2}

Foam	Time to ignition (s)	Time to extinction (s)	Observations
A	4	100	Volatiles erupted violently into furnace and ignited. Sample burned fiercely with very smoky flame. Surface receded as it charred. Flames were abating after 80s but soft foam curled away from char and then burned vigorously to flimsy remains except for front face.
A	4	80	In a repeat run the softened foam contracted but did not separate from the char. There was still extensive combustion, and the back face softened and charred. The remaining char, although shrunken, was sound.
B	7	100	Ignition occurred when volatiles were projected into furnace, and sooty flame ensued. Combustion prolonged when char cracked to form vent for volatile materials. Internal decomposition continued and back face melted and charred at centre.
C	12	80	Vigorous projection of decomposition products. The flame extinguished when relatively non-permeable char formed on surface. Centre of back face charred and melted.
D	4	45	Sooty flame spread all over front face after 10s. Flame flashed over other faces but did not become established. Back softened but no burn through. Char is firm, even though split where irradiated, and shrunken.
E	NO IGNITION		Sparse white fumes, and decrepitation. After 5 minutes irradiated area had fissures and front 6mm of char was soft and friable and had receded 3mm. Around this, char medium brown for 20mm. No signs of softening or burn through.

Table 3.5 : Radiation intensity, 25.2 kW m^{-2}

Foam	Time to ignition (s)	Time to extinction (s)	Observations
A	$2\frac{1}{2}$	85	Burned with copious grey smoke. At extinction sample thickness only 12mm. Back face then melts onto existing char and chars. The residue is fragile and distorted.
B	3	120	Copious smoke as flame spread over all sample. The foam softened as it burned and fell from clamp after 120 s when only fragile skin remained.
C	3	140	Very smoky flame spread all round sample. Rear face was seen to melt, decompose then burn. Only skin remained.
D	$2\frac{1}{2}$	60	Flame spread all over surface for 45 s until surface was charred, when flame died except on irradiated face. White fumes were still emitted and a little softening was in evidence. Sample suffered moderate shrinkage and just charred through. Fissures in surface about irradiated zone.
E	5	125	Small flame with grey smoke for 25 s, spreading upwards on heated face only. Then smaller flame on irradiated area as surface decrepitates under thermal shock. After 5 minutes integrity of sample is still good although there are fissures about the irradiated area, which is a friable and fine char. Flame did not spread off front.

3.3

3.3.1 WEIGHT LOSS.

The data from the weight loss experiments are presented here in both tabular and graphical forms.

Table 3.6 : Foam A

Temperature °C	Fractional Weight Loss After			
	7 min	20 min	60 min	180 min
160	0.067	0.077	0.125	0.167
200	0.159	0.225	0.255	0.264
245	0.366	0.350	0.376	0.383
290	0.478	0.472	0.500	0.538
333	0.587	0.599	0.629	0.698
360	0.639	0.666	0.711	0.806
400	0.716	0.772	0.860	0.940

Table 3.7 : Foam B

Temperature °C	Fractional Weight Loss After			
	7 min	20 min	60 min	180 min
160	0.057	0.113	0.168	0.180
200	0.180	0.236	0.276	0.282
245	0.343	0.354	0.356	0.370
290	0.453	0.475	0.488	0.545
333	0.580	0.600	0.617	0.713
360	0.665	0.690	0.742	0.814
400	0.748	0.802	0.834	0.923

Table 3.8 : Foam C

Temperature °C	Fractional Weight Loss After			
	7 min	20 min	60 min	180 min
160	0.125	0.160	0.192	0.232
200	0.224	0.278	0.318	0.332
245	0.383	0.384	0.408	0.417
290	0.512	0.534	0.525	0.556
333	0.620	0.648	0.688	0.784
360	0.690	0.726	0.790	0.870
400	0.772	0.815	0.891	0.938

Table 3.9 : Foam D

Temperature °C	Fractional Weight Loss After			
	7 min	20 min	60 min	180 min
160	0.106	0.114	0.124	0.131
200	0.142	0.200	0.311	0.382
245	0.426	0.437	0.440	0.445
290	0.537	0.540	0.546	0.597
333	0.520	0.588	0.653	0.733
360	0.645	0.685	0.772	0.885
400	0.710	0.770	0.913	0.948

Table 3.10 : Foam E

Temperature °C	Fractional Weight Loss After			
	7 min	20 min	60 min	180 min
160	0.124	0.151	0.152	0.155
200	0.170	0.185	0.217	0.230
245	0.238	0.240	0.254	0.268
290	0.291	0.325	0.312	0.364
333	0.334	0.374	0.425	0.631
360	0.370	0.410	0.510	0.756
400	0.450	0.616	0.850	0.930

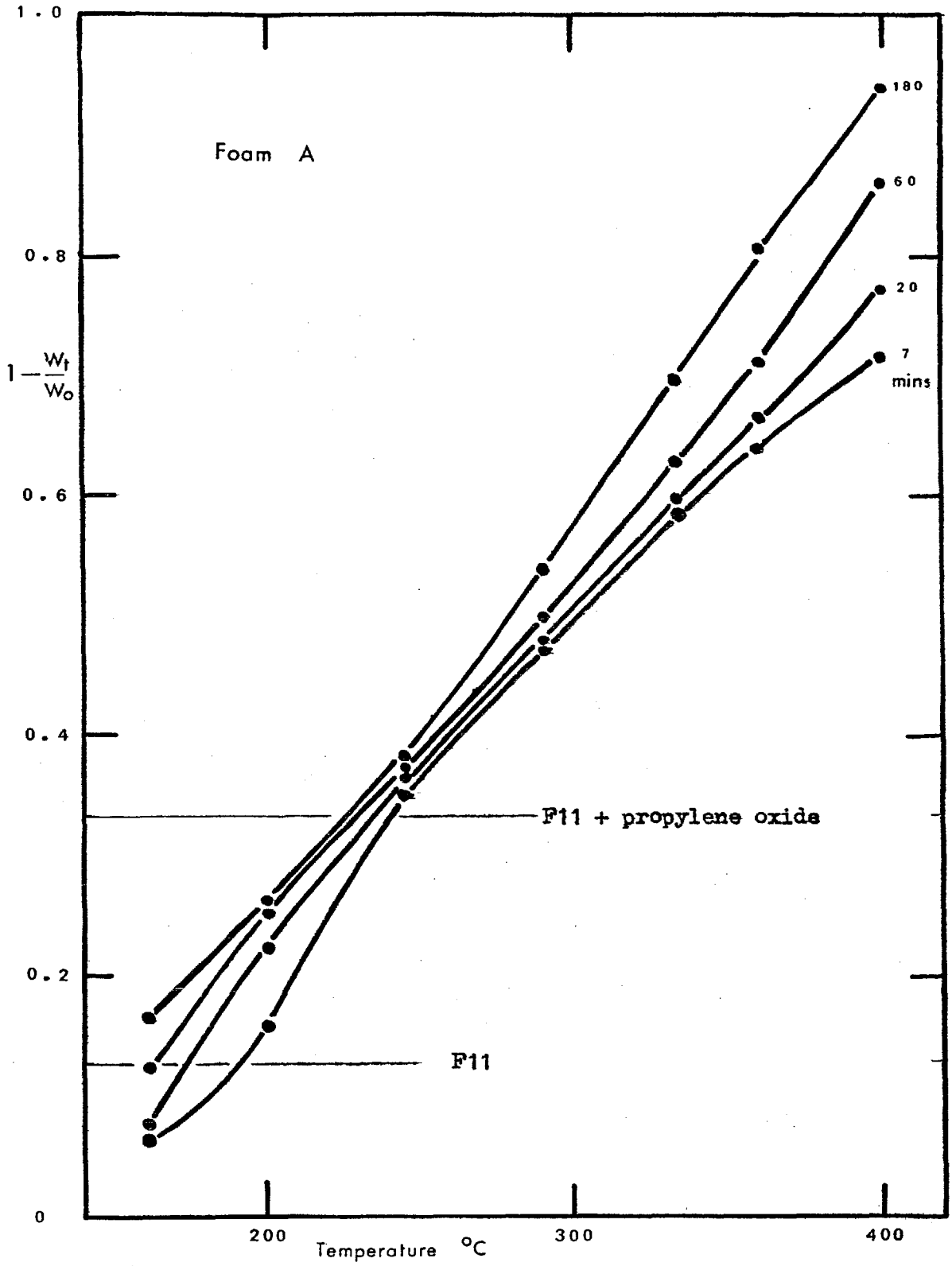

Figure 3.6 : Fractional weight loss vs temperature after various exposure times, Foam A

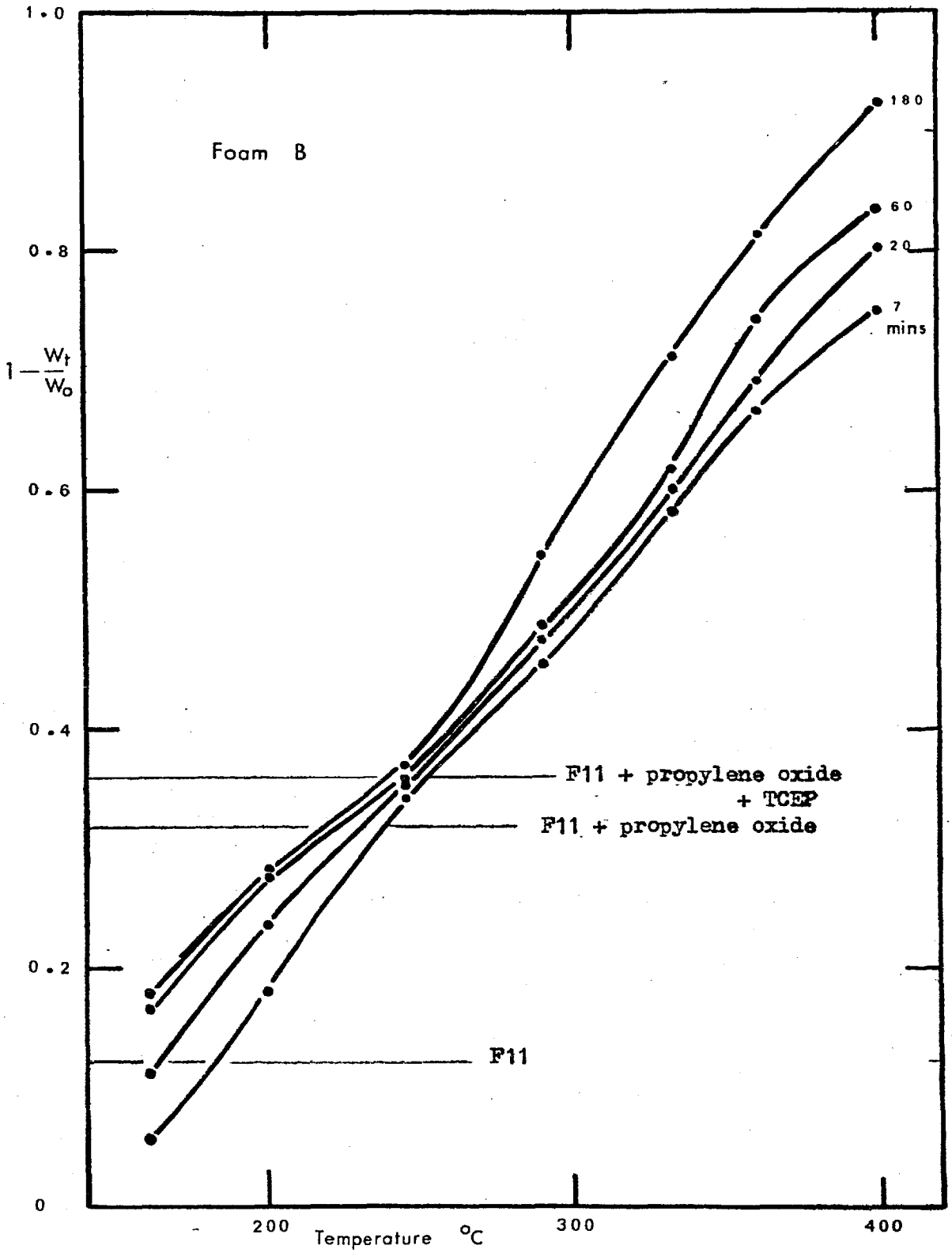

Figure 3.7 : Fractional weight loss vs temperature after various exposure times, Foam B

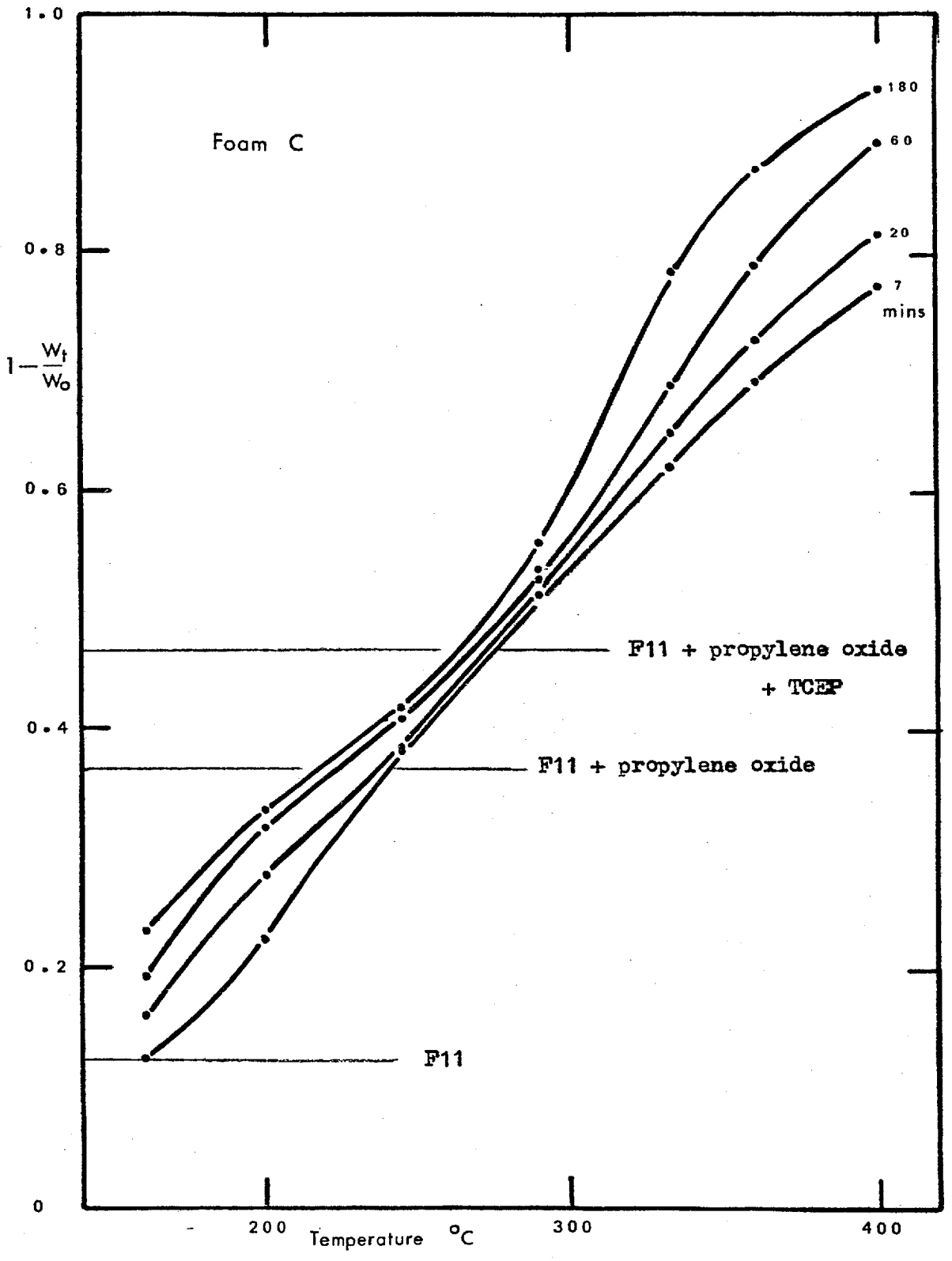

Figure 3.8 : Fractional weight loss vs temperature after various exposure times, Foam C

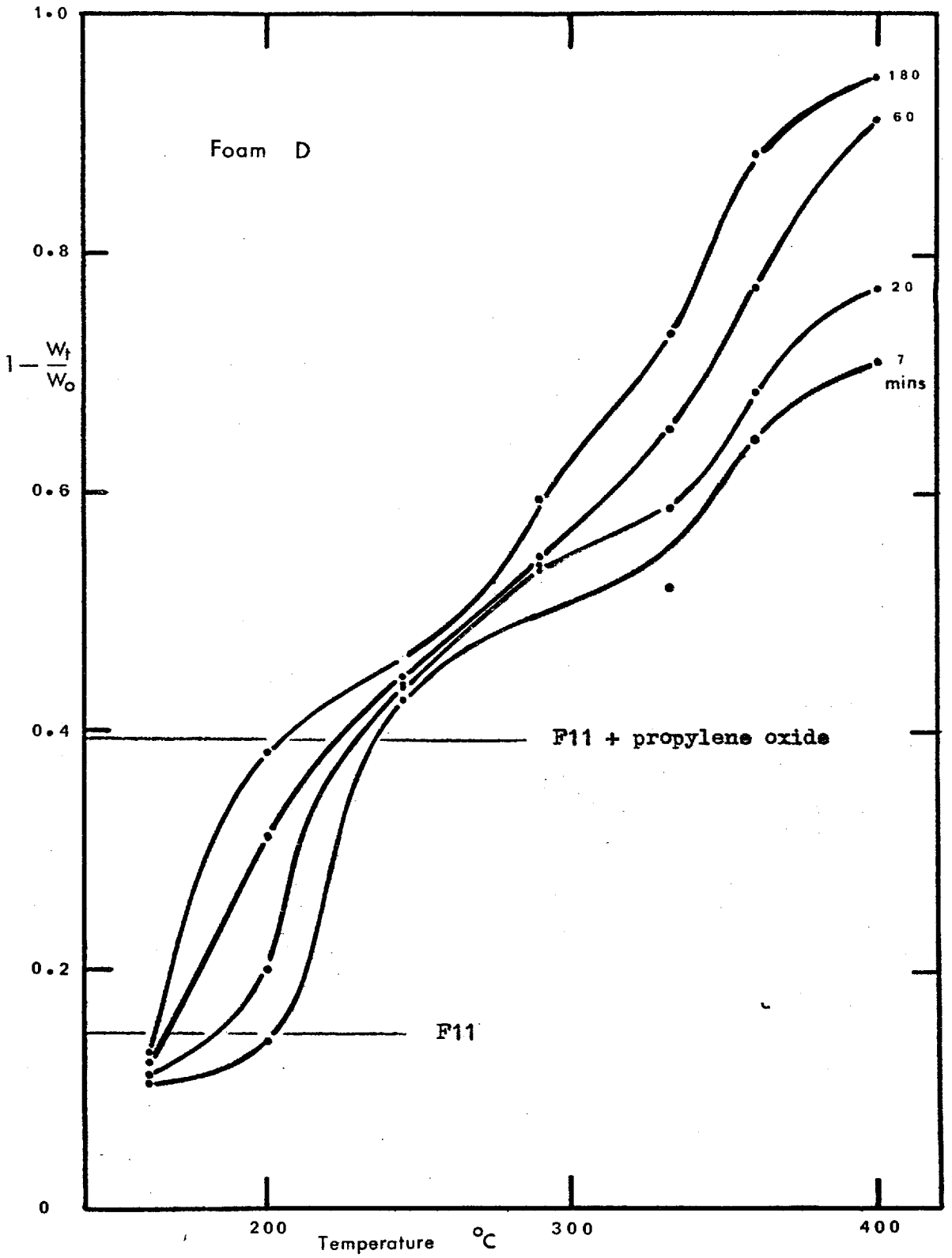

Figure 3.9 : Fractional weight loss vs temperature after various exposure times, Foam D

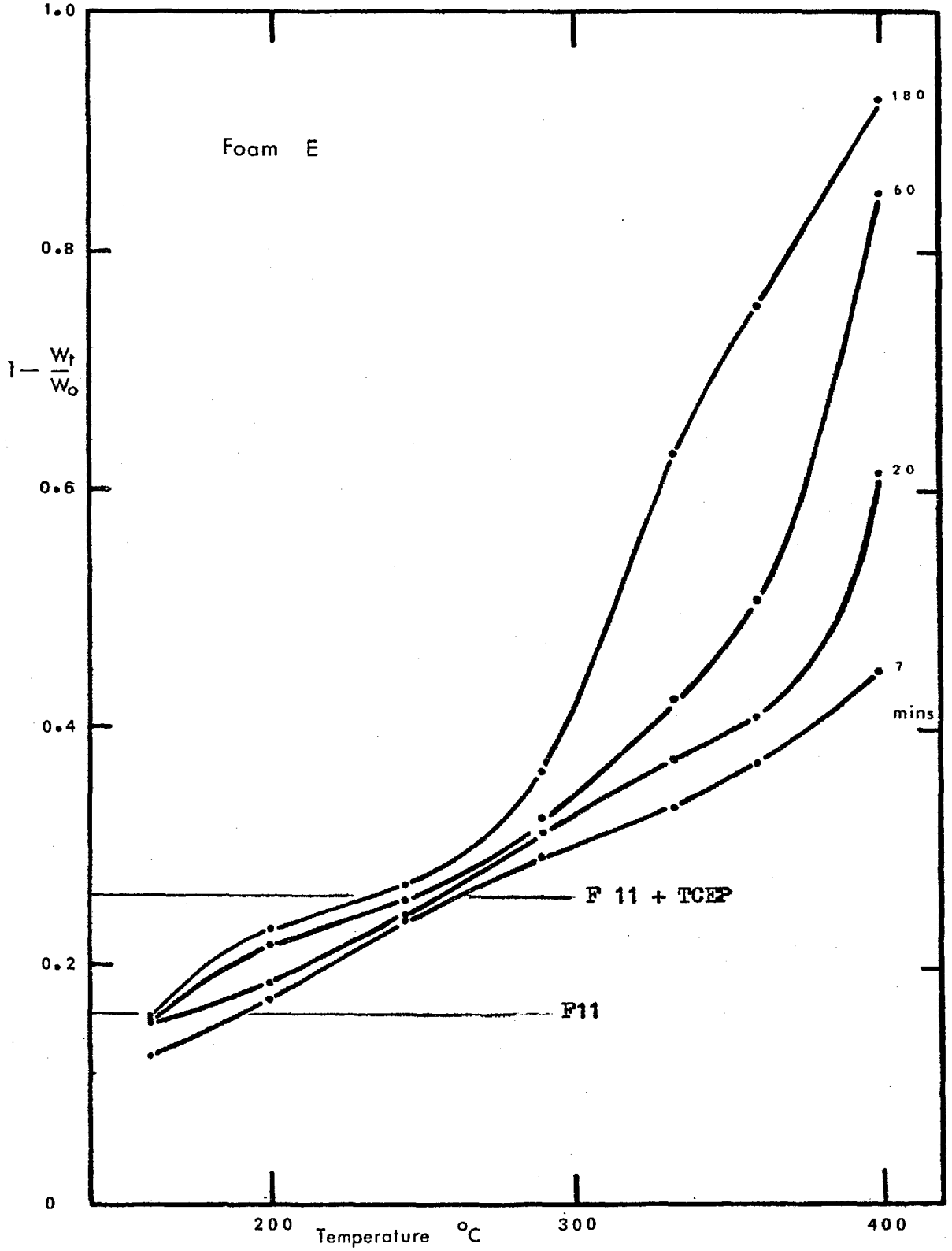

Figure 3.10 : Fractional weight loss vs temperature after various exposure times, Foam E

3.3.2 Charred Foams

These tables list the characteristics of the foam samples after exposure in the weight loss determinations.

Key:

Temperature:- This is the equilibrium temperature at which the weight loss determination was made.

Time :- The time of exposure of the sample to the elevated temperature.

Strength :- Measured on an arbitrary scale ranging from 1 (very frail) to 5 (strong as original foam).

Shrinkage :- L <30% volume loss

M 30-75% volume loss

H >75% volume loss

Cell Size :- Size of the predominant cell type

a <1mm

b 1-5mm

c >5mm

s indicates the formation of a compact shell of thickness approximately ½mm

If, by virtue of the existence of distinct zones, one cell size did not predominate throughout the sample, then both sizes are shown.

Melting :- m slight signs of softening

M indication of major softening

Table 3.11 : Foam A

Temperature °C	Time (min)	Strength	Shrinkage	Cell Size	Melting	Comment
160	7	5	L	a	-	no iridescence
	20	5	L	a	-	slightly brown
	60	5	L	a	-	light brown
	180	5	L	a	-	dark brown
200	7	5	L	a	-	micro cracking
	20	5	L	ab	-	" ", dark brown
	60	5	L	ab	m	cell walls breaking,
	180	5	L	ab	m	black
245	7	4	H	cs	M	strong brittle shell
	20	4	H	cs	M	" " "
	60	4	H	cs	M	" " "
	180	4	H	cs	M	" " "
290	7	1	M	cs	M	weak shell
	20	1	M	cs	M	
	60	1	M	cs	M	
	180	1	M	cs	M	
333	7	1	M	cs	M	
	20	1	M	cs	M	
	60	1	M	cs	M	
	180	1	M	cs	M	
360	7	1	L	s	M	shell only
	20	1	M	s	M	" "
	60	1	M	cs	M	flimsy filling
	180	1	H	cs	M	" "
400	7	1	L	s	M	
	20	1	M	s	M	
	60	1	H	cs	M	
	180	1	H	cs	M	

Table 3.12 : Foam B

Temperature °C	Time (min)	Strength	Shrinkage	Cell Size	Melting	Comment
160	7	5	L	a	–	
	20	5	L	a	–	light brown
	60	5	L	a	–	
	180	5	L	a	–	iridescent, dark brown
200	7	5	L	a	–	
	20	5	M	ab	m	
	60	5	M	ab	m	
	180	5	M	ab	m	black centre, brown mass
245	7	3	H	bc	M	red interior, thick skin
	20	2	H	bc	M	
	60	3	H	bc	M	black
	180	2	H	bc	M	
290	7	1	M	s	M	shell only
	20	1	M	bc	M	
	60	1	M	c	M	
	180	2	M	bc	M	
333	7	1	M	cs	M	
	20	1	M	cs	M	
	60	2	M	cs	M	
	180	3	M	cs	M	
360	7	1	L	s	M	
	20	1	L	bcs	M	soft golden filling
	60	1	M	bs	M	soft iridescent filling
	180	1	H	bs	M	" "
400	7	1	M	bs	M	very frail filling,
	20	1	M	bs	M	iridescent,
	60	1	H	bs	M	thin shell,
	180	1	H	bs	M	little remaining,

Table 3.13 : Foam C

Temperature °C	Time (min)	Strength	Shrinkage	Cell Size	Melting	Comment
160	7	5	L	a	–	yellow
	20	5	L	a	–	light brown
	60	5	L	a	–	light brown
	180	5	L	a	–	dark brown
200	7	5	L	a	–	
	20	5	M	b	m	orange centre
	60	5	M	b	m	reddish centre
	180	5	H	b	m	
245	7	3	H	c	M	dark red glassy interior
	20	2	M	cs	M	
	60	2	H	c	M	
	180	3	M	c	M	fragile black interior
290	7	1	L	c	M	
	20	1	L	c	M	
	60	2	M	c	M	
	180	1	M	c	M	
333	7	2	L	c	M	
	20	2	L	bc	M	
	60	3	M	b	M	
	180	3	H	bc	M	
360	7	1	L	bc	M	soft iridescent filling
	20	1	M	bc	M	" "
	60	1	M	bc	M	" "
	180	1	H	b	M	" "
400	7	1	M	b	–	iridescent filling
	20	1	M	bc	–	" "
	60	1	H	bc	–	" "
	180	1	H	b	–	dull grey interior

Table 3.14 : Foam D

Temperature °C	Time (min)	Strength	Shrinkage	Cell Size	Melting	Comment
160	7	5	L	a	–	
	20	5	L	a	–	just discolouring
	60	5	L	a	–	
	180	5	L	a	–	
200	7	5	L	a	–	light brown
	20	5	L	a	–	dark brown
	60	5	M	ab	m	brown & black, soft centre
	180	5	M	ab	m	"
245	7	4	M	ac	M	3mm wall, rest melted, black
	20	4	M	ac	M	" "
	60	4	M	ac	M	" "
	180	4	M	ac	M	" "
290	7	3	L	ac	M	thick cellular wall
	20	3	L	ac	M	"
	60	4	M	ac	M	"
	180	4	M	ac	M	"
333	7	3	L	b	M	1mm skin
	20	3	L	c	M	
	60	3	M	c	M	
	180	3	M	c	M	
360	7	3	L	bc	M	2mm skin, frail interior
	20	3	M	bc	M	" "
	60	2	M	bc	M	
	180	2	H	bc	M	small
400	7	3	L	c	M	
	20	2	M	c	M	
	60	1	H	c	m	
	180	1	H	b	m	very small

Table 3.15 : Foam E

Temperature °C	Time (min)	Strength	Shrinkage	Cell Size	Melting	Comment
160	7	5	L	a	–	sample cracking
	20	5	L	a	–	"
	60	5	L	a	–	" apart
	180	5	L	a	–	" "
200	7	4	L	a	–	many fissures, pale brown
	20	4	L	a	–	" light brown
	60	4	L	a	–	" brown
	180	4	L	a	–	" "
245	7	4	L	a	–	mid brown) cracks
	20	4	L	a	–	dark brown) breaking up
	60	4	L	a	–	gold/black) sample
	180	4	L	a	–	)
290	7	5	L	a	–	grey except centre, cracking
	20	5	L	a	–	
	60	5	L	a	–	
	180	5	L	a	–	
333	7	5	L	a	–	only minor cracks
	20	4	L	a	–	"
	60	4	L	a	–	"
	180	4	M	a	–	"
360	7	5	L	a	–	black and cracking
	20	5	L	a	–	" "
	60	4	M	a	–	no cracks, becoming friable
	180	3	H	a	–	" "
400	7	5	L	a	–	
	20	4	M	a	–	
	60	2	H	a	–	becoming friable
	180	1	H	a	–	very small

3.3.3 ACTIVITY OF CHARS

The following graphs (figures 3.11-3.18) record the the temperature rises when oxygen was passed over the heated chars as described in section 2.4.3

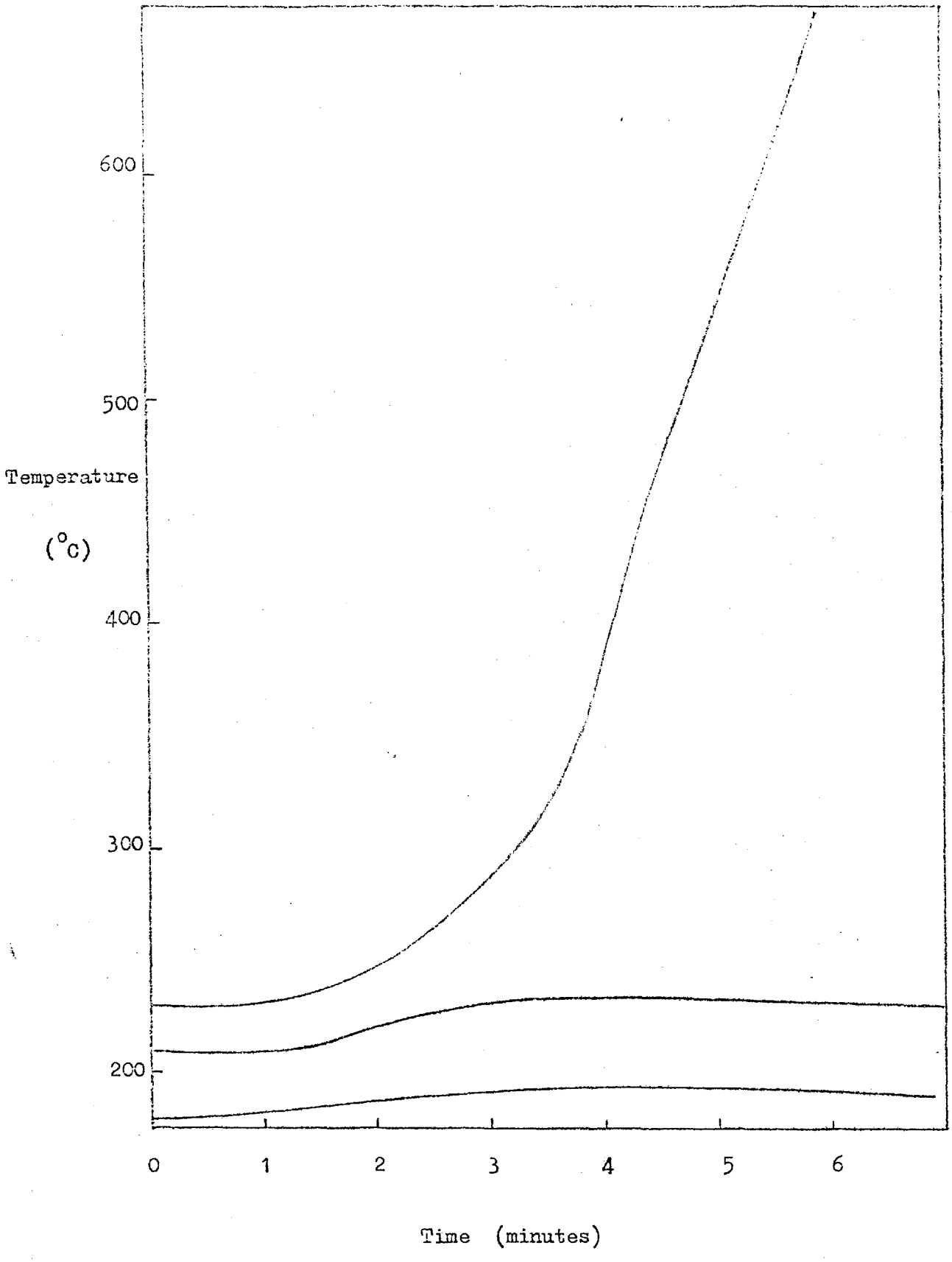

Figure 3.11 ; Char activity - Foam A, char from radiant panel.

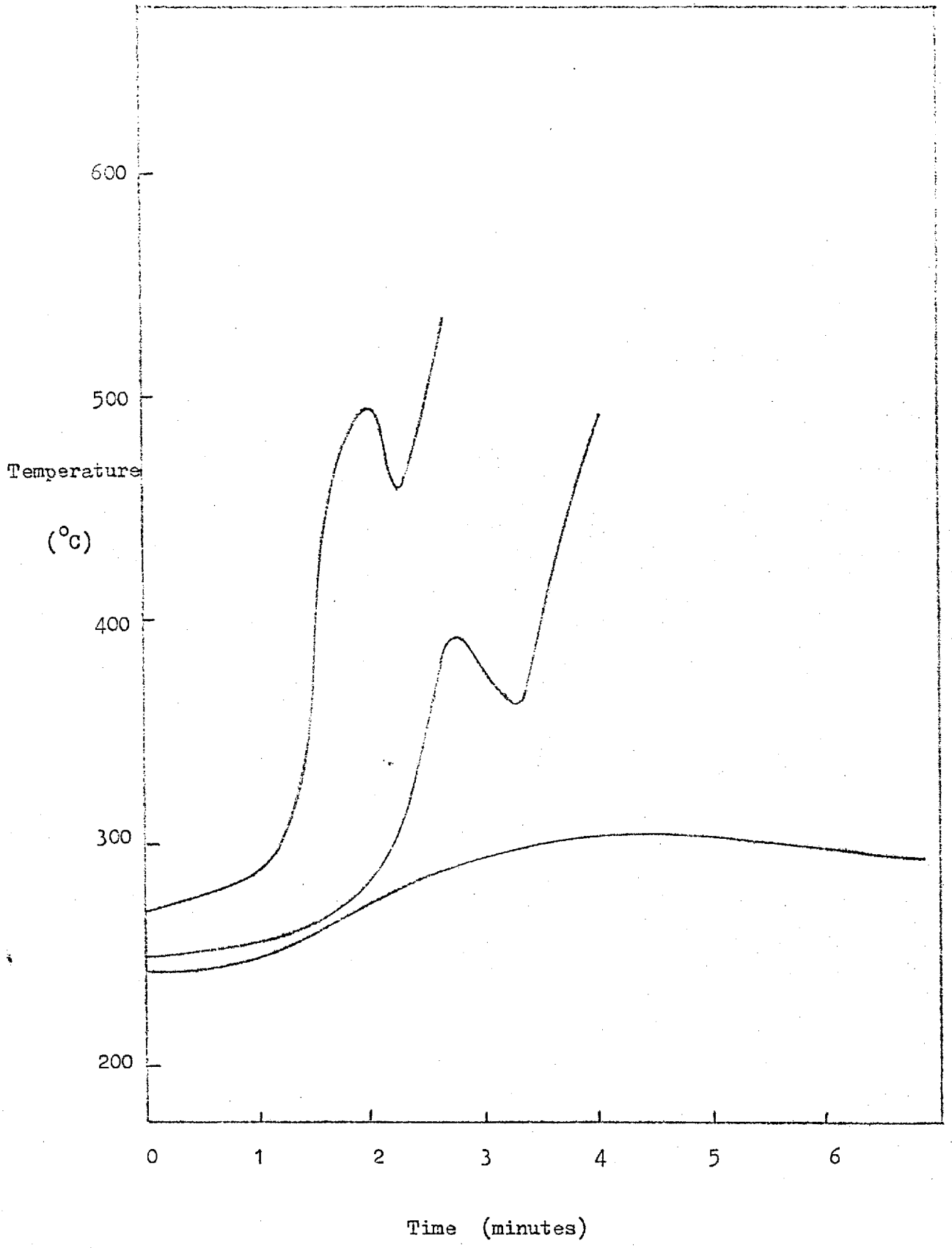

Figure 3.12 ; Char activity - Foam A, char from weight loss furnace.

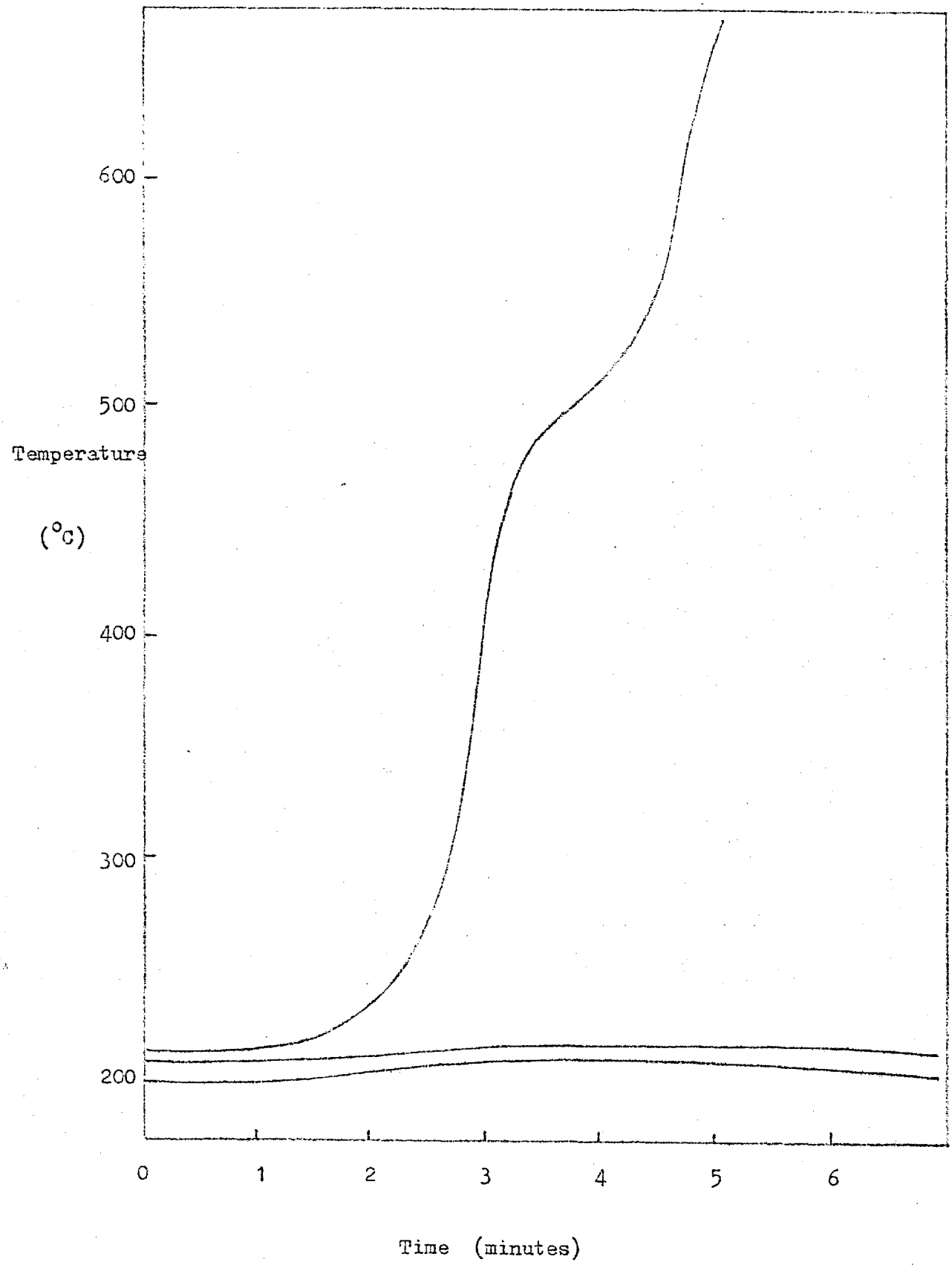

Figure 3.13 ; Char activity - Foam B, char from radiant panel.

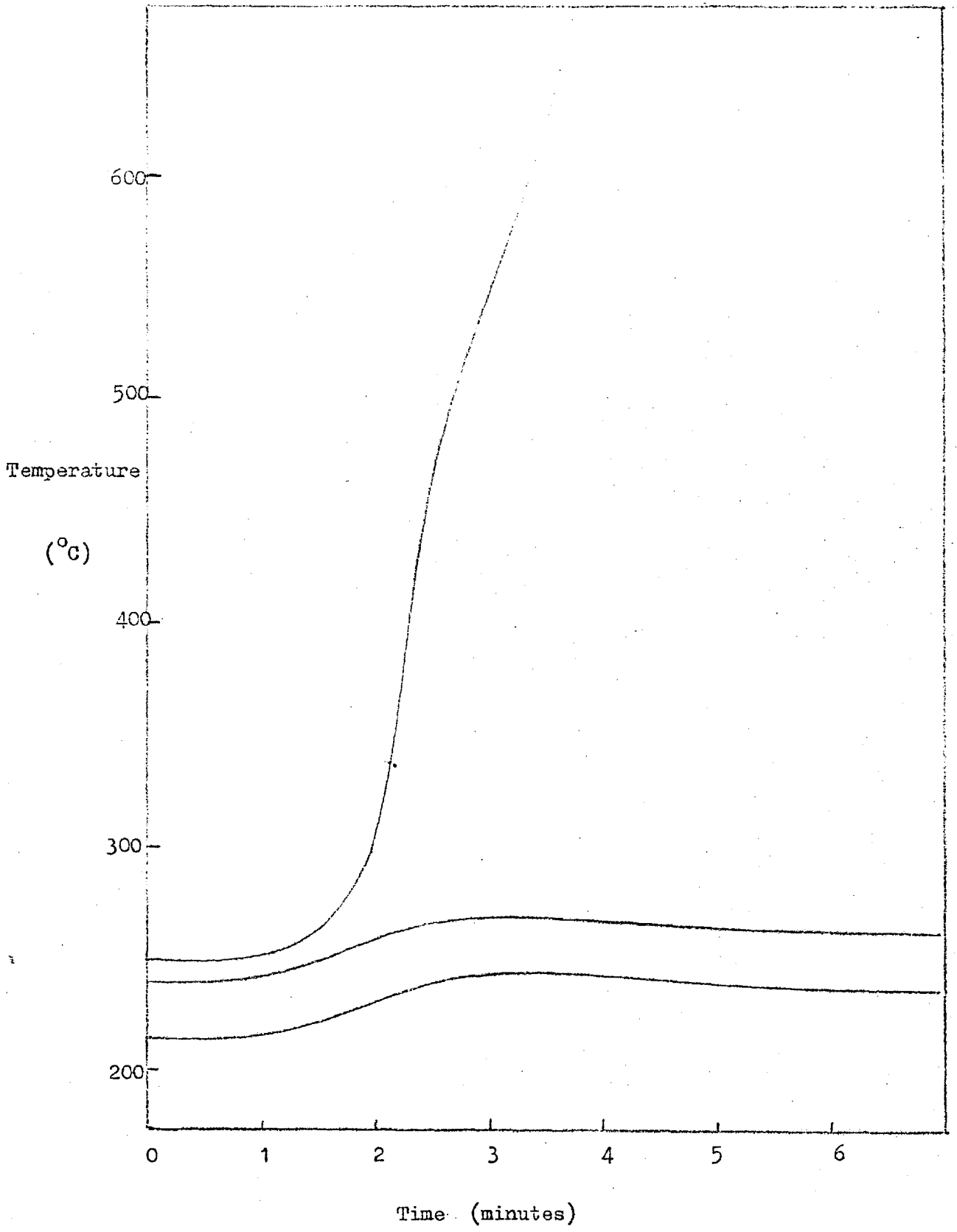

Figure 3.14 ; Char activity - Foam C, char from radiant panel.

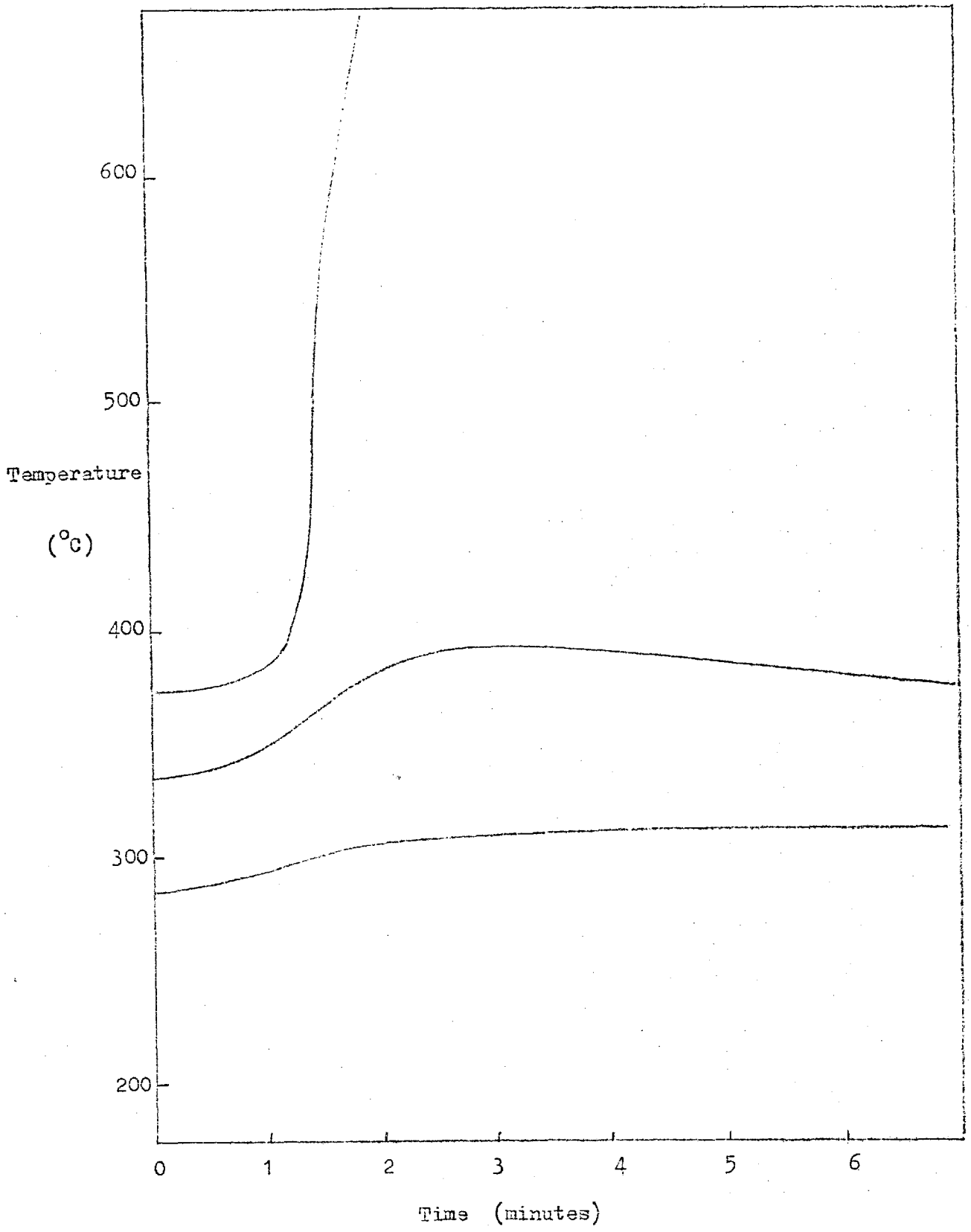

Figure 3.15 ; Char activity - Foam C, interior of char from weight loss furnace.

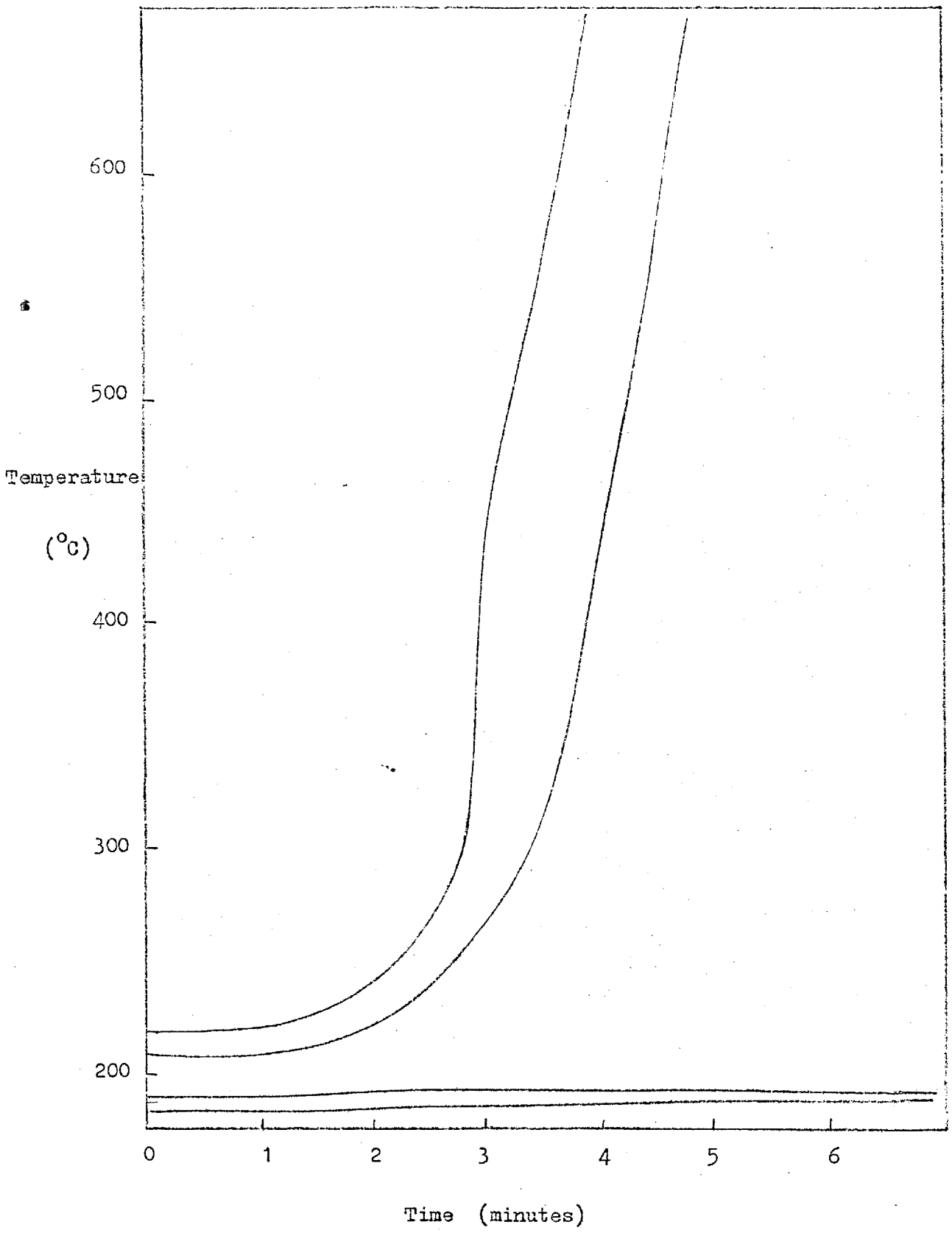

Figure 3.16 ; Char activity - Foam D, char from radiant panel.

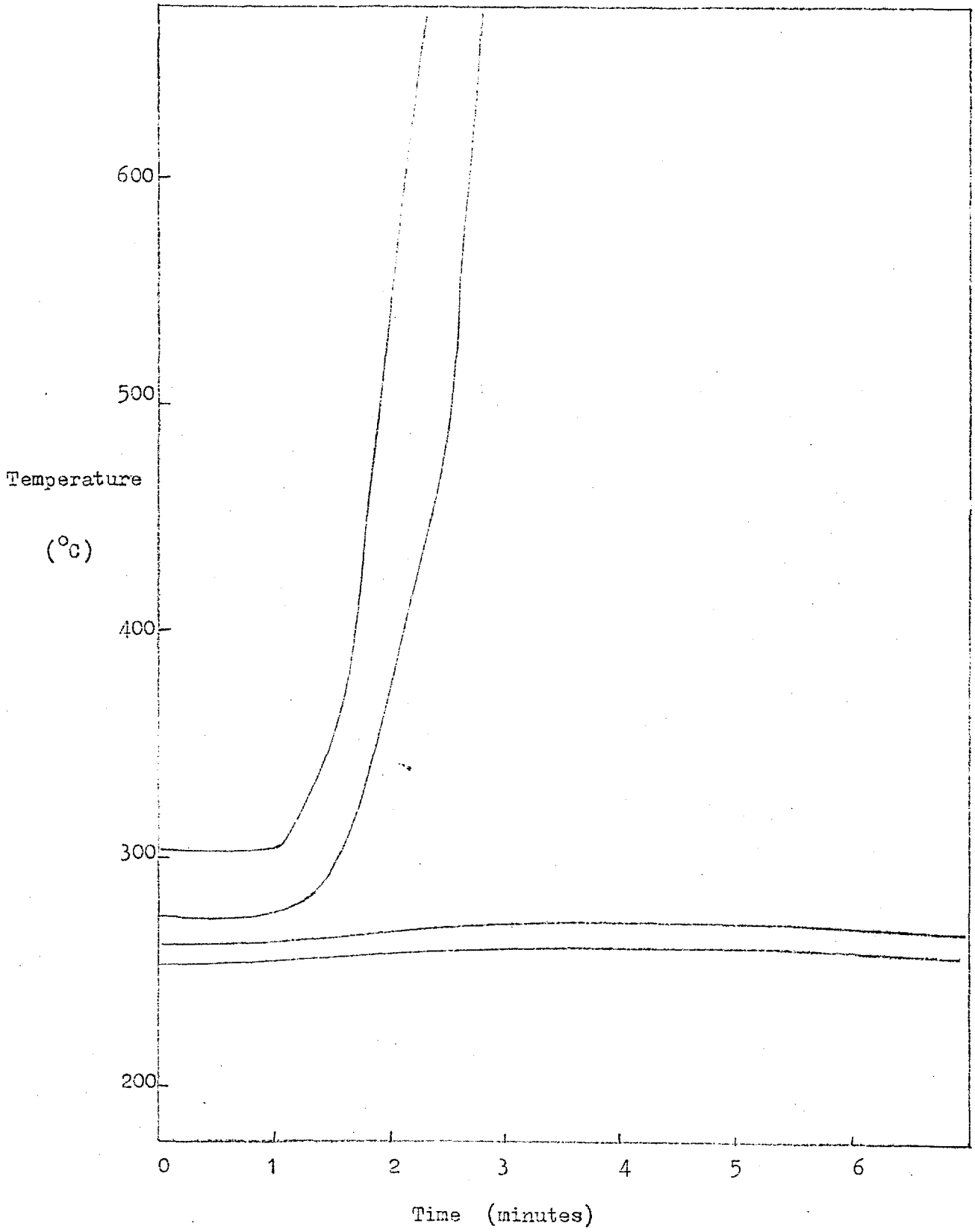

Figure 3.17 ; Char activity - Foam E, char from radiant panel.

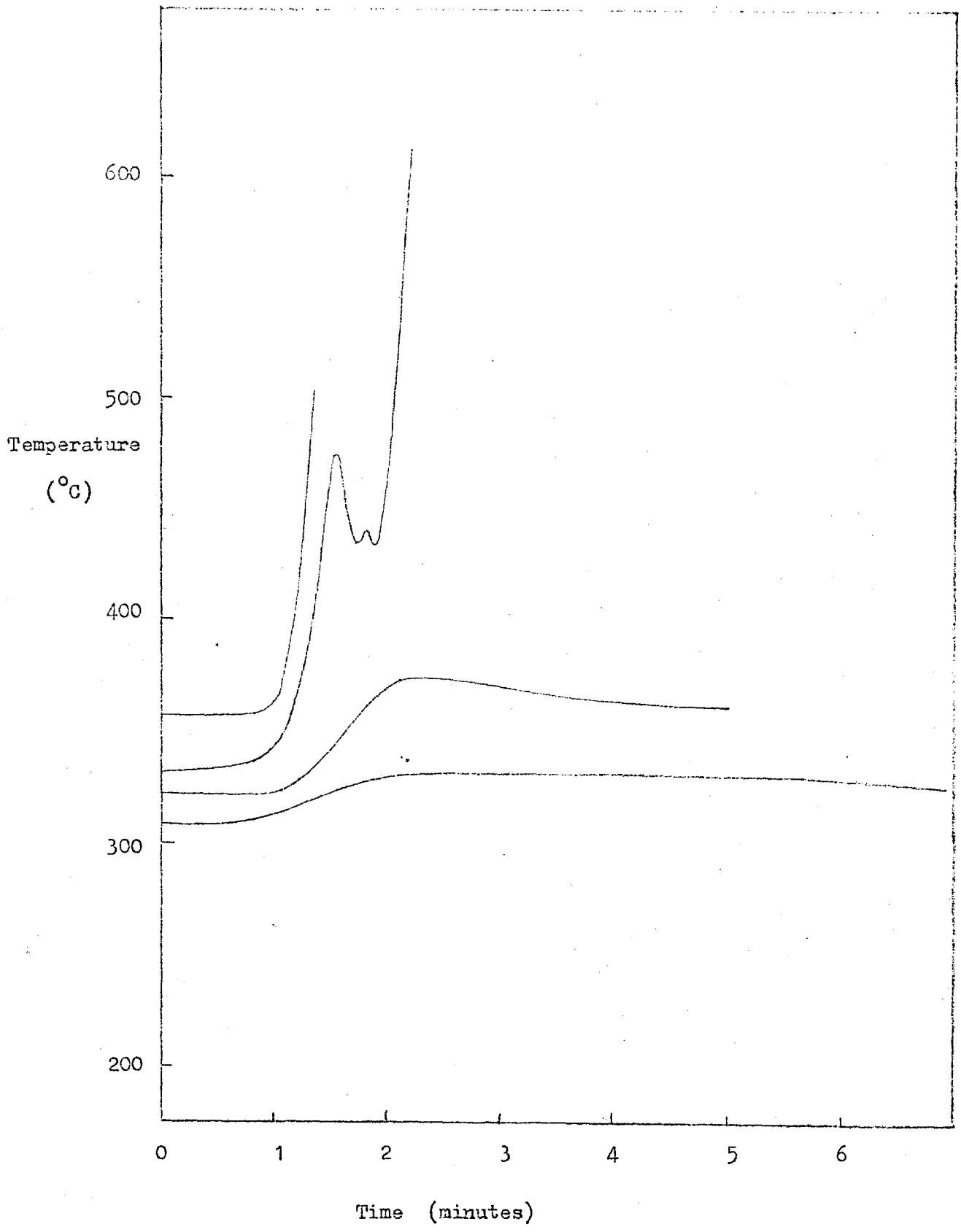

Figure 3.18 : Char activity – Foam E, char from weight loss furnace.

3.4 DIFFERENTIAL THERMAL ANALYSIS

Figures 3.19 - 3.21 are the thermograms for Foams A-E, the additional foams formulated (F1-F5) and for some of the raw materials used in urethane foams.

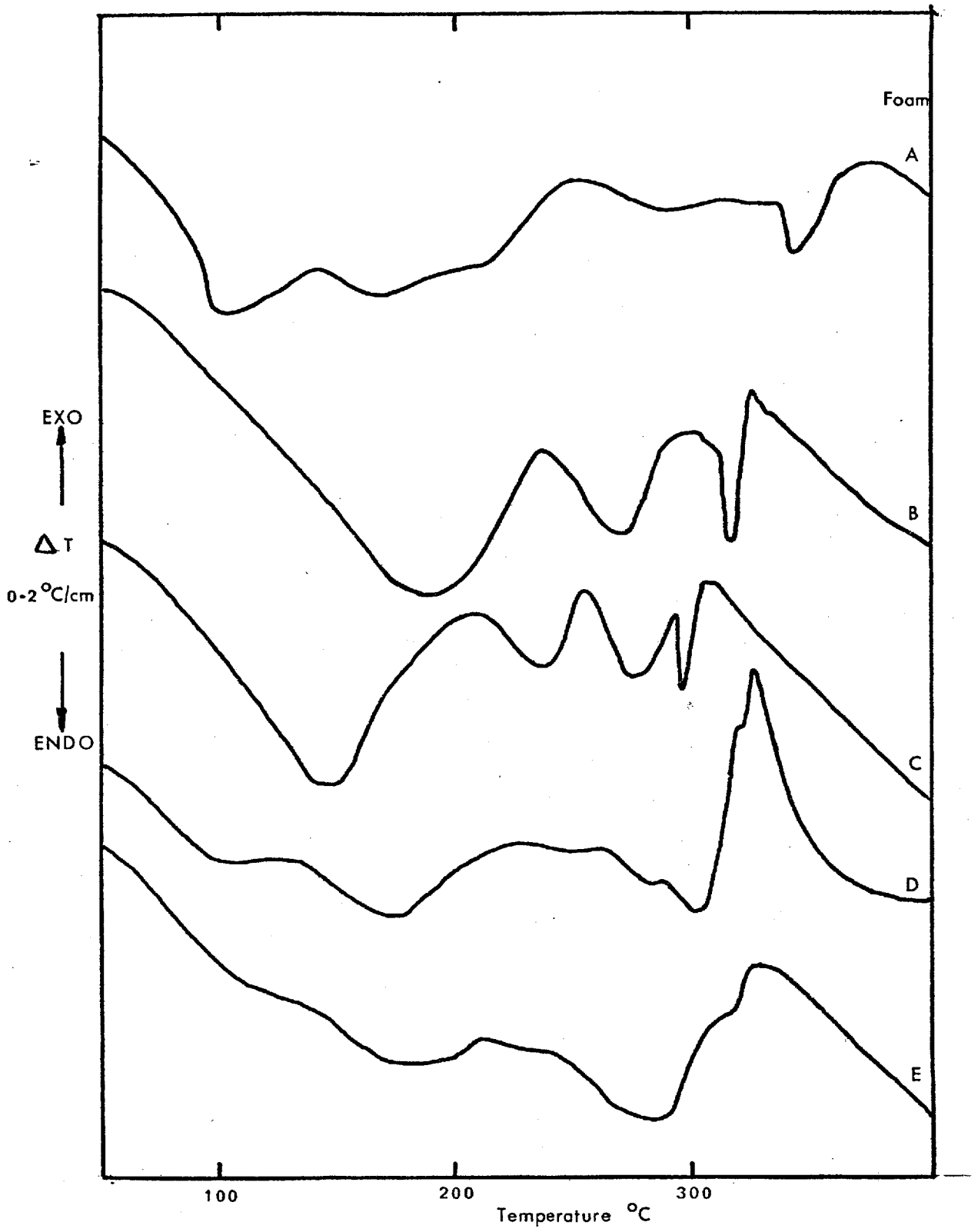

Figure 3.19 : Differential Thermal Analyses, Foams A–E

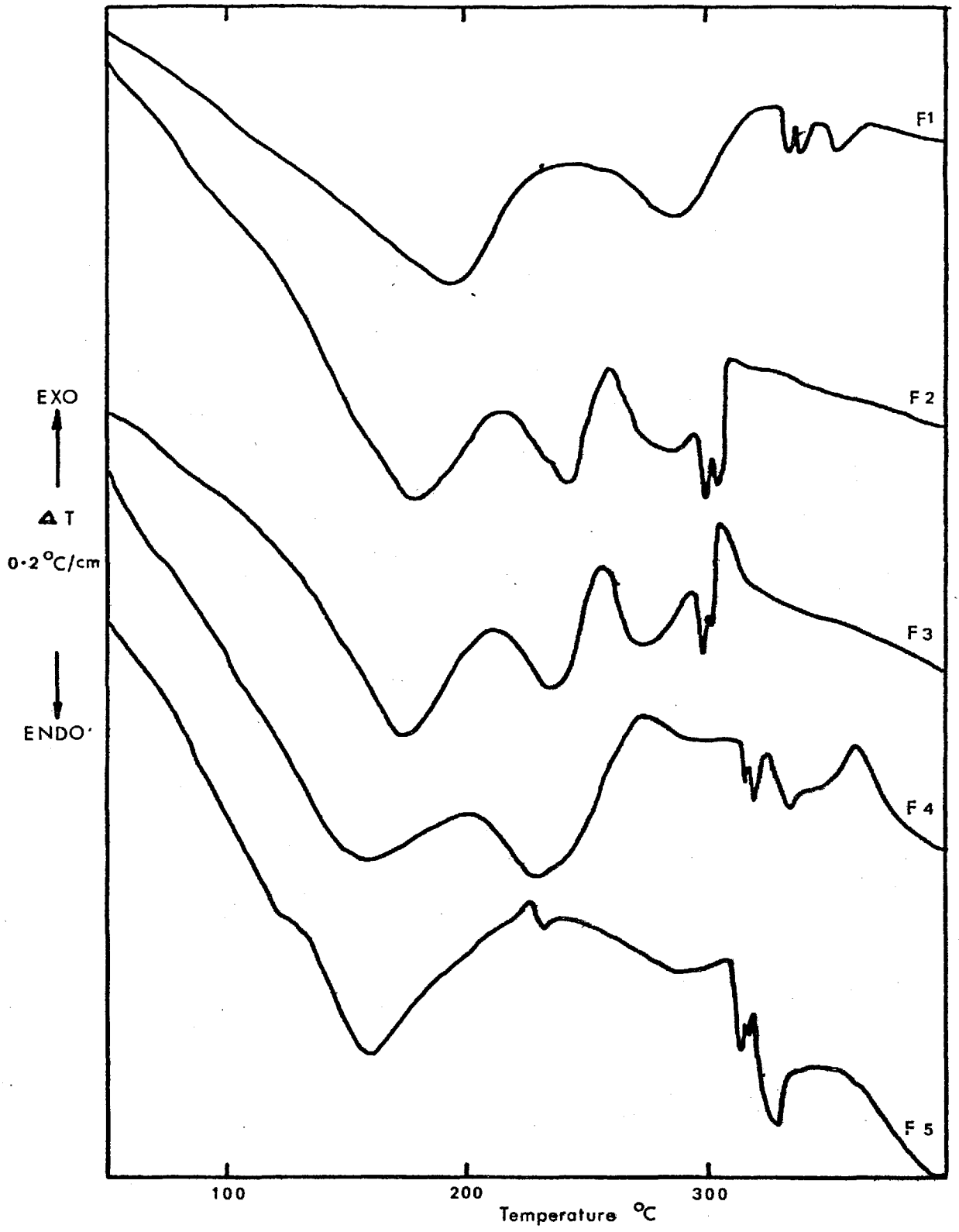

Figure 3.20 : Differential Thermal Analyses,
Foams F1-F5

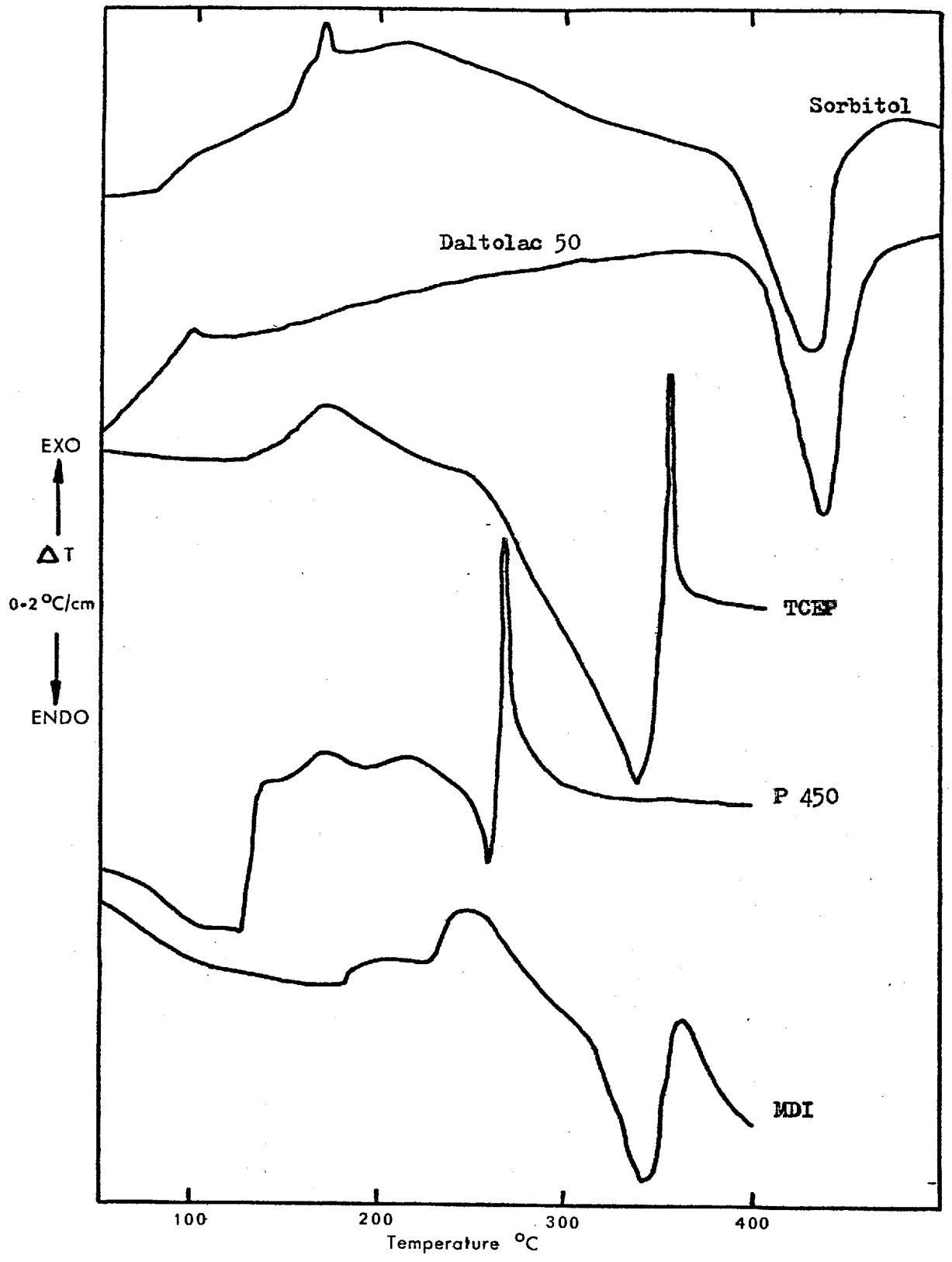

Figure 3.21 : Differential Thermal Analyses, raw materials

3.5 PYROLYSIS PRODUCTS

3.5.1 Chromatography

As noted in the experimental section positive identification of samples was not possible with the apparatus used. It was, however, possible to make some useful observations. No output signal was produced when the gaseous products were introduced into the column either directly from the pyrolyser or by injection through the septum. Concentration of the decomposition products by solution in various organic liquids did not enable analyses to be made.

3.5.2 Chloride determination

In this test all the foams gave similar results. The aqueous extract of the pyrolysis products was of a pale yellow-green colour, and it reduced silver nitrate solution to give a black precipitate of silver, in some cases leaving a liquor that gradually turned pink. The test for chloride ions produced positive results, although in the case of foams A and D the solution went turbid but did not throw down a heavy precipitate as did the others. Universal papers showed the pH to be approximately 7.

3.5.3 Mass Spectrometry

3.5.3.1 Table 3.16 shows the peaks produced on analysis of the pyrolysis products of the foams. The output signal was weak unless noted with m (medium) or s (strong).

Samples of foams A and B were also pyrolysed at temperatures of 200°C and 160°C. The resulting mass spectrographs of the gaseous products did not vary significantly from those at 250°C.

3.5.3.2 The charred foam samples remaining after pyrolysis at 250°C were inspected and the observations are recorded below.

Foam A : Sample had shrunk to ½ original size and a hard cellular reddish char resulted.

Foam B : Behaviour similar to Foam A, but exterior of sample was of a darker colour.

Foam C : Much shrinkage. The strong reddish char exhibited signs of melting.

Table 3.16 : Summary of mass spectrograms

Temperature of pyrolysis :- 250°C

FOAM A	FOAM B	FOAM C	FOAM D	FOAM E	Background
14	14	14	14 s	14	14
			15		
16 m	16 s	16 m	16 m	16	16
17	17		17		17
18 m	18 m	18	18 m	18	18
20	20		20	20	
22	22	22	22		
26		26	26		
27 m	27	27 m	27	27	
	27½		27½	27½	
28 ss	28 ss	28 ss	28 ss	28 ss	28 s
29 m	29 m	29	29 m	29 m	
31	31	31	31 m	31 m	
32 ss	32 ss	32 ss	32 ss	32 ss	32 s
			34		
35 m	35 m	35 m	35 m	35 m	
36 m	36 m	36 m	36 s	36 m	36
37	37	37	37 m	37	
38	38	38	38 m	38	38
			39		
40 m	40 m	40	40 s	40 m	40
		41	41	41	
		42	42		
		43	43		
44 s	44 s	44 s	44 ss	44 s	44 s
45	45	45	45		
46	46	46			
47	47	47	47 m	47	
49	49	49 m	49 m	49	
		50	50		
50½	50½	50½	50½	50½	
		51			
51½		51½	51½	51½	
			52		
			58½		
		61			
62 m	62	62 m		62	
63		63		63	
64		64			
66 m	66	66 m	66 m	66 m	
			67		
68	68	68	68	68	
82	82	82	82	82	
84	84	84	84	84	
86	86	86	86	86	
		98	91		
		100	100		
101 s	101 s	101 s	101 s	101 s	
103 s	103 s	103 s	103 s	103 s	
			104		
105 m	105 m	105 m	105 m	105 m	
117	117	117	117 m	117	
119	119	119	119 m	119	
	121		121		

Foam D : The black char was approximately half the size of the original sample.

Foam E : The sample split along several approximately longitudinal places, but only discoloured slightly.

4 DISCUSSION

4.1 HEAT PENETRATION

4.1.1 The temperature histories of axial points of cylindrical samples, the ends of which were exposed to thermal radiation of intensity 4.2kW m^{-2} are shown in figures 3.1-3.5. The shapes of the curves are in general agreement with predictions - the nearer an element was to the heat source, the more quickly was its equilibrium temperature attained. The temperature decreased with distance from the heated face and after 15 minutes the gradient was tending to a constant value as exists in steady state equilibrium.

The heat flux into the end of the sample has the form of a step function and the response to this is governed by the nature of the foam which has a finite value of conductivity and a thermal capacity and so absorbs heat as its temperature rises. The effect of this is to introduce a time delay and to change the step function to a sigmoid, the flatness of which depends on the distance from the heated face and which is asymptotic to the equilibrium temperature. As the face distant from the heated one is not perfectly insulated the equilibrium condition will not be uniform temperature throughout but there will be a constant gradient and a heat flux through the sample.

The temperature measured by the shielded thermocouple at the surface is that of the evolved materials expelled as the foam decomposes. When such evolution has ceased it is a measure of the air temperature in this region.

4.1.2 The temperature-time histories show deviations from theoretical profiles which must be explained in terms of the nature and behaviour of the materials.

Rigid polyurethane foams of low density are composed mostly of the blowing agent with only a matrix of polymer to form the cells that hold the gas. Assuming a density of 6 kg m^{-3} for the gas and 1000 kg m^{-3}

for the solid, it can be shown that the volume of solid in a 30 kg m^{-3} foam is only 2½% of the total volume. Thus the foams under investigation consist of thin walled cells of diameter ½ to 1½mm filled with vaporised trichlorofluoromethane. It is readily appreciated that conduction through a solid cannot be strictly applied to such a material. The gas in the cells will not remain stationary within the cell and there will be flux due to convective transfer. In order to effect any heat transfer between the cell walls and the gas there must be a temperature difference between them, which requires the existence of an associated transfer coefficient. Heat can also be transferred by conduction around the cell walls, and by radiation from one side and absorption by another.

When a sample of foam is exposed to thermal radiation the surface absorbs energy and is heated. A temperature gradient then exists between the surface and the interior of the sample causing heat flux into the sample which heats the material. As the temperature of an element rises it reaches the softening temperature of the polymer and cell walls become more readily deformable. At this temperature there are probably also reactions occurring in the polymer, modifying the chemical structure. The nature of these reactions depends on the availability of oxygen, whether the element is near the surface or not, and the time taken to reach the temperature, among other factors. One result of these reactions is to make the cell membranes permeable. Some of these reactions involve fragmentation resulting in short chain molecules being evolved. The volume of the gaseous products is greater than the voids in the form so the gases must be emitted from the interior. The path of least resistance is through the heated section of the foam where reactions have already weakened if not perforated the cell walls. Depending on whether the reactions are exothermic or endothermic and to what degree, the element under consideration will be further heated or not, and the gaseous products on their way to the surface will be heated or cooled by contact with the cell surfaces upon which further reactions may occur. Thus the temperature and nature of the materials upon emergence at the surface

depend upon any number of factors, not least among which are the temperature of the reacting foam that produced it, the temperature of the intervening foam, and the duration of the passage.

The 'surface' temperatures shown in figures 3.1-3.5 all rise in the first minute to a value over 200°C, and after a few minutes variation settle to a value near 220°C. The steady lower value for Foam B is probably due to poor positioning of the shielded thermocouple at too great a distance from the sample and the failure to ensure that the thermocouple was cleaned of all deposits from earlier experiments which would tend to insulate the thermocouple. Foam E is exceptional in its behaviour - the higher surface temperature of 260°C means that the decomposition products are hotter which indicates that the fragmentation reaction for the isocyanurate ring occurs at a higher temperature than the corresponding breakdown in conventional urethanes. When the heated portion has decomposed the flow of materials out of the surface abates, and the surface thermocouple merely measures the ambient temperature. As the foam softens and chars there is often accompanying contraction as surface tension plays its part, and the heated surface recedes from its original position and the thermocouple. This is the major cause of the fall in surface temperature after a few minutes exposure.

Comparison of the graphs for each of the materials tested shows little difference between foams A, B, C and D. The differences in final temperature reached at each depth are attributed to variations in the positioning of the thermocouples and the resulting error in the distance from the heated face, with the exception of those recorded at a depth of 40mm. In foams B and C the temperatures are significantly higher at 40mm, and it is also seen that the gradient at 30mm is higher in these two samples than in either foam A or D, although the other curves are comparable. Review of the components of the foams shows that foams B and C are the only two of the polyurethanes containing the fire retardant additive TCEP. This is a viscous liquid boiling at approximately 220°C

under atmospheric pressure. A material such as this in a foam could enhance the process of heat transfer by a "fluxing" process. As the foam is heated the TCEP vaporises and permeates down the concentration gradient into a cooler part of the foam where it then condenses, releasing its considerable latent heat of vaporisation. Thus the temperature at a depth inside the foam is raised more quickly, and even to a higher value than it would be without the addition of a volatile flame inhibitor. The effect of this process is not reflected in the temperatures near the surface as these elements undergo rapid heating by conduction from the high temperature surface.

The behaviour of foam E reflects the differing basic nature of the isocyanurate based foams. The initial temperature rise is of the same rapid rate as the other materials but where as in these the exothermic chemical reactions raise the temperatures quickly to their final values, the decomposition of the isocyanurate foam proceeds more slowly at a higher temperature, thus delaying the attainment of final temperatures. The slow decomposition is evidenced by the continuing issue of volatile materials, albeit as a thin stream, long after the other materials appear inert. The high degree of cross-linking in isocyanurate foams gives a high softening temperature that is not reached before decomposition. As the char does not suffer amalgamation of cells but retains the basic cell geometry of the original material the thermal conductivity does not rise as a result of the increased convection, and the volatiles being evolved come into more intimate contact with the char, providing effective heat transfer to cool the hotter zones and delay the rise to maximum temperatures. Cracks are produced in the surface by thermal stress and as the exposure continues these fissures become wider and deeper, allowing the radiation to penetrate deeper into the sample. As a result of this the temperatures continue to rise long after the other foams have reached a steady state. Although it is suggested that foam E may contain TCEP it is not possible in these curves to find positive confirmation as

there are other factors of greater influence.

It is seen that the temperatures inside the foam soom rose above that at the surface, which indicates that the radiant panel was not the sole source of heat even if the diathermancy of the foam was not negligible. It is possible that exothermic reactions occurred as the foam was heated, which could raise the temperature, but the effect is seen to have transcended the decomposition period, which near the surface was less than one minute, and was maintained in the charred foam. Alternatively, the source of heat could have been oxidation of the char by oxygen that diffused in through the surface of the sample. As the sample charred there was shrinkage at the exposed face which caused a gap between the sample and the glass holder which provided additional surface for the oxygen to diffuse through. If the reaction was controlled by the rate of diffusion of oxygen this could explain the apparently slow reaction and the steady high temperatures.

4.1.3 Diffusivity

a) From the temperature histories shown in figures 3.1-3.5 the values of the thermal conductivities recorded in Section 3.1 were calculated as follows:

Consider an opaque isotropic semi-infinite solid at zero initial temperature, the surface temperature of which is f(t). The temperature at any point is given by

$$v = \frac{2}{\sqrt{\pi}} \int_{\frac{x}{2\sqrt{\alpha t}}}^{\infty} f\left(t - \frac{x^2}{4\alpha\mu^2}\right) e^{-\mu^2} \, d\mu \qquad \ldots\ldots\ldots(1)$$

where v – temperature
t – time
x – distance from face
α – thermal diffusivity

If $f(t) = kt^{\frac{1}{2}n}$, (k = constant),

$$v = k\Gamma\left(\tfrac{1}{2}n + 1\right)(4t)^{\frac{1}{2}n} \; i^n \operatorname{erfc}\left(\frac{x}{2\sqrt{\alpha t}}\right) \qquad \ldots\ldots\ldots(2)$$

When the surface is held at a constant temperature then n=o and

$$v = k\ \mathrm{erfc}\left(\frac{x}{2\sqrt{\alpha t}}\right) \qquad \ldots\ldots\ldots(3)$$

Thus after time t the temperatures at x_1 and x_2 are given by

$$v_1 = k\ \mathrm{erfc}\left(\frac{x_1}{2\sqrt{\alpha t}}\right) \qquad \ldots\ldots\ldots(4)$$

$$v_2 = k\ \mathrm{erfc}\left(\frac{x_2}{2\sqrt{\alpha t}}\right) \qquad \ldots\ldots\ldots(5)$$

$$\therefore \quad \frac{v_1}{v_2} = \frac{\mathrm{erfc}\left(\frac{x_1}{2\sqrt{\alpha t}}\right)}{\mathrm{erfc}\left(\frac{x_2}{2\sqrt{\alpha t}}\right)} \qquad \ldots\ldots\ldots(6)$$

or

$$\frac{v_1}{v_2} = \frac{\mathrm{erfc}(a)}{\mathrm{erfc}\left(a\frac{x_2}{x_1}\right)} \quad \ldots\ldots(7) \quad \text{where} \quad a = \frac{x_1}{2\sqrt{\alpha t}}$$

$\frac{v_1}{v_2}$ and $\frac{x_2}{x_1}$ are known from measurements and it is desired to find the value of a.

A log-log plot of erfc(y) against y is drawn.

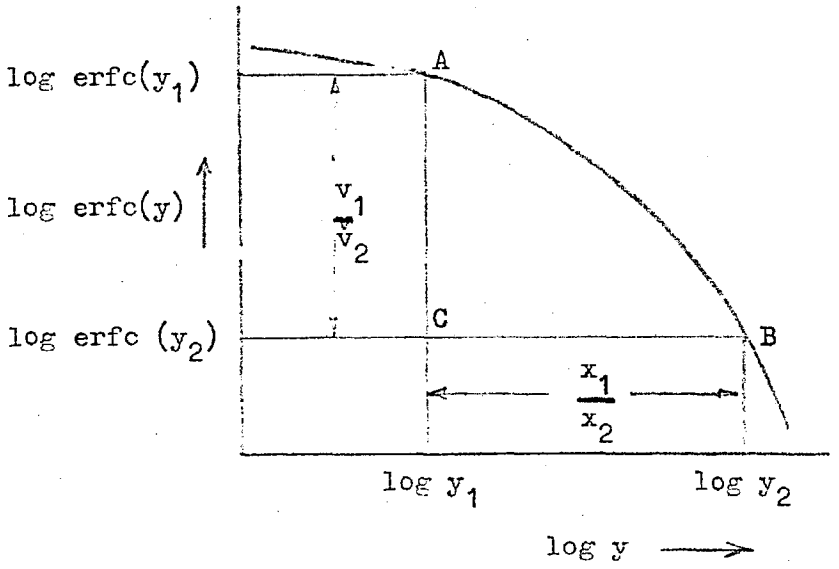

$$\log \mathrm{erfc}(y_1) - \log \mathrm{erfc}(y_2) = \log \frac{\mathrm{erfc}(y_1)}{\mathrm{erfc}(y_2)}$$

but $y_1 = a$ and $y_2 = a\frac{x_2}{x_1}$

so $$AC = \log \frac{\mathrm{erfc}(a)}{\mathrm{erfc}\left(a\frac{x_2}{x_1}\right)} = \log\left(\frac{v_1}{v_2}\right)$$

Also $\log y_2 - \log y_1 = \log \left(\frac{y_2}{y_1}\right)$

so $$BC = \log \frac{a\frac{x_2}{x_1}}{a} = \log \frac{x_2}{x_1}$$

The positions of A and B are found by trial and a value of y_1 is read off. $$y_1 = \frac{x_1}{2\sqrt{\alpha t}}$$

$$\therefore \alpha = \frac{1}{t}\left(\frac{x_1}{2\ y_1}\right)^2 \qquad \text{.....(8)}$$

b) The average values of the diffusivity for each of the foams and values for some common building materials [12] are shown in table 4.1.

Table 4.1 : Thermal Diffusivity

Material	Thermal Diffusivity $m^2s^{-1} \times 10^{-6}$
Foam A	0.86
Foam B	0.91
Foam C	0.78
Foam D	0.78
Foam E	1.01 *
Air	18.7
Crown glass	0.58
Concrete	0.42
Brick	0.38
Ground cork	0.14
Wood (spruce, with grain)	0.45
Wood (spruce, across grain)	0.24

* Average excluding those values over 2×10^{-6}

The thermal diffusivity, $\alpha = \frac{\lambda}{\rho C_p}$

where λ – thermal conductivity

ρ – density

C_p – specific heat at constant pressure.

Thus ρC_p is the specific heat per unit volume and $\frac{\lambda}{\rho C_p}$ represents the ratio of heat transmitted to heat absorbed in the conducting medium. As such it is a measure of the insulating ability, by volume, of a material : a lower value of α means that a smaller proportion of the incident heat is transmitted.

The thermal diffusivity of the urethane foams is seen to be about 2 to 3 times that of other common insulating materials, but when it is considered that the other materials contain 10 to 60 times the mass in an equivalent volume the urethane foams stand out as excellent insulators.

4.2 SPONTANEOUS IGNITION

4.2.1 The observations made in the preliminary experiments are recorded in Section 3.2.1. From these it is seen that ignition did not occur when the intensity of radiation was less than 8.4kW m^{-2}. The ignition temperature as measured by a shielded thermocouple at the surface is similar for all the urethane foams and does not change significantly with intensity. The isocyanurate based material exhibits a much higher ignition temperature. The time to ignition decreased as the intensity increased but as the time was generally less than 5 seconds the accuracy of the measurements is not high. Figure 4.1 shows the relationship between the intensity and the ignition time. The dog leg in the curve for foam A was probably accentuated by experimental errors, but it does indicate that at higher intensities of radiation the factor limiting ignition is likely to be of a physical nature, eg mixing, or time to project material from the solid, and not the radiant intensity.

In these experiments the gaseous products of decomposition discharged from the heated face in streams which were drawn into the furnace where high temperatures prevailed in the vicinity of the red hot elements. When heated in this way the volatiles ignited and flame flashed back to the surface of the sample where it was sustained by the evolving stream. A low intensity of radiation caused only slow decomposition so the heat output from the subsequent combustion of the decomposition products was not sufficient to cause further decomposition outside the irradiated area, as evidenced by the lack of spread of flame beyond the irradiated area and the extinction of the flame when the radiative source was removed. The lack of ignition at 6.3 kW m^{-2} was due to the failure of the volatiles to reach the interior of the furnace in sufficient quantity to form a flammable mixture. The foams did decompose but the rate of reaction was not high enough to produce the necessary concentration for ignition. If the intensity was increased beyond 16 kW m^{-2} the time to ignition would not decrease continuously as the limiting factor appears to be the production of volatiles for projection into the furnace. This is governed by heat penetration into the surface layer of foam, but at

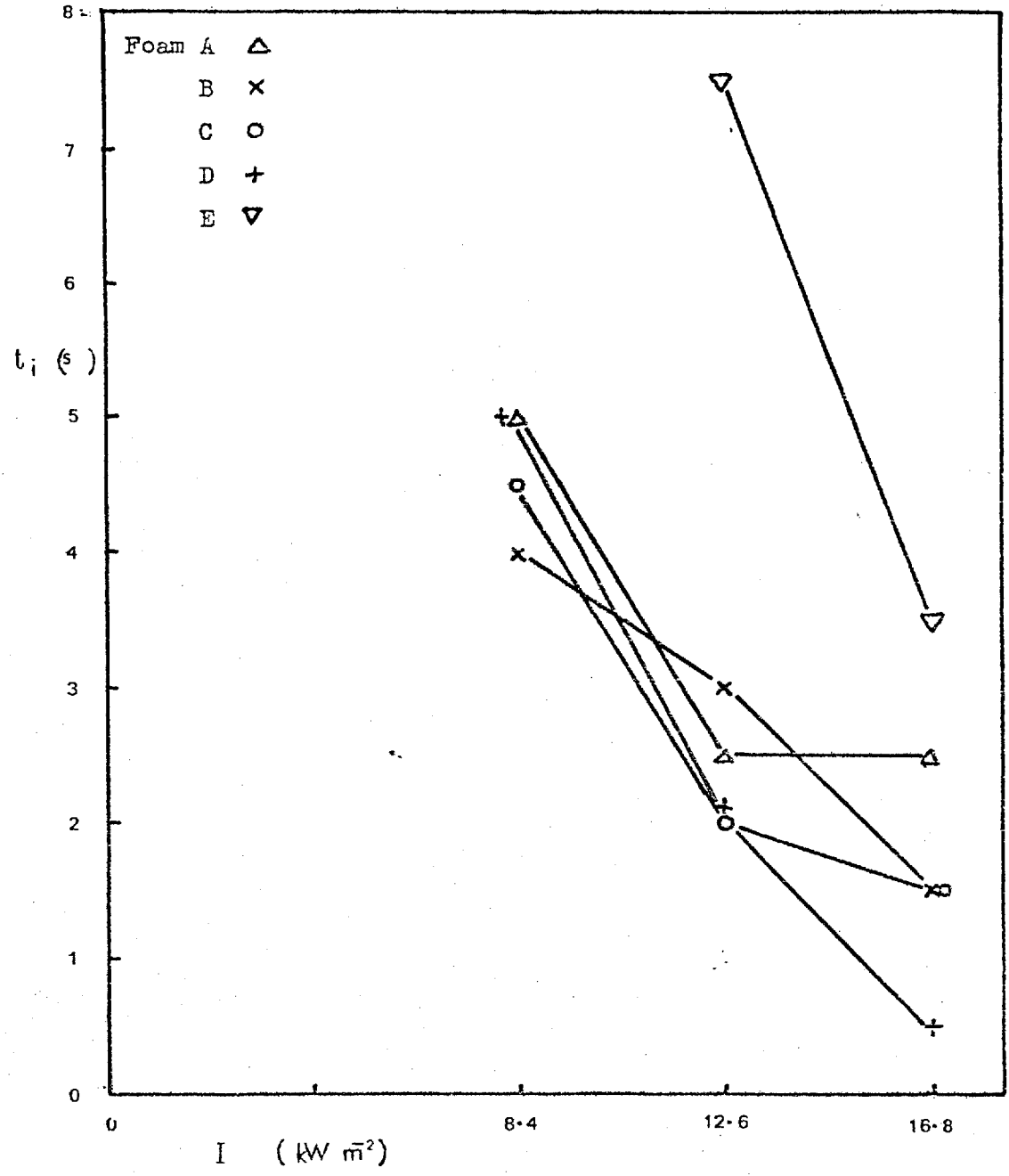

Figure 4.1 ; Ignition time versus incident radiant intensity.

high intensities the decomposition temperature is reached almost instantaneously so the only time delay is that needed to produce the volatile matter and transport it to the hot furnace.

The conditions of these experiments are similar to those employed when studies of pilot ignition are made [13] in as much as there is an external source of ignition independent of the material. This situation has significance in practical situations. At the scene of a fire the fuels are heated both by radiation from the flames and by the hot atmosphere before the flames reach the fuel. Thus decomposition of a material commences before it is directly involved in the fire and if the products of decomposition are volatile they will be mixed with the atmosphere and carried to the flame where they can provide further fuel or alternatively produce a flammable atmosphere capable of propagating flame to points remote from the seat of the fire.

4.2.2 The observations recorded in Section 3.2.2 were made with a positive pressure of nitrogen in the furnace which prevented the convective draught into the furnace aperture. This effectively delayed ignition until a much higher intensity was employed. At an intensity of 16.8 kW m^{-2} the samples underwent considerable decomposition but the evolved volatiles were swept upwards by the convective current set up at the heated face and did not enter the furnace.

When the intensity was increased to 21 kW m^{-2} there was violent eruption of streams of volatile material from the heated face and some of these entered the furnace aperture upon which ignition occurred. The polyurethane foams all burned with a very sooty flame but this did not spread beyond the front face and top of the sample. There was extensive combustion but eventually sufficient char built up to give protection to the rear of the sample. Foams B and C containing TCEP showed emission of streams of materials as Foam A, but ignition was delayed. This could be due to the boiling out of the fire retardant additive with the decomposition products as it could prevent them supporting a flame. Further decomposition

would then produce a volatile stream not so protected by TCEP. The slow spread of flame over the face of Foam D indicates that the incorporation of a phosphorylated polyol had altered the kineticparameters of decomposition as combustible products were not produced so rapidly when the foam was subjected to the lower intensity of the flame radiation. Fracture of the surface cells as a result of thermal shock threw small particles of foam up from the surface and the resulting combustion of these was responsible for the flash of non-sustained flame all over the sample [17]. The isocyanurate-based foam E is particularly susceptible to this behaviour, as is evidenced by observations made in the weight loss experiments. The thermal stresses made the sample surfaces crack audibly, and at low temperatures when charring was slight, these cracks extended until the sample was reduced to several pieces.

On increasing the intensity to 25.2 kW m^{-2} the TCEP was seen to produce only a marginal increase in ignition time and subsequent behaviour of Foams A, B and C show no significant differences. When a char was formed on the surface of Foam D the flame was extinguished except where the sample was irradiated as elsewhere insufficient combustible products were being evolved.

The isocyanurate based sample, Foam E, did not ignite until it was subjected to 25.2 kW m^{-2} and even then the scale of combustion was minor compared with the other samples.

When the sample of foam undergoes decomposition volatile products are evolved from the heated face, but whatever their temperature they cannot ignite as they have no oxygen content. This has to be provided by mixing with the surrounding atmosphere. The convective current at the heated face sweeps the gas stream upwards as it mixes, out of the irradiated volume and into cooler regions where it loses heat. As the atmosphere that dilutes the stream is cooler than the stream this also reduces the temperature. Spontaneous ignition occurs when the mixture comes within the flammable limits and at the same time has reached the

ignition temperature. In these experiments some of the gas stream, diluted with entrained air, is expelled into the furnace where it receives the additional heat required to raise it to its ignition temperature. The flame propagates back to the sample where the exothermic combustion provides the energy to sustain the reaction.

4.2.3 Table 4.2 [14] shows the practical effects of various intensities of radiation.

Table 4.2 : Effects of radiant heat

Effect	Intensity, kW m^{-2}
Summer sunshine in England	0.67
Causes pain in 3s	10.5
Spontaneous ignition of wood after long time	29.4
" " " cotton fabric after 5s	42.0
" " " fibre board after 5s	52.5

By way of comparison the intensities received from a single bar electric fire at 5, 10 and 15 cm distances are 10, 5 and 3.4 kW m^{-2} respectively.

4.2.4 Theories of flame spread across a surface of a solid vary with the type of material under consideration, but there are certain aspects common to them all. It is agreed that radiation forward from the flame is the major heat transfer process and that conduction along the solid surface can be disregarded.

In the combustion of plastic fuels McAlevy and Magee [15] view the spreading as a continuous diffusive gas phase ignition. The advancing flame heats the surface by radiation, the surface vaporises, and the vapours diffuse away from the surface to react exothermically with the oxygen in the atmosphere. The reaction then feeds back more heat to the surface, thus increasing the vaporisation rate; the heat release is increased by the increased vapour production, leading to a thermal "run-away" to ignition. Ignition occurs just as the flame reaches the location. Direct surface attack by oxygen is unimportant in spreading the flame.

Tarifa, del Notario and Torrilbo[16] admit that much vital data on evaporation and chemical kinetics is missing, so making it difficult to evaluate flame spreading analytically. They note that the flame spreads as a thin bluish flame front which moves very close to the surface of the plastic fuel. In this region combustion probably occurs with the fuel/oxidant ratio close to the minimum for flame propagation. Behind this front is the body of the flame where combustion is independent of conditions in the advancing front. Thus the spreading process is controlled by the mixture conditions at the surface, and the propagation velocity can be calculated for the one dimensional case with the mixture conditions at the front. In the regime of low fuel surface temperature the heat transfer by radiation ahead of the flame controls the spreading rate. At a certain temperature, because of the exponential nature of the vapour release characteristics, the fuel vapour fraction at the surface increases rapidly and the flame spread increases similarly. This temperature must be close to the "ignition temperature of the fuel" as it is usually defined. Above this temperature a combustible mixture exists all over the fuel surface, and the flame propagates through this mixture with the heating of the surface having no influence on the process.

Similar models have been forwarded for the candle-like burning of plastics[19]. In these cases the plastic either evaporates or undergoes a well defined depolymerisation reaction to provide the vapour to supply the flame. No such simple process occurs when polyurethane is heated so this type of model cannot be applied to the material.

Although of a completely different nature cellulosic materials provide a more acceptable parallel to urethanes in their combustion behaviour. The flow diagram of events in a fire[18] are shown in figure 4.2; drawn for wood, this describes quite well the processes followed by all complex polymeric materials, including polyurethane. Several observations affecting the processes can be made.

i) Char thickness, and hence resistance to removal of vapours increases with time.

ii) The increased residence time allows the reactions of the pyrolysis products, and those between the products and the charred material to proceed to a greater extent.

iii) Surface fissures form and deepen as exposure continues and they decrease the effects of points i) and ii).

iv) There is a multitude of chemical reactions occurring simultaneously in the material and the inter-action between the reactions is unknown and impossible to assess.

v) The preheating rate varies with the position inside the material, the time elapsed, the temperature at the point under consideration and therefore also the kinetics of the reactions.

vi) Possible back condensation of products in the virgin material will alter the characteristics of the material and thus its subsequent behaviour.

Figure 4.2 : Diagram of events in a fire

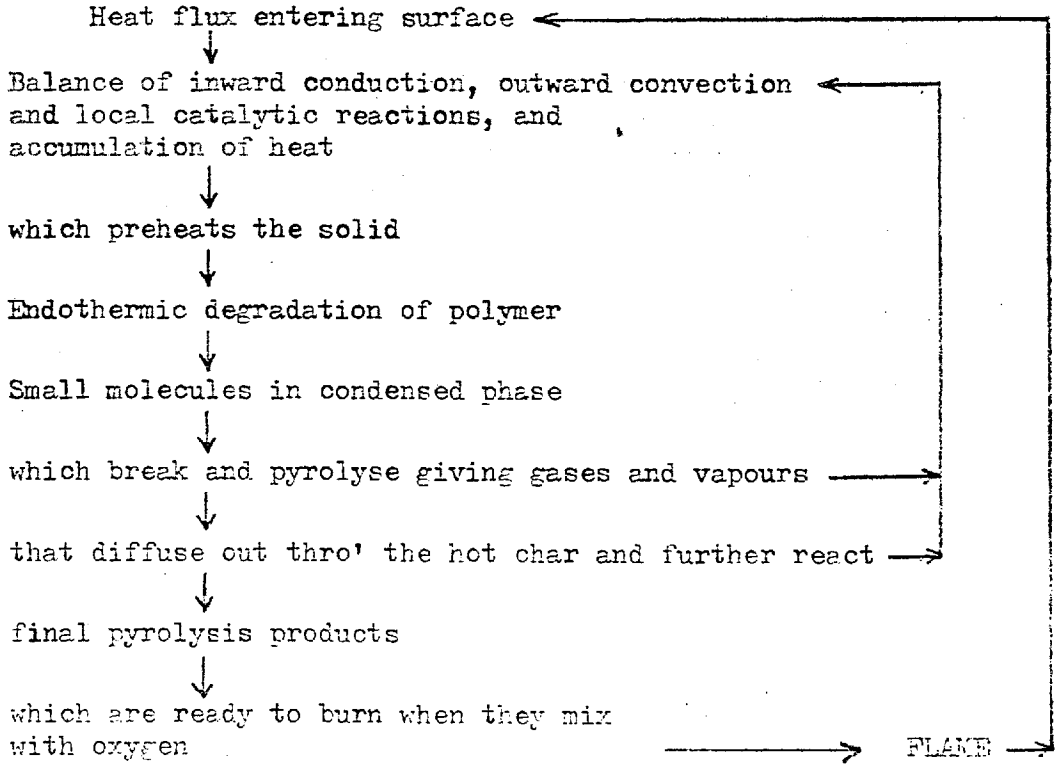

4.2.5 It is immediately apparent that an analytical solution to the combustion of this type of material is not possible, but that the best solution is to be gained by fitting the behaviour to models, the forms of which are suggested by theoretical considerations.

One such model is that due to Simms and Law [20]. In the system considered there is a constant radiative intensity at the face and heat losses are by Newtonian cooling. It is assumed that ignition occurs when the surface temperature reaches a fixed value. The results are considered in terms of two dimensionless parameters, an energy modulus and a cooling modulus. If θ_F is the temperature of the surface above ambient when combustion occurs, then

$$\text{Energy modulus} = \frac{It}{\rho C_p (\alpha t)^{\frac{1}{2}} \theta_F}$$

$$= \frac{It}{(\rho C_p \theta_F . \lambda t \theta_F)^{\frac{1}{2}}}$$

which represents the ratio between the heat directed at the surface and the geometric mean of the heat absorbed by and conducted through the surface layer.

Cooling modulus, $\beta = H (\alpha t)^{\frac{1}{2}} / \lambda$, where H is the Newtonian cooling co-efficient.

$$\therefore \beta = \frac{Ht}{\rho C_p (\alpha t)^{\frac{1}{2}}}$$

$$= \frac{Ht \theta_F}{\rho C_p (\alpha t)^{\frac{1}{2}} \theta_F}$$

Thus the cooling modulus is a ratio of the heat lost from and the heat retained in the material.

It is postulated that the results fit a relationship of the form

$$\frac{It}{\rho C_p (\alpha t)^{\frac{1}{2}} \theta_F} = \frac{\beta}{1 - \exp \beta \operatorname{erfc} \beta}$$

Simms and Law tested wet wood under conditions of pilot and spontaneous ignition. Their results form a good correlation with their model when values of 380°C and 545°C are given to θ_F for pilot and spontaneous

ignition respectively.

Other workers have used these moduli [21] and have set up models with similar form [22].

The model was applied to the results of the spontaneous ignition experiments performed in this work. The specific heat of the foams was estimated from values for solid polymer and the blowing agent to be 1480 J kg^{-1} $^{o}C^{-1}$, and a mean value of 10^{-6} m^2 s^{-1} was taken for the thermal diffusivity. The mean density was 30 kgm^{-3}. The Newtonian cooling co-efficient for natural convection is an imprecise parameter and, depending on the source, estimates vary from 6.27 [23] W $m^{-2}s^{-1}$, through 12.5 [24] W $m^{-2}s^{-1}$ to 13.2 [25] W $m^{-2}s^{-1}$ for these experimental conditions. The values for θ_F were suggested by temperatures recorded by the surface mounted thermocouple used in the preliminary experiments. Higher temperatures were used for the secondary experiments to reflect the effect of the positive pressure of nitrogen in the furnace, and the lower cooling coefficient takes account of the less violent air currents past the sample face.

The calculated values of the Energy and Cooling moduli are shown in tables 4.3 and 4.4

Table 4.3 : Energy Moduli (based on Section 3.2.1)

I (kW m^{-2})		8.4	12.6	16.8
t (s)	β (-)	Energy	Modulus	(-)
0.5	0.159			1.34
1.5	0.276			2.31
2.0	0.318		2.00	
2.5	0.356		2.23	3.00
3.0	0.390		2.45	
3.5	0.421			2.01*
4.0	0.450	1.88		
4.5	0.478	2.00		
5.0	0.503	2.11		
7.5	0.617		2.22*	

H = 10.0 $Wm^{-2}{}^{o}C^{-1}$ and θ_F = 200°C (except * when θ_F = 350°C)

Table 4.4 : Energy Moduli (based on Section 3.2.2)

I (kW m^{-2})		21.0	25.2
t(s)	β(-)	Energy Modulus	(-)
2.5	0.223		3.26
3.0	0.245		3.67
4.0	0.282	3.44	
5.0	0.315		3.18*
7.0	0.374	4.55	
12.0	0.490	5.95	

H = 6.27 $Wm^{-2}\ {}^{o}C^{-1}$ and θ_F = 275°C (except * when θ_F = 400°C)

These results are plotted in figure 4.3 and can be seen to fit the model approximately. The points from the early experiments show scatter as consequence of the uncertainties of plume projection. The low values of θ_f required to obtain this correlation indicate that the ignition is by a pilot mechanism, and bear no relation to the self ignition temperature of 520°C determined for similar foams[26] by the Setchkin Test [27]. In the Setchkin Test the sample is heated by a stream of hot air, as shown in figure 4.4. The self ignition temperature is the lowest temperature, with optimum air flow, at which the specimen will ignite in the absence of an external flame source.

4.2.6 As the model above is based on the assumption that ignition occurs at a fixed temperature it is reasonable to calculate the surface temperatures of the irradiated samples.

Consider a thickness l of the irradiated face of the sample.

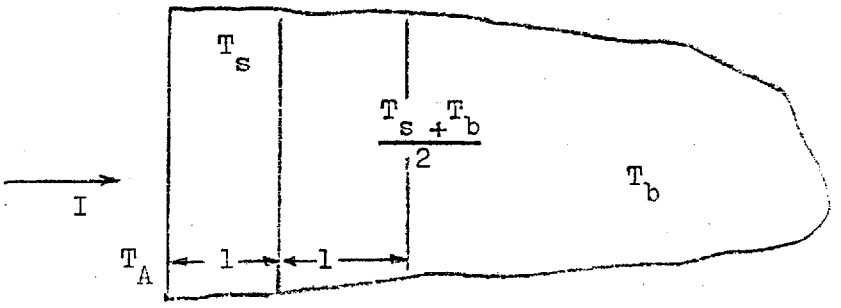

Let T_s = temperature of surface layer,

T_A = air temperature in region of the face,

T_b = temperature in the bulk of the sample,

and the temperature at depth 2l be $(T_s + T_b)/2$

For unit area during the interval δt,

heat received from furnace = $I\,\delta t$

radiation received from atmosphere = $\sigma T_A^4\,\delta t$

radiation lost from sample (black body) = $\sigma T_s^4\,\delta t$

heat conducted from face into body of sample = $\lambda \cdot \frac{T_s - T_b}{2} \cdot \frac{1}{2l} \cdot \delta t$

convective loss from face = $H\,(T_s - T_A)\,\delta t$

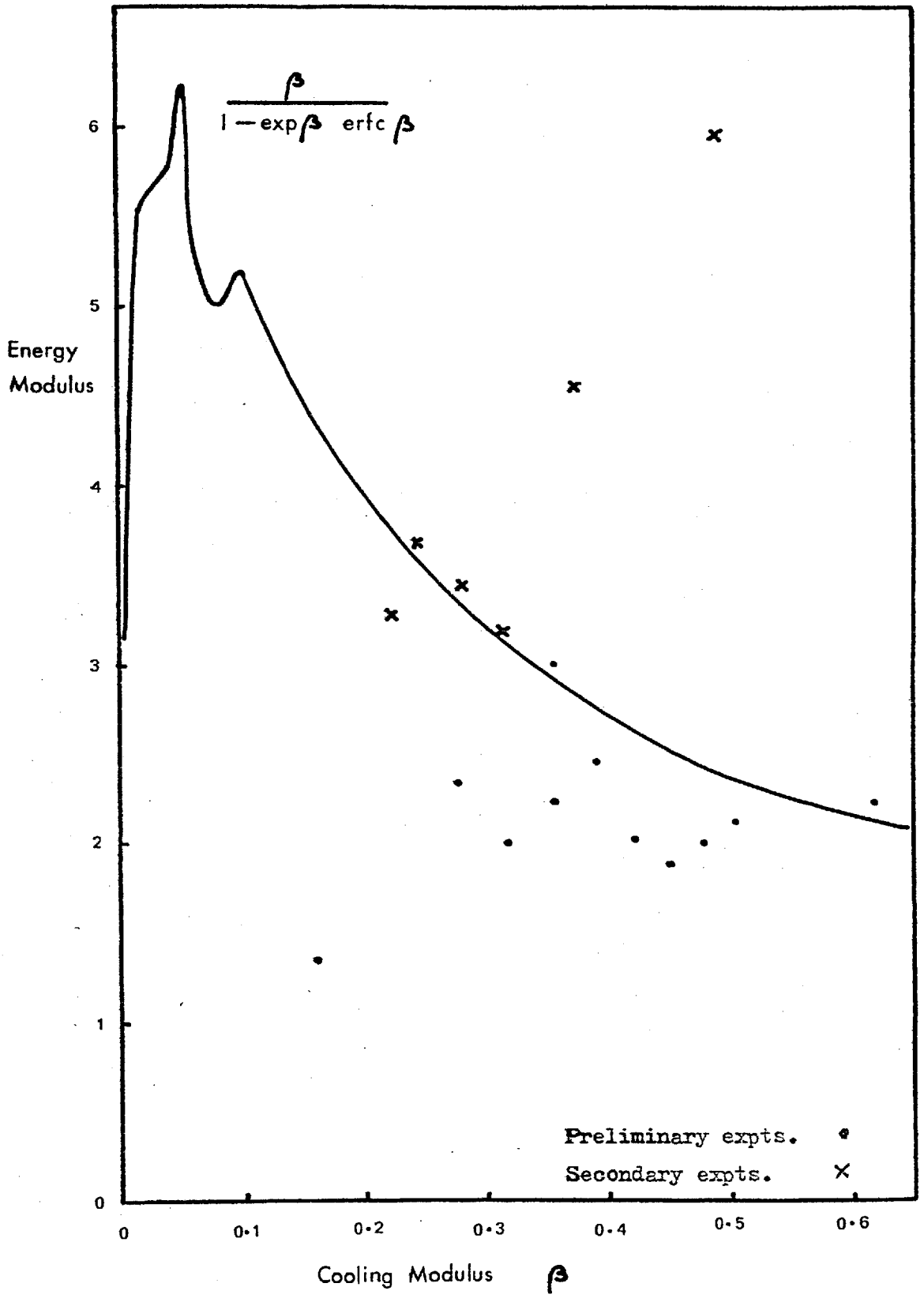

Figure 4.3 ; Fit of experimental data to model of Simms and Law.

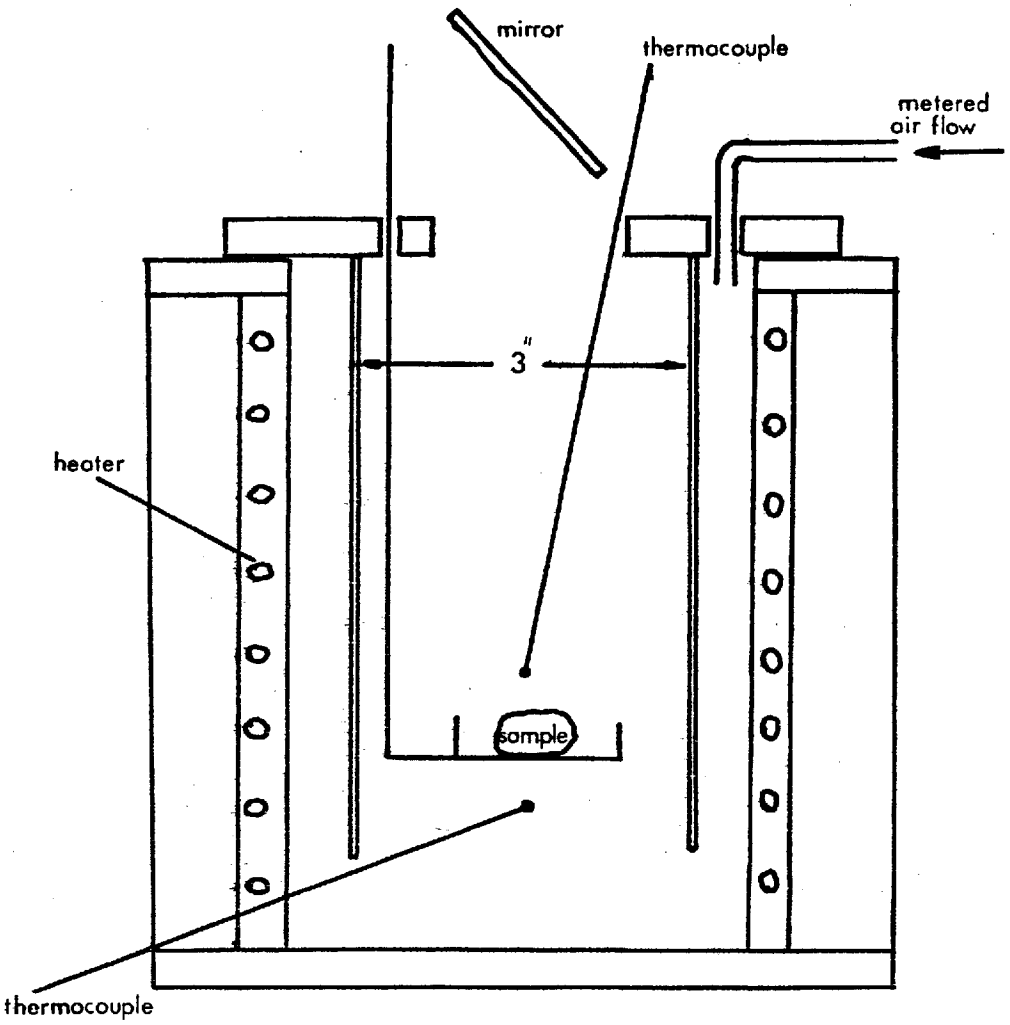

sample holder $1\frac{1}{2}'' \varnothing \times \frac{1}{2}''$

sample 3 g

Figure 4.4 ; Cross-section of Setchkin Test apparatus.

$$\therefore \quad \text{net heat in} = I\,\delta t - \sigma(T_s^4 - T_A^4)\delta t - \frac{\lambda}{2l} \cdot \frac{T_s - T_b}{2}\delta t - H\,(T_s - T_A)\,\delta t,$$

heat accumulated $= \delta T_s \rho\, C_p\, l$

A heat balance then gives

$$\frac{dT_s}{dt} = \frac{1}{l\,\rho\,C_p}\left[I - \sigma(T_s^4 - T_A^4) - \frac{\lambda}{2l}\left(\frac{T_s - T_b}{2}\right) - H(T_s - T_A)\right] \quad \ldots(9)$$

if $T_A = mT_s + n$,

$$\frac{dT_s}{dt} = \frac{1}{l\rho C_p}\left[I - \sigma T_s^4 + \sigma(mT_s+n)^4 - \frac{\lambda}{4l}T_s + \frac{\lambda}{4l}T_b - H(1-m)T_s + Hn\right] \quad \ldots(10)$$

$$\therefore \frac{dT_s}{dt} = \frac{1}{l\rho C_p}\left[(I + \sigma n^4 + \frac{\lambda}{4l}T_b + Hn) + T_s(4\sigma n^3 m - \frac{\lambda}{4l} - H(1-m)) + T_s^2\, 6\sigma m^2 n^2 + T_s^3\, 4\sigma m^3 n + T_s^4(m^4 - 1)\sigma\right] \quad \ldots(11)$$

This is of the form

$$\frac{dT_s}{dt} = \frac{1}{s}\left[a + bT_s + cT_s^2 + dT_s^3 + pT_s^4\right] \quad (a, b, c, d, p, s - \text{constants}) \quad \ldots(12)$$

$$\therefore \quad \frac{dT_s}{\frac{a}{p} + \frac{b}{p}T_s + \frac{c}{p}T_s^2 + \frac{d}{p}T_s^3 + T_s^4} = \frac{p}{s}\,dt \quad \ldots(13)$$

If the polynomial denominator has roots $\lambda_1, \lambda_2, \lambda_3, \lambda_4$ then

$$\frac{dT_s}{(T_s - \lambda_1)(T_s - \lambda_2)(T_s - \lambda_3)(T_s - \lambda_4)} = \frac{p}{s}\,dt \quad \ldots(14)$$

Separating the fractions and integrating gives (a', b', c', d', - constants)

$$\int \frac{a'\,dT_s}{T_s - \lambda_1} + \int \frac{b'\,dT_s}{T_s - \lambda_2} + \int \frac{c'\,dT_s}{T_s - \lambda_3} + \int \frac{d'\,dT_s}{T_s - \lambda_4} = \int \frac{p}{s}\,dt \quad \ldots(15)$$

$$\therefore \quad a' \ln(T_s - \lambda_1) + b' \ln(T_s - \lambda_2) + c' \ln(T_s - \lambda_3) + d' \ln(T_s - \lambda_4) = \frac{p}{s}t + \text{const} \quad \ldots(16)$$

$$\therefore \quad (T_s - \lambda_1)^{a'}(T_s - \lambda_2)^{b'}(T_s - \lambda_3)^{c'}(T_s - \lambda_4)^{d'} = \exp(\tfrac{p}{s}.t) \times \text{constant} \quad \ldots(17)$$

It can be seen that this equation is not readily soluble for T_s, so an analytical solution for T_s is not possible. The equation for the temperature gradient has to be solved iteratively.

The following values were given to the variables:

$l = 2.5 \times 10^{-3}$ m

$\rho = 30$ kg m^{-3}

$C_p = 1480$ J kg^{-1} °C^{-1}

$T_b = 300^{\circ}K$

$\lambda = 4.6 \times 10^{-2}$ W m^{-1} $^{\circ}C^{-1}$

$H = 8.4$ W m^{-2} $^{\circ}C^{-1}$

and T_A was taken as $473^{\circ}K$ when $I = 4.2$ kW m^{-2},

so $T_A = 273 + 0.78125\ (T_s - 273)$

$$\therefore \frac{dT_s}{dt} = 0.009 \left[I - 5.73 \times 10^{-8} \left(T_s^4 - (0.78125T_s + 59.71875)^4\right) - 9.2\ (T_s - 300) - 8.4(0.21875T_s + 59.71875) \right] \quad \ldots(18)$$

At equilibrium $\frac{dT_s}{dt} = 0$. Values of T_s were tried to find the surface temperature giving zero gradient. The gradient $\frac{dT_s}{dt}$ has the form $f(T_s)$.

Consider the case when $I = 8.4$ kW m^{-2}, and let the first estimate of T_s be $605^{\circ}K$.

Then, $f(T_s = 605) = 0.009 \left[8.4 \times 10^3 - 5.73 \times 10^{-8} \left(605^4 - 0.78125 \times 605 + 59.71875)^4 \right) - 9.2(605 - 300) - 8.4\ (0.21875 \times 605 + 59.71875) \right]$

$= 18.74$

As the gradient had a positive value a higher value of T_s, $625^{\circ}K$, was taken as the second estimate, then

$f(625) = 9.9$

The third estimate was $650^{\circ}K$,

$f(650) = -2.06$,

thus the equilibrium temperature was between $625^{\circ}K$ and $650^{\circ}K$,

$f(640) = 2.86$

$f(645) = 0.42$

$f(646) = -0.51$

it is seen that the value of T_s lies between $645^{\circ}K$ and $646^{\circ}K$ because the gradient changes sign in this interval. To the nearest degree, $\underline{T_s = 645^{\circ}K}$.

Then $T_A = 273 + 0.78125\ (645 - 273)$

$\underline{T_A = 564\ ^{\circ}K}$

The values of T_s and T_A calculated in the same fashion for differing incident intensities are shown in table 4.5

Table 4.5 : Equilibrium surface temperatures

I (kW m^{-2})	T_s (^oK)	T_A (^oK)
4.2	530	473
6.3	589	520
8.4	645	564
12.6	732	632
16.8	798	683
21.0	852	726
25.2	898	761

Equation (18) is of the form $\frac{dT_s}{dt} = f(T_s)$, so

$$\int_{T_o}^{T_t} \frac{dT_s}{f(T_s)} = \int_o^t dt \qquad \cdots(19)$$

which can be integrated numerically.

Simpson's rule with five ordinates (i.e. four strips) gives the following expression [64] for integration of a continuous function. (See figure 4.5),

$$\int_a^b g(x)\,dx \cong \frac{h}{3}\left[g_o + g_4 + 4\,(g_1 + g_3) + 2g_2\right] \qquad \cdots(20)$$

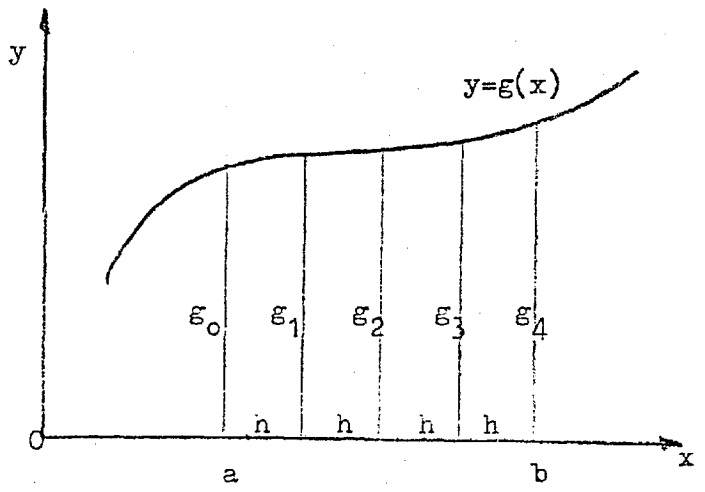

Figure 4.5 : Simpson's rule with 4 strips

This is applied to equation (19) to find the time taken for the surface to reach a temperature of 525°K when subjected to 4.2 kW m^{-2}:

thus $$t = \int_{273}^{525} \frac{dT_s}{f(T_s)} = \int_{273}^{525} F(T_s)\, dT_s \ .$$

For 4 strips, $h = \frac{525 - 273}{4} = 63^{\circ}K$, so the function needs to be evaluated at 273°K, 336°K, 399°K, 462°K and 525°K. Then, for $I = 4.2$ kW m^{-2},

$f(273) = 53.288$ $\qquad F_0 = \frac{1}{f(273)}$

$f(336) = 43.576$ $\qquad F_1 = \frac{1}{f(336)}$

$f(399) = 32.224$ $\qquad F_2 = \frac{1}{f(399)}$

$f(462) = 18.397$ $\qquad F_3 = \frac{1}{f(462)}$

$f(525) = 1.096$ $\qquad F_4 = \frac{1}{f(525)}$

Application of equation (20) gives

$$\int_{273}^{525} \frac{dT_s}{f(T_s)} = \frac{63}{3} \left[F_0 + F_4 + 4(F_1 + F_3) + 2F_2 \right]$$

$$= \underline{38.8 \text{ s}}$$

Thus, at $I = 4.2$ kW m^{-2}, the surface temperature reaches 525°K in 38.8s. This indicates that the surface reaches a steady temperature in approximately one minute and justifies the assumption of a constant surface temperature in the diffusity calculations.

In order to find the temperature attained by the surface after a given time the integration shown in equation (19) was used, but it was evaluated by the trapezium rule [65], which uses the following expression (see figure 4.6)

$$\int_a^b g(x)\, dx \cong \frac{h}{2} (F_0 + 2F_1 + F_2) \qquad \ldots (21)$$

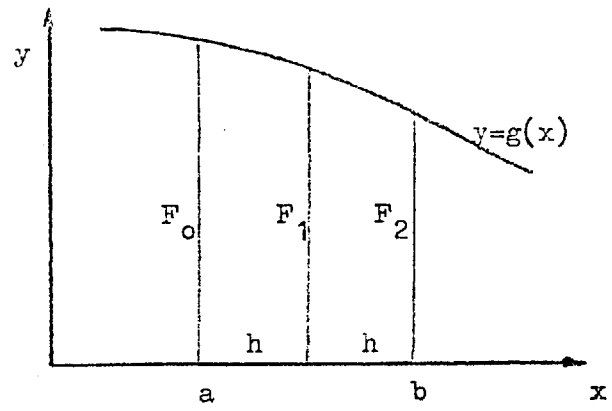

Figure 4.6 : Trapezium rule

Again $F(T_s) = \frac{1}{f(T_s)}$, and $f(T_s) = \frac{dT_s}{dt}$ as defined in equation (18).

Consider, for example, the time required for the surface to reach $700^{\circ}K$ when subjected to 16.8 kW m^{-2}:

$$h = \frac{700-273}{2} = 213^{\circ}K,$$

then $f(700) = 0.009 \left[16.8 \times 10^3 - 5.73 \times 10^{-8} (700^4 - (0.71875 \times 700 + 59.71875)^4) - 9.2(700-300) - 8.4(0.21875 \times 700 + 59.71875)\right]$

so $f(700) = 48$, $\therefore F_2 = 0.02083$,

$f(486) = 113$, $F_1 = 0.00885$,

$f(273) = 153.5$, $F_0 = 0.00652$.

These values are then substituted into equation (21),

$$\int_{273}^{700} F(T_s)dT_s = \frac{213}{2} (0.00652 + 2 \times 0.00885 + 0.02083)$$

$$= \underline{4.8}$$

Thus after 4.8 seconds a surface exposed to 16.8 kW m^{-2} reaches a temperature of $700^{\circ}K$. Similar calculations produced the range of values shown in table 4.6.

Table 4.6 : Surface temperature history, I = 16.8 kW m^{-2}

t(s)	T_s (^oK)
2.21	550
3.8	660
4.8	700
7.57	740
8.9	750
11.15	760

The integral was evaluated using other values for the intensity of radiation, and the ensuing results are shown in tables 4.7 - 4.10.

Table 4.7

Surface temperature
I = 8.4 kW m^{-2}

t(s)	T_s(^oK)
3.24	460
4.42	500
6.67	550
10.95	590
13.7	600
20.6	620

Table 4.8

Surface temperature
I = 12.6 kW m^{-2}

t(s)	T_s(^oK)
2.49	500
3.26	550
4.34	600
6.05	650
9.12	690
11.1	700

Table 4.9

Surface temperature

$I = 21.0 \text{ kW m}^{-2}$

t(s)	$T_s(^{\circ}K)$
1.65	550
2.77	660
3.17	698
3.92	742
4.72	770
5.66	790
8.06	815
10.9	830

Table 4.10

Surface temperature

$I = 25.2 \text{ kW m}^{-2}$

t(s)	$T_s(^{\circ}K)$
1.42	550
2.28	670
2.52	700
2.86	730
3.11	750
4.0	800
5.08	830
8.3	860

The trapezium rule decreases in accuracy as the curve being integrated deviates from the straight line, thus the times are less accurate as the temperature approaches the equilibrium temperature.

The information contained in tables 4.6–4.10 is presented graphically in figure 4.7. If one assumes that ignition occurs when the surface reaches a fixed temperature it is possible to construct a family of curves showing the variation of ignition time with incident intensity for each fixed surface temperature. Such a family is shown in figure 4.8.

A comparison between predicted and actual ignition times is made in figures 4.9 and 4.10. At the lower intensities the experimental results correspond quite well with the theoretical curves. The equivalent surface temperature is seen to be approximately $500^{\circ}K$ ($225^{\circ}C$) which is close to the temperatures measured by the surface mounted thermocouple in the preliminary ignition experiments. The theoretical critical surface temperature for Foam E is approximately $650^{\circ}K$ ($380^{\circ}C$) which agrees with the measured value.

At higher intensities the correlation between theory and practice is not so clear. Indicated ignition temperatures range from $720^{\circ}K$

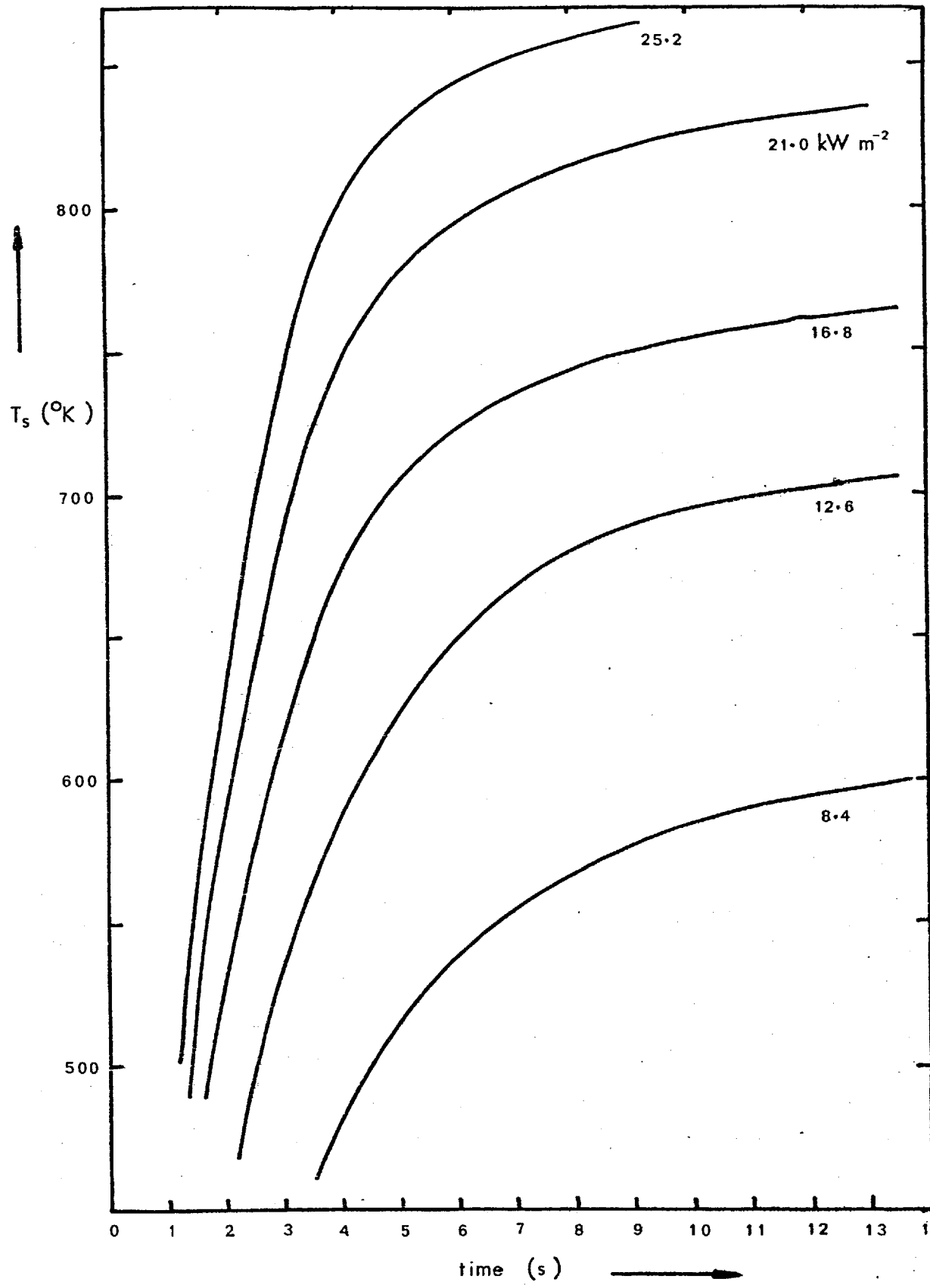

figure 4.7 ; Variation of surface temperature with incident intensity

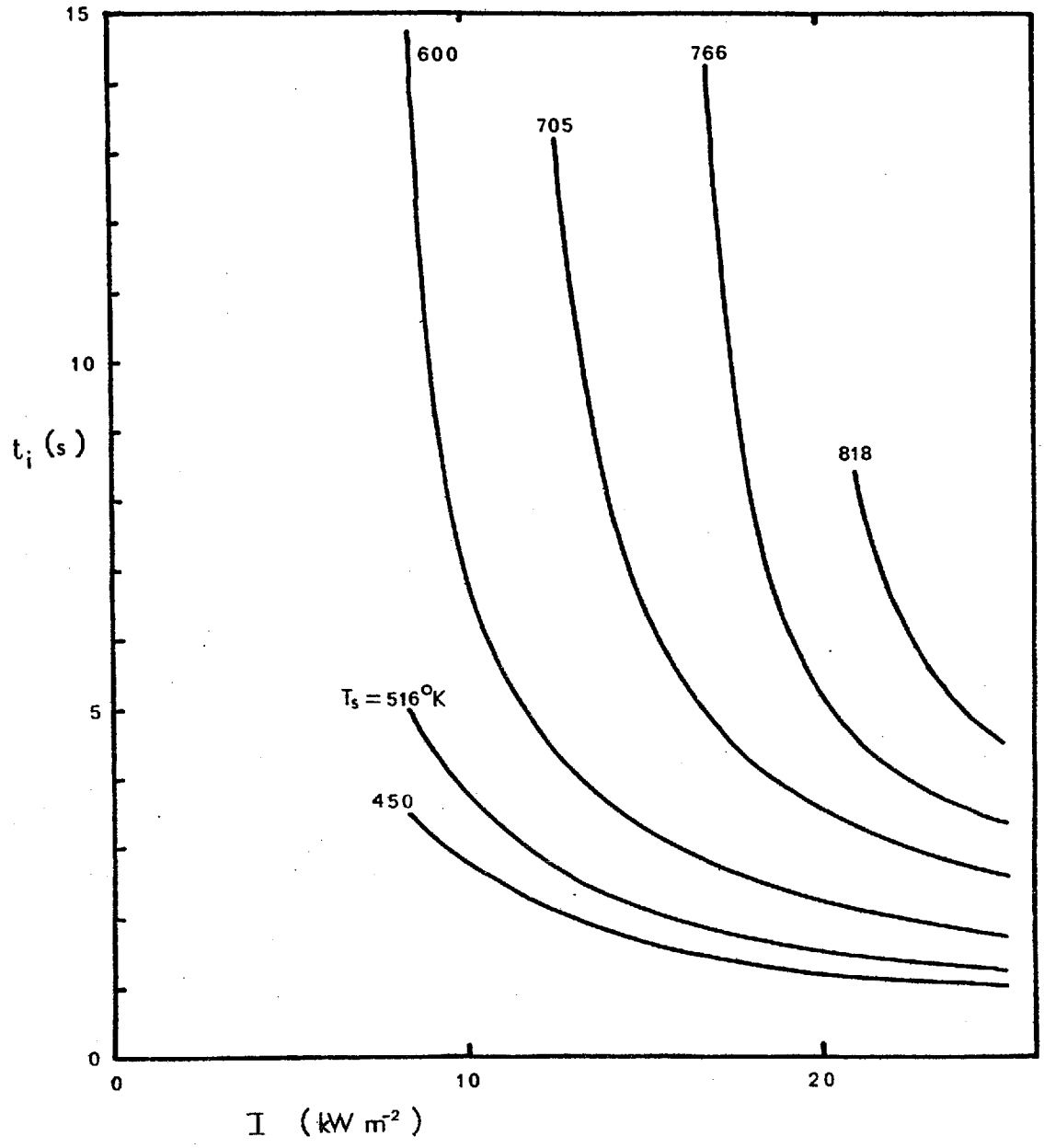

Figure 4.8 ; Theoretical variation of ignition time with incident intensity, for a range ofvalues of critical surface temperature.

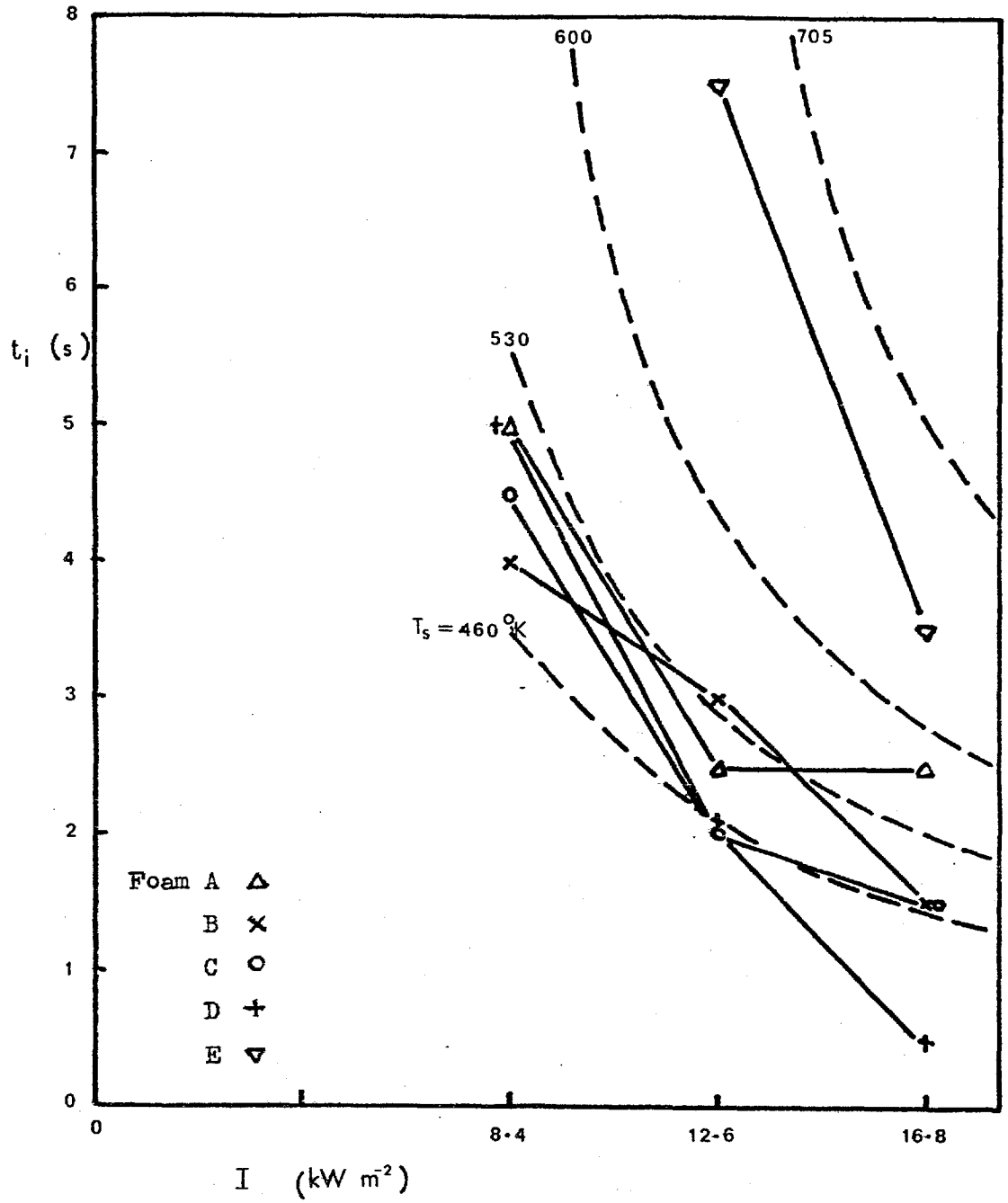

Figure 4.9 ; Comparison of predicted and experimental ignition times, for preliminary experiments.

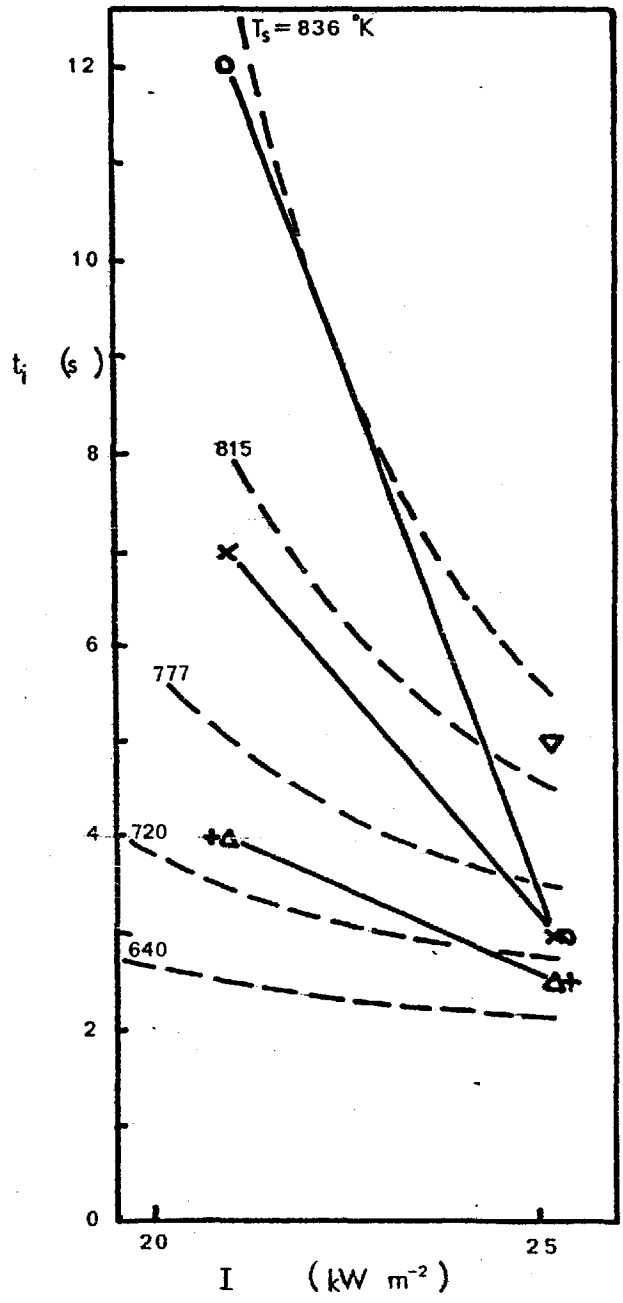

Foam A △
B ×
C ○
D +
E ▽

Figure 4.10 ; Comparison of predicted and experimental ignition times, for secondary experiments.

(450°C) upwards.

From these results it can be deduced that the surface temperature is a major factor governing ignition, but its precise role cannot be defined because of the vagaries of the experimental circumstances. As discussed in section 4.2.1, factors involving the physical movement of the evolved materials are likely to have an auxiliary controlling effect and in the short term these are liable to show severe perturbations, for example a change in the cell structure at the surface can completely alter the direction of a jet of volatiles and so change the mixing pattern. Probably the major cause of scatter in these results was the furnace used as the radiation source. It was not intended to be so, but the furnace also acted as a pilot ignition source. In this capacity it was very poorly situated; the usual position for a pilot source is a short distance above the sample [20, 21, 22, 28]. Being at some distance from the sample and at the same height means that in order for the evolved materials to reach the ignition source they had to be projected violently from the sample. When the furnace was flushed with nitrogen this difficulty was aggrevated. This factor effectively prevented ignition at lower rates of decomposition and increased the minimum ignition intensity.

No consideration of the frequency dependence of the emissivity of the foam was taken, and no measurement of the spectral distribution of the radiation source was made, although it is seen that these factors can influence the absorption of heat in the sample [22].

These low density, 30 $kg\,m^{-3}$, foams will have a higher minimum ignition intensity than a more dense foam. When the sample is first exposed the surface temperature has to rise to the equilibrium value, and while it is doing so the foam is decomposing at a lower rate than necessary to form a flammable mixture with the air. By the time the temperature has risen high enough to cause reaction at a sufficient rate for ignition, the surface layer of the foam has reacted to form a char which insulates the bulk of the foam and prevents it reaching a high

enough temperature to cause a flammable mixture to be formed. Thus, even though the radiation intensity may be above the minimum value for a dense foam, the low density may preclude ignition.

Under conditions met in practical applications of urethane foams the behaviour is likely to be modified by the size of the sample. The minimum intensity for ignition decreases as the area of irradiated surface increases [29]. For fibre insulation board [67] the minimum intensity for ignition of a large area is half the value for an area of $10cm^2$ and 2/3 of that for $100cm^2$. Another implication of a small experimental sample is the short residence time of the evolved materials in the heated zone. On a large scale, the mixing conditions would be altogether different; once mixed with air the evolved products would pass up over more heated surface and could be heated sufficiently to reach the critical temperature before passing into the cool zone. A larger plume could also produce a flammable mixture at a distance from the heated material and so the source of pilot ignition could be distant from the seat of the fire it produces.

In the case of a vertical surface [63] the ignition time also depends on the height of the sample. When the radiant intensity is below a critical level the ignition time decreases as the height increases, but above the transitional radiation level there is no height dependence. This is explained in terms of the time, t_{ss}, to establish a steady-state free convection boundary layer in the gas at the solid surface. At low values of irradiance $t_i > t_{ss}$ and the height dependent heat losses through the boundary layer cause the top of the panel to be hotter than the bottom and so cause the pyrolysis rate and time to ignition to be dependent on the height. At high value, greater than approximately 170 kW m^{-2} for cellulosic solids, $t_i < t_{ss}$ and ignition occurs before the boundary layer is set up.

For ignition of a gas by a hot surface, Zeldovitch [66] considered the effect of various factors, including the shape and dimensions of the igniting surface, movement of the gas, and chemical kinetics, in terms of the heat flux in the gas and the critical balance of generated heat versus heat lost that limits a thermal explosion. He noted that if the combustion temperature was lower than the ignition temperature as calculated from the heat balance, there could be no ignition however hot was the ignition surface because the propagation of flame was nothing more than ignition of cold gas by the hot combustion products.

4.3 Weight Loss

4.3.1 The results of the weight loss experiments are given in tables 3.3 – 3.7. The information is presented graphically in figures 3.6 – 3.10 with additional lines showing the concentrations of the blowing agent (F11), the propylene oxide content of the foam and TCEP. In some of the foams F11 is introduced in the polyether (Daltolac 51) and as a separate constituent.

Propylene oxide is used to extend the polyethers and its concentration is calculated from the hydroxyl number and the polyether functionality. Daltolac 50 has a hydroxyl number of approximately 480, and an insignificant acid number of less than 1.

The hydroxyl number is the weight in mg of potassium hydroxide equivalent to one gramme of the polyol resin. The molecular weight of potassium hydroxide is 56, so

56g KOH ≡ 1g resin, signifies 1 (OH) group/g of resin

∴ 56mg KOH ≡ 1g resin, signifies 1 (OH) /1000g resin

If hydroxyl number is 480, there are $\frac{480}{56}$ (OH) /1000g resin

= 1 (OH) /116.7g resin

But Daltolac 50 is a propoxylated toluene diamine, a tertol, so the 4 hydroxyl groups are contained in 467g of resin: this is the molecular weight of Daltolac 50. The molecular weight of toluene diamine is 122, therefore the remainder, 345, is due to propylene oxide. Propylene oxide has a molecular weight of 58, thus each molecule of Daltolac 50 contains 6 molecules of propylene oxide, which is 74% by weight.

Similarly Propylan RF33 is a propoxylated sucrose adduct with a hydroxyl number of 490 – 500.

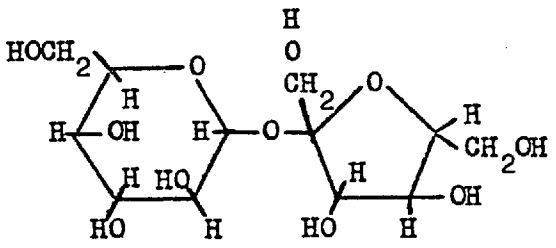

Sucrose.

Sucrose has a functionality of 8. This gives $9\frac{1}{2}$ – 10 molecules of propylene oxide per molecule of polyether, some 62.5%.

Propylan P450 is a propoxylated phosphoric acid with approximately 7% of phosphorus. If P450 were

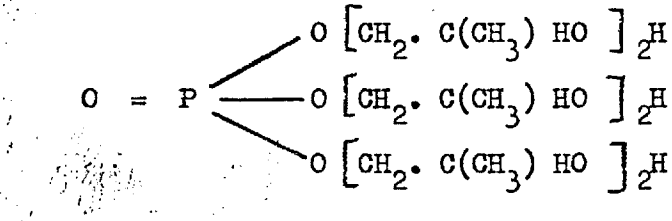

the phosphorus content would be 7% and propylene oxide would account for 78%. The hydroxyl number would agree with the published value of 385.

The following table summarises the concentrations of these materials in the experimental foams:

Table 4.11 : Composition of foams

	FOAM				
% of	A	B	C	D	E
F11	12.8	12.1	12.5	14.7	16
Propylene oxide	20.5	19.5	24.3	24.6	0*
TCEP	0	5.3	9.9	0	10*

*Estimated

In order to get some idea of the degree of crosslinking the excess isocyanate over stoichiometric requirements was calculated.

MDI has a molecular weight of 250 but is a diisocyanate so the equivalent weight is 125.

Daltolac 50 has a molecular weight of 467, and, being a tertol, each molecule combines with 4 equivalents of isocyanate. Thus 1 part of Daltolac 50 needs $\frac{4 \times 125}{467}$ = 1.07 parts of MDI.

Similarly the isocyanate requirements of the other polyols were calculated and are shown in table 4.12.

Table 4.12 : MDI requirements of polyols

Polyol	MDI requirement, W/W
Daltolac 50	1.07
Propylan RF33	1.1
Propylan P450	0.84
Glycerol	4.0
Water	14

From these data and the formulations in section 2.1.1 the excess isocyanate in the foams was derived.

Eg for Foam D:

MDI demand of RF33 = 70 x 1.1 = 77

MDI demand of P450 = 30 x 0.84 = 25.2

∴ Total MDI demand = 102.2

but MDI used = 128, therefore excess = 25%

Table 4.13 : MDI in foams, excess over stoichiometric demand

Foam	Excess MDI
A	38%
B	38%
C	19%
D	25%

There was insufficient data for a calculation for Foam E to be made.

The excess MDI reacts with the active hydrogen in the urethane group to form allophanate linkages which add to the rigidity of the matrix.

4.3.2 Inspection of the curves in figures 3.6 - 3.10 reveals several features of interest. Firstly the weight loss at 160°C is in all cases approximately equal to the weight fraction of trichlorofluoromethane which, as the blowing agent, can be expected to be first lost as it is only a gas enclosed in the cells of the material. Considering foams A,B and C it can be seen that as the concentration of TCEP is increased so the material loses the first fraction more quickly. To enable the F11 to escape it would be necessary to provide a path, which could be created either by rupture of the cell walls by physical or chemical forces, or by rendering the cell walls permeable to diffusion of the vapour. The inclusion of TCEP is a physical process so the cell walls must be intrinsically more susceptable to gaseous diffusion when the vapour pressure of the TCEP increases with temperature and there is less of it in the solid

matrix of the foam. Permeability might be enhanced by the plasticising effect of the TCEP.

Secondly there is a distinct "pinch" in the curves at a weight fraction corresponding to the loss of F11 + propylene oxide + TCEP, where they are present in the formulations. This indicates that one set of reactions is complete and that another has yet to commence. The temperatures at which these critical weight losses are reached are shown in table 4.14.

Agreement among the values for the widely differing foams suggests that similar processes are responsible in all cases. The boiling point of TCEP is 220°C,[33] but with the accompanying decomposition and possible elevation of the boiling point it is reasonable to expect complete vaporisation at approximately 260°C.

Table 4.14 : Temperatures at critical weight losses

	Foam A	Foam B	Foam C	Foam D	Foam E
a), % F11	12.8	12.1	12.5	14.7	16
b), " + propylene oxide	33.3	31.6	36.8	39.3	-
c), " " + TCEP	-	36.9	46.7	-	26
Temperature for b), °C	220-240	220-240	220-240	205-235	-
Temperature for c), °C	-	240-250	265-275	-	230-260

Above 250°C the polyurethane foams A, B and C exhibit an approximately linear relationship between temperature and weight loss, but the foam with phosphorylated polyol, D, shows more time dependence. Up to 340°C the secondary reactions in foam E are relatively slow, but above this temperature the foam volatolises rapidly.

4.3.3 In order to ascertain the relevance of the experimental results after 7 minutes it is necessary to consider the heat penetration. Consider an infinite cylinder of radius a, with a temperature of zero.

The surface is raised to a temperature of Tr = a. Figure 4.11 shows the variation of temperature with radius and time.[34]

For the samples in question $\alpha = 1 \times 10^{-6}$ m^2 s^{-1} and a = 16.5mm

When t = 60 s, $\frac{\alpha t}{a^2} = 0.2262$ and $T_r = 0.50\ T_{r=a}$

t = 120 s, $\frac{\alpha t}{a^2} = 0.4524$ and $T_r = 0.92\ T_{r=a}$

t = 180 s, $\frac{\alpha t}{a^2} = 0.6786$ and $T_r = 0.97\ T_{r=a}$

Thus within 3 minutes the whole of the sample is within 3% of the surface temperature, which justifies an assumption of instant heating to furnace temperature.

4.3.4 It is suggested that the first effect of heating the foam is to drive out the blowing agent. This can be accomplished by rupturing the cells, or by making the walls permeable to the F11, so allowing it to escape as it expands on heating.

The case of the cell walls being ruptured by the increased pressure of the gas is first considered.

If the density of solid polymer is 1000 kg m^{-3}, the density of F11 vapour is 6 kg m^{-3} and that of the foam is 30 kg m^{-3}, let x be the volume fraction of solid in the foam. Then $30 = 1000\,x + (1 - x)\,6$

$$\therefore \quad x = .024$$

The solid is the continuous phase in this mixture, so the solid fraction of the cross sectional area = $1 - 0.976^{2/3} = 0.016$. Typically the cells have a diameter of $\frac{1}{2}$ mm. Consider an area 10 mm square, and assume regular arrangement of the cells on a square matrix. The total length of the cell boundaries is then 40 x 10 mm. If t_w is the thickness of the cell walls,

$$\text{area of solid} = 400 \times t_w \quad \text{mm}^2$$

$$= 0.016 \times 100 \quad \text{mm}^2$$

$$\therefore \quad \text{thickness of walls, } t_w = 0.004 \text{ mm}$$

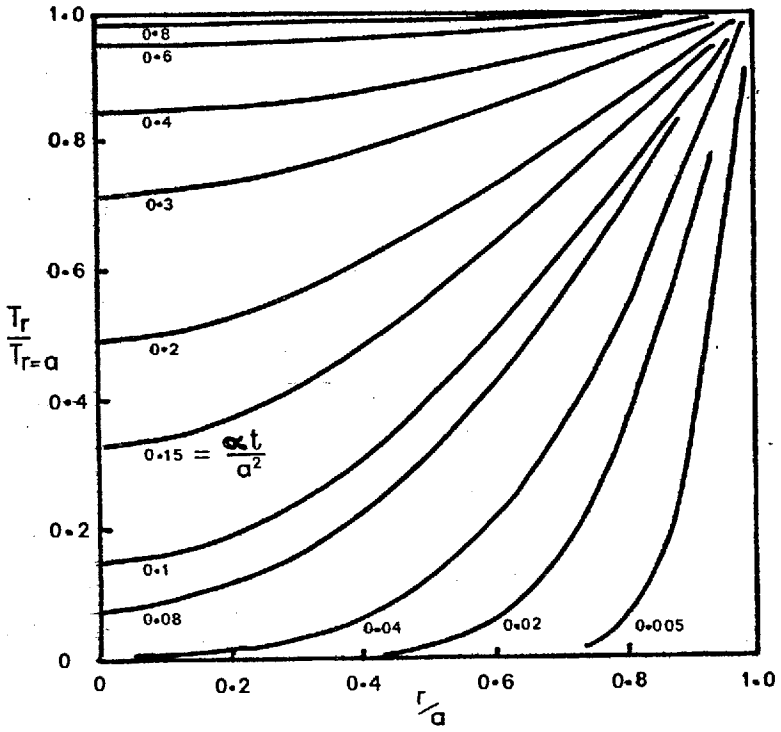

Figure 4.11 ; Temperature profile of infinite cylinder of radius a, initially at zero temperature, and surface raised to temperature $T_{r=a}$.
(from reference 34)

The tensile strength of the polymer is approximately 1.4×10^4 kN m^{-2} (2000 psi) and the modulus of elasticity is 34.5×10^4 kN m^{-2} (50×10^3 psi)[35]

Modulus of elasticity = stress/strain

When the material fractures the stress is equal to the tensile strength,

so $$34.5 \times 10^4 = \frac{1.4 \times 10^4}{dL/L}$$

$$\therefore \frac{dL}{L} = 0.0406$$

$$\therefore \frac{L + dL}{L} = 1.0406$$

Consider an area the crossection of which has length L. This is distorted to a length L + dL, with a radius of curvature of r_c (figure 4.12)

Figure 4.12 :
Curvature of distorted surface

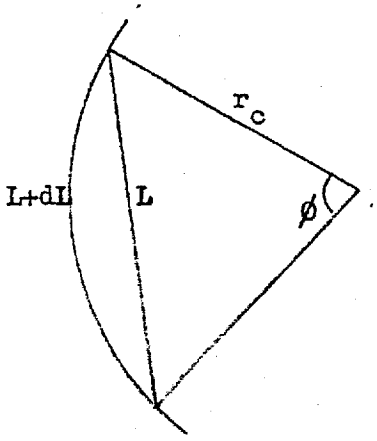

Then $$L + dL = \frac{\phi}{360} \cdot 2\pi r_c$$

$$L = 2 r_c \sin \frac{\phi}{2}$$

$$\therefore \frac{L + dL}{L} = \frac{\pi}{360} \cdot \frac{\phi}{\sin \frac{\phi}{2}}$$

but $$\frac{L + dL}{L} = 1.0406$$

$$\therefore 1.0406 = \frac{\pi}{360} \cdot \frac{\phi}{\sin \frac{\phi}{2}}$$

$$\therefore \frac{\phi}{\sin \frac{\phi}{2}} = 120.0$$

By inspection this is seen to have a solution $\underline{\phi = 60^\circ}$,

therefore $L/r_c = 2 \sin 30^\circ, = 1$

To find the pressure, ΔP, required to maintain a surface of thickness t_w at a radius of r_c let us consider the hemisphere shown in figure 4.13.

Figure 4.13 ;

Pressure to maintain curvature

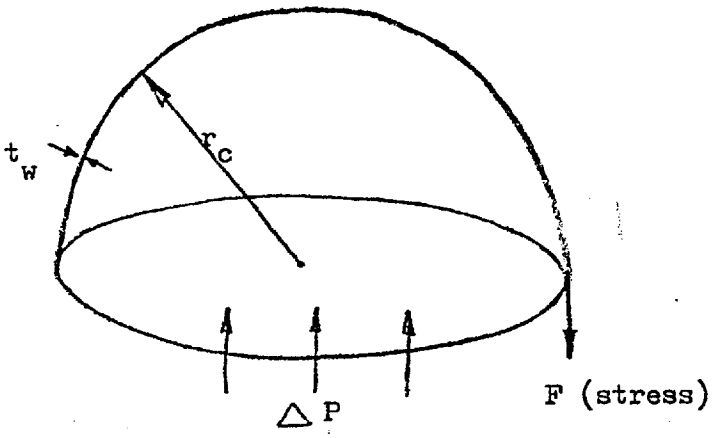

The force due to pressure = $\Delta P \ \pi \ r_c^2$

and the total stress at the rim of the shell = $F. \ 2 \ \pi \ r_c \ t_w$

at steady state these are equal, so

$$\Delta P \ \pi \ r_c^2 = F. \ 2 \ \pi \ r_c \ t_w$$

$$\therefore \quad \Delta P = \frac{2. F. t_w}{r_c}$$

At fracture the stress, F, $= 1.4 \times 10^4$ kN m^{-2}

$r_c = 0.5$ mm and $t_w = 0.004$ mm

$$\therefore \quad \Delta P = \frac{2 \times 0.004 \times 1.4 \times 10^4}{0.5}$$

$$\Delta P = 224 \text{ kN } m^{-2}$$

Therefore the pressure difference across the cell wall needed to cause rupture is 224 kN m^{-2}. If the external pressure is atmospheric, 100 kN m^{-2}, and the internal pressure was atmospheric at room temperature, then the temperature at which the internal pressure is sufficient to rupture the wall would be $\frac{324}{100} \times 273 \cong 880^{\circ}K$ ($610^{\circ}C$). This is clearly far higher than the temperature at which the F11 is lost, so this is not the release mechanism.

Weight losses approaching the F11 content occurred at temperatures as low as $160^{\circ}C$. Reference to the tables in section 3.3 reveals that there is evidence of chemical degradation even at these temperatures: discoloration

the foam and an iridescence of the cell membranes are found. If there was sufficient reaction to cause these changes it is most unlikely that the physical characteristics of the material would be unchanged and membranes 0.004 mm thick remain impermeable. Investigating polyisocyanurate foams Einhorn[36] found that after 5 minutes at 100°C there was no damage, but that 5 minutes at 300°C produced blisters on the cell membranes.

4.3.5 Activation energies for decomposition of the foams can be derived from the measurements of weight loss.

Suppose that the foam undergoes a reaction such that the product is volatile and is lost from the solid. If the reaction proceeds according to a first order mechanism,

then $$\frac{dW_t}{dt} = -kW_t$$

where W_t = weight of foam at time t

k = rate of reaction

$$\therefore \quad \frac{dW_t}{W_t} = -kdt$$

Integration yields $\ln W_t = -kt + \text{constant}$

At $t = 0$, $W_t = W_o$ so constant $= \ln W_o$,

$$\therefore \quad \ln \frac{W_o}{W_t} = kt$$

But k is of the form $A.\exp(-E_{act}/RT)$, $\therefore \ln \frac{W_o}{W_t} = tA.\exp(-E_{act}/RT)$,

$$\therefore \quad \ln \ln \frac{W_o}{W_t} = \ln At - \frac{E_{act}}{RT}$$

Thus a plot of $\ln \ln W_o/W_t$ versus $1/T$ has a gradient of $-\frac{E_{act}}{R}$ and an intersept of $\ln At$.

In the decomposition of polyurethane foams the loss of the blowing agent is a physical process and as such cannot be accounted for in such a treatment. Therefore a corrected original weight, $W_o' = W_o$ (1-fraction of F11), is used.

Values of $\ln \ln W_o' / W_t$ calculated from the results of section 3.3.1 are shown in tables 4.15 - 4.19.

Table 4.15 : Foam A

$\frac{10^3}{T^\circ K}$	$\ln \ln W_o' / W_t$			
	7 min	20 min	1 h	3 h
2.31				- 3.08
2.11	- 3.32	- 2.14	- 1.85	- 1.78
1.93	- 1.14	- 1.23	- 1.10	- 1.06
1.78	- 0.67	- 0.69	- 0.59	- 0.45
1.65	- 0.29	- 0.25	- 0.16	0.06
1.58	- 0.13	- 0.04	0.10	0.41
1.49	0.12	0.29	0.60	0.98

Table 4.16 : Foam B

$\frac{10^3}{T^\circ K}$	$\ln \ln W_o' / W_t$			
	7 min	20 min	1 h	3 h
2.31			- 2.90	- 2.67
2.11	- 2.67	- 1.97	- 1.64	- 1.60
1.93	- 1.23	- 1.18	- 1.17	- 1.10
1.78	- 0.75	- 0.66	- 0.62	- 0.42
1.65		- 0.24	- 0.19	0.11
1.58	- 0.04	0.04	0.20	0.44
1.49	0.22	0.40	0.51	0.89

Table 4.17 : Foam C

$\frac{10^3}{T^\circ K}$	ln ln W_o'/W_t			
	7 min	20 min	1 h	1 h
2.31		- 3.20	- 2.53	- 2.04
2.11	- 2.12	- 1.65	- 1.39	- 1.31
1.93	- 1.05	- 1.05	- 0.94	- 0.90
1.78	- 0.54	- 0.46	- 0.49	- 0.39
1.65	- 0.18	- 0.09	0.03	0.34
1.58	0.04	0.15	0.36	0.65
1.49	0.30	0.44	0.73	0.97

Table 4.18 : Foam D

$\frac{10^3}{T^\circ K}$	ln ln W_o'/W_t			
	7 min	20 min	1 h	3 h
2.31				
2.11		- 2.75	- 1.54	- 1.13
1.93	- 0.93	- 0.88	- 0.87	- 0.84
1.78	- 0.49	- 0.48	- 0.46	- 0.29
1.65	- 0.55	- 0.32	- 0.11	0.15
1.58	- 0.13	0.00	0.28	0.70
1.49	0.08	0.27	0.83	1.03

Table 4.19 : Foam E

$\frac{10^3}{T^oK}$	ln ln W_o'/W_t			
	7 min	20 min	1 h	3 h
2.31				
2.11		- 3.50	- 2.66	- 2.44
1.93	- 2.33	- 2.30	- 2.13	- 1.98
1.78	- 1.78	- 1.52	- 1.61	- 1.28
1.65	- 1.46	- 1.22	- 0.97	- 0.20
1.58	- 1.25	- 1.04	- 0.62	0.21
1.49	- 0.86	- 0.25	0.54	0.91

The results are plotted in figures 4.14 to 4.18. It can be seen that the curves are not the straight lines the model predicts, but that they diverge at both high and low values of T. At low temperatures the weight loss does not differ by much from the F11 concentration, so any variation or inaccuracy in this figure will have a large effect on the ordinate. Mean gradients of the curves were measured in three regions and activation energies calculated from them. Table 4.20 holds the values,

Table 4.20 : Activation Energies

$10^3/T^oK$	Activation Energy kJ $mole^{-1}$		
	1.5 - 1.6	1.65 - 2.1	~2.2
Foam A	54	33	54
Foam B	34	34	54
Foam C	30	30	45
Foam D	51	22	-
Foam E	78	29	20

which are a little lower than the 80 kJ $mole^{-1}$ quoted for the pyrolysis of wood[18] or the 100 kJ $mole^{-1}$ typical value for the oxidation of wood fibreboard, cotton linters, natural rubber foams and cork.[37]

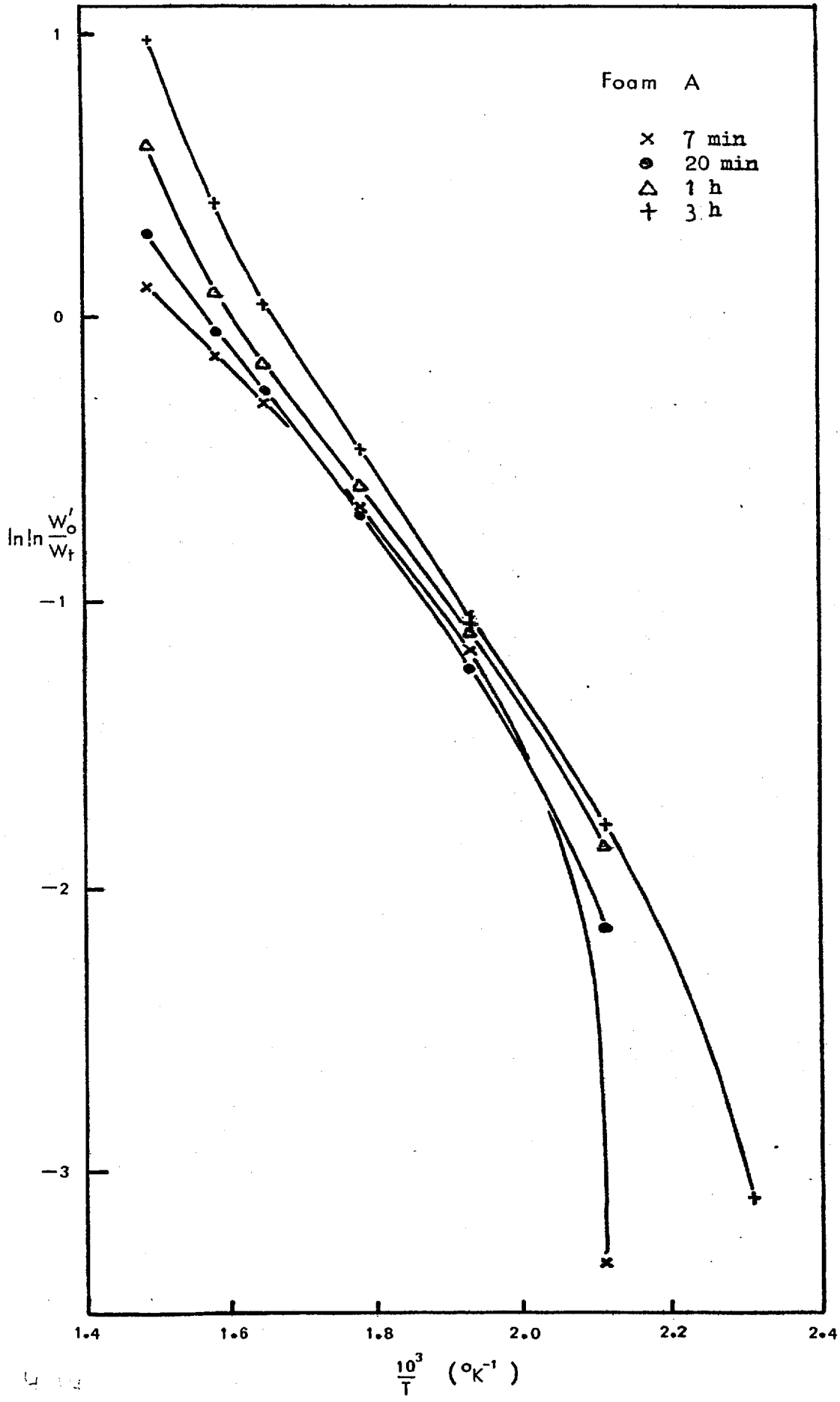

Figure 4.14 ; Arrhenius plot of weight loss results – Foam A.

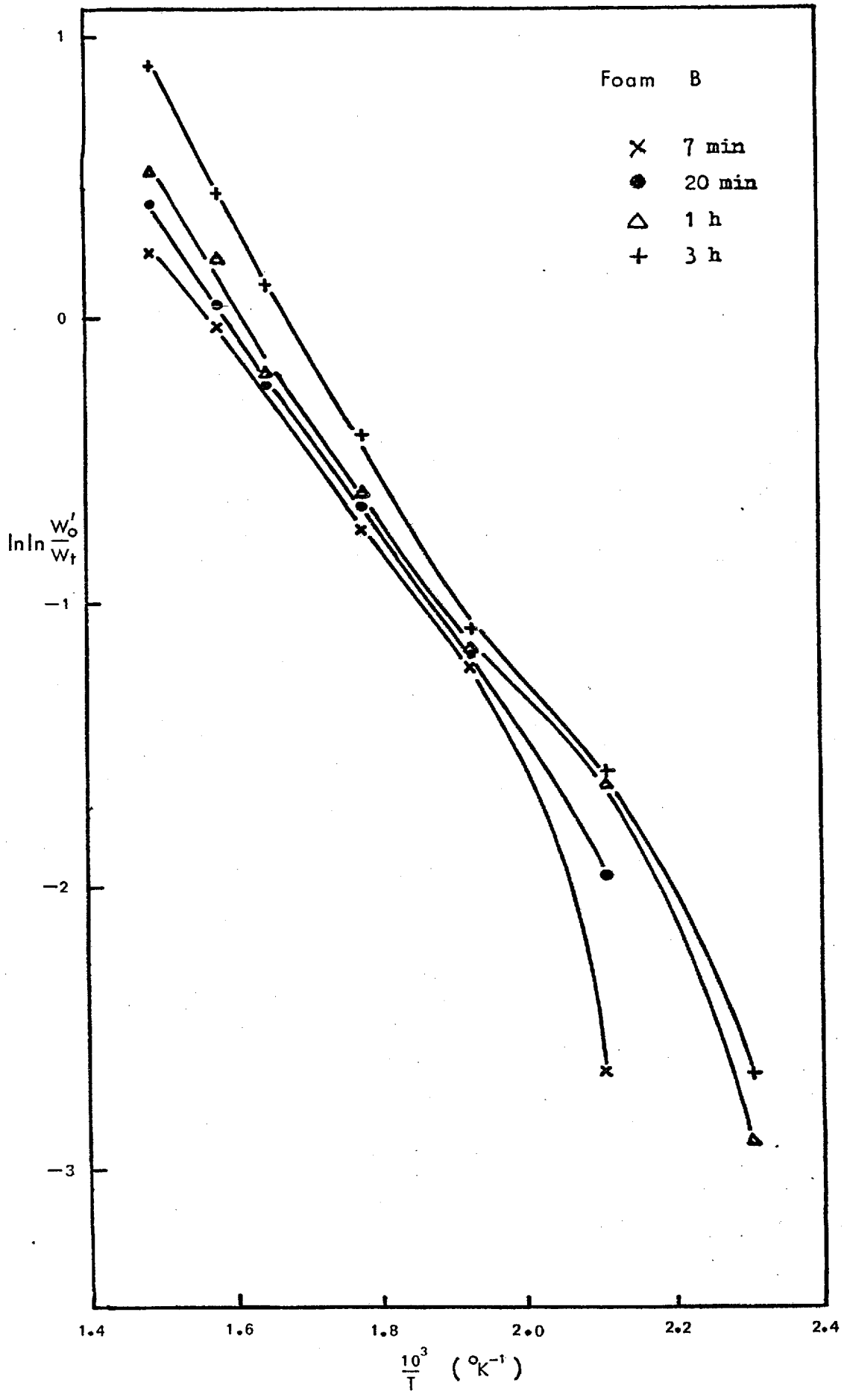

Figure 4.15 ; Arrhenius plot of weight loss results - Foam B.

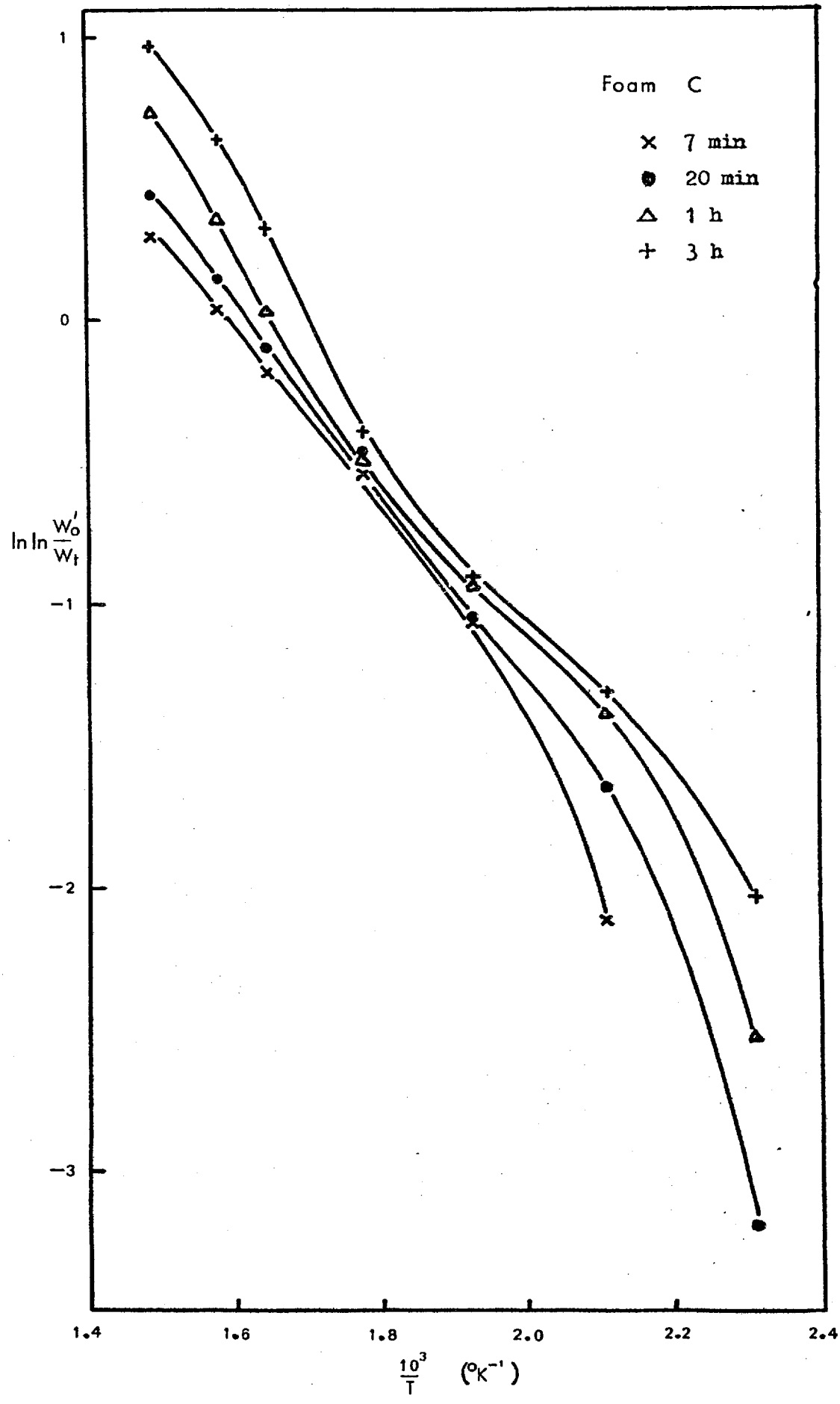

Figure 4.16 ; Arrhenius plot of weight loss results – Foam C.

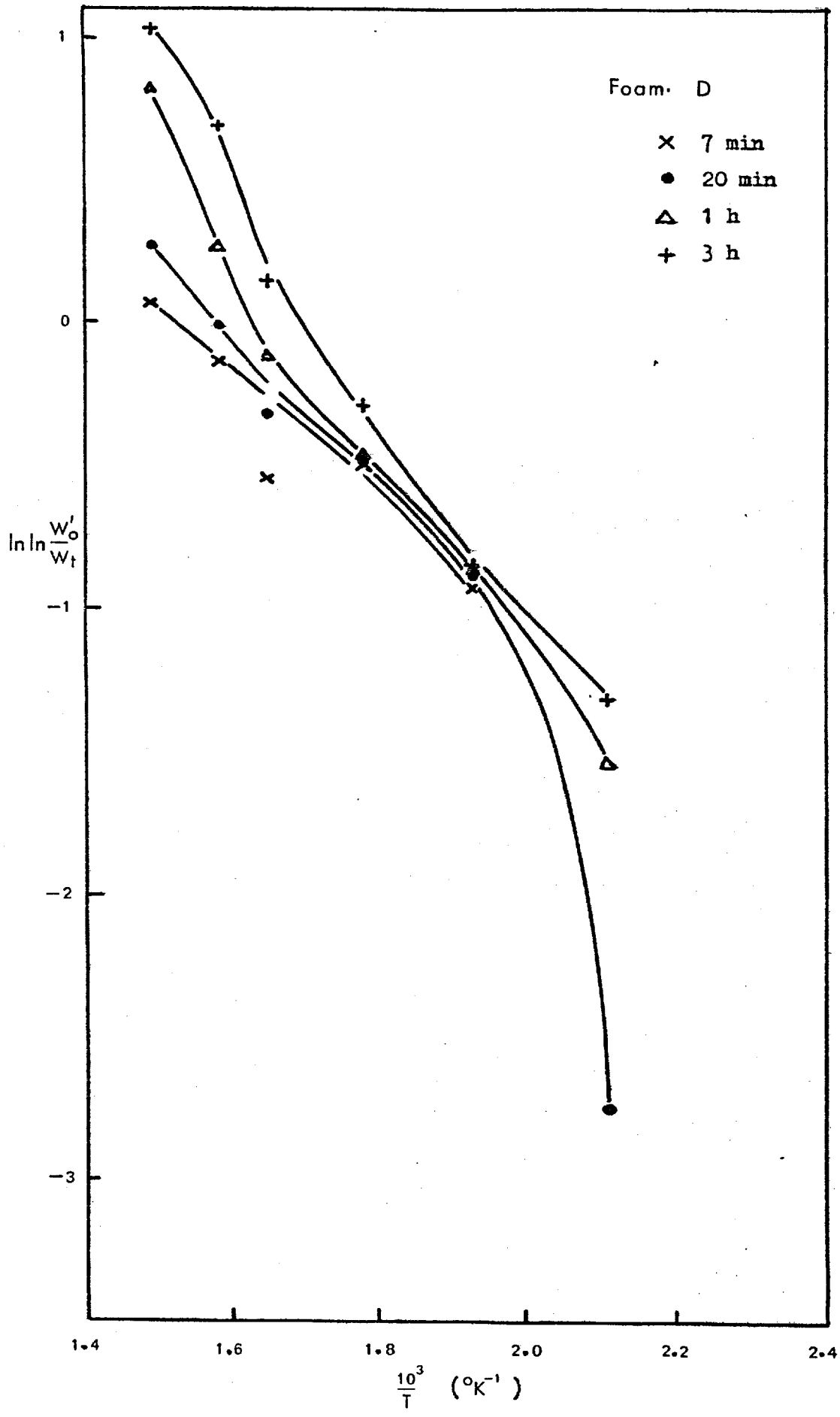

Figure 4.17 ; Arrhenius plot of weight loss results – Foam D.

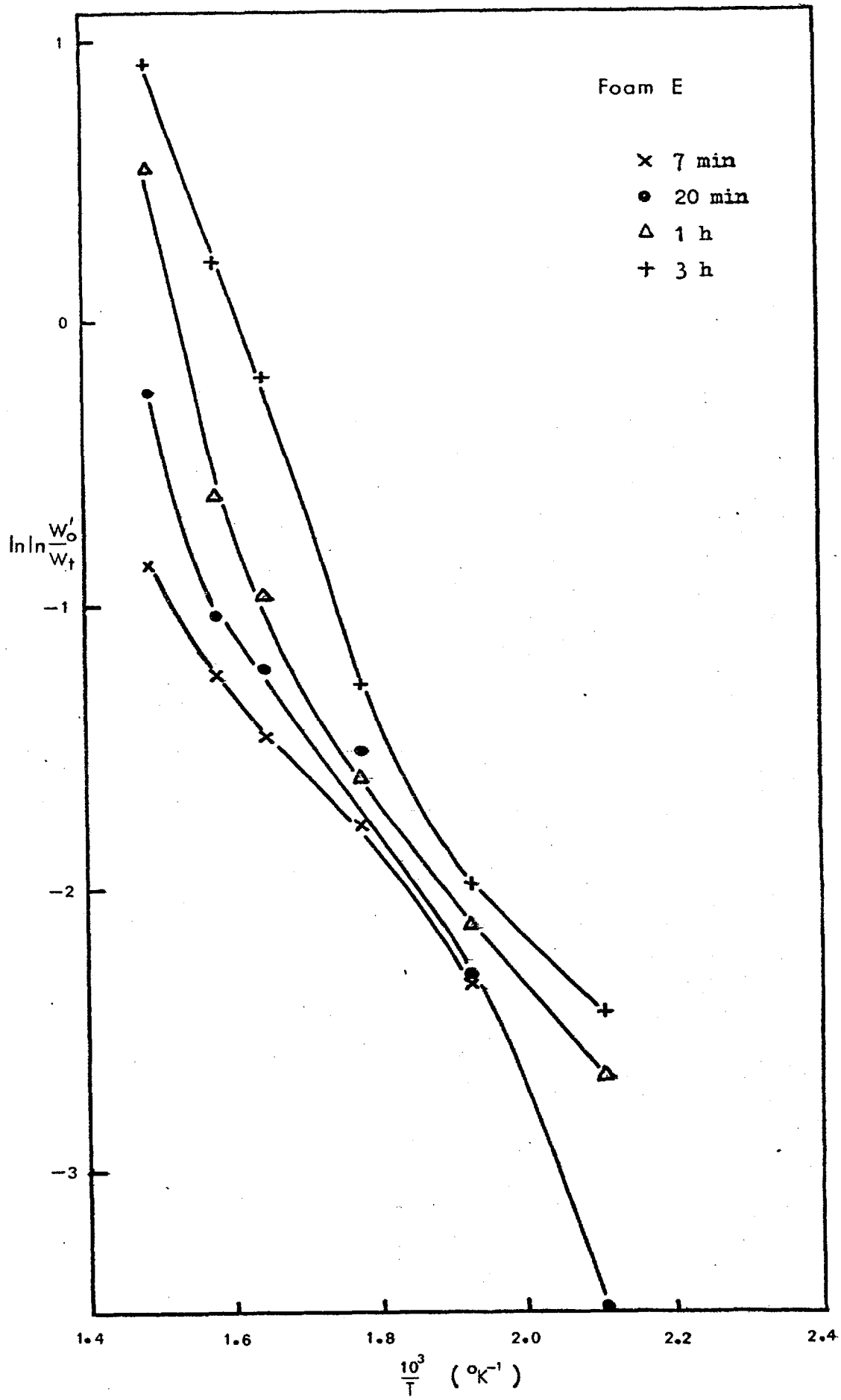

Figure 4.18 ; Arrhenius plot of weight loss results – Foam E.

Using a similar technique Gamadia investigated polyurethane foams of higher density. Results for foams of density 64 kg m^{-3} are shown in tables 4.21 and 4.22.

Table 4.21 : Rigid foam, with 30 parts TCEP. 64 kg m^{-3}

	Fractional weight loss	
Temperature, ^{o}C	after 5 min	after 10 min
230	0.075	0.102
270	0.175	0.257
300	0.230	0.336
330	0.485	0.527

Table 4.22 : Flexible (high modulus) foam. 64 kg m^{-3}

	Fractional weight loss	
Temperature, ^{o}C	after 5 min	after 10 min
230	0.060	0.100
270	0.105	0.300
300	0.330	0.420
330	0.420	0.445

For the rigid foam a blowing agent fraction of 0.05 is assumed, but the flexible foam is of an open cell structure and so no gas is encapsulated. The Arrhenius plots for these data are shown in figures 4.19 and 4.20. Using the gradients denoted by the broken lines, activation energies have been calculated to be 71 kJ $mole^{-1}$ for the rigid foam and 52 kJ $mole^{-1}$ for the flexible foam. These values are higher than those for the lower density foams, probably on account of the greater surface area in the materials upon which the volatile products can crack to produce carbon, so decreasing the rate of global weight loss.

These calculations were made assuming complete conversion of solid to gas, without any solid residue. If such an allowance is made, then the shape of

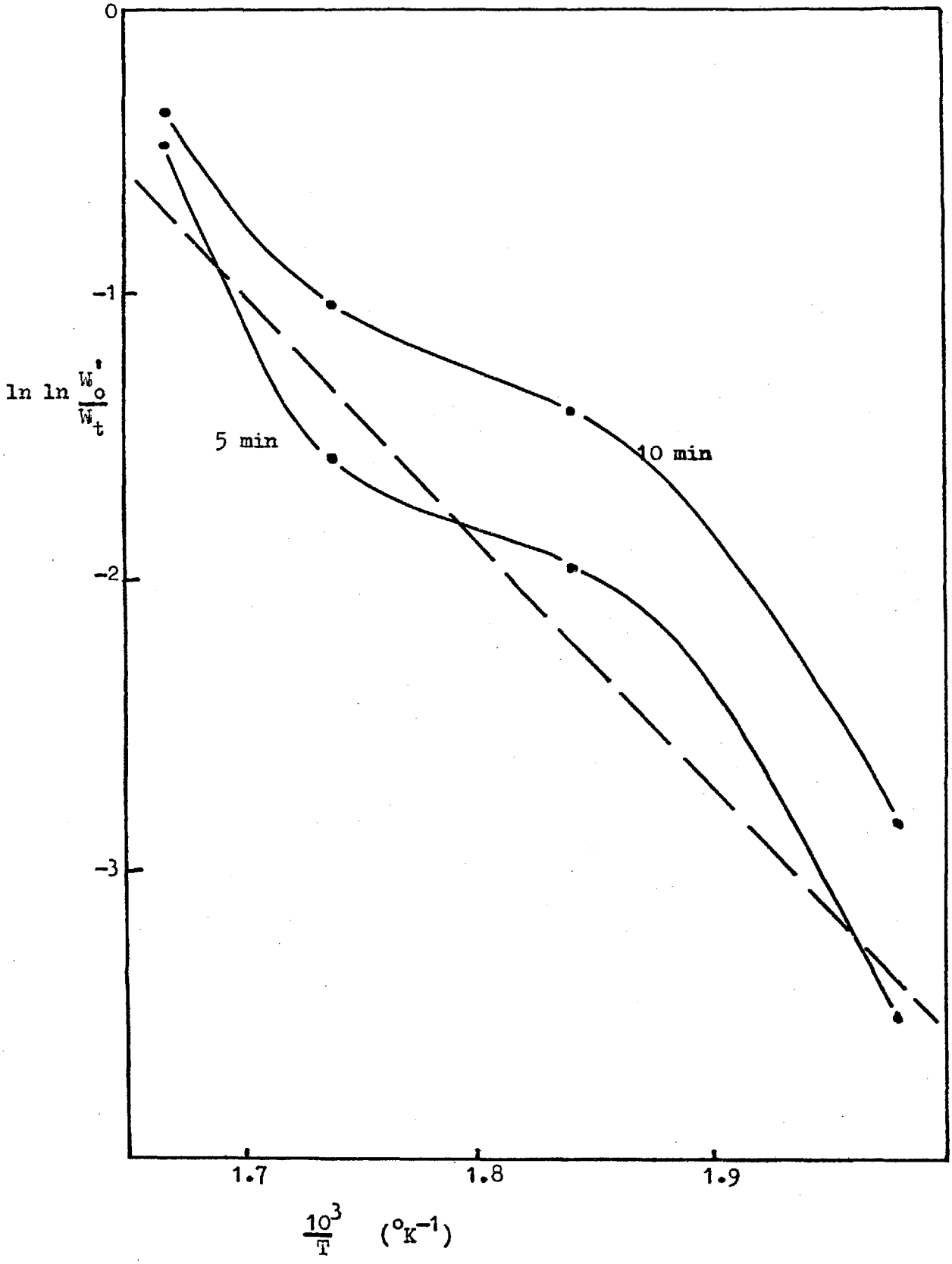

Figure 4.19 ; Arrhenius plot from weight loss - Rigid foam with 30 parts TCEP, and density 64 kg m^{-3}.

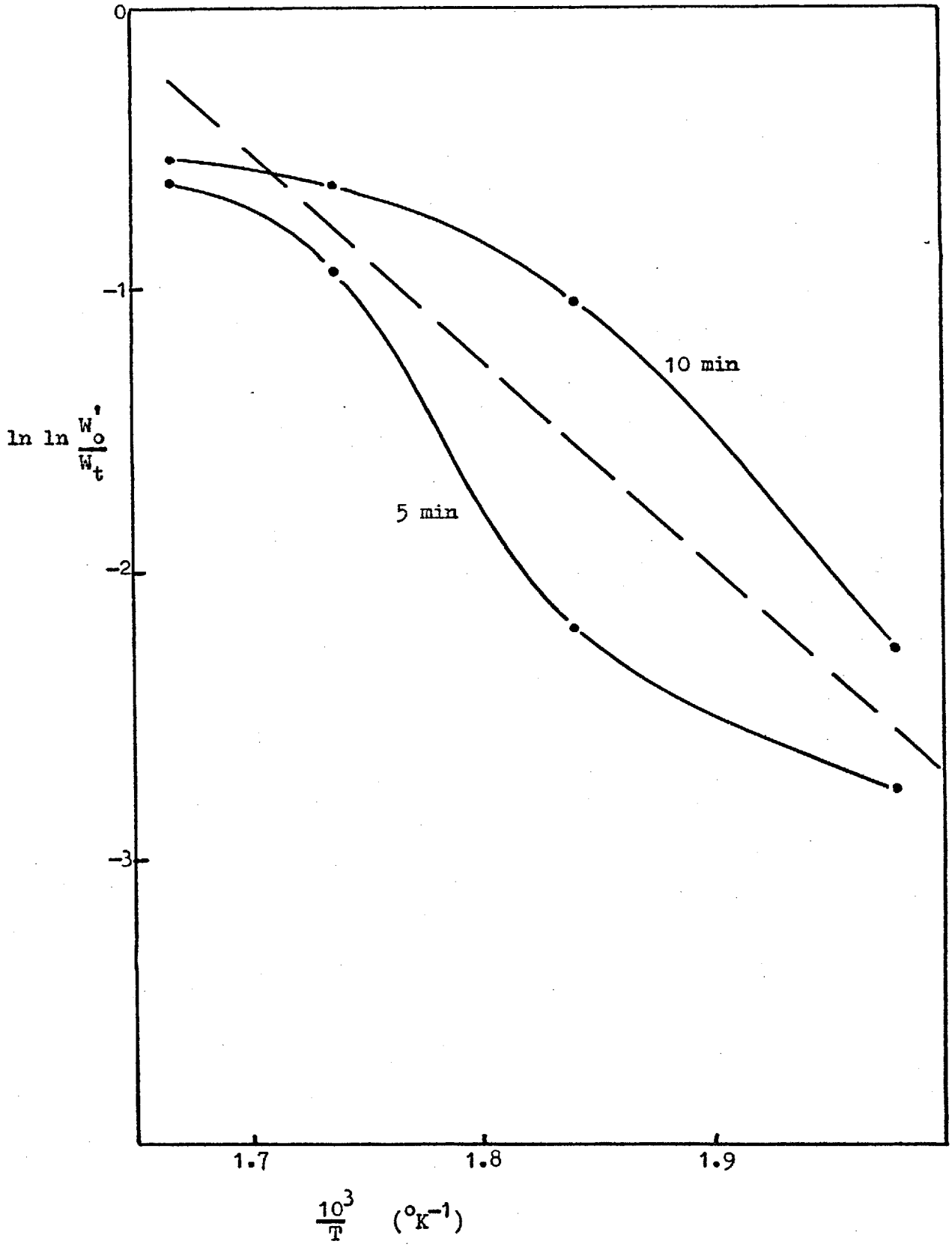

Figure 4.20 ; Arrhenius plot from weight loss - Flexible (high modulus) foam of density 64 kg m^{-3}.

the Arrhenius plot is changed.

If reaction of unit weight produces x solid residue, then let y_t be the weight of reactive solid at time t. When y_t remains, $y_o - y_t$ has reacted to give a residue of $x(y_o - y_t)$, thus the total weight remaining, W_t

$$= y_t + x(y_o - y_t),$$

$$\therefore \quad y_t = \frac{W_t - x\,y_o}{1-x} \qquad \text{and} \quad d\,y_t = \frac{1}{1-x}\,dW_t$$

$$\text{But} \quad \frac{dy_t}{dt} = -ky_t$$

$$\therefore \quad \frac{1}{1-x}\,\frac{dW_t}{dt} = -k\,\frac{W_t - xy_o}{1-x}$$

$$\therefore \quad \frac{dW_t}{W_t - xy_o} = -kdt, \quad \text{which on integration gives}$$

$$\ln (W_t - xy_o) = -kt + \text{constant}$$

$$\text{At } t = o, \quad W_t = W_o', \quad \text{and } y_o = W_o',$$

$$\therefore \quad \ln \frac{W_o' - xW_o'}{W_t - xW_o'} = +kt,$$

$$\therefore \quad \ln \ln \frac{W_o' - xW_o'}{W_t - xW_o'} = \ln At - \frac{E_{act}}{RT}$$

There is no simple relationship between $\ln \ln \frac{W_o' - xW_o'}{W_t - xW_o'}$ and $\ln \ln \frac{W_o'}{W_t}$, but one such typical curve for the case of $W_o' = 0.872$ and $x = 0.057$ is shown in figure 4.21.

The amended family of curves allowing for 5% of the original sample remaining as char is shown for Foam A in figure 4.22. Comparison with figure 4.14 shows that there is a positive displacement of the curves, a natural consequence of decreasing the numerator and denominator of the fraction, but little difference in gradient even at high temperatures - the activation energy calculated at $1/T = 1.5 \times 10^{-3}$ is 57 kJ mole^{-1}.

The activation energy found by this means must obviously be a global value as there is not one single reaction occurring, but a great number. Many are

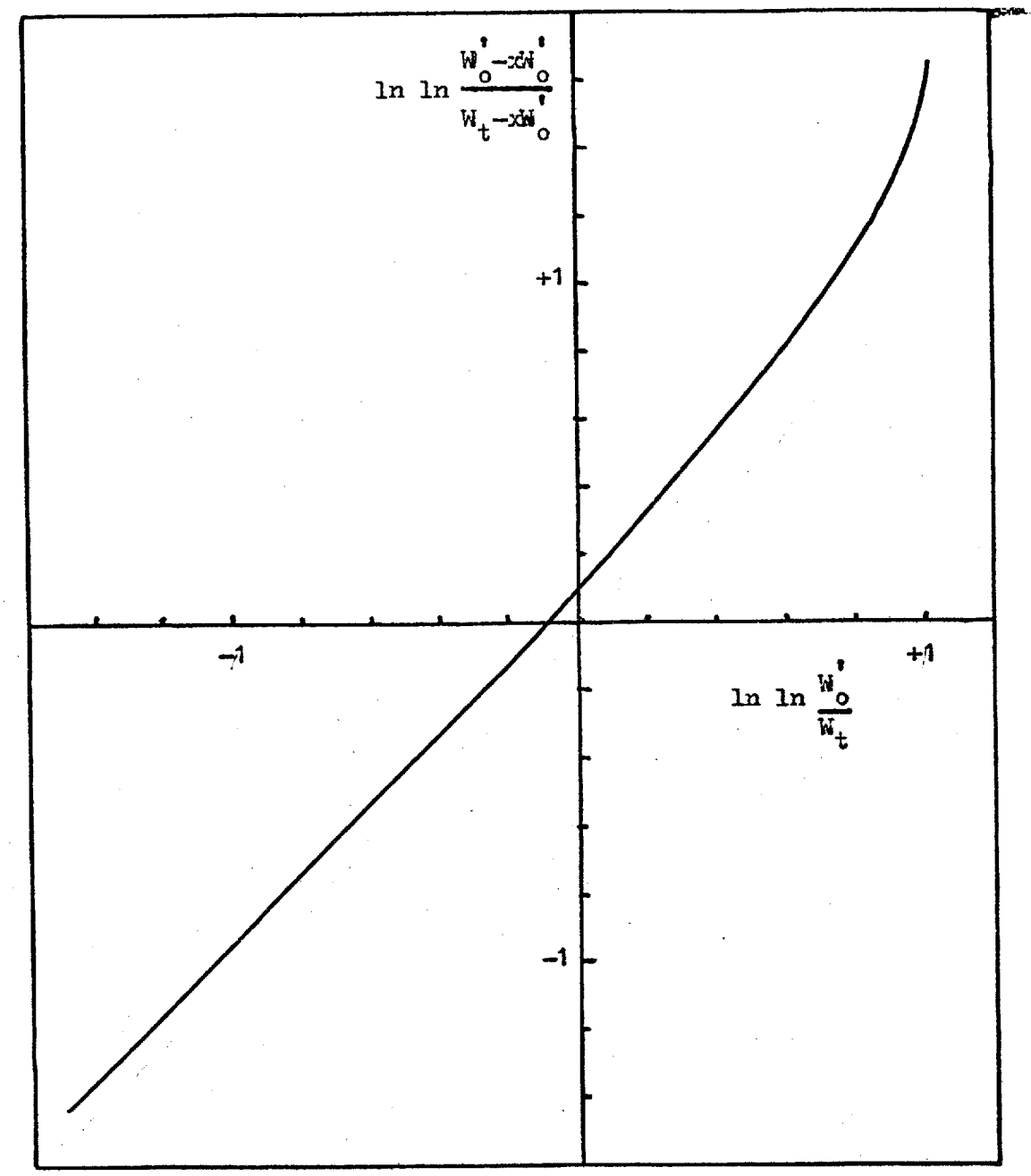

Figure 4.21 ; Effect of solid residue on Arrhenius plots of weight loss results (for the case W'_o=0.872, x=0.057)

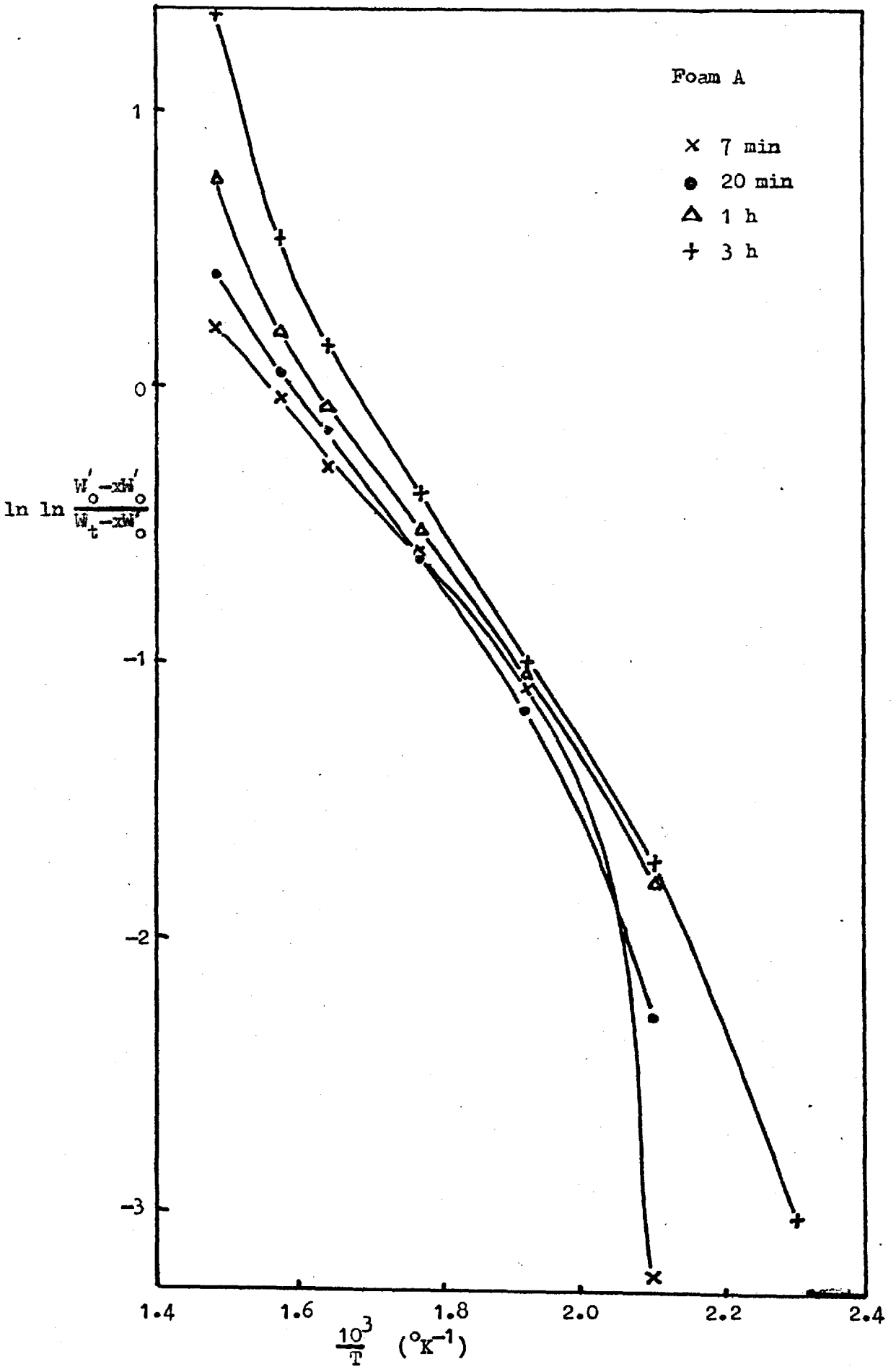

Figure 4.22 ; Arrhenius plot of weight loss results – Foam A,

(allowing for 5% remaining as char).

simultaneous reactions, but others are sequential, depending on the products of prior reactions. There are reactions between the gaseous and solid phases and these are particularly dependent on the nature of the surface which is constantly changing. Some reactions cause no loss of weight and others condense the gaseous materials. When the foam is subjected to different temperatures there are different reaction schemes as one or another reaction is favoured by the prevailing conditions, and this has effect on the subsequent reactions too.

Thus it is seen that the global activation energy is of limited value in a real situation and should be used with caution.

In addition to the variations caused by multiple reaction systems, there is also the problem of defining an activation energy for a solid or solid/gas reaction. In the above calculation weight of solid was taken as a measure of concentration, but it is doubtful that this truly represents the correct picture even if a unimolecular first order reaction does occur, especially if the reacting 'molecule' is a section of the polymeric matrix. In solid reactions the expression 'mole' has limited applicability as it is not possible to define it meaningfully - in a highly crosslinked structure such as rigid polyurethanes the 'molecule' could extend throughout the mass of the sample.

4.3.6 Characteristics of Char

Observations and measurements made on the samples of foam utilised in the weight loss experiments are recorded in section 3.3. As all these measurements were taken when the samples had cooled, the assessment of strength may well have been inaccurate as the softened foam became quite rigid when the temperature fell. The other observations were not affected by this cooling.

The foams A, B and C all showed some signs of decomposition at 160°C as was evidenced by the discolouration, but even after 180 minutes there was no loss of strength or breakdown of the cellular structure. When subjected to a temperature of 200°C the walls of the cells started to degenerate

producing larger cavities within the foam (figure 4.23). This did not weaken the foam as the effect was countered by the increase in rigidity of the struts and membranes that remained intact, and a reduction in size of the sample. As the time increased so did the slight signs of softening of the materials become apparent as an iridescence of the glazed surfaces. The presence of TCEP produced greater shrinkage and an earlier onset of softening.

The condition of these foams after exposure to 245°C was markedly altered – shrinkage was high and the interior was weak, with large cells as shown in figure 4.24. Overall sample strength was provided by the rigid shell which was more substantial in the foam without added TCEP. The insides of the shells were glazed and, when cooled after seven minutes exposure, the interior structure of foam C exhibited a glass-like texture. At 290°C and 330°C foams A and B behaved in similar fashions. Both were reduced to a weak shell with a weak large-celled interior, and suffered medium shrinkage, except that foam B after seven minutes was only an empty shell (figure 4.25). Foam C however only suffered low shrinkage for the shorter exposure times, and showed a tendency to greater strength as the shrinkage increased and cell size decreased with time of exposure.

At 360°C and 400°C all three foams became very weak, although the shrinkage varied with exposure time. Foam A reduced to a thin shell and sometimes contained a flimsy filling as shown in figure 4.26. Foams B and C were both composed of a very frail iridescent filling of medium cell size in a continuous carbonaceous shell, which in the case of foam C was very thin.

Up to 200°C the reactions made little change to the physical appearance of the foam, but at temperatures above this the materials undergo reactions which have shorter chain length products that have a melting or softening point below the reaction temperature. The decrease in initial shrinkage at the elevated temperatures indicates that the low softening point products further decompose to give non-softening products before sufficient time has

Figure 4.23 ; Char from weight loss experiment

Foam D, 1 hour at 200°C.

Figure 4.24 ; Char from weight loss experiment,

Foam C, 1 hour at 245°C.

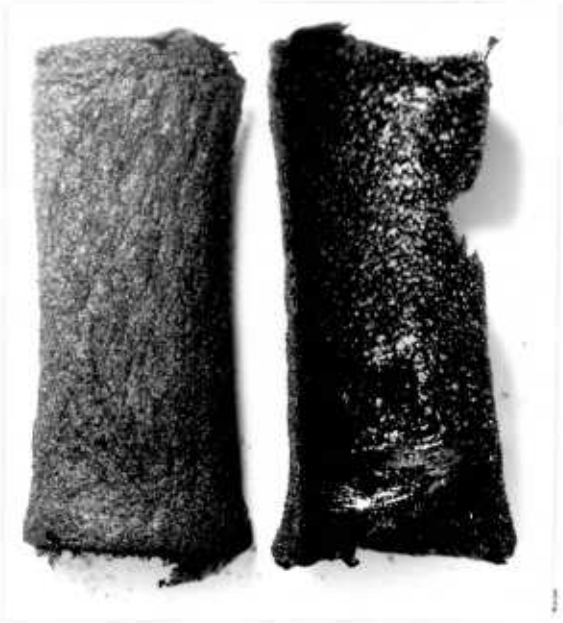

Figure 4.25 ; Char from weight loss experiment,
Foam B, 7 minutes at 290°C.

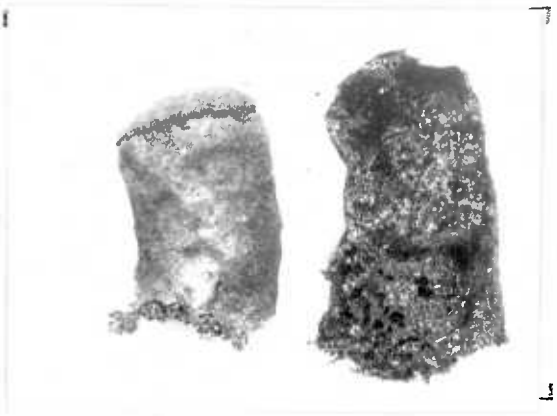

Figure 4.26 ; Char from weight loss experiment,
Foam A, 1 hour at 400°C.

elapsed to allow the softened material to coalesce. This is a result of the complexity of a material which undergoes many reactions simultaneously when heated, the course of the reactions depending on the balance of factors influencing the individual rates of reaction.

The major effect of the added TCEP appeared to be to increase the softening of the material which is to be expected as it is frequently used as a plasticiser,[33] but at higher temperatures it may have assisted in the production of the soft iridescent core of the sample.

Table 3.14 shows the observations made on foam D. Up to 200°C the behaviour was the same as that of foams A, B and C, but at higher temperatures the char had markedly different characteristics. The strength slowly decreased with increasing temperature but even at 360°C the sample was still moderately strong. The formation of a relatively thick outer shell of finely textured char was responsible for delaying the onset of frailty. The inner volume may have been weak with large cells but the outer portion appeared to "crack" the volatile matter produced at the centre and to lay down a char with small cells (figure 4.27) that provided continuing strength. As heating continued this slowly decomposed and the sample size decreased correspondingly.

Even at 400°C foam D did not immediately lose its strength. Although it was decomposing steadily there was still a reasonable amount of substantial char after 20 minutes of exposure, but after one hour the char was of little use as an insulant (figure 4.28).

The mode of degradation of the isocyanurate based material, foam E, differed in several important aspects from that of the other materials studied. The strength of the charred sample was comparable with that of the untreated foam until it suffered prolonged exposure to temperatures in excess of 350°C, and at no stage did softening become apparent or the cell structure show signs of breakdown. At the lower experimental temperatures the surface of the samples was broken by a plethora of small cracks which

Figure 4.27 ; Char from weight loss experiment, Foam D, 20 minutes at 290°C.

Figure 4.28 ; Char from weight loss experiment, Foam D, 1 hour at 400°C.

enlarged as time continued. At 245°C these fissures developed until the sample was rift in several approximately parallel planes along the cylindrical axis and direction of rise as evidenced in figure 4.29. These cracks were probably started by the thermal shock on introduction of the sample to the high temperature environment. Any stresses left in the material after manufacture, or weaknesses introduced during sample preparation would automatically act as nuclei for the development of these fissures. Expansion in a network of material as rigid as this isocyanurate foam could produce areas of high stress where the tensile strength could be exceeded, especially in the plane of foam rise where the bubbles are elongated and the cross sectional area of solid decreased.

An increase of the temperature to 290°C started chemical decomposition that turned the foam grey and rendered it less liable to cleavage. The more rapidly this degradation occurred the less the extent of the physical fragmentation.

A further phase in the degradation was apparent after prolonged exposure at 360°C. This was the failure of the strength of the char.As the internal black honeycomb became fragile and grey the size of the sample underwent dramatic reduction (figure 4.30).

From these observations it is obvious that the different materials offer varying degrees of insulation after they have been exposed to hot atmospheres. After exposure to 250°C and above, with no combustion, the foams A, B and C were reduced to little more than a flimsy shell which would be detached from its position by any slight draught. At temperatures up to 200°C the foams retained their integrity and the factor limiting their efficiency was the shrinkage suffered. Performance in this respect decreased as the concentration of TCEP increased, probably on account of the action of this additive as a plasticiser.

Incorporation of phosphorus into the structure of the foam improved the nature of the char. Degradation of the foam structure at temperatures in

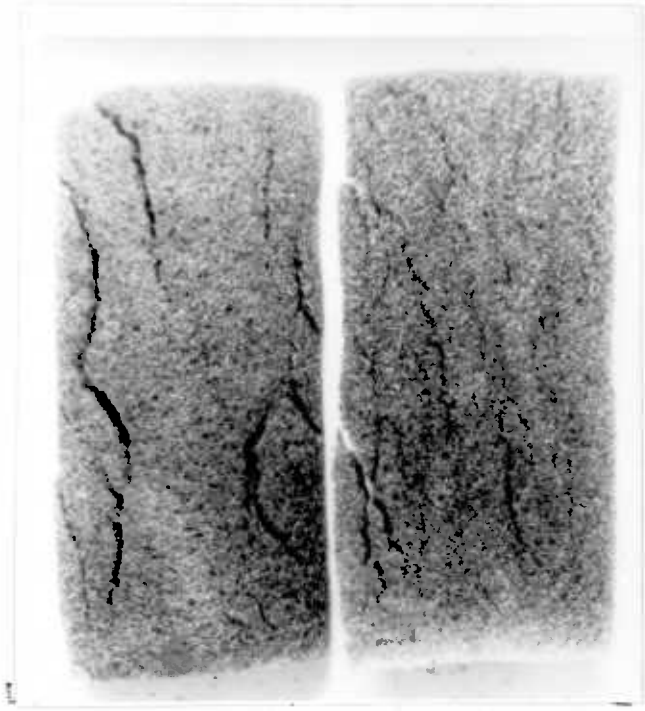

Figure 4.29 ; Char from weight loss experiment,
Foam E, 1 hour at 245°C.

Figure 4.30 ; Char from weight loss experiment,
Foam E, 3 hours at 400°C.

excess of 200°C again occurred as would be expected from the presence of urethane groups but the resulting char was acceptably strong up to temperatures greater than 330°C. A marginal improvement in the shrinkage of the sample resulted from the addition of phosphorus, but the real gain was in the thick cellular wall that was formed around the softened interior. It was a shell that would resist removal by a strong draught and would not shatter upon the infliction of minor physical damage.

Dimensional stability of the isocyanurate foam, E, was very good up to 360°C. The char retained a degree of strength only a little below that of the original foam right up to this same temperature. The char was homogeneous and capable of providing continued protection against both thermal and physical damage even at high temperatures. The problem posed at lower temperatures was of a different nature. At temperatures between 160°C and 250°C the physical breakage of the foam was the cause of loss of strength and protection. This behaviour could not occur when the foam was faced with a solid material, as in a composite panel, and could presumably be prevented by coating the surface with a thin coating to render any faults innocuous as nucleifor splitting.

Rigid urethane foams of density 64 kg m^{-3} and 128 kg m^{-3} suffer similar thermal damage[40] as did foams A, B and C: viz, the interior melts to give a structure with large glazed cavities, and a thin shell is formed on the surface. The higher density foam produces a slightly stronger shell, but it is insufficient to offer any real protection. The improvement in dimensional stability appears to be due to the higher internal pressure of volatile materials and a less permeable shell, which counteract the tendency to shrink on softening.

Figures 4.31 to 4.35 record the state of the samples from the ignition experiments recorded in table 3.5. The samples were exposed to 25.2 kW m^{-2} for 5 minutes. The rectangular outline in the figures indicates the side elevation of the original sample, 100 mm x 50 mm.

Figure 4.31 ; Sample from ignition experiment after 5 minutes exposure at 25.2 kW m^{-2} - Foam A.

Figure 4.32 ; Sample from ignition experiment after 5 minutes exposure at 25.2 kW m^{-2}, - Foam B.

Figure 4.33 ; Sample from ignition experiment after 5 minutes exposure at 25.2 kW m^{-2}, - Foam C.

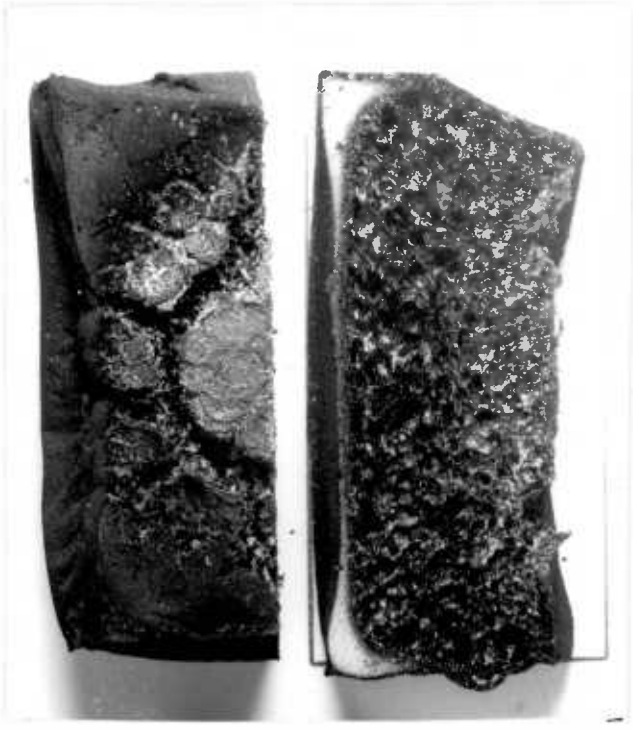

Figure 4.34 ; Sample from ignition experiment after 5 minutes exposure at 25.2 kW m^{-2}, - Foam D.

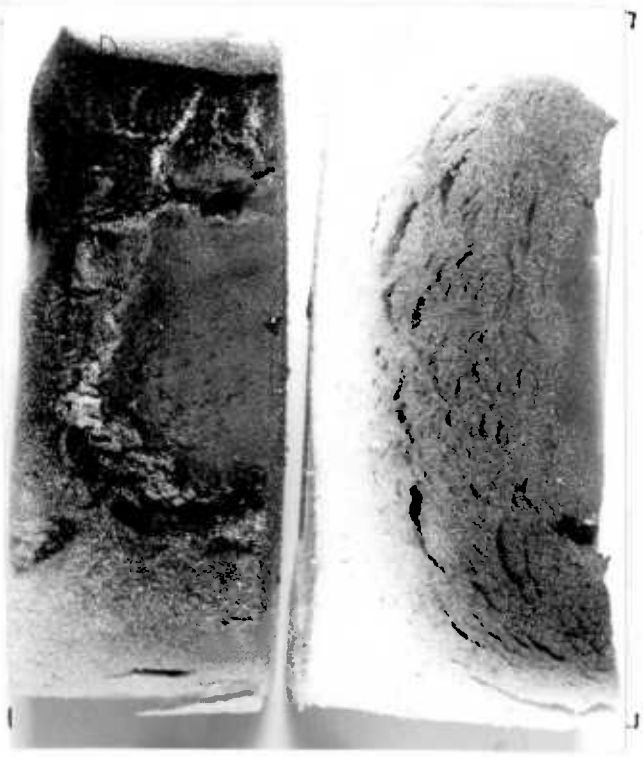

Figure 4.35 ; Sample from ignition experiment after 5 minutes exposure at 25.2 kW m^{-2}, - Foam E.

It is seen that foams A, B and C were almost completely consumed, the only part remaining being the bottom of the back face where convection currents hindered the spread of flame.

The addition of phosphorus in foam D did not prevent reaction at the rear face of the sample, but the resulting char was strong and offered continued service as an insulating layer after the flame had extinguished.

The behaviour of foam E was fully in accord with the observations of the chars from the weight loss experiments. As the temperature increased from the back face to the front there was a graduation in char properties, from slight discolouration, through cracks in the body of the foam, and a strong dark char, to the soft grey char at the irradiated area of the surface. The extent of damage is seen in figure 4.35 which shows that after 5 minutes exposure to 25.2 kW m^{-2} this material offered protection little short of that which it had given before irradiation.

4.3.7 Activity of Chars

An activation energy for the oxidation of the char can be derived from the experiments described in section 2.4.3.

Assuming all the heat of reaction raises the temperature of the reacting mass then,

$$\triangle H_R = \rho C_p \triangle T ,$$

but the rate of heat generation is proportional to the rate of reaction, so

$$\rho C_p \frac{dT}{dt} = A \exp \left[- \frac{E_{act}}{RT} \right]$$

$$\therefore \quad \log \frac{dT}{dt} = \log \frac{A}{\rho C_p} - \frac{E_{act}}{2.3\ RT}$$

and a plot of $\log \frac{dT}{dt}$ versus $\frac{1}{T}$ will have a slope of $- \frac{E_{act}}{2.3\ R}$

This is a simple model as it does not make provision for heat losses to the gas stream and surroundings, or take account of the diminishing size and varying density of the sample, but nevertheless it provides a useful estimate of the activation energy.

Measurements made from the results in section 3.3.3 and derived values are given in the following tables.

Table 4.23: Foam A, char from radiant panel

$\frac{10^3}{T}$ ($^oK^{-1}$)	T ^oK	T ^oC	$\frac{dT}{dt}$ ($^oC\ min^{-1}$)	log $\frac{dT}{dt}$
1.97	508	235	17.5	1.243
1.91	523	250	30	1.477
1.825	548	275	50	1.699
1.75	573	300	68	1.833
1.605	623	350	150	2.176

Table 4.24: Foam A, char from weight loss furnace

$\frac{10^3}{T}$ ($^oK^{-1}$)	T ^oK	T ^oC	$\frac{dT}{dt}$ ($^oC\ min^{-1}$)	log $\frac{dT}{dt}$
1.825	548	275	43	1.634
1.75	573	300	105	2.021
1.675	598	325	205	2.312
1.605	623	350	400	2.600

Table 4.25: Foam B, char from radiant panel

$\frac{10^3}{T}$ ($^oK^{-1}$)	T ^oK	T ^oC	$\frac{dT}{dt}$ ($^oC\ min^{-1}$)	log $\frac{dT}{dt}$
2.05	498	225	35	1.544
1.91	523	250	75	1.875
1.825	548	275	130	2.115
1.75	573	300	200	2.300
1.675	598	325	350	2.545

Table 4.26: Foam C, char from radiant panel

$\frac{10^3}{T}$ ($^oK^{-1}$)	T ^oK	T ^oC	$\frac{dT}{dt}$ ($^oC\ min^{-1}$)	log $\frac{dT}{dt}$
1.875	533	260	35	1.544
1.825	548	275	70	1.845
1.75	573	300	160	2.205
1.675	598	325	280	2.447

Table 4.27: Foam C, char from weight loss furnace

$\frac{10^3}{T}$ ($^oK^{-1}$)	T ^oK	T ^oC	$\frac{dT}{dt}$ ($^oC\ min^{-1}$)	log $\frac{dT}{dt}$
1.533	653	380	25	1.400
1.515	660	387	50	1.700
1.485	673	400	110	2.040
1.434	698	425	600	2.778

Table 4.28: Foam D, char from radiant panel

$\frac{10^3}{T}$ ($^oK^{-1}$)	T ^oK	T ^oC8	$\frac{dT}{dt}$ ($^oC\ min^{-1}$)	log $\frac{dT}{dt}$
2.05	498	225	20	1.30
1.91	523	250	45	1.65
1.825	548	275	95	1.98
1.75	573	300	185	2.27

Table 4.29: Foam E, char from radiant panel

$\frac{10^3}{T}$ ($^oK^{-1}$)	T ^oK	T ^oC	$\frac{dT}{dt}$ ($^oC\ min^{-1}$)	log $\frac{dT}{dt}$
1.792	558	285	55	1.741
1.750	573	300	92	1.964
1.675	598	325	200	2.300
1.605	623	350	250	2.400

Table 4.30: Foam E, char from weight loss furnace

$\frac{10^3}{T}$ ($^oK^{-1}$)	T ^oK	T ^oC	$\frac{dT}{dt}$ ($^oC\ min^{-1}$)	log $\frac{dT}{dt}$
1.632	613	340	63	1.800
1.605	623	350	100	2.00
1.543	648	375	200	2.30
1.485	673	400	350	2.544
1.434	698	425	600	2.779

Inspection of the curves in figures 3.11 - 3.18 revealed a similar basic behaviour for all the chars tested. When the exothermic reactions occurred and rapid rises in temperature were recorded, the graphs showed that the curves were not simple but appeared to be a curve with a peak superposed on it, indicating that one reaction proceeded over the period recorded, but another persisted for only part of the time. For example the char from Foam B (figure 3.13) showed a secondary reaction between $2\frac{1}{2}$ and $4\frac{1}{2}$ minutes and the weight loss char from foam A gave a very clear auxiliary reaction (figure 3.12). This feature was particularly noticeable in the chars from Foams A and E produced in the weight loss furnace. The samples were not subjected to such high temperatures during charring as were the other samples and appreciable proportions of molecules stable at the temperature of preparation could have been

formed. The char from Foam C formed by pyrolysis was expected to show a different behaviour as the sample taken was the insubstantial golden foamed filling from the carbonaceous shell. This filling was probably formed when the core of the sample had melted onto the charred outer shell and at some stage a volatile component of the ensuing decomposition products had boiled and foamed the liquid portion which further reacted to solidify in the form of the sample taken.

When the activation energy was calculated from these data no attempt was made to separate the peaks of the various reactions, but the global value was derived for all the reactions that contributed to the exponential temperature rise.

The plots of $\log \frac{dT}{dt}$ versus $\frac{1}{T}$ are shown in figure 4.36 and tables 4.31 and 4.32 give the activation energies calculated from the gradients of these lines.

Table 4.31: Activation Energies of chars from radiant panel

Foam	E_{act} (kJ $mole^{-1}$)
A	51
B	51
C	86
D	62
E	91

Table 4.32: Activation Energies of chars from weight loss furnace

Foam	E_{act} (k J $mole^{-1}$)
A	90
C	254
E	87

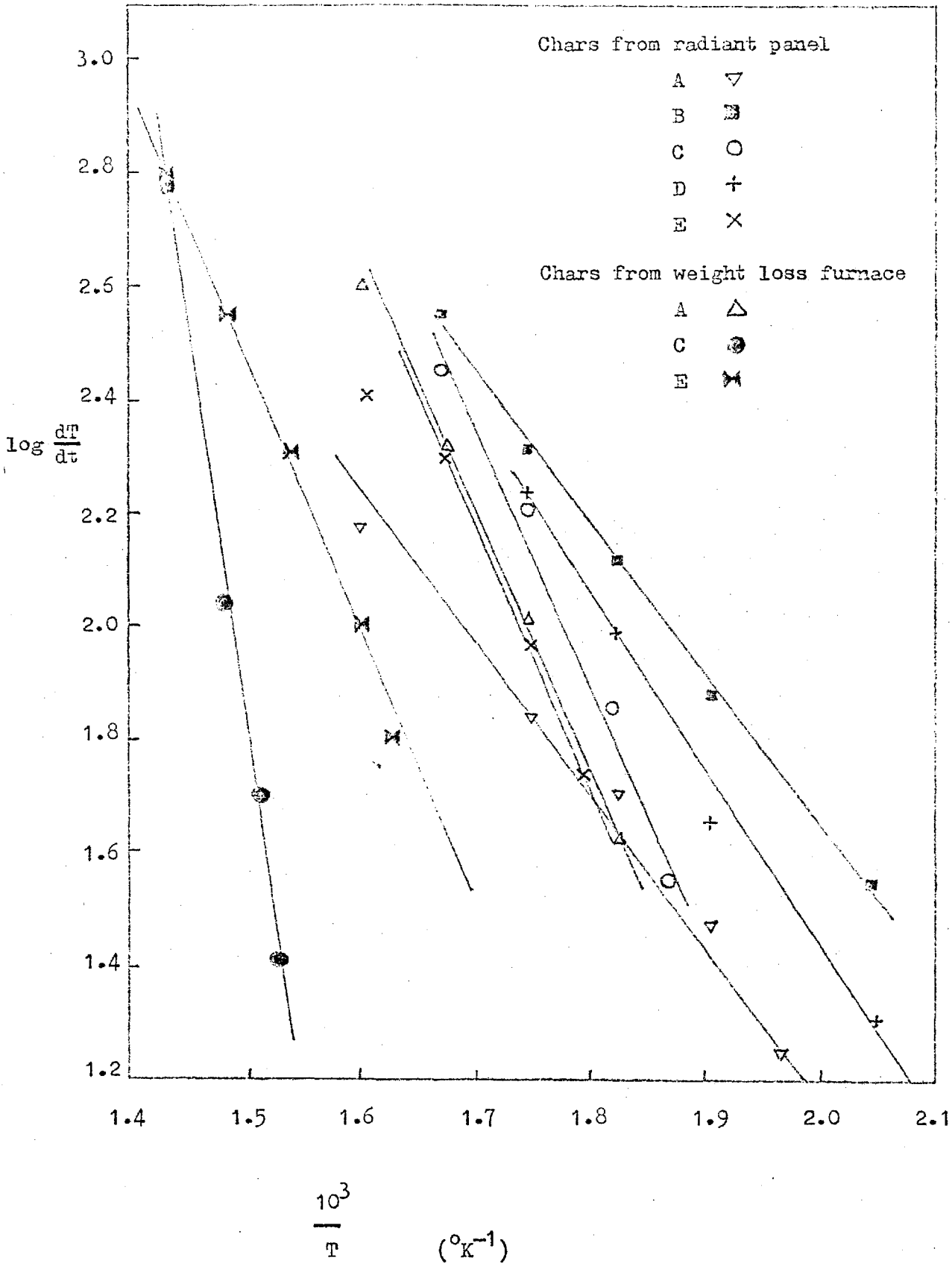

Figure 4.36 ; Arrhenius plot for char activity.

To derive the gradients of the curves in section 3.3.3 the tangents were found at several temperatures by inspection and measured on the axes of the graphs. When the values of $\frac{dT}{dt}$ were taken from the temperature histories it was necessary to use only one run for each material as the pre-exponential constant in the expression for the rate of reaction was varied by the packing and size of the sample, and this variation would produce a meaningless Arrhenius plot.

Table 4.31 shows that when the chars were produced by flaming combustion in air the values of activation energy were similar for all foams. Foams A and B differed only in their TCEP content and the activation energies were the same, which offers confirmation that the TCEP boils out of the foam and does not significantly modify the course of combustion or char formation. Foam C did not contain excess MDI to promote cross linking, as did foams A and B, and when exposed to the radiant panel the sample suffered softening and partial collapse as it burned, which resulted in a more compact char with a fine cellular structure. The softening also allowed the internal surfaces of the char to show a glazed effect and this resulted in the char having a higher activation energy as the surface was not so highly developed and could not present such a large surface area for gaseous attack.

The phosphorus in foam D promoted the formation of a good residual char but did not appear to reduce the activity of this char when it was reheated in an oxygen stream. At 62 kJ $mole^{-1}$ the activation energy was of the same order as those of chars from the other polyurethane foams, and the slightly higher value reflected the trend towards higher activation energies recorded for forms of carbon on increasing density. [49]

The char from foam E had the same activation energy whether produced by combustion or by pyrolysis at 360°C. The "take-off" temperature was the minimum temperature to which the char needed to be heated in

nitrogen for there to be an exponential rise in temperature when pure oxygen was passed over the char. The temperature rise depended on the rate of heat generation which was a function of the rate of reaction, which was itself dependent on the temperature: this positive feedback produced a thermal explosion, while the reactive species was rapidly expended. The 'take-off' temperature was 55°C higher for the pyrolysed sample of foam E than for the air produced char. This was a general result - the radiant panel chars had a take-off temperature in the region of 200-250°C and the pyrolysis char was inactive until some 25-80°C higher, as shown in table 4.33.

Table 4.33: 'Take-off' temperatures of chars

	Radiant panel	Pyrolysis
Foam	Take-off temperature (°C)	
A	225	250
B	215	-
C	250	335
D	210	-
E	270	325

During combustion the samples were subjected to temperatures in excess of 400°C, the equilibrium temperature for a surface receiving 12.6 kW m^{-2} (figure 4.7), but only for a maximum of 5 minutes duration. Upon extinction of the flame the char was seen to be coated with a soft soot from the luminous fuel-rich, diffusion flame.

The pyrolysed chars were exposed to lesser temperatures, but for a period of 1 hour which allowed the foams to soften and surface tension to concentrate the viscous material into a smooth surfaced matrix while they decomposed at a relatively slow rate. Besides producing a char of different composition this made for a poorly developed internal surface with a low concentration of active sites which produced a low rate of

gas/solid reaction and hence a char more resistant to oxidation than that from flaming combustion. The steady elevated temperature also promoted the formation of polymeric structures stable at that temperature, such as isocyanurate and carbodiimide, which necessitated a higher temperature to cause further degradation of the char than would otherwise have been required.

The difference between the chars produced by pyrolysis of foams A and C was to some extent due to the TCEP content: foam A did not soften and form a compact mass so extensive repolymerisation was not favoured. The sample of char used from foam C was the insubstantial golden foam-like material that filled the shell of compact char (section 4.36). This flimsy filling was apparently not predominantly carbonaceous but was a brittle lacquer-like material and could have been an isocyanurate polymer formed after the urethane links had dissociated. This was not inconsistent with the DTA data in figure 3.19 and would explain the very high activation energy and 'take-off' temperature. Furthermore the DTA results showed that the trimerisation occurred at a higher temperature in foam A than in the other foams so this would also prevent formation of the stable structure as there would be greater degradation before the structure was consolidated by the trimerisation.

The activation energies determined for the chars were generally lower than for the oxidation of carbon: high porosity graphite at between 450 and 650°C in a dry atmosphere showed an activation energy of 250 kJ $mole^{-1}$, in moist atmosphere 190 kJ $mole^{-1}$, and nuclear graphite in wet oxygen 105 kJ $mole^{-1}$ at 510°C, although at lower temperatures smaller activation energies had been found. For porous brown coal char an activation energy of 135 kJ $mole^{-1}$ has been calculated. The char produced from the foams was not pure carbon but contained a great assortment of other species rich in nitrogen and hydrogen which could not be expected to oxidise with the same reaction kinetics as carbon,

thus the values of activation energy derived were global values for the mixture of structures present.

The 'take-off' temperature of the char is important as it relates to secondary combustion in a fire. When the flames have extinguished, any charred remains are still hot and if a draught of fresh air should play on them there is a distinct possibility of exothermic reaction that could cause an increase in temperature and eventually a fresh outburst of flames when not expected.

The temperatures at which these chars thermally exploded were lower than would be experienced in practical events because pure oxygen was used in the experiments. If air were passed over the char the nitrogen content would not interfere chemically but would reduce the concentration of oxygen at the surface by a factor of five and would also act as a heat sink, carrying away some of the heat produced by oxidation of the char and reducing the degree of positive feedback that caused the thermal explosion. Quantification of these effects is not simple: at a low rate of reaction the heat dissipation would have most bearing, increasing the 'take-off' temperature as a higher heat release rate was needed to balance the heat removal by nitrogen. At higher rates of reaction the hindrance of the nitrogen molecules at the solid surface would have increasing significance, especially at internal surfaces where the gas penetrated by diffusion through the porous material as the smaller molecule of nitrogen diffuses 7% faster than oxygen because the rate of diffusion is inversely proportional to the square root of the molecular weight. The effect of this would be to limit the rate of reaction and hence the release of heat which means that the rise in temperature would be less than exponential and the maximum would be limited by this process. As a result the char would not be consumed so rapidly as by pure oxygen.

Another factor which had some effect on the rate of oxidation of the char was the production of gaseous reaction products. When the supply of oxygen was restricted the probable product was carbon monoxide, two molecules of which would be produced from each molecule of oxygen. This increase in volume must lead to increased internal gas pressure which opposes diffusion into the char and further reduces the concentration of oxygen at the internal surfaces.

In order to gauge the effect of heat dissipation by nitrogen on the 'take-off' temperature it was assumed that the criterion for thermal explosion was the attainment of a certain value of $\frac{dT}{dt}$. But $\frac{dT}{dt}$ is proportional to the rate of reaction,

$$\therefore \frac{dT}{dt} = \text{const} \cdot A \exp\left(-\frac{E_{act}}{RT}\right)$$

$$= A' \exp\left(-\frac{E_{act}}{RT}\right)$$

If only part of the heat produced raised the temperature of the reacting mass then

$$\frac{dT}{dt} = K A' \exp\left(-\frac{E_{act}}{RT}\right)$$

Thus for a constant value of $\frac{dT}{dt}$, T varied when the proportion of heat lost changed.

$$K_1 A' \exp\left(-\frac{E_{act}}{RT_1}\right) = K_2 A' \exp\left(-\frac{E_{act}}{RT_2}\right)$$

$$\therefore \exp\left(-\frac{E_{act}}{RT_1}\right) = \frac{K_2}{K_1} \exp\left(-\frac{E_{act}}{RT_2}\right)$$

$$\therefore -\frac{E_{act}}{RT_1} = \ln\frac{K_2}{K_1} - \frac{E_{act}}{RT_2}$$

$$\therefore T_1 = -\frac{E_{act}}{R}\left[\ln\frac{K_2}{K_1} - \frac{E_{act}}{RT_2}\right]^{-1}$$

The case was considered where $E_{act} = 50\ kJ\ mole^{-1}$ and the 'take-off' temperature in pure oxygen was 250°C (523°K). If it was assumed that in pure oxygen all the heat produced heated the char (K = 1), but in

air that half was dissipated by the gas stream ($K = \frac{1}{2}$), then the 'take-off' temperature in air would have been,

$$T_1 = -\frac{50 \times 10^3}{8.3}\left[\ln\left(\frac{1}{\frac{1}{2}}\right) - \frac{50 \times 10^3}{8.3} \cdot \frac{1}{523}\right]^{-1}$$

$$= 560\ ^{o}K \quad (= 287\ ^{o}C)$$

If 2/3 of the heat of reaction was dissipated ($K = 1/3$) then the 'take-off' temperature would be 307 ^{o}C.

Thus it is seen that, even when allowance has been made for loss of heat of reaction in the air, the 'take-off' temperature that had to be attained before thermal explosion could occur was comparable with that reached by a surface receiving 8.4 kW m^{-2} (figure 4.7), which is quite a moderate intensity of radiant heat (cf section 4.2.3).

4.4 DIFFERENTIAL THERMAL ANALYSIS

4.4.1 In view of the complexity of the traces of the differential thermal analyses of the foams A to E, figure 3.19, a further batch of foams was formulated in order to determine the effect of each component and to determine the cause of each peak. These foams are detailed in Table 2.1 and the differential thermal analyses are shown in figure 3.20.

The formulations of foams F2 and F3 differed only in that the latter contained the catalyst dibutyltin dilaurate which has been reported[41] as accelerating degradation of urethane foams. There are no significant differences between the traces for these two foams which indicates that this effect is minimal in a well formulated material.

TCEP was included in foams F2, F3 and F4. Inspection of the results shows that these three materials showed an endothermic peak in the region of 210°C - 255°C which was not shown by the other foams. This is the range in which one expects TCEP to show itself as it is known that TCEP boils with decomposition at 220°C, and the resulting fragments can be expected to react with the active sites on the polymer chain. Of the original samples foams B, C and E were known to have TCEP as an additive. The curves for foams C and E show definite endothermic peaks in the same range although that for foam E coincides with the peak of an exotherm and so is less visually apparent. This is the reason why the curve for foam B appears to be without the endotherm although it is known to contain TCEP. Closer inspection shows that there is a change of gradient at 250°C where the endothermic effect of the TCEP has terminated.

Common to all curves is an endothermic peak in the range 255°C - 300°C, which can be assigned[36,42,43] to the breakage of the urethane link. It is noted that in the sorbitol based materials, F4 and F5, the peak is at a slightly higher temperature and is not so endothermic. The reason for this is that the aliphatic base with its higher functionality

promotes stronger crosslinking, and the balance between the reactions by which the urethane group fractures is altered. Reference to the results for foam D in figure 3.19 shows that a sucrose based polyether also has this effect.

Once the urethane cleavage has taken place the thermographs all show a short series of endothermic peaks, but at varying temperatures. This is possibly evidence of the trimerisation of the isocyanate formed on fracture of the urethane link, and indication that the temperature of reaction is controlled by the other reaction products which serve to catalyse the reaction. It is seen that this peak is very small in foam E as would be expected from the lower frequency of urethane groups present in this polymer. Were the reaction at this temperature the decomposition of isocyanurate as reported[36,42,43] then the peak for foam E would be at least as pronounced as those for the other foams, which is not the case.

Reference to the curve for MDI in figure 3.21 shows that the raw material itself undergoes a fairly abrupt endotherm at 320°C, whilst the foams reacted at temperatures ranging from 295°C to 355°C. This is not inconsistent with a reported[32] temperature of 350°C for isocyanurate formation.

The presence of TCEP in the foam lowered the temperature at which this reaction occurred when the polyether was Daltolac 51, but not when an aliphatic polyether was used.

The introduction of a phosphorylated polyol had the effect of producing a reaction at a temperature of 120°C (F5) and an increased endothermicity over 250°C, probably by virtue of its promoting reactions with carbonaceous products. Foam D is also seen to undergo some reaction in the region 100° - 130°C as rearrangement of the phosphorus segment of

the network occurs. The endothermic peak shown by foam A is atypical and is probably due to absorption of water into the sample or apparatus.

The temperature at which the first reactions were evidenced on the thermographs varied between the foams but was generally between 150°C and 200°C, except for the initial reaction in the phosphorylated foams. As the foams were heated and the energy of the system increased the hydrogen bonding between adjacent chains within the material would weaken, and then reactions would occur at the active sites on the macromolecule. The ether linkages in the propoxylated polyols rotate easily[44] and the freedom of movement makes these parts of the molecule susceptible to easy degradation. The possible reactions are numerous so the range of reaction temperatures will be extended.

Table 4.34 shows the temperature at which the exothermic peak commenced for each foam analysed.

Table 4.34: Temperature of initial reaction

Foam	Temp °C	Foam	Temp °C
F1	190	A	190
F2	175	B	185
F3	175	C	150
F4	155	D	180
F5	155	E	190

Foams F1, F2 and F3 were based on Daltolac 50, derived from tcluene diamine. The tin catalyst in F3 had no effect, but the TCEP in F2 and F3 promoted degradation at a temperature some 15°C lower than in F1. No corresponding effect was seen in foams F4 and F5 both of which were based on a sorbitol polyether, but only the former contained TCEP. There was no evidence to show that the additional phosphorus in F5 had the same effect as the TCEP in F4. The extent to which the aliphatic nature of the sorbitol polyether was instrumental in lowering the

temperature at which reaction commenced cannot be certified as the degree of extension by propoxylation was unknown.

The effect of TCEP was seen to some extent on comparison of foams A and B. The start of the peak in foam A was obscured by a small exothermic peak between 170°C and 215°C that was not identified. The low decomposition temperature of foam C was not due completely to the increased concentration of TCEP but was enhanced by a modified formulation lacking the glycerol of foams A and B. Being a short chain triol the glycerol would generally stiffen the structure and shorten the average distance between crosslinking bonds, thus aiding stability.

The sucrose base of the Propylan RF33 is heterocyclic and no reduction of the initial reaction temperature was observed.

The isocyanurate based foam E did not show appreciable reaction until 190°C, but lack of detailed knowledge of the formulation prevented significant conclusions being drawn.

It is of interest to note that the temperatures in table 4.34 correspond to the temperatures at which a weight loss equal to the F11 content was recorded. This is consistent with a material which under heating suffers molecular reorganisation to produce permeable cell walls which allow the entrained blowing agent to escape.

4.4.2 The effects of the experimental problems on the results should also be noted. In view of the nature of the samples and their small size it was not possible to maintain uniformity between runs, which resulted in varying values of thermal capacity, conductivity and thermocouple contact efficiency. The effect of this on the output would be variations in the position and size of the peak for a given reaction. The residence time of the volatile products in the sample and hence the degree to which they were able to react with the foam solids was controlled by the packing of the sample and its behaviour during the

experiment. In some cases the volatile matter permeated out through the solid, but in other cases it propelled a plug of solid sample along the sample tube thus preventing interaction of the phases and often leaving the thermocouple bead not in contact with the sample. Besides the shift of position and size of peak produced by the physical displacement, there was the effect of the segregation of the phases which altered the course of reaction and could thus change the shape and span of the peaks of the complex series of interactions occurring.

The characteristics of the chromel/alumel thermocouples varied from one to the next and a new thermocouple was used for each experimental run with the result that the mismatch between the sample and reference thermocouples was not constant. The mismatch determined the shape of the baseline so absolute measurements were not reliable and interpretations of comparative magnitues were limited in accuracy.

4.4.3 Piloyan et al[45] derived the activation energies of reactions from DTA traces. They considered a general peak of the form in figure 4.37.

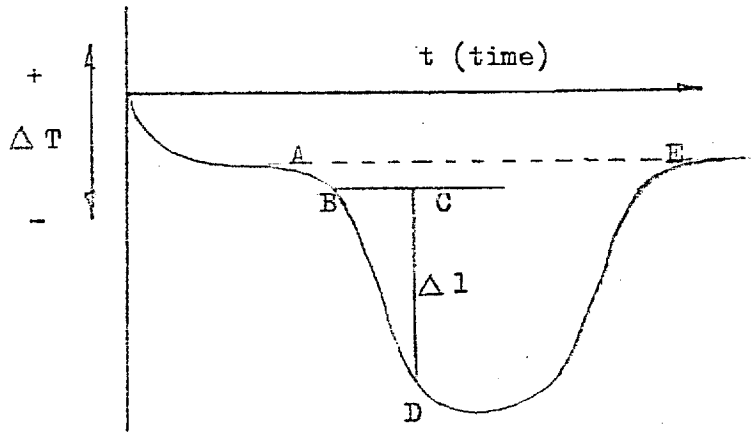

Figure 4.37:
General DTA peak

$\Delta 1$, the height of the peak, was measured as the length CD, and the datum was the line through the point of maximum curvature, B, not the base line AE.

If a = activity of the reacting species

S = heat of reaction

$$\Delta 1 \propto S \frac{da}{dt}$$

but $$\frac{da}{dt} = A_o f(a) \exp\left[-\frac{E_{act}}{RT}\right] \qquad \text{(Arrhenius)}$$

$$\therefore \ln \Delta 1 = \text{const} - \ln f(a) - \frac{E_{act}}{RT}$$

When $0.05\ a_o < a < 0.8\ a_o$ then T has a greater effect on $\Delta 1$ than a if the heating rate is $10 - 40^{\circ}C/min$

$$\therefore \ln \Delta 1 = \text{const} - \frac{E_{act}}{RT}$$

Thus a plot of $\log_{10} \Delta 1$ versus $\frac{1}{T}$ has a gradient of $-\frac{E_{act}}{2.3\ R}$

The peak assigned to the fracture of the urethane link was extracted from each of the samples, figure 4.38, and a datum line drawn through the point of maximum curvature. The measurements taken from these curves, and derived numbers are shown in table 4.35.

$\text{Log}_{10}\ \Delta 1$ was plotted against the reciprocal of the absolute temperature and the resulting curves are shown in figure 4.39. The lines G1 and G2 represent the gradients corresponding to activation energies of 460kJ mole^{-1} and 125 kJ mole^{-1} respectively, and can be seen to provide a realistic estimate of the range of values indicated.

In agreement with kinetic theory, the activation energy for each material was seen to decrease with increasing temperature. The position of the curves on the temperature scale varied between foams in a similar fashion in both figures 4.38 and 4.39.

The activation energy of the foams containing TCEP (F2, F3, F4, B and C) was generally higher at the early stages of reaction than that of foams without, but rapidly fell to a lower value. This effect was less apparent in some of the foams containing aliphatic polyols (A, B and F4) although F5, with sorbitol and phosphorylated polyol, had an activation energy that fell to a low value within a very short temperature range.

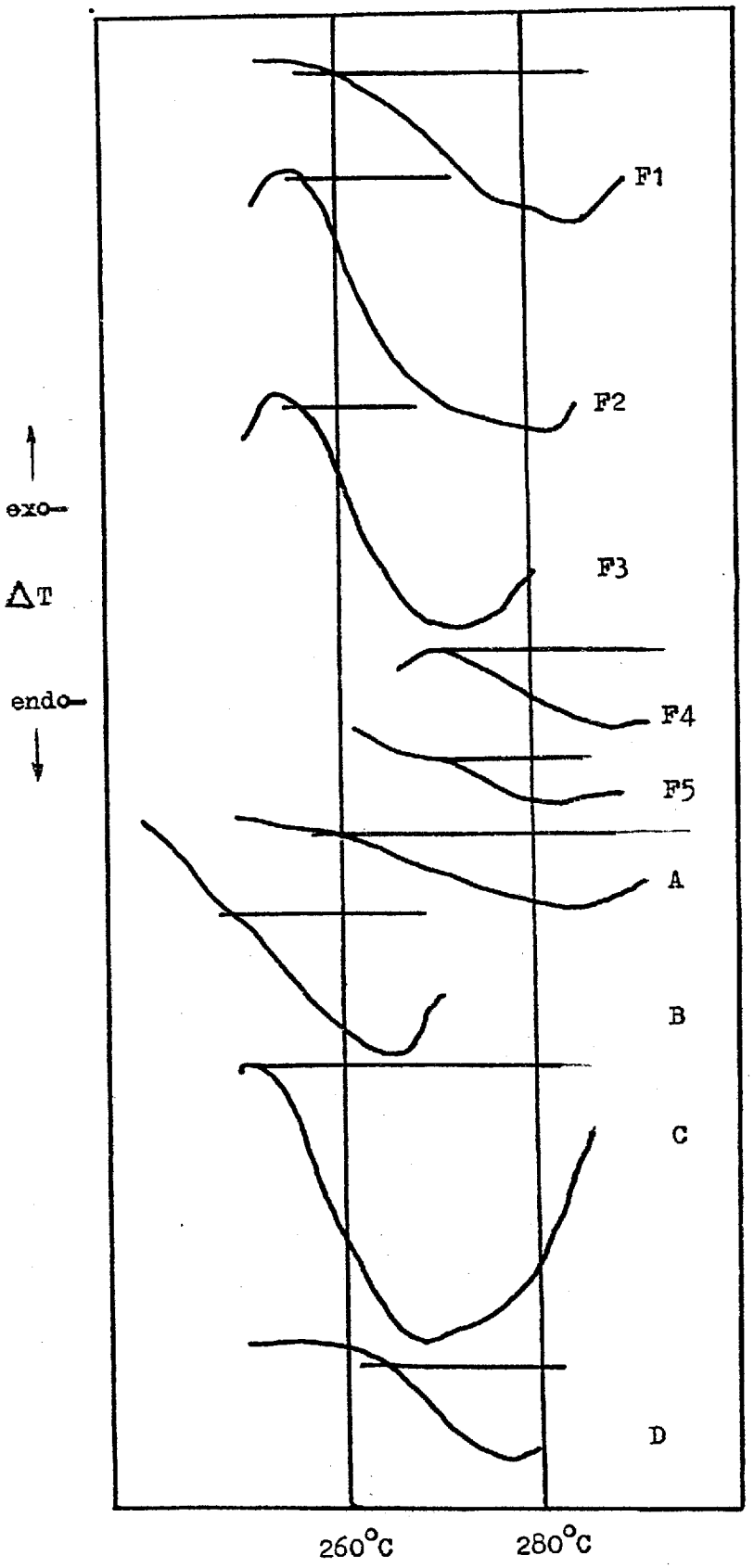

Figure 4.38 ; Extracted peaks from DTA thermograms.

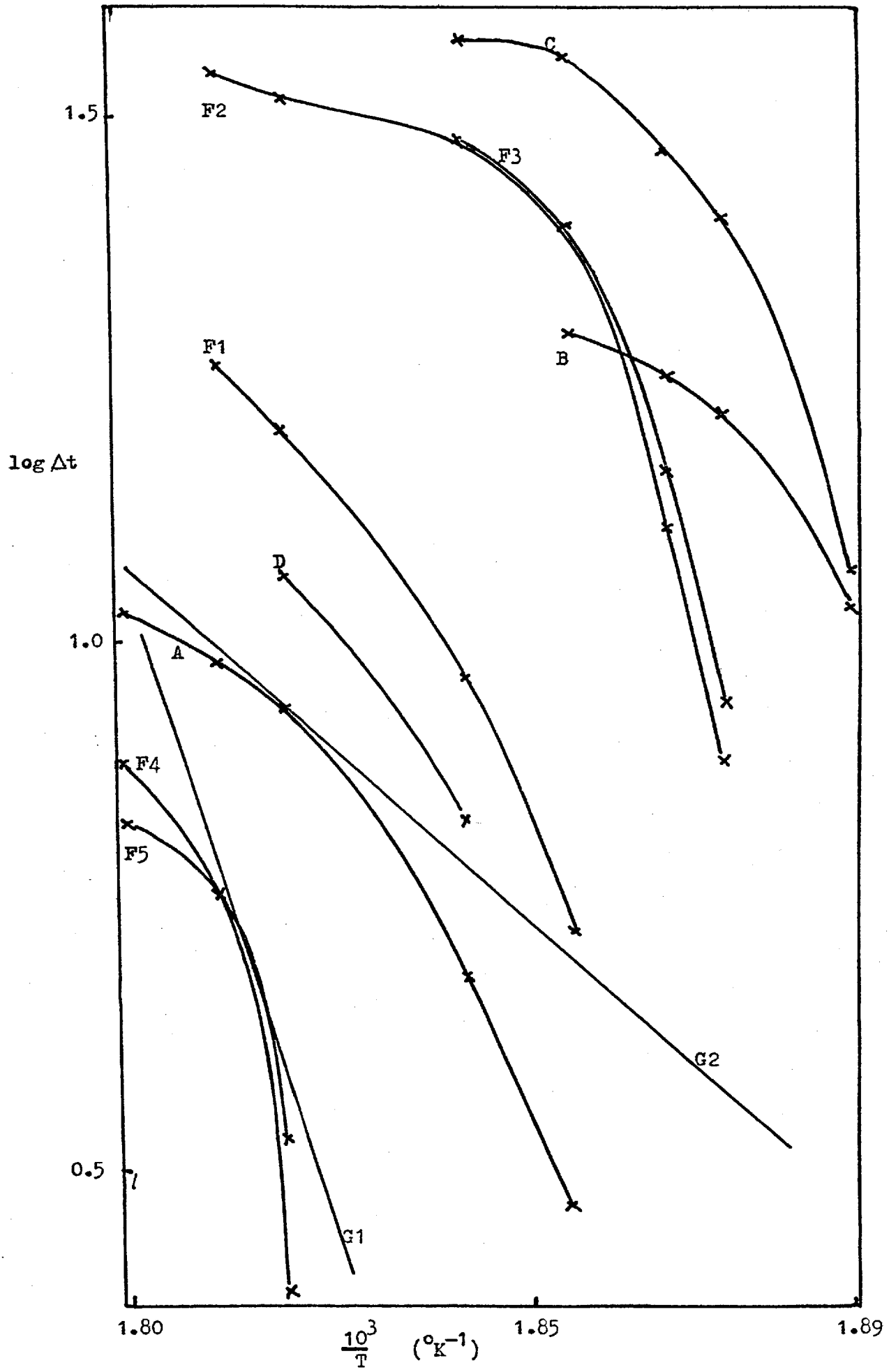

Figure 4.39 ; Arrhenius plot for DTA peaks (figure 4.38)

Table 4.35 Δl and log Δl at various temperatures

$\frac{10^3}{T}$ ($^oK^{-1}$)	1.890	1.875	1.868	1.855	1.842	1.820	1.812	1.800
T ^oK	529	533	535	539	543	549	552	556
T ^oC	256	260	262	266	270	276	279	283
FOAM		Δl (mm) $\log_{10} \Delta l$						
F1	–	–	–	5.5 0.74	9.5 0.98	16.5 1.218	19 1.28	–
F2	–	9 0.954	15 1.176	25.5 1.41	31 1.49	34 1.53	36 1.557	–
F3	–	8 0.902	14 1.148	25.5 1.41	31 1.49	–	–	–
F4	–	–	–	–	–	2.5 0.40	6 0.78	8 0.902
F5	–	–	–	–	–	3.5 0.545	6 0.78	7 0.845
A	–	–	–	3 0.477	5 0.699	9 0.954	10 1.00	11 1.043
B	11 1.043	17 1.23	18.5 1.266	20 1.305	–	–	–	–
C	12 1.08	26 1.415	30 1.477	37 1.57	38.5 1.585	–	–	–
D	–	–	–	–	7 0.875	12 1.08	–	–

Owing to the large degree of superimposition it was not possible to separate successfully the peaks of the thermographs for each reaction. This rendered any attempt to recover quantitative data highly inaccurate, but did not prevent qualitative observations being made.

It is of interest to note that the thermographs of the foams cannot be constructed from those of the raw materials from which they are made, which demonstrates that the foams do not simply dissociate on heating, but that the various segments of the polymer chain interact to produce a variety of new fission sites.

4.5 PYROLYSIS PRODUCTS

4.5.1 Gas-Liquid Chromatography

The GLC experiments were performed with the object of identifying some of the products of pyrolysis, with emphasis being placed on the fate of the chlorine content of the foams.

For this reason the ionisation detector chosen was used in an electron capture mode. The carrier gas is ionised by the radio active β emitter source thus enabling a current to flow between the detector electrodes. The operating conditions should be regulated to restrict the effective carriers of current to the thermal electrons. The presence of any electron capturing molecules depletes the gas stream of electrons and so reduces the current flowing. Halogenated hydrocarbons and other polar organic compounds are effective electron capturing species. This is a very sensitive and selective type of detector having a lower limit of detectability of approximately 10^{-12} g/ml[46], although it has been used in a pulsed voltage mode to detect a concentration of the order of 10^{-14} g/ml[47]. Argon is the usual carrier gas but a satisfactory alternative is oxygen free nitrogen.

When no response was found on the injection of the pyrolysis products, samples of known organic liquids were introduced to test the response of the equipment. Full scale response was given by 0.1 μ l (approximately 10^{-4} g) of methanol, ethanol and hexanol and by similar quantities of simple ketones, although there was not much separation of the peaks which made identification of the species by this means very doubtful. Variation of the flow rate of the carrier gas did not improve this aspect.

When 0.1 μ l samples of various halogenated hydrocarbons were injected the output showed saturation in the form of a large initial peak that slowly decayed with sharper peaks superimposed on it. This behaviour may be caused by an excessively large concentration of strongly

electron capturing species and it could be partially due to the inherent problems of this type of detector, anomalous electron transport effects within the ionisation chamber and excessive sensitivity to contaminants.[46] Fenimore et al.[48] found that traces showing this feature were produced when the detector volume was large and mixing within it allowed incomplete exhaustion of the outgoing portion of gas. The detector used had a volume of some 3 ml, against the 0.1 ml volume of modern versions.[46] The mixing effect would be aggravated by a low flow rate, but as the electron capture detector is sensitive to concentration, not mass flow rate, a higher carrier gas flow would decrease the sensitivity.

This detector is sensitive to polar organic molecules which are capable of removing the thermal electrons from the ionised carrier stream. Thus it shows a large fall in current with halogenated materials, and can be used to detect molecules containing electrophilic groups such as $>C=O$, $-C\equiv N$, $-NO_2$ and $-COOR$. It will not detect the permanent gases, carbon dioxide, water or cyanogen, some of which even desensitise its response.

From the failure of the samples of pyrolysis products to produce any peaks whether injected directly or as an extract it must be implied that there were no significant amounts of gases containing the electrophilic groups. The yellowish smoke produced in pyrolysis, if injected into the column, has a very long residence time which is probably due to its polymerisation within the column to give tarlike products with very low vapour pressures.

4.5.2 Chloride determination

All the foams A, B, C, D and E gave positive results when aqueous extracts of their pyrolysis products were tested for the chloride ion. It is of interest to note that A and D gave only turbidity, for these were the two foams that did not contain TCEP, which gives hydrogen chloride on decomposition.[33] Thus it appears that F11 does give some

measure of hydrogen chloride when the foam decomposes.

Rapid reduction of the silver nitrate solution indicated a strong reducing agent which suggests the presence of aldehydes in the gas stream. The colours exhibited by the liquor imply molecules containing nitrogen in conjunction with a benzene ring for these are often highly coloured.

4.5.3 Mass Spectrometry

In view of the lack of positive results from the gas chromatographic investigation of the products of pyrolysis an analysis was made by mass spectrometry, and the results obtained are shown in section 3.5.3.

It was obvious from the physical appearance of the samples that major changes of structure had occurred. All but foam E had suffered major shrinkage and the lack of sharp edges in the char from foam C emphasised the effect of softening. As in the weight-loss experiments the sample of foam E split under the thermal stress but suffered only minor discolouration. The chars from foams A, B and C were various shades of red, but that from foam D was nearly black owing to the carbon-forming effect of the phosphorylated polyol which promotes a higher yield of char.[52,58]

The spectrograms produced from foams A and B when pyrolysed at the lower temperatures of 200°C and 160°C, showed no significant variations from those at 250°C which indicated that degradation of the propylene oxide molecular extensions commenced at a temperature below 160°C and was the major reduction up to 250°C. This was supported by figures 3.6 to 3.10 which showed that weight loss commenced below 140°C and by 250°C - 260°C was approximately equal to the combined weight fraction of F11, propylene oxide and, where added, TCEP. A large portion of the weight loss below 200°C was due to the blowing agent which was released when the weakening of the hydrogen bonds and rearrangement of the

polymer crosslinking rendered the cell walls permeable, but the mass spectrograms showed that there was also some loss due to fragmentation of the urethane matrix.

An idealised structure for foam A is shown in figure 4.40. Foam B differed only in the inclusion of TCEP, but as this was a non-reactive additive it was not bound into the polymer but merely held in the lattice. The absence of glycerol from foam C decreased the degree of crosslinking, but the inclusion of water in the formulation partially compensated for this by promoting the formation of urea groups. Foam D was based on different polyols and the effect of the higher functionality in increasing the crosslinking can be seen in the idealised structure (figure 4.41). The details of the components of foam E were not known but, from the general similarity of the mass spectrogram of its pyrolysis products to those of the other foams tested, it could be assumed that a propoxylated polyol was included in the formulation. The peculiarity of foam E was the partial trimerisation of the isocyanate content, presumably as the result of the inclusion of a suitable catalyst in the mix.

What was not taken into account in the idealised structures was the excess of MDI in the formulations. This reacted with the active hydrogen atoms of the urethane groups to give allophanate groups and increased the crosslinking in the structure. The crosslinking of the polymer chains was further increased by hydrogen bonding which was not shown in the figures 4.40 and 4.41. An example of crosslinking by hydrogen bonding of polymer chains that would not otherwise interact is shown in figure 4.42. The hydrogen bond in general occurs between hydrogen and the highly electronegative elements of small atomic volume, nitrogen, oxygen and fluorine. It is a relatively weak bond usually having a dissociation energy of about 20 kJ[59] against the value of 460 kJ for an oxygen-hydrogen bond.[60]

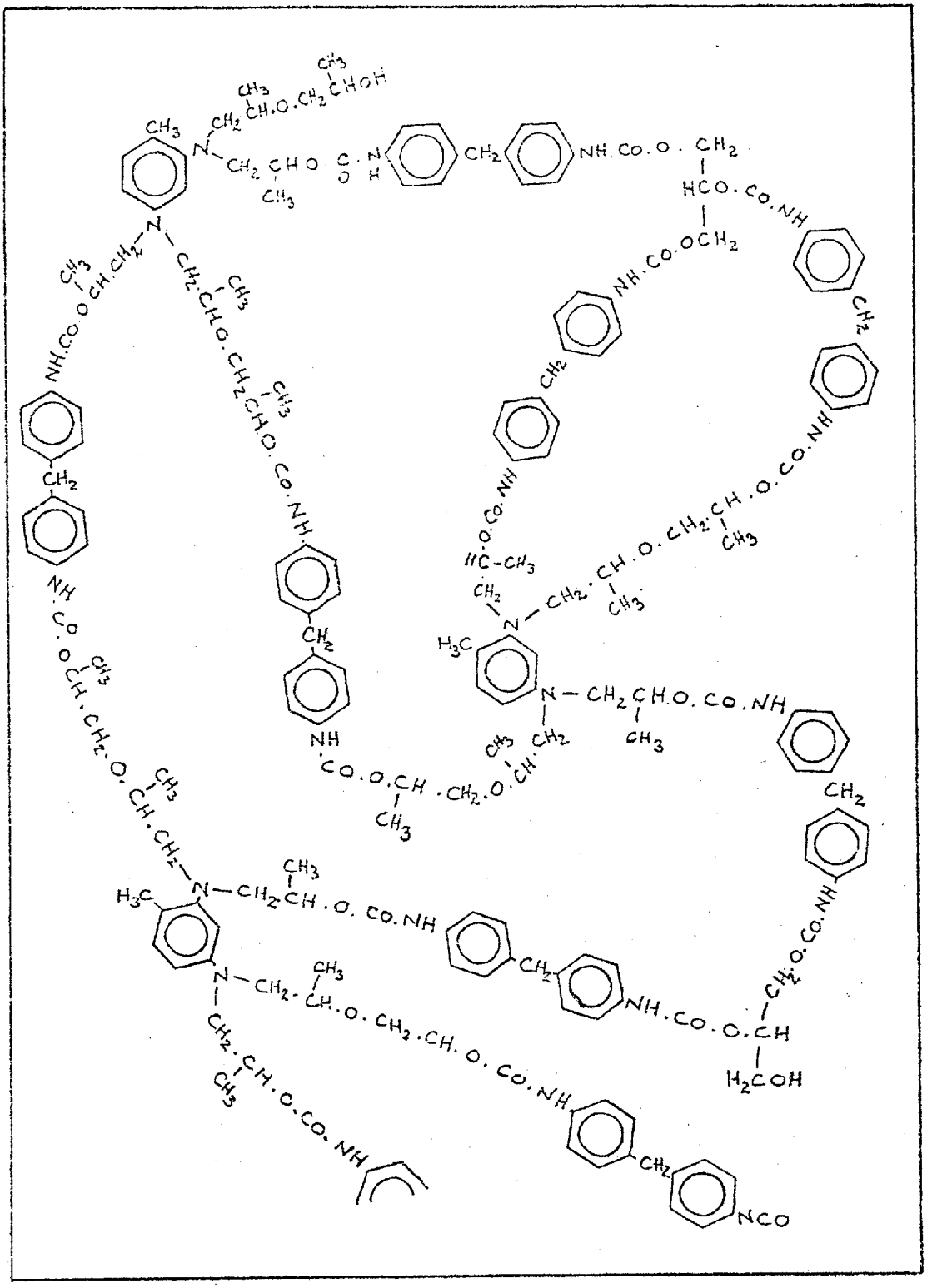

Figure 4.40 ; Idealised structure of Foam A.

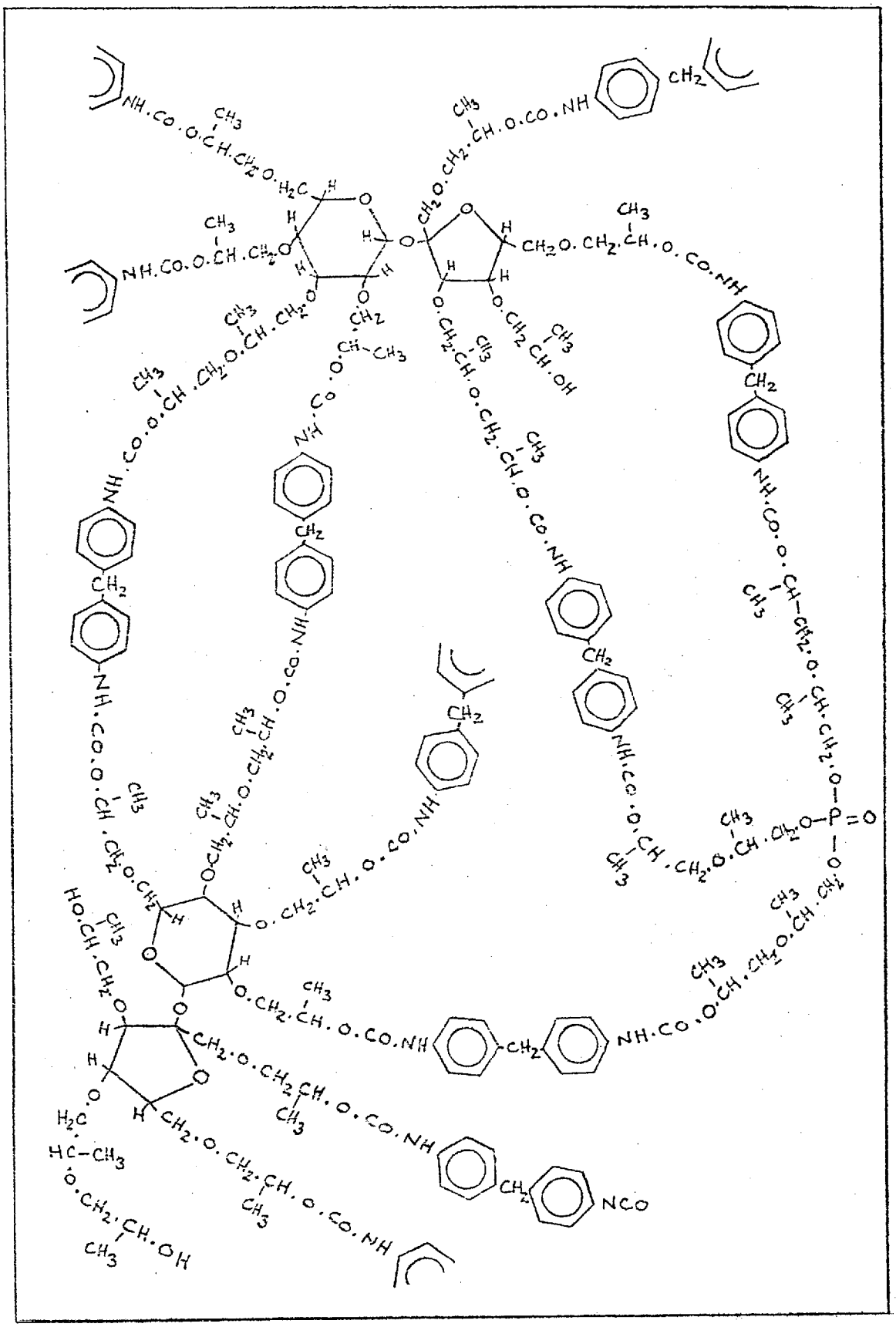

Figure 4.41 ; Idealised structure of Foam D.

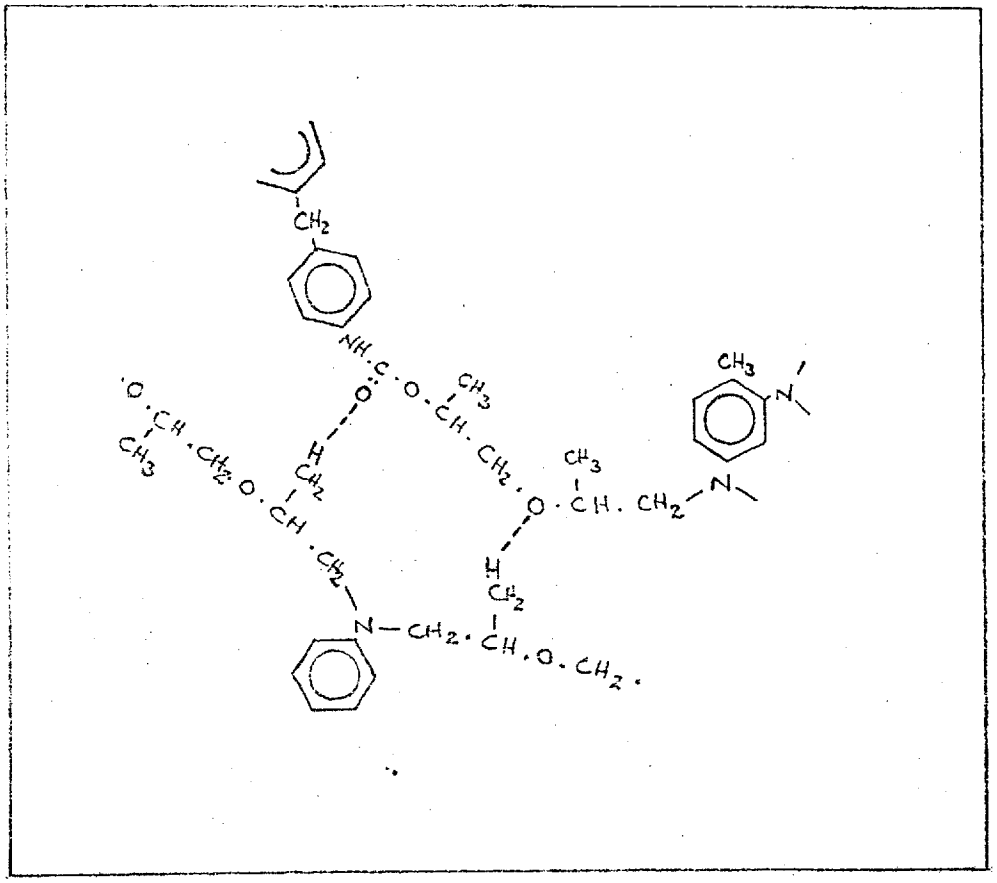

Figure 4.42 ; Crosslinking of polymer chains by hydrogen bonding.

Common to the structures of all the materials tested were the urethane group and the polyether linkages. As the foam was heated the molecular chains were thermally excited and the relatively weak hydrogen bonds were broken, which left the matrix less tightly formed and allowed the blowing agent to start permeating out.

Further heating put more strain on the polyether chains which were able to rotate freely into close proximity with other sections of the molecule, and these chains started to fracture and release small volatile fragments. With increasing temperature there was more fragmentation of the polyether chains and the rate of urethane group failure increased. The three main routes of urethane breakage were [50] ;

1) dissociation to isocyanate and alcohol

2) fragmentation to primary amine, carbon dioxide and alkene

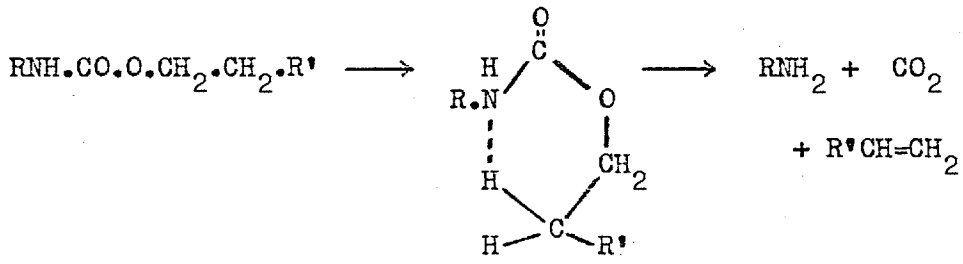

3) formation of secondary amine and carbon dioxide

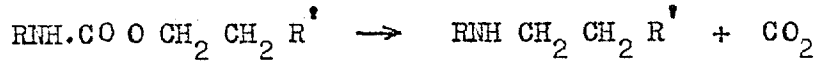

From the evidence of the DTA results it would appear that the simple dissociation of the urethane groups to give isocyanate endings was of importance as there was subsequent trimerisation of them in the charred material. From studies of the pyrolytic degradation of the polythiolcarbamate formed from diphenylmethane diisocyanate and 1,6 - hexanedithiol, Dyer and Osborn [51] found that 20% of the polymer decomposed to give a primary amine and 80% dissociated to give the parent isocyanate and dithiol.

It was expected that the major component of the pyrolysis products of all the foams would be the blowing agent, fluorotrichloromethane, and this proved to be the case. $CFCl_3$ has a molecular weight of 136, 138, 140 or

142 depending on the isotopes of the chlorine atoms present; the isotope of carbon ^{13}C has only 1.1% occurrence and ^{19}F is the only naturally occurring isotope of fluorine, so these may be disregarded. The mass spectrograms showed no peaks with a mass to charge ratio $(\frac{m}{e})$ in this range, but this large molecule would be largely dissociated in the high energy source chamber. If the $CFCl_3$ was double charged the $\frac{m}{e}$ peaks would be at 68, 69, 70 and 71 but only 68 was found, so the species was not present.

If dissociation took place by removal of the fluorine atom the species CCl_3^+ would remain with a $\frac{m}{e}$ of 117, 119, 121 or 123. The relative heights of the expected peaks can be predicted from the relative abundance of the chlorine isotopes – ^{35}Cl, 75% and ^{37}Cl, 25% approximately. Thus the probability of a ^{35}Cl atom is $\frac{3}{4}$ and of a ^{37}Cl atom $\frac{1}{4}$.

The probability of combinations of the three chlorine atoms are as follows:

$$3 \times {}^{35}Cl \quad [105] : \frac{3}{4} \cdot \frac{3}{4} \cdot \frac{3}{4} = \frac{27}{64}$$

$$2 \times {}^{35}Cl + 1 \times {}^{37}Cl \quad [107] : \frac{3}{4} \cdot \frac{3}{4} \cdot \frac{1}{4} \cdot 3 = \frac{27}{64}$$

$$1 \times {}^{35}Cl + 2 \times {}^{37}Cl \quad [109] : \frac{3}{4} \cdot \frac{1}{4} \cdot \frac{1}{4} \cdot 3 = \frac{9}{64}$$

$$3 \times {}^{37}Cl \quad [111] : \frac{1}{4} \cdot \frac{1}{4} \cdot \frac{1}{4} = \frac{1}{64}$$

Thus the CCl_3^+ peaks at $\frac{m}{e}$ of 117, 119, 121 and 123 would be in the ratios 27: 27: 9: 1. Measurement of these peaks on the spectrogram of foam D showed peaks of heights 52mm, 48mm, 16mm and 2mm respectively, which are in a ratio of 26: 24: 8: 1, sufficiently close to the predicted value to confirm the presence of three chlorine atoms. The absence of peaks other than 117 and 119 for some of the other samples was caused by lack of sufficient amplification to show the relatively small peaks.

In a similar fashion the relative abundances of combinations of two chlorine atoms were calculated;

$$2 \times {}^{35}Cl \quad [70] : \frac{3}{4} \cdot \frac{3}{4} = \frac{9}{16}$$

$${}^{35}Cl + {}^{37}Cl \quad [72] : \frac{3}{4} \cdot \frac{1}{4} \cdot 2 = \frac{6}{16}$$

$$2 \times {}^{37}Cl \quad [74] : \frac{1}{4} \cdot \frac{1}{4} = \frac{1}{16}$$

From the mass spectrogram of foam C the peaks at $\frac{m}{e}$ 101, 103 and 105 were 34, 21 and 4 mm high giving a ratio of $8\frac{1}{2} : 5\frac{1}{4} : 1$ which indicated that the species was $CFCl_2^+$.

Measurements of the relative sizes of the peaks also confirmed the presence of the following species;

$C\,Cl_2^+$ - 82, 84, 86

$CF\,Cl^+$ - 66, 68

$C\,Cl^+$ - 47, 49

it is also possible for a radical to carry a multiple charge and this appeared to happen in several cases, viz:

$C\,Cl_3^{++}$ - $58\frac{1}{2}$, . . .

$CF\,Cl_2^{++}$ - $50\frac{1}{2}$, $51\frac{1}{2}$ . . .

$C\,Cl_2^{++}$ - 41, 42, 43

but the small sizes of the peaks made confirmation by relative occurrence impossible.

The peak at $\frac{m}{e}$ = 31 was probably due to CF^+, and HF^+ could have contributed to the one at 20. The relative sizes of the peaks at $\frac{m}{e}$ 35, 37 and 36, 38 confirmed that these were due to Cl^+ and HCl^+ respectively, but it could not be determined whether the species were the result of dissociation of larger species or present in their own right.

Nuckolls[54] found that a mixture of $CFCl_3$ and air passed over heated iron produced appreciable amounts of Cl_2, $COCl_2$, HF and HCl. In the more complex environment of the pyrolysing foam these species would be produced

and then would react with the other pyrolysis fragments to give a variety of products dependent on the constantly varying situation. In the mass spectrograms the peaks at $\frac{m}{e}$ of 98, 100, 102 ($COCl_2^+$), 49, 50, 51 ($COCl_2^{++}$) and 63 ($COCl^+$) suggested the presence of phosgene.

There was no way of assessing the contribution to these peaks of any 1.2-dichloroethane[55] that was produced from the TCEP.

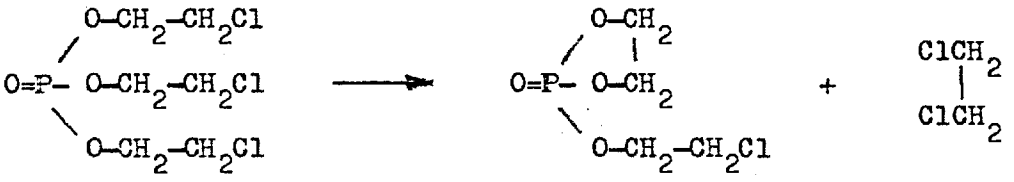

(TCEP)

The "condensation" may proceed internally as shown, or there could be a bimolecular reaction producing a polymeric ethyl phosphate. Fragments from dissociation of 1.2-dichloroethane could account for $\frac{m}{e}$ 61 to 64 ($CH_2 \cdot CCl^+$ and $CH_2 \cdot CHCl^+$).

Degradation of the polyether linkage, - C.O.C -, proceeded along many lines, among which the following would have played an important role:

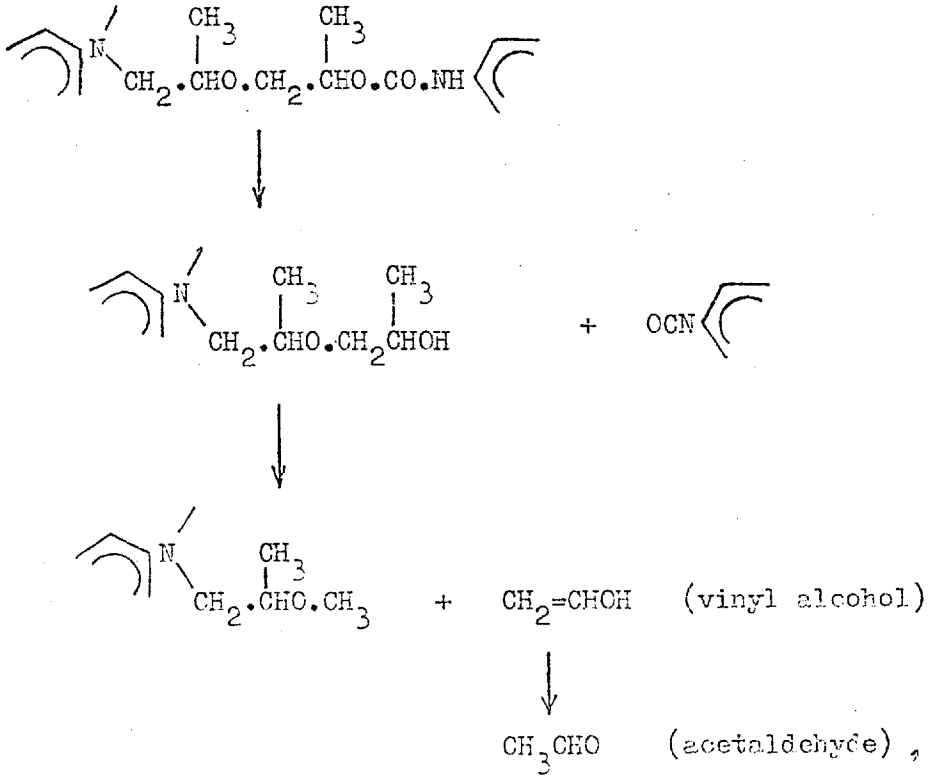

and

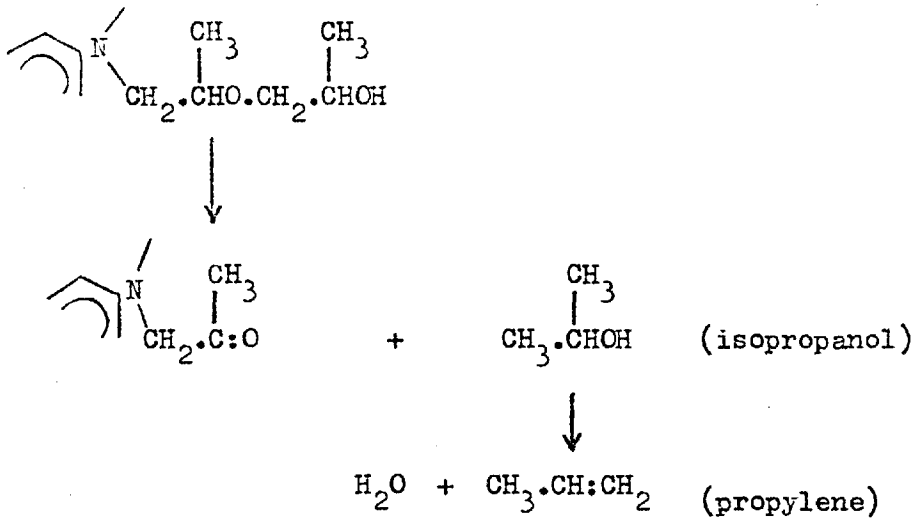

and

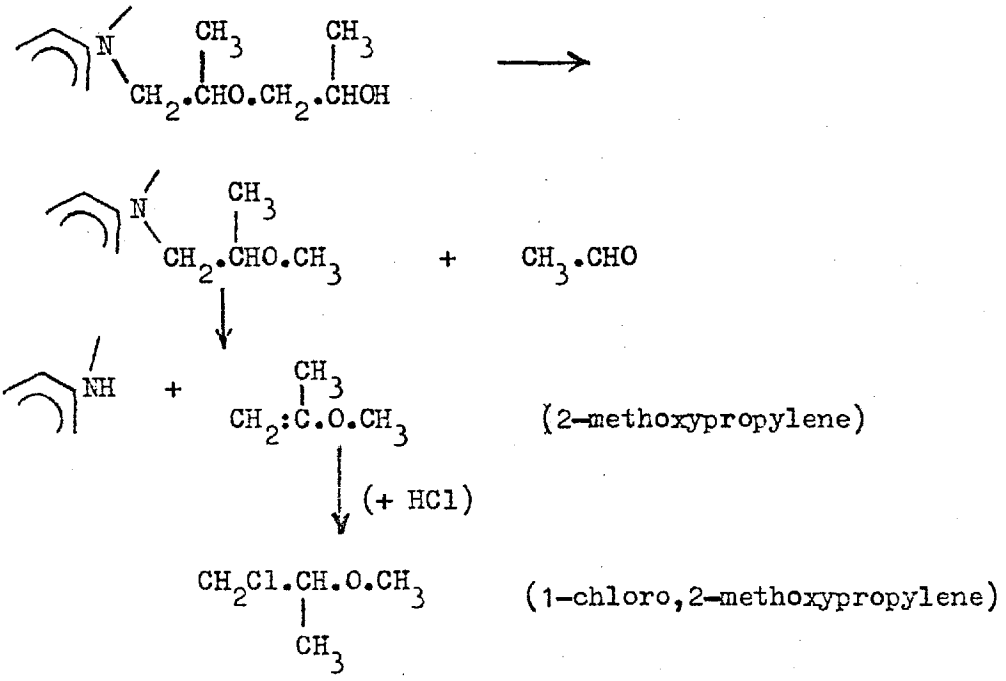

Alternatively CO_2 may be expelled,

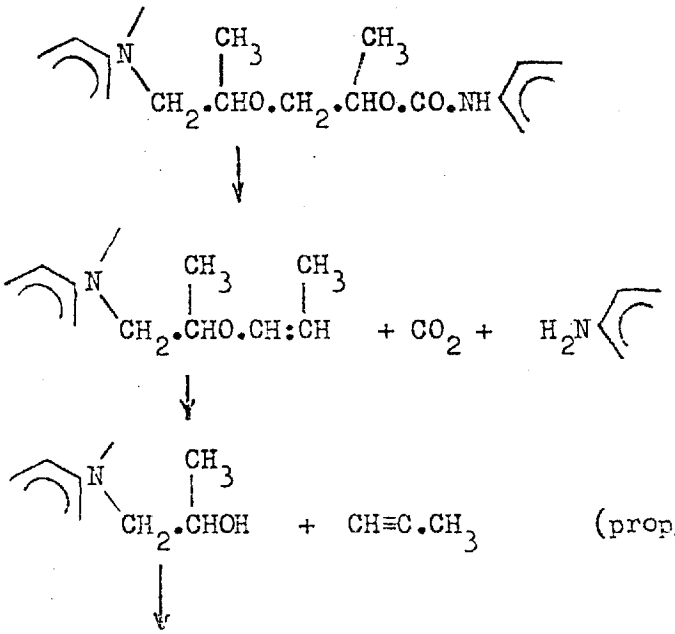

and

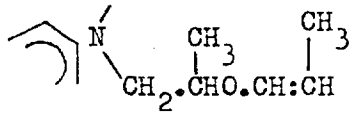

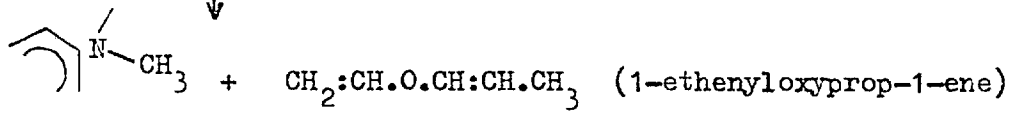

or

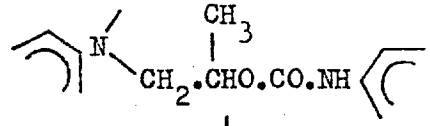

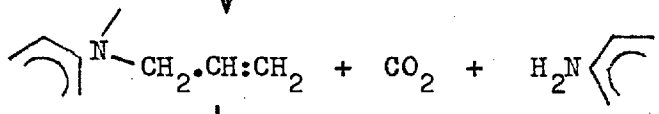

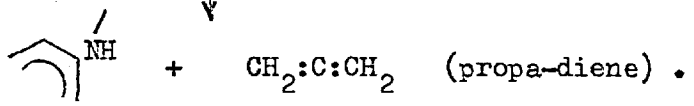

Following the formation of a secondary amide, a nitrile could be formed;

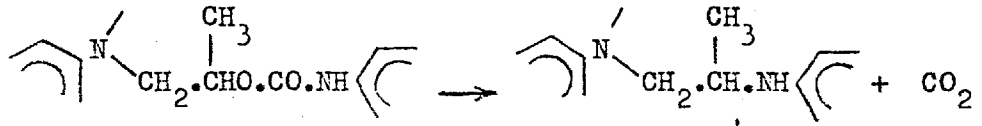

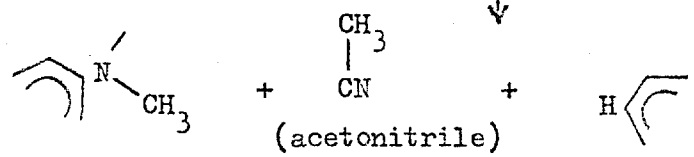

(acetonitrile)

Some of the products may have reacted further to consolidate the char, e.g.

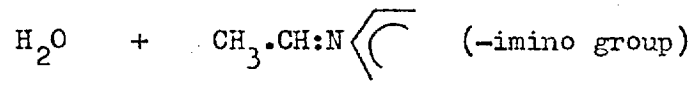

and

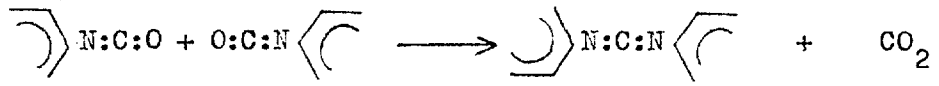

in addition to the formation of the isocyanurate trimer.

Fragmentation and dehydration of glycerol and sorbitol would have given rise to a variety of alcohols and unsaturated compounds in a similar fashion.

The wealth of possible products can be seen from these examples. In practice only a few of the products are present in large proportions, but which the few will be is not readily ascertained from theory.

The mass spectrograms bore peaks which indicated fragments of many of the above pyrolysis products as shown in table 4.36.

Using these fragments it was possible to build up a range of pyrolysis products which was consistent with the results of the chloride test - hydrogen chloride to give chloride ions in solution, aldehydes to reduce the silver, nitriles and other similar compounds to produce the pungent, choking smell experienced, and a wealth of unsaturated molecules to burn with a smoky luminous flame. From the fact that the peak at $\frac{m}{e} = 39$ was produced only in foam D it appeared that the phosphorylated foam did release a little of its phosphorus in the volatile products as reported by Napier and Wong[56], and confirmed by Einhorn et al[61].

The results were not at variance with those of other workers on similar materials. Backus et al[52] found that when heated in air the foams produced a variety of species below 240°C among which were CO_2, $CFCl_3$, CO, some unsaturated gas and a mixture characterised by the -NH, -CH,-C6H,-COC-and H_2O infra red bands, which was consistent with the oxidation of the polypropylene oxide extensions. Combustion at 530°C produced[53] a similar set of products; CO, CO_2, HCHO, CH_3.CHo, higher aldehydes and ketones, phenol, cresol, alkylphenols, amines, and traces of HCN and HCl.

The effect on the charred residue was generally to produce a more highly crosslinked matrix as the long extensions between the carbon rings of the polyol and the isocyanate had been eliminated.

Table 4.36: Analysis of mass spectrograph peaks (excluding chlorine-bearing species)

m/e	Fragments	Possible sources of fragments
14	CH_2^+, N^+	methane, alkanes, amines
15	CH_3^+, NH^+	alkanes, amines
16	CH_4^+, O^+, NH_2^+	methane, CO_2, amines
17	OH^+	water, alcohol
18	H_2O^+	
20	HF^+, $C.O.C^{++}$, $C.CO^{++}$	polyether, ketones
22	CO_2^{++}, CH_2CN^{++}	acetonitrile, amines
26	CN^+	cyanide, amine, isocyanate
27	HCN^+, CNH^+	cyanide, amine
28	CO^+, $C_2H_4^+$, N_2^+, CH_2N^+	CO, CO_2, alkene, alkane, amine
29	CHO^+, $C_2H_5^+$	aldehyde, alkane
31	CF^+, P^+	F11, phosphorylated polyol, TCEP
32	O_2^+, CH_3OH^+, HP^+, CHF^+	F11
39	POP^{++}, $C_3H_7^+$	phosphorylated polyol, alkane
40	$C.CO^+$, NCN^+, $C.C.C^+$	ether, ketone, carbodiimide
42	NH_2CN^+, NCO^+	isocyanate
44	CO_2^+, $CH_2.O.CH_2^+$, CH_3CHO^+, CH_2CN^+	ether, aldehyde, acetonitrile, amide
45	CH_3CN^+, $C_2H_5.O^+$, $CH_3.O.CH_2^+$	ether, aldehyde, amide
46	$C_2H_5OH^+$, $HCOOH^+$	alcohol, formic acid
47	PO^+	phosphorylated polyol, TCEP
50	$C:C.CN^+$	unsaturated amine
52	$C_6H_5\ NCH^{++}$	toluene amine
68	$C.O.C.O.C^+$	polyether

It was not possible to deduce the absolute identity of the species present from the mass spectrograms, but only to gain clues as the molecules dissociated into small fragments in the sampling chamber, and took multiple charges.

Under fixed spectrometer conditions each compound gives a constant response of a series of peaks, but without extensive calibration of hundreds of peaks and repeated checking against standard mixtures it is not possible to analyse a mixture of any complexity. To gauge the involved nature of such calculations it is significant to note that n-butane, a simple alkane, gives at least 37 peaks.[57]

4.6 MODEL OF POLYURETHANE FOAM

4.6.1 Theoretical Considerations

4.6.1.1 Fourier's Conduction law states that the heat flux is proportional to the temperature gradient, and the constant of proportionality is defined as the thermal conductivity.

$$\frac{q}{A} = \lambda \frac{dT}{dx}$$

Consider a slab of foam being used as insulation. This will be treated as an infinite slab so that the heat flux is only in one dimension. Figure 4.43 shows the conditions if the slab is in contact with fluids at different constant temperatures each side.

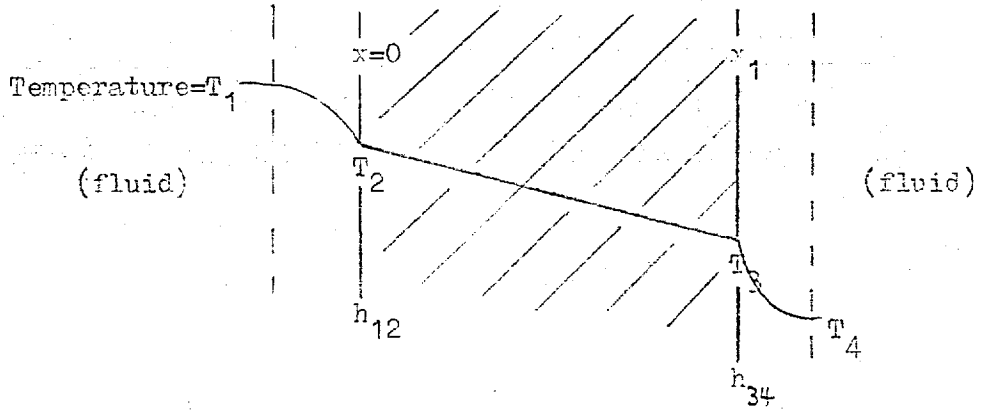

Figure 4.43

h_{12} is the total heat transfer coefficient between the fluid at T_1 and the surface of the slab.

At steady state there is no temperature variation with time, and the heat flux in the x direction, $\frac{q}{A}$, is constant. The heat flow through each "layer" may be expressed in terms of the boundary temperatures:

$$\frac{q}{A} = h_{12} (T_1 - T_2) \qquad \text{.....(1)}$$

$$\frac{q}{A} = \lambda \frac{(T_2 - T_3)}{x_1} \qquad \text{.....(2)}$$

$$\frac{q}{A} + H_{34} (T_3 - T_4) \qquad \text{.....(3)}$$

There are three equations so the three unknowns, $\frac{q}{A}$, T_2 and T_3 can be found thus defining the performance of the insulant. If the x=o face were subjected to thermal radiation of intensity I and the foam were opaque, then the first equation would be modified to

$$\frac{q}{A} = h_{12} (T_1 - T_2) + I \qquad \text{.....(4)}$$

but the system would still be solvable and the temperature gradient within the slab would still be linear.

If the solid slab generated heat at the constant rate of q_r/unit volume then the temperature gradient within the slab would be non-linear.

At a distance x from the face

$$\frac{q}{A} + q_r x = -\lambda \frac{dT}{dx}$$

This can be integrated

$$\int \left(\frac{q}{A} + q_r x\right) dx = -\int \lambda \, dT,$$

$$\therefore \quad \frac{q}{A} x + q_r \frac{x^2}{2} + C = -\lambda T,$$

but $T = T_2$ at $x = 0$

$$\therefore \quad C = -\lambda T_2$$

$$\therefore \quad \frac{q}{A} x + q_r \frac{x^2}{2} = \lambda (T_2 - T)$$

so at $x = x_1$

$$\frac{q}{A} x_1 + q_r \frac{x_1^2}{2} = \lambda (T_2 - T_3) \qquad \text{.....(5)}$$

At the lower temperature boundary all the generated heat would be transmitted to the fluid thus

$$\frac{q}{A} + q_r x_1 = h_{34} (T_3 - T_4) \qquad \text{.....(6)}$$

Re-arrangement of equations (1) (2) and (3), for the inert material, gives $T_1 - T_2 = \frac{q}{A} \frac{1}{h_{12}}$ .....(7)

$$T_2 - T_3 = \frac{q}{A} \frac{x_1}{\lambda} \qquad \text{.....(8)}$$

$$T_3 - T_4 = \frac{q}{A} \frac{1}{h_{34}} \qquad \text{.....(9)}$$

Adding (7) (8) and (9) gives

$$T_1 - T_4 = \frac{q}{A} \left(\frac{1}{h_{12}} + \frac{x_1}{\lambda} + \frac{1}{h_{34}}\right)$$

$$\frac{q}{A} = (T_1 - T_4) \left(\frac{1}{h_{12}} + \frac{x_1}{\lambda} + \frac{1}{h_{34}}\right)^{-1} \qquad \text{.....(10)}$$

When the solid generates heat the flux from fluid at T_1 is found by solution of equations (1) (5) and (6);

$$\frac{q}{A} = \left(T_1 - T_4 - \frac{q_r x_1^2}{2\lambda} - \frac{q_r x_1}{h_{34}}\right) \left(\frac{1}{h_{12}} + \frac{x_1}{\lambda} + \frac{1}{h_{34}}\right)^{-1} \qquad \text{.....(11)}$$

Thus it can be seen that if the insulation generates heat within itself it is more effective in preventing heat loss from a body, but at the same time more heat is transmitted to the cold side: for an inert solid the flux into the cold fluid is

$$\frac{q}{A} = (T_1 - T_4) \left(\frac{1}{h_{12}} + \frac{x_1}{\lambda} + \frac{1}{h_{34}}\right)^{-1},$$

but when there is heat generation the corresponding flux is

$$\frac{q}{A} + q_r x_1 = (T_1 - T_4) \left(\frac{1}{h_{12}} + \frac{x_1}{\lambda} + \frac{1}{h_{34}}\right)^{-1} - \left(\frac{q_r x_1^2}{2\lambda} + \frac{q_r x_1}{h_{34}}\right) \left(\frac{1}{h_{12}} + \frac{x_1}{\lambda} + \frac{1}{h_{34}}\right)^{-1} + q_r x,$$

and the difference between these two fluxes is

$$\left(q_r x_1 \frac{1}{h_{12}} + \frac{q_r x_1^2}{2\lambda}\right) \left(\frac{1}{h_{12}} + \frac{x_1}{\lambda} + \frac{1}{h_{34}}\right)^{-1}$$

At low temperatures (less than approximately 100°C) rigid polyurethane foam behaves essentially as an inert material and the steady state equations can be used to predict the equilibrium temperature distribution. The design temperature, that is the temperature it attains in normal usage or operation, should never be high enough to initiate any reactions,

but in cases of poor design or unforeseen conditions the temperature may rise too high, and heat will be generated. In this case the behaviour will tend to that derived above for a material with internal heat generation, but as there would be a critical temperature which needed to be exceeded before the exothermic reactions occurred the slab would behave as a composite with only the hotter portion generating heat, (figure 4.44)

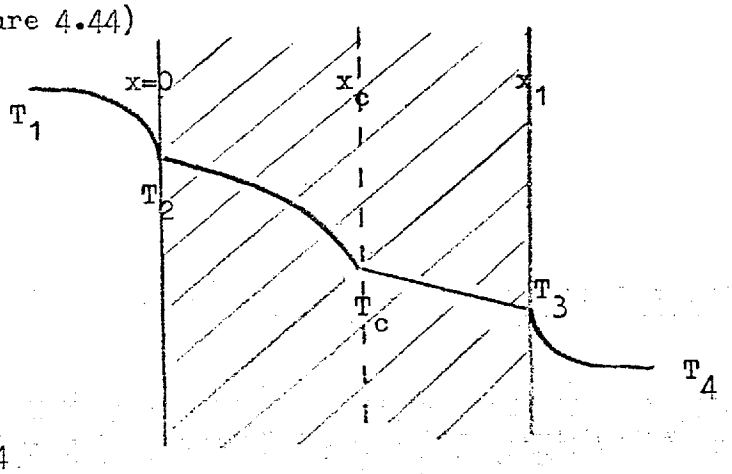

Figure 4.44

then $\frac{q}{A} + h_{12}(T_1 - T_2)$,

$$\frac{q}{A} x_c + q_r \frac{x_c^2}{2} = \frac{\lambda}{x_c} \cdot (T_2 - T_c) ,$$

$$\frac{q}{A} + q_r x_c = \frac{\lambda}{x_1 - x_c} \cdot (T_c - T_3) ,$$

$$\frac{q}{A} + q_r x_c = h_{34} \quad (T_3 - T_4).$$

These four equations in four unknowns ($\frac{q}{A}$, T_2, T_3, x_c) require numerical solution.

In practice a steady state such as this would never be reached because the reactions generating the heat would consume the reactants. A steady rate of generation would not be established as the rate of reaction would also vary with the temperature.

Thus in real situations the steady state conditions will prevail when the temperatures are low and the polyurethane behaves as an inert material, and possibly in the char remaining after combustion of the form.

4.6.12 Thermal damage, that is charring, ignition and continued burning of solids when the temperature is raised by radiative heating or by exposure to a heated atmosphere, is approached in terms of the heating of the solid. The solid is not in thermal equilibrium so steady state considerations are not applicable. As the solid is heated its characteristics change with the changing chemical structure. Parameters that are usually considered to vary slowly and continuously with temperature, such as specific heat and thermal conductivity, undergo sudden fluctuations due to both the altered nature of the material and the changes in density that result from the evolution of volatile fragments. As it is not practical to forecast the chemical reactions that will occur on heating owing to the complex nature of interactions so the variations in thermal parameters are not readily pre-determined.

If it is assumed that the specific heat and thermal conductivity are constant then the following equation represents one dimensional heat flow in a diathermic (i.e. one which has the quality of transmitting radiant heat) self-heating material:

$$\lambda \frac{\partial^2 T}{\partial x^2} = \rho C_p \frac{T}{t} + q_r \rho + u \qquad \text{.....(1)}$$

where q_r = rate of heat generation per unit mass

u = absorption of radiant heat per unit volume.

When the heat loss from the front surface is due to convective cooling and the slab is thick enough to be considered semi-infinite the boundary conditions are

$$\lambda \frac{\partial T}{\partial x} = H (T - T_o) \quad \text{at} \quad x = o, \; t > o$$

$$\frac{\partial T}{\partial x} = o \quad \text{at} \quad x = \infty$$

It is conventionally assumed that the absorption per unit volume is given by the Lambert-Beer attenuation law:

$$u = \alpha I e^{-\alpha x} \qquad \text{.....(2)}$$

where α the attenuation co-efficient

and I is the incident radiant intensity.

Thus the radiation absorbed between the surface and a depth of x is

$$\int_o^x aI\, e^{-ax}\, dx$$

$$= aI\, \frac{1}{-a} \left[e^{-ax} \right]_o^x$$

$$= \underline{I(1-e^{-ax})} \qquad \text{.....(3)}$$

The less transparent a material is to radiant heat, the greater is the value of the absorption coefficient, and hence a greater proportion of the radiation is absorbed in a given distance.

The rate of heat generation per unit mass is proportional to the rate of reaction;

$$q_r = H_r \frac{dc}{dt} \qquad \text{.....(4)}$$

where c is the concentration of the reacting species. For an nth order reaction $\frac{dc}{dt} = -k\, c^n$ .....(5)

and $c = c_o$ at $t = o$

k, the rate of reaction has the form $A_o e^{\frac{-Eact}{RT}}$

where A_o is the frequency factor

Eact is the activation energy

R is the universal gas constant.

When there are several reactions occurring simultaneously the heating effect is represented by the summation of the terms,

$$q_r = \sum H_{ri} \frac{dci}{dt}$$

where $\frac{dci}{dt} = -k_i \cdot c_i^{ni}$ and $c_i = c_{io}$ at $t = o$

The problem in practical definition of the concentration is discussed in section 4.3.5.

Considering the case of a single n-th order reaction,

$$\frac{dc}{dt} = -k\,c^{n} \quad ,$$

$$\therefore \quad \int c^{-n}\,dc = \int -k\,dt \quad ,$$

$$\therefore \quad \frac{c^{1-n}}{1-n} = -kt - A \quad ,$$

but $c = c_o$ at $t = o$,

$$\therefore \quad \frac{c_o^{1-n}}{n-1} = A \quad ,$$

so $$\frac{c^{1-n}}{n-1} = kt + \frac{c_o^{1-n}}{n-1} \quad ,$$

$$\therefore \quad c^{n} = \left[(n-1)\,kt + c_o^{1-n}\right]^{\frac{n}{1-n}} \qquad \text{.....(6)}$$

When equations (2), (4), (5) and (6) are substituted into equation (1) with the appropriate boundary conditions to give

$$\lambda \frac{\partial^2 T}{\partial x^2} = \rho\, C_p \frac{\partial T}{\partial x} - \rho H_r A_o \exp\left(-\frac{Eact}{RT}\right)\left[A_o \exp\left(\frac{-Eact}{RT}\right).\, t(n-1) + c_o^{1-n}\right]^{\frac{n}{1-n}} + a.I\,e^{-ax} \qquad \text{.....(7)}$$

with $$\lambda \frac{\partial T}{\partial x} = H(T - T_o) \quad \text{at } x = o,\ t > o$$

$$\frac{\partial T}{\partial x} = o \quad \text{at } x = \infty,$$

it can be seen that the resulting system does not lend itself to analytical solution.

If the chemical heating effect is small enough to be disregarded and the radiation is absorbed in a short enough distance for the material to be considered opaque, then the system is considerably simplified and is reduced to a semi infinite opaque solid with its surface maintained at a temperature f(t). Thermal damage can be considered separately. In Section 4.2.5 it has been shown that the variation of the surface temperature with time is a complex relationship, but inspection of figure 4.5 shows that for the first $\frac{1}{2}$ minute or so the function could be approximated by $\sqrt{t}$. This is in agreement with the function of the surface temperature derived by Carslaw and

Jaeger [62] for a semi infinite solid receiving a constant flux at the surface. When the temperature is initially zero and the flux at x = o is a constant, F_o, the temperature at the surface of a semi infinite solid is given by

$$v_{x=o} = \frac{2F_o}{K}\left(\frac{\alpha t}{\pi}\right)^{\frac{1}{2}}$$

and the temperature at any point is given by

$$v = \frac{2F_o\sqrt{\alpha t}}{K} \cdot \text{ierfc}\ \frac{x}{2\sqrt{\alpha t}}$$

This expression could be used for the initial period and will give the temperature distribution within the body of the material, but, as seen in section 4.2.6, the surface temperature reaches a steady value in less than one minute. During this time the heat will have penetrated effectively to less than 20mm.

$$\frac{v_{(x=x)}}{v_{(x=o)}} = \frac{\frac{2F_o\sqrt{\alpha t}}{K}\ \text{ierfc}\ \frac{x}{2\sqrt{\alpha t}}}{\frac{2F_o}{K}\left(\frac{\alpha t}{\pi}\right)^{\frac{1}{2}}}$$

$$= \sqrt{\pi}\ \text{ierfc}\ \frac{x}{2\sqrt{\alpha t}}$$

Consider then t = 60s, $\alpha \simeq 10^{-6}\ m^2\ s^{-1}$ and $x = 2 \times 10^{-2}$m

$$\therefore \quad \frac{v_{(x)}}{v_{(o)}} = \sqrt{\pi}\ \text{ierfc}\ \frac{2 \times 10^{-2}}{2\sqrt{(6\times10^{-5})}}$$

$$= \sqrt{\pi}\ \text{ierfc}\ (1.3)$$

$$= \underline{0.032}$$

This means that the temperature rise at 20mm depth is only 3% of that at the surface. Similarly it is found that the rise at 15mm is 6% and at 10mm 25%.

After this initial period when the surface temperature is building up to a constant value the system can be considered, as in section 4.1.3, as having a constant surface temperature. The solution of the

case with non-uniform initial temperature distribution is not analytically feasible, but as most above the temperature is nearly uniform, even after the initial surface temperature build up, for all but the shallow surface layer. Thus the use of the expression

$$v = \text{erfc} \frac{y}{2\sqrt{\alpha t}}$$ to define the temperature at any point is valid for all but the zone close to the surface where the limiting constant value is soon attained.

When calculating the thermal damage to the foam it is essential to know the rate constants of all the reactions that occur. Polyurethane foam is not a simple repeating polymer, which means that it is not easy to determine all the rate data required to solve equation (7) above. In practice it is assumed that the material decomposes in one or two stages for each of which global kinetic data are derived from experimental data, in a similar manner to that used in sections 4.3.5, 4.3.7 and 4.4.3. If it is assumed that the thermochemical effects are small and can be ignored in the heat balance, then the solution of the diffusion equation is substituted into the equations for the degradation of the foam and an expression of the chemical degradation is derived.

From the form of the Arrhenius rate constant it is seen that the rate of reaction is finite at all temperatures, but from experimental observations it is apparent that there is a critical temperature below which the rate of reaction is insignificant. For an nth order reaction the rate of reaction, $\frac{dc}{dt} = -k\, c^n$ and $k = A_o \exp(\frac{-Eact}{RT})$, thus it is seen that the rate of reaction is proportional to $\exp(\frac{-Eact}{RT})$ which is temperature dependent. Theoretically the activation energy is itself temperature dependent, ($E_{act} = E + RT$), but this hardly affects the linear Arrhenius plot.

The form of the rate constant used, $k = A_o \exp(\frac{-E_{act}}{RT})$, is derived from the collision theory in gaseous reactions. It can be

applied quite successfully to reactions in liquids, but its applicability to reactions in solids is rather more dubious. The exponential portion of the expression represents the probability of a colliding molecular pair having energy greater than the activation energy. The pre-exponential factor, or frequency factor, is the rate of collision of the gas molecules, and for gaseous reactions this is proportional to the square root of the temperature. In a solid the mean position of the molecules is fixed and they vibrate about these positions so collisions between portions of the molecules are limited by their orientation and position in the molecule.

The activation energies calculated from the weight loss results, and for the char oxidation vary with temperature in no fixed manner. This is not surprising as the temperature range covered is several hundred degrees, and a multiplicity of reactions must be taking place.

Consider a reaction with an activation energy of 50kJ $mole^{-1}$. At 290°C the exponential portion of the reaction rate constant can be evaluated as

$$\exp\left[\frac{-50 \times 10^3}{8.3 \times (290+273)}\right] = 2.2 \times 10^{-5}$$

Values calculated at other temperatures are shown in table 4.37.

Table 4.37 : Reaction rates (E_{act} = kJ $mole^{-1}$)

Temperature °C	$\exp(\frac{-E_{act}}{RT}) \times 10^{-5}$
80	0.0039
100	0.0105
120	0.021
140	0.045
160	0.1
200	0.35
245	0.9
290	2.2
333	4.5
360	7.5
400	12

From this table it can be seen that the rate of reaction varies non-linearly with temperature, but the pre-exponential constant A_o has to be known to determine the rate of reaction. Now $k = -\frac{dc}{dt} \cdot \frac{1}{c}$ which is the fractional rate of reaction. If the reaction is 1st order and $A_o = 10^{13}$ sec^{-1} then k can be evaluated at several temperatures:

k_{30^oC}	=	0.0004 s^{-1}	(0.04% s^{-1})
k_{100^oC}	=	0.001 s^{-1}	(0.1% s^{-1})
k_{160^oC}	=	0.01 s^{-1}	(1% s^{-1})
k_{245^oC}	=	0.09 s^{-1}	(9% s^{-1})
k_{290^oC}	=	0.22 s^{-1}	(22% s^{-1})

To gauge the effect of these reaction rates it is useful to calculate the time ($t_{1/2}$) taken for the concentration to be reduced to half the initial concentration, C_o.

$$\frac{dc}{dt} = -kc$$

$$\therefore \int\frac{dc}{c} = \int -kdt$$

$$\therefore \ln c = -kt + \text{const} \quad \text{, but } c = c_o \text{ at } t = o$$

$$\therefore \ln \frac{c}{c_o} = -kt$$

when $\frac{c}{c_o} = \frac{1}{2}$

$$\ln \tfrac{1}{2} = -kt_{\frac{1}{2}}$$

$$\therefore t_{\frac{1}{2}} = \frac{0.7}{k}$$

For the values of k above the corresponding 'half life' times are

T = 80°c	$t_{\frac{1}{2}}$ = 1800 s (30 minutes)
100°c	700 s
160°c	70 s
245°c	7.7 s
290°c	3.2 s

These figures are a good practical guide to the speed of reaction. From them can be estimated a critical temperature that will allow time to counter the hazard before the reaction has proceeded too far. It can be seen that for these values of activation energy and frequency factor a temperature of 80°C is the limit in the short term where some 20 minutes are required to react to the danger.

Using the same equations it is possible to model the weight loss of the reacting foam, since all that is required is knowledge of the proportion of the reaction products that are volatile, and the calculations are then performed as in section 4.3.5.

Closely associated with this weight loss model are the considerations of ignition of the material when exposed to heating. When considering auto ignition the build up of heat in the solid which leads to a thermal explosion is of importance [37, 38], but when ignition is caused by heating from an external source the controlling mechanisms are different. As there is limited access of oxygen to the interior of rigid polyurethane foams there is little oxidative self heating of the type that leads to spontaneous ignition at low ambient temperatures in stacks of wool [70] or sawdust. If urethane foams have been poorly formulated, secondary curing, with its accompanying exotherm, can occur when the ambient temperature rises above the normal operating temperature. At temperatures over 250°C high modulus polyurethane foams show an increased weight loss and an exothermic reaction when heated in oxygen rather than nitrogen [69], but isocyanurate foam did not show this behaviour even at temperatures in excess of 330°C [39].

As the temperature at the surface is raised above the critical level the foam begins to decompose and release volatile matter which mixes with the atmosphere near the surface and is then carried away by convection currents.

The volatile matter is evolved from the foam in small turbule t jets which increase the efficiency of mixing. On the small scale, the additional projection of volatiles towards possible sources of ignition can be important but for larger systems it has less significance. At some stage of the mixing the concentration of volatile products will fall within the flammability limits and if the temperature is high enough the mixture will ignite spontaneously. There would appear to be a critical heating rate or irradiance value which limits the ignition in two ways. As the air with which the volatiles mix is at a lower temperature it exerts a cooling effect and thus to obtain a combustible mixture at the ignition temperature the evolved volatiles must be at a considerably higher temperature than the ignition temperature. This effect is diminished in the case of a large vertical sample as the rising mixture is heated by convection from the hot face of the material [63], and in the case of pilot ignition where the extra heat is provided externally. If the surface temperature rises slowly the surface will decompose slowly and the rate of evolution of volatile fragments will be low, giving a narrow region of mixture within the flammability limits, which means that the high heat losses from this region ensure that the positive feedback essential to ignition cannot occur. By the time the surface has reached a high enough temperature to give the high rate of decomposition needed there will be no unreacted molecules remaining in the surface layer.

In view of the critical nature of the rate of evolution of volatiles and their temperature it is appreciated that the criterion for ignition of a fixed surface temperature as postulated by several authors [20,22] is correct in practice.

Once these criteria for ignition are incorporated in the model there is need to add an expression for the heat fed into the solid from

the flame at the surface. This can only be done if the amount and nature of the volatile fragments is known as the degree of exothermicity and emissivity of the flame are required.

4.6.2 Requirements of a model of behaviour

To make a complete model of the behaviour of polyurethane foams is not simple as polyurethanes are complex materials and the effects of altering the formulation are highly interactive. The history of the sample is very important, but it is likely to be unknown. Some of the requirements of a model are now listed.

A: Heat flux within the sample is most likely three dimensional and due to several causes:

1) external sources - transfer by radiation, conduction and convection
2) internal generation - from an unknown and constantly changing balance of reactions
3) mass transfer - escaping volatiles remove heat and condensing materials such as TCEP effectively transfer heat
4) flaming combustion at the surface feeds heat to the solid
5) the char may oxidize exothermally when fresh air plays on the material
6) poor formulations can promote secondary curing at quite unexpected times.

B: Physical changes in the foam can be important and have a great effect on the usefulness of a material.

1) softening and melting - few rigid foams melt and flow but the softening allows some consolidation of the heated foam. Plasticisers such TCEP affect the degree of softening

2) shrinkage is the result of - softening

- chemical ablation (evolution of volatiles)

- physical removal of char

3) The permanence of the char is vital as a brittle char that blows away is no use as an insulant: the strength of the charred foam requires assessment.

C: Reactions are varied and depend largely on the past treatment of the foam. Among the facets to be considered are:

1) reactions in the chains of the polymer matrix as assessed by DTA

2) most reactions give some volatile fragments that are removed from the site of formation. These may further react as they diffuse from the material, either to give smaller fragments or to consolidate the char

3) the behaviours under oxidative and pyrolytic conditions are different and in practice neither can be strictly applied

4) when there is ignition of the volatile fragments whether the heat input is sufficient to maintain the supply of fuel to the flame

5) the criteria for ignition by spontaneous ignition or by a pilot source must be tested against the conditions prevailing.

6) when the char is oxidised the nature of the layer on which the volatile fragments are cracked is altered and this will affect the course of the cracking reactions

7) the concentrations and identities of the volatile products of pyrolysis and of their products of oxidation need to be assessed in order to ascertain whether there are any toxic components and whether they present a hazard. Analysis by gas chromatography is useful for assessing this.

3) reactions at low temperatures do not produce volatile products but they do render cell walls permeable, (vide section 4.3.4) and allow the blowing agent to escape and potentially reactive gases to diffuse into the foam.

9) kinetic data and activation energies are required for all the reactions that take place. Until it is known precisely what reactions do occur this is not easy, and global values have to be used. By their very nature these are neither constant or precise, but they do allow some rough quantitive evaluations to be made.

4.6.3 In view of the complexity of the heat diffusion equation derived in section 4.6.1.2 any model formulated would need to be based on numerical solution. As an indication of the manner in which a model could be developed the case of one-dimensional flux through an infinite slab is considered. This represents any large area of foam that is heated at one face, and approximates to many practical situations.

The thickness of the slab, L, is divided into n layers of thickness Δx with half thickness layers at the surfaces, and the temperatures and properties of the solid are assumed to be constant within each layer. T_m is the temperature of the nth layer.

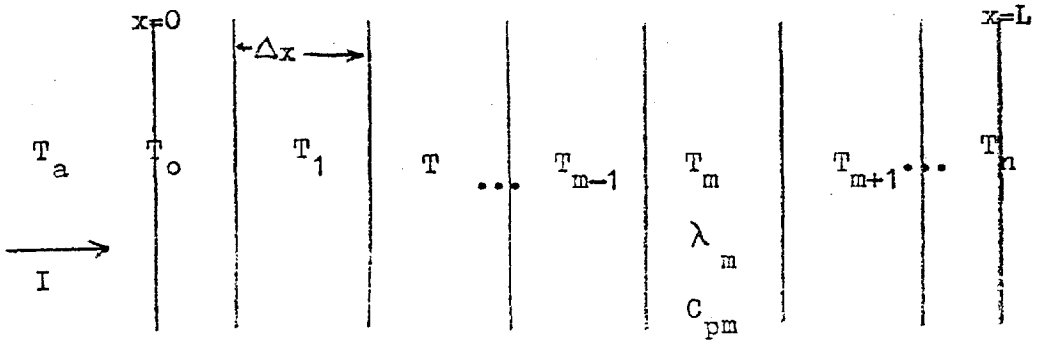

Consider now a unit area of the general layer, m,

heat flux from layer m-1 $= \lambda_m (T_{m-1} - T_m) / \Delta x$

heat flux to layer m+1 $= \lambda_m (T_m - T_{m+1}) / \Delta x$

$\therefore$ net flux into layer m $= \lambda_m (T_{m-1} - 2T_m + T_{m+1}) / \Delta x$

if after time Δt the temperature of layer m is T_m then the rate of heating of the layer is

$$\frac{\Delta x \ \rho \ C_p \ (T_m' - T_m)}{\Delta t}$$

$$\frac{\lambda_m (T_{m-1} - T_{m+1})}{\Delta x} = \frac{\Delta x \ \rho \ C_p \ (T_m' - T_m)}{\Delta t}$$

$$\therefore \quad T_m' = T_m + \frac{m(T_{m-1} - 2T_m + T_{m+1}) \Delta t}{(\Delta x)^2 \ \rho C_p}$$

At the surface, layer '0', the flux in is derived from convective heating/cooling and from radiative transfer, so heat flux into surface = $I - \sigma \epsilon (T_o^4 - T_a^4) - H(T_o - T_a)$

heat flux into layer 1 $= \lambda_o (T_o - T_1) / \Delta x$

and rate of heating of layer $= \frac{\Delta x}{2} \ \frac{\rho \ C_p \ (T_o' - T_o)}{\Delta t}$

$$\therefore \quad T_o' = T_o + \frac{2 \Delta t}{\Delta x \ \rho \ C_p} \left[I - \sigma \epsilon (T_o^4 - T_a^4) - H(T_o - T_a) - \lambda_o \frac{(T_o - T_1)}{\Delta x} \right]$$

A similar equation is derived for the other face of the slab. With these relationships it is possible to follow the temperature history throughout the slab if the properties of the material are known. No

allowance is made for thermochemical effects because the DTA results (figure 3.19) show a temperature variation of less than 1°C due to chemical reaction.

Inspection of the weight loss results in section 3.3.1 reveals that interpolation for temperatures between the experimental points would be permissable as the curves do not deviate markedly from straight lines. There is rapid weight loss during the first 7 minutes, but thereafter it soon reaches a steady value, so a linear interpolation is the simplest method of reaching the time variation of the weight loss, and it does not introduce great inaccuracy. Thus from the experimental results it is possible to derive the functions $W_t(T, t)$ and $\frac{dW_t}{dt}(T, t)$ in empirical form.

With these data a history of the weight fraction remaining at any point of the slab can be followed using the relationship

$$W_{t+\Delta t,m} = W_{t,m} + \Delta t \quad \frac{dW_t}{dt}(T_m, t).$$

Knowledge of the weight fraction remaining is then used to determine the properties used in the equations for temperature after a further interval Δt.

The mean density of the foam decreases as the weight loss increases and can be represented by $\rho_o \frac{W_t}{W_o}$, where ρ_o is the density of the virgin foam, as density is the weight of material per unit volume.

The specific heat, C_p, increases slightly with increasing weight loss and tends to the value of the gas within the char matrix. This has a much smaller effect on the thermal capacity of the foam than the density and can be disregarded.

Weight loss also affects the thermal conductivity of the solid. As there is less solid the cross-sectional area of the relatively high

conductivity path is decreased, which decreases the overall conductivity, but the increasing cell size that accompanies the weight loss allows greater circulation of the gas and so increases the convective heat transfer through the foam. This effectively increases the apparent thermal conductivity.

In addition to the weight loss there is also shrinkage of the sample as recorded in section 3.3.2. An approximate relationship between shrinkage, and temperature and time can be formulated empirically, and then a factor applied to the linear dimension, x, and to the increment Δx, to make provision for this in the layers where shrinkage has occurred.

The spontaneous ignition experiments show that there is a critical surface temperature that has to be exceeded before ignition will occur, and T_o can be tested to check if the condition is met. Alternatively, and probably more accurately, the rate of weight loss can be evaluated in the heated layers near the surface, by means of the empirical relationships derived from the weight loss experiments, to see if there is a sufficient supply of fuel to sustain a flame. If there is no pilot source of ignition, the temperature has to be much higher to cause auto ignition of the volatile matter, as determined in the Setchkin apparatus (section 4.5.2).

When the foam does ignite there is radiation of heat from the flame to the surface of the foam, and this must be calculated with the aid of an assessed flame temperature, and emissivity.

When using the iterative model of this type the increments of length and time can be varied depending on the accuracy required. Where rate of change of temperature and weight fraction are low the grid can be made coarse, with savings of time and effort, without prejudicing the accuracy.

In situations with different geometry and boundary conditions the heat balance at the surface elements have to be remade, and when it is required a three-dimensional or two-dimensional grid can be formed, but correspondingly more work must be put into the solution.

If extensive data on the products of decomposition were obtained by identification of the volatile fragments with gas chromatography and mass spectrometry, and by following the fracture of bonds and groups in the solid with the aid of infra-red spectrometry, then the differential thermographs could be used to obtain rate data for the reactions. In this manner a detailed model of the degradation of the polymer could be formulated and the quantities of toxic products could be assessed. A model of this nature requires much research to identify the reactions in even a simple system and care must be exercised when applying the data to a different system as the interaction of reactions is finely balanced and much changed by additional components or varying conditions.

5 CONCLUSIONS

In a foam of density 30 kg m^{-3} the solid accounts for only 2% of the volume.

Inclusion of TCEP in a foam enhances the process of heat transfer through the foam by its 'refluxing' through the material.

Rigid urethane foams of density 30 kg m^{-3} have a thermal diffusivity of approximately 0.85×10^{-6} m^2 s^{-1}. This is about 3 times that of other common building materials, but in view of their very low density polyurethane foams are excellent insulators.

The position and nature of the pilot source affect the ignition time when a foam is subjected to thermal irradiation.

The presence of TCEP in a foam increases the time to ignition while the concentration of the additive in the volatile products of pyrolysis is high, but the concentration is soon reduced below an effective level.

Fracture of the surface cells as a result of thermal shock throws small particles of foam up from the surface and the resulting combustion of these is a major factor in the flash of non-sustained flame over the sample surface. The brittle isocyanurate foam is particularly susceptible to this behaviour.

The surface temperature is the major factor governing ignition. With pilot ignition the polyurethane foams have a critical surface temperature of ca 225°C and the isocyanurate foam 380°C, and the minimum radiation intensities of 8.4 and 12.6 kW m^{-2} respectively.

The surface temperature is critical because it controls the rate of pyrolysis, and ignition only occurs when there is a sufficient supply of volatile matter to sustain a flame.

At temperatures over 160°C the blowing agent is lost quickly from the foam when the cell walls are rendered permeable by rearrangements in the polymer chains.

Degradation of the polymer chains at 240°C releases volatile molecules thus eliminating the propylene oxide that is used to extend the polyols.

The TCEP is eliminated from the foam by 260°C.

The global activation energies of 30 - 55 kJ $mole^{-1}$ calculated from the weight loss results for the polyurethane foams are lower than the values (80 - 100 kJ $mole^{-1}$) quoted for pyrolysis of wood and natural insulating materials.

The phosphorylated foam has a lower activation energy at the lower temperatures used, only 22 kJ $mole^{-1}$ at 200°C.

Below 350°C the isocyanurate based foam has a low activation energy (less than 30 kJ $mole^{-1}$), but above it rises sharply to nearly 80 kJ $mole^{-1}$.

Discolouration shows that the urethane foams start decomposing below 160°C.

At 200°C the charred urethanes have good strength and suffer little shrinkage in spite of extensive reaction, but by 245°C they are frail and distorted.

Incorporation of TCEP results in higher shrinkage at temperatures of 200°C upwards, and softening of the foam.

Foams based on phosphorylated polyols produce a char with useful strength up to 300°C, largely on account of the thick cellular wall that is formed.

The isocyanurate foam exhibited fracture of the sample as a result of thermal shock.

There is no sign of melting at all in the isocyanurate foam, and the cellular structure is preserved in the char. At 330°C the char offers similar strength to the virgin foam, and shows only small shrinkage.

The chars oxidise in an air stream when heated to some 300°C, and the low activation energies confirm that the chars contain materials other than carbon in appreciable proportions.

In a well formulated foam an organic tin catalyst does not accelerate degradation of the urethane foam.

The urethane link fractures in the temperature range 250 - 300°C. The foams based on higher functionality polyols show urethane degradation at the higher end of this range.

An estimate of the activation energy for the urethane fracture gives values between 125 kJ $mole^{-1}$ and 460 kJ $mole^{-1}$.

Trimerisation of the isocyanate groups occurs at temperatures ranging from 295°C to 355°C depending on the catalysing species present.

Phosphorylated foams show an exothermic reaction at 120°C due to reorganisation of their structure.

The presence of TCEP promotes lowering of the initial reaction temperature by approximately 15°C.

The products of pyrolysis of the foams do not contain any strongly electrophilic molecules in large enough concentrations to be measured by gas chromatography, but there is evidence of aldehydes being present.

TCEP does evolve hydrogen chloride when heated, as does to a small extent the blowing agent, F11.

The mass spectrograms of the pyrolysis products at 250°C are very similar for all the foams tested.

Pyrolyses between 160°C and 250°C produce similar mixtures of products.

Dissociation of the molecules in the mass spectrometer prevents absolute identification of the species present, but clues to their identities can be gained from the fragments. Among the species indicated are the alkanes, alkenes, aldehydes, carbon dioxide, amines, ketones and ethers expected from the fracture of the polymer chains.

There is some evidence of phosgene, cyanides, acetonitrile and isocyanate in the pyrolysis products.

The phosphorylated polyol does release some of its phosphorus in the volatile stream.

The complexity of the problem prevents an analytical model of the polyurethane foam being formed, but it is possible to formulate, with the aid of experimental data, an empirical model to describe the behaviour of a foam when it is subjected to a variety of environments.

APPENDIX I

Calculation of heat flux from radiative source

Symbols:

q	heat flux from furnace	$W\ m^{-2}$
A_T	total area of disc	m^2
A_R	area of disc receiving heating from source	m^2
T_A	ambient temperature	^oK
T_D	temperature of disc	^oK
G	emissivity of surface of disc	-
σ	Stefan-Boltzmann constant	$(5.73 \times 10^{-8}\ W\ m^{-2}\ ^oK^{-1})$
C	Newtonian cooling coefficient	

Subscripts 1, 2 represent different source apertures.

The disc receives heat from the source and by radiation from the atmosphere. At steady state the heat received

$$= G\ q\ A_R + A_T\ \sigma\ G\ T_A^4$$

Heat is lost by radiation to the surroundings and by natural convective cooling. At steady state the heat lost

$$= A_T\ \sigma\ G\ T_D^4 + A_T\ C(T_D - T_A)^{\frac{5}{4}}$$

Completing the heat balance at steady state gives

$$G\ q\ A_R + A_T\ \sigma\ G\ T_A^4 = A_T\ \sigma\ G\ T_D^4 + A_T\ C(T_D - T_A)^{\frac{5}{4}}$$

which simplifies to

$$q\ \frac{A_R}{A_T} - \sigma\ (T_D^4 - T_A^4) = \frac{C}{G}\ (T_D - T_A)^{\frac{5}{4}}$$

This equation contains an unknown factor $\frac{C}{G}$, which needs to be eliminated. The value of q, the heat flux is kept constant, and the value of A_R changed by using a different source aperture, and the new equilibrium temperatures measured. The following equations hold

$$q \frac{A_{R1}}{A_T} - \sigma (T_{D1}^4 - T_{A1}^4) = \frac{C}{G} (T_{D1} - T_{A1})^{\frac{5}{4}}$$

$$q \frac{A_{R2}}{A_T} - \sigma (T_{D2}^4 - T_{A2}^4) = \frac{C}{G} (T_{D2} - T_{A2})^{\frac{5}{4}}$$

Elimination of the factor $\frac{C}{G}$ between these equations, and rearrangement gives

$$q = \frac{A_T \sigma (T_{D1}^4 - T_{A1}^4) (T_{D2} - T_{A2})^{\frac{5}{4}} - (T_{D2}^4 - T_{A2}^4) (T_{D1} - T_{A1})^{\frac{5}{4}}}{A_{R1} (T_{D2} - T_{A2})^{\frac{5}{4}} - A_{R2} (T_{D1} - T_{A1})^{\frac{5}{4}}}$$

APPENDIX II

List of symbols.

a Constant

a Radius of cylinder

a Activity of reacting species

a Absorption coefficient

A_o Frequency factor

b Constant

C_p Specific heat at constant pressure

c Constant

c Concentration of reacting species

d Constant

E_{act} Activation energy

H Newtonian cooling coefficient

H_R Heat of reaction

h_{ij} Heat transfer coefficient between i andj

I Intensity of radiation

k Constant

k Rate constant of reaction

l Thickness of layer

p Constant

q Heat flux

q_r Rate of heat generation / unit mass

R Universal gas constant (8.3 J $mole^{-1}$ $^{o}K^{-1}$)

s Constant

S Heat of reaction

t Time

t_i Time to ignition

t_{ss} Time to establish steady state convective boundary layer

T Temperature

T_S Temperature at surface

T_a Temperature, ambient

u Absorption of radiant heat / unit volume

v Temperature

W Weight of foam

x Distance

α Thermal diffusivity

λ Thermal conductivity

ρ Density

θ_F Temperature above ambient at ignition

β Cooling modulus

$$\operatorname{erfc}(x) = \frac{2}{\sqrt{\pi}} \int_x^\infty e^{-t^2}\, dt$$

$$\operatorname{ierfc}(x) = \int_x^\infty \operatorname{erfc}(x)\, dx$$

REFERENCES

1 Saunders J H and Frisch K C; "Polyurethanes – Chemistry and Technology" part I, (Interscience, New York) 1962.

2 Department of Employment, H M Factory Inspectorate; Technical Data Note 29, (HMSO, London) 1971.

3 Plastics and Rubber Weekly, p6, 12 October 1973.

4 Singh A, Weissbein L and Mollica J C; Rubber Age, 99, 77 (Dec 1966).

5 Ferrigno T H; "Rigid plastic foams" 2nd Ed, p23, 1967 (New York; Rheinhold Publishing Corporation).

6 Buist J M and Lowe A; British Polymer J, 3, 104 (1971).

7 Zapp J A; Arch. Ind. Health, 15, 324 (1957).

8 Europlastics Monthly, British Plastics Edition; Nov 1972.

9 Anderson J J; Ind Eng Chem, 55, 260 (1963).

10 US Nat. Res. Council; "International Critical Tables of Numerical Data, Physics, Chemistry and Technology", Vol 1, p59 (McGraw Hill, New York) 1926.

11 Carslaw H S and Jaeger J C; "Conduction of heat in solids", 1957, p63 (London, Oxford University Press).

12 Ibid, Appendix VI.

13 Simms D L, Combustion and Flame, 7, 253 (1963).

14 Lawson D I, Fire Research Bulletin, No 1, "Fire and the Atomic bomb" 1954 (London, HMSO)

15 McAlevy R F and Magee R S, 12th Symposium (International) on Combustion 1968, 1969 (Pittsburgh: Combustion Institute).

16 Tarifa C S, Del Notario P P and Torrilbo A M, 12th Symposium (International) on Combustion, 1968, 1969 (Pittsburgh, Combustion Institute).

17 Mitchell D W, Nagy J and Murphy E M, Bureau of Mines, Report of Investigations No 6366, 1964 (US Dept of Interior).

18 Murty Kanury A; Combustion and Flame, 18 (1) 75 (1972).

19 Fennimore D C and Jones; Combustion and Flame, 10, 295 (1966).

20 Simms D L and Law M; Combustion and Flame, 10, 295 (1966).

21 Garg D R and Stewart F R; Combustion and Flame, 17, 287 (1971).

22 Wesson H R, Welker J R and Sliepcevich C M; Combustion and Flame, 16, 303 (1971).

23 Carslaw H S and Jaeger J C, "Conduction of Head in Solids", 1957, p21 (London, Oxford University Press).

24 Chapman A J, "Heat Transfer" 2nd Ed, 1967, sect 9.5 (New York, Macmillan).

25 McAdams W H, "Heat Transmission" 3rd Ed, 1954 (New York, McGraw Hill).

26 Wilson W J; Private communication.

27 Chellis L N; Electro-technology 68 (6) 77 (1961).

28 Gross D, Loftus J J, Lee T G and Gray V E; US Dept of Commerce, Nat. Bur. of Standards, Building Science Series 18, (1969).

29 Simms D L; Combustion and Flame, 4, 293 (1960).

30 Technical Information, PC/U 65, (Imperial Chemical Industries Ltd, 1965).

31 Technical Information, U/R 8A, (Lankro Chemicals Ltd, 1965).

32 Burbridge J, Private communication.

33 Technical Information, OC28 (British Celanese Ltd, 1971).

34 Carslaw H S and Jaeger J C; "Conduction of heat in solids", 1957, p200 (London, Oxford University Press).

35 Clauser H R ed: "Encyclopaedia of Engineering Materials and Processes" (Reinhold Publishing Corp. New York, 1963).

36 Einhorn I N, Seader J D, Drake W O, Mihlfeith C M and Kanakia M D; Polym. Eng. Sci. 12, 167 (1972).

37 Gross D and Robertson A F; J Res. Nat. Bur. Standards, 61, 413 (1958).

38 Walker I K, Harrison W J and Hooker C N; N.Z J Science, 8, 319 (1965).

39 Gamadia R K; Private communication.

40 Gamadia R K; 1966, DIC Thesis, Imperial College of Science and Technology.

41 Buist J M, Hurd R, and Lowe A; Chemistry and Industry, 1544 (1960).

42 Nicholas L and Gmitter G T; J Cellular Plastics, 1, 85 (1965).

43 Woolley W D: British Plastics, 3, 186 (1971).

44 Bunn C W; J Polymer Science, 16, 323 (1955).

45 Piloyan G O, Ryabchikov I D and Novikova O S; Nature, 212, 1229 (1966).

46 Morris C J O; Laboratory Practice, 23, 515 (1974).

47 Maggs R J, Joynes P L, Davies A J and Lovelock J E; Anal. Chemistry, 43, 1966 (1971).

48 Fenimore D C, Loy P R and Zlatkis A; Anal. Chem, 43, 1972 (1971).

49 Lang F M and Magnier P; "Chemistry and Physics of Carbon, 3", Ed. Walker P L, 1966 (Marcel Dekker Inc. New York).

50 Saunders J H and Frisch K C; "Polyurethanes – Chemistry and Technology" Part I, p 106 (Interscience, New York) 1962.

51 Dyer E and Osborn D W; J Polymer Science, 47, 349 (1960).

52 Backus J K, Darl W C, Gemeinhardt P G and Saunders J H; J Cellular Plastics, 1, 178 (1965).

53 Trace R; "Health hazards due to fires in plastics", SMRE, Jan 1971.

54 Nuckolls A H; Underwriters Laboratory Report, Miscellaneous Hazard No 2375 (1933).

55 J Cellular Plastics, 5, 122 (1969).

56 Napier D H and Wong T W; British Polymer J, 4, 45 (1972).

57 Wilson H N; "An approach to chemical analysis" p339, Permagen Press, Oxford, (1966).

58 Einhorn I N, Mickelson R W, Shah B and Craig R; J Cellular Plastics, 4, 188 (1968).

59 Moore W J; "Physical Chemistry", 4th edition, 1966, p550, (Longmans, London).

60 Ibid. p59.

61 Einhorn I N; Science, 187, 742 (1974).

62 Carslaw H S and Jaeger J C; op. cit. p75.

63 Alvares N J, Blackshear P L and Murty Kanury A; Combustion Science and Technology, 1, 407 (1970).

64 Stephenson G; "Mathematical Methods for Science Students", 1965, p234 (Longmans, London).

65 Ibid. p232.

66 Zeldovitch Ya B; J Experimental Theoretical Physics (USSR), 9, 1530 (1939).

67 Simms D L; Fire Research Note No 361/1958, (London, HMSO) 1958.

68 Smith I W and Tyler R J; Combustion Science and Technology, 9, 87 (1974).

69 Boult M A, Gamadia R K and Napier D H; in "Fourth Symposium on Chemical Process Hazards with special reference to plant design", I Chem E Symposium Series No 33, (Instn Chem Engrs, London) 1972.

70 Walker I K and Harrison W J; N Z J Science, 8, 106 (1965).

71 Fish A; Combustion and Flame, 8, 84 (1964).

72 Hilado C J; J Cell. Plastics; 4, 67 (1968).

73 Jacques J K; Trans J Plast Inst, Conf Suppl No 2, 33 (1967).

74 Piechota H; J Cell Plastics, 1, 351 (1965).

75 Papa A J; Ind Eng Chem, Prod Res Develop, 9, 478 (1970).

76 Ferrigno T H; "Rigid Plastics Foams" 2nd Ed. (Reinhold, New York) 1967.

77 Saunders J H and Frisch K C; "Polyurethanes - Chemistry and Technology" - Part II (Interscience, New York) 1962.

78 Sheridan J E and Haines C A; J Cell Pl, 7, 135 (1971).

79 Hilado C J; Fire Technology, 3, 314 (1967).

80 Hilado C J; Ind Eng Chem, Prod Res & Devel, 6, 154 (1967).

81 Learmouth G S and Thwaite D G; Br Polym J, 1, 154 (1969).

82 Darr W C, Gremeinhardt P G and Saunders J H; Ind Eng Chem, Prod Res & Devel, 2, 194 (1963).

83 Rosser W A and Wise H; 9th Comb Symp (Int), p733 (Pittsbgh, Combustion Institute) 1962.

84 Papa A J and Proops W R; J Appl Polym Sci, 16, 2361 (1972).

85 Miles C E and Lyons J W; J Cell Plastics, 3, 539 (1967).

86 Dombrow B A; "Polyurethanes" 2nd Ed (Reinhold Publishing Corp, New York) 1965.

87 Tilley J N, Nadean H G, Reymore H E, Waszeciak P H and Singh A A; J Cell Plastics, 4 22 (1968).

88 Bott R, Frith J G and Jones T A; Br Polym J, 1, 203 (1969).

89 Coleman E H; Plastics, 24 (264) 416 (1959).

90 Seader J D, Einhorn I N, Drake W O and Mihlfeith C M; Polym Eng & Sci, 12, 125 (1972).

91 Madorsky S L and Straus S; J Polym Sci, 36, 183 (1959).

92 Woolley W D; Br Polym J, 4, 27 (1972).

93 Plastics and Rubber Weekly; p27, 5 April 1974.

Behaviour of polyurethane foams under controlled heating

M. A. Boult, B.Sc.(Eng.), A.C.G.I.

D. H. Napier, M.Sc., Ph.D., C.Eng., A.R.I.C., M.Inst.F.*

Department of Chemical Engineering and Chemical Technology, Imperial College

Knowledge of the behaviour of new materials is essential if engineering designers are to avoid unsuitable applications. To avoid undesirable consequences it is necessary to evaluate the properties, behaviour and hazards of new materials at an early stage of development.

Polyurethane foams have replaced traditional materials in many applications, and whilst the behaviour of traditional materials is comparatively well documented, that of polyurethane is still in several ways a matter for testing and experimentation. One reason for this is that the term "polyurethane foam" covers a large range of materials differing widely in chemical composition and physical properties.

The major uses of rigid polyurethane foam are in insulating applications, lagging pipework, containers and, increasingly, for filling cavity walls in brickwork. It also finds application as major and minor components in furniture, and as packaging. The flexible foams are used extensively in packaging, clothing, furniture, automobile and aircraft trimmings and in some insulation situations.

In common with other organic materials, polyurethane foam burns vigorously once the combustion is well established; this is well illustrated by the case of the firing of a large stack of foam. When the material is distributed in a structure and there may be local ignition with subsequent local combustion, other criteria of assessment must be applied. This, in effect, is the standpoint adopted in this paper where objective assessment of the behaviour in specified environments has been attempted. Thus the concern is more with the production of smoke and the stability of the char than with the softening and flaming occurring in violent large-scale combustion.

The incorporation of fire retardants into the formulation can enhance the performance, eg smoke production may be reduced and heat penetration may be limited, but other factors also require consideration. For example, tris (chlorcethyl) phosphate (TCEP) distils and decomposes producing hydrogen chloride, and phosphorus polyols reduce the temperature of initial decomposition of the foam.

*Acknowledgment

The authors wish to thank the British Rigid Urethane Foam Manufacturers Association who are supporting this work.

Types of foam

All polyurethanes are based on the urethane linkage formed when an organic compound containing a hydroxyl group reacts with an isocyanate,

$$R{-}OH + R'NCO \rightarrow R{-}O{-}\overset{\overset{O}{\|}}{C}{-}\overset{\overset{H}{|}}{N}{-}R'$$

By the reaction of alcohols containing more than one hydroxyl group (polyols) with isocyanates a three-dimensional structure can be built up.

Many formulations can be used to produce foams of widely differing properties. The broadest classification comprises the two classes of flexible and rigid foams; the former is usually of an open cell structure and the latter has closed cells.

Classification may also be based on the raw materials used in manufacture. The polyhydroxyl compound can be a polyester-or a polyether-based material, and the isocyanate used may commonly be toluene di-isocyanate (TDI) or diphenyl methane di-isocyanate (MDI).

Flexible foams were originally all made from an ester based compound, but this is no longer the case as the reaction produces water that must be driven off, making the product costly. Besides having a wide range of molecular weights commercial polyesters contain unreacted starting material which reduces the hydrolytic stability[1].

In spite of these shortcomings polyesters still command a place among urethanes because they are inherently less flammable than polyethers[2] and, when halogenated compounds are used it is possible to formulate foams having superior fire retardant properties. Thus flexible foams are made from polyethers with some substituted esters added as a fire retardant. TDI is the most common polyisocyanate for these open cell foams and the blowing agent is usually the carbon dioxide produced by reaction of isocyanate with the water included in the formulation.

Rigid foams differ from flexible foams in that there is a high degree of crosslinking between the polymer chains. The principal commercially available polyether rigid foams are made by starting from compounds of propylene oxide and materials such as glycerol, sorbitol and sucrose. MDI is the commonest isocyanate used in rigid foam manufacture as it is safer to handle than TDI and gives desirable chemical characteristics, and the foam is blown by trichlorofluoromethane added as solvent.

Fire retardants can be divided into two classes, the physical additives and those that are chemically bonded in the foam. Most of the retardants used depend upon phosphorus or halogens or both for their effectiveness. Halogens act by inhibiting flame reactions, and phosphorus by promoting char formation.

Among the additives there are some solids but these are rarely used in low density systems as they have detrimental effects on the physical properties of the foam. Liquids such as tris (chloroethyl) phosphate (TCEP) and other halogenated alkyl phosphates are in common use.

The chemically incorporated fire retardants can be phosphorus-or halogen-containing isocyanates, but by far the majority are polyhydroxyl compounds containing these elements. The acids of phosphorus are frequently extended with propylene oxide to decrease the isocyanate demand, and chlorine or bromine is introduced on account of the mutually beneficial effect that exists between halogens and phosphorus in fire retardance[3].

Miscellaneous methods The introduction of heat resistant groups into the foam structure is gaining importance. The most notable such group is the isocyanurate ring formed by the joining together of three isocyanate molecules. Although the isocyanurate ring is stable to over 300°C[4, 5], the friability of the foams it produces limits the extent of its use[6].

Behaviour of foam

Heat penetration When polyurethane foam is exposed in a fire it decomposes as do all organic materials. Of greater interest is its behaviour under the conditions that exist before ignition occurs.

Some investigations relating to heat penetration were performed by subjecting one end of a cylindrical sample to a known intensity of thermal radiation and measuring the temperatures along the cylinder axis at various distances from the heated face. The intensities used were 4·2 kW/m² and 21·0 kW/m². The lower of these values approximates to exposure to a single bar electric fire at six inches distance. The intensities received from other frequently encountered sources of radiant heat are shown in Table I[7]. Typical temperature histories are shown in Fig 1[8]. The foams examined were rigid, of nominal density 32 kg/m³. Values of thermal diffusivity were calculated by assuming the system approximated to a semi-infinite body subjected to constant radiation[9]. These values and those of some typical building materials are shown in Table II.

The curves showing heat penetration are of the expected shape, but there are notable differences between the heating rates of the different foams. The heat penetration rate was higher for the foam containing TCEP than for that without flame retardant due to the "fluxing" of the additive through the material assisting heat transfer and breakdown of the cell walls. It was also observed that a decrease in heat penetration rate occurred in the order A B D C, which correlates with the decreasing cell size of the char. The surface temperatures were measured by a shielded thermocouple at the face, and the shrinkage of the foam away from the thermocouple caused the drop in temperature observed. Isocyanurate foam behaved differently from the others as shown by the

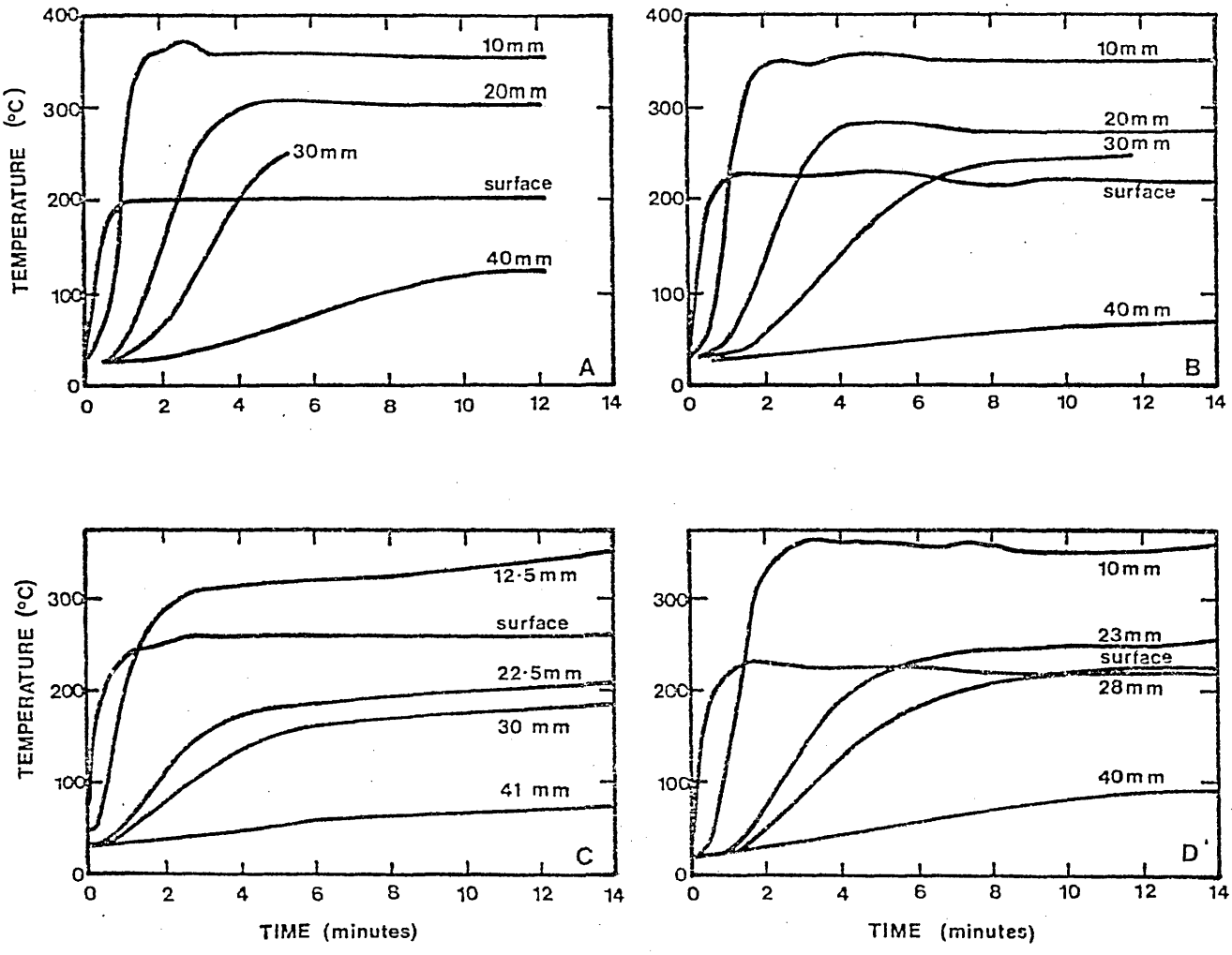

Fig 1. Thermal penetration by irradiation. Temperature histories at various depths below heated face.
A: Polyurethane foam, 20 parts of TCEP
B: Polyurethane foam, no additive
C: Isocyanurate foam
D: Phosphorylated polyurethane foam (high char)
The foams were all rigid, of a nominal density of 32 kg/m³, and were subjected to an intensity of 4·2 kW/m².

curves in Fig 1. The foam did not shrink and the charring was more gradual. Cracks were formed in the exposed surface by the stresses produced in heating. These resulted in fissures in the material at which decomposition continued, thus widening them and aiding the process of heat penetration.

The results from exposure to 21·0 kW/m² show that the effects of a fivefold increase of intensity are

Table I: Radiation intensities in some practical systems

	kW/m²
Summer sunshine in England	0·67
Radiation to cause pain in 3 sec.	10·5
Spontaneous ignition of wood after an extended period	29·4

Table II: Values of thermal diffusivity of polyurethane foams and of some building materials

Material	Thermal conductivity (W/m°C) ×10⁻³	Thermal diffusivity (m²/s) ×10⁻⁶
A. Polyurethane foam, 20 parts TCEP in mix B. Polyurethane foam C. Isocyanurate foam D. Polyurethane foam with phosphorylated polyol	23·1	0·81
Air	23·9	17·8
Crown glass	1150·0	0·58
Brick	825·0	0·38
Wood (spruce, across grain)	123·0	0·24
Ground cork	41·0	0·14

minimised by the char layer formed, as the temperatures at a depth of 10mm reach a value of about 440°C.

Weight loss Although not a complete index of performance of a material resulting from the imposition of extreme thermal conditions, loss of weight reflects the alteration in chemical and mechanical properties of the material.

For low density foams (32 kg/m³) it appears that the weight loss after maintaining at a fixed temperature for one hour is proportional to the temperature over the range between 200 and 360°C, the losses varying from approximately 25 per cent to 80 per cent. The initial rate of loss is high, three-quarters of the weight loss occurring during the first 10 minutes of exposure if the temperature is over 200°C. Under the same conditions foams containing TCEP suffer greater loss than those without by virtue of the fact that the TCEP acts as a plasticizer thus allowing the foam to soften and flow before decomposing.

Higher density foams suffer a smaller loss, for example doubling the density reduces the loss in one hour at 330°C to less than 50 per cent. The greater surface area of char produced allows a more complete heterogeneous cracking of the volatile materials as they are evolved from the interior of the sample. If the temperature is greater than 230°C the use of an inert atmosphere greatly reduces the rate of weight loss, which indicates the desirability of cladding any foam panels with non-porous material. This effect is much less noticeable in isocyanurate based foams as the fraction of low stability urethane groups is smaller.

Ignition When an exposed face of foam is subjected to radiant heat and the temperature rises to about 200°C, decomposition commences and volatile products are evolved from the face. In some potential fire situations, eg overheating by close proximity to domestic heating, pilot ignition sources are absent and flaming combustion is therefore less

Table III: Surface ignition observations on thermal irradiation

Radiation intensity (kW/m²)	Foam	Ignition Time (s)	Ignition Temp. (°C)	Observations
6·3	1	No ignition		Chars have large cavities. Considerable shrinkage, even charring
	2			
	3			
	4			
	5			
8·4	1	5	250	Black sooty smoke. Flame extinguished without irradiation.
	2	4	230	Grey sooty smoke. Some spread of combustion.
	3	4·5	225	Grey sooty smoke.
	4	5	225	Some spread of flame, some shrinkage. Good char.
	5	No ignition		
12·6	1	2·5	250	Combustion penetrated and spread.
	2	3	240	Complete combustion of irradiated area. Extensive spreading.
	3	2	230	Extensive combustion; material softened.
	4	2	240	Flame spread over whole face. Good char.
	5	7·5	400	Small flame, self-extinguished after 20 seconds.
16·8	1	2·5	250	Complete combustion of irradiated area. Some spread of flame.
	2	1·5	240	Almost complete combustion.
	3	1·5	240	Extensive combustion. Material softened.
	4	<0·5	250	Considerable spread of combustion. Good char.
	5	3·5	380	Small transient flame. Some white smoke.

Rigid Foam
32 kg/m³

1: no additive.
2: 20 parts TCEP in mix.
3: 30 parts TCEP in mix.
4: phosphorylated polyol.
5: Isocyanurate, no additive incorporated.

likely. When convective mixing of the volatile products with air occurs the mixture temperature will be even lower and the ignition temperature will not be attained. The radiant absorptivity of such gas mixtures appears to be low and the source of radiant heat does not contribute appreciably to the heating of the mixture.

The convection currents induced by the heated face rapidly dilute the evolved materials so that only a very small region is within the flammable limits and the whole mixture is swept away from the hot zone. This aids circulation so that combustibles will reach the source of the heat, but the dilution will be so great that there can be no ignition. By the time the surface has reached a higher temperature the material near the surface will have reacted to form a carbonaceous char, which limits the penetration of heat into the unreacted foam and so decreases the rate of decomposition. The results of preliminary experiments are reported in Table III and the conclusion has been reached that an intensity in excess of about 8 kW/m^2 appears to be needed to ignite low density rigid urethane foams, and about 12 kW/m^2 for isocyanurate based material.

In the case of pilot ignition, the size and intensity of the igniting flame determines what is likely to occur. Only qualitative experiments were performed, but these were sufficient to identify two quite different patterns of behaviour. If a small flame is put to a piece of foam then there is transient ignition as flame flashes across the surface. There is decomposition of the area close to the point of application of the flame and combustion of the products, but this is only transient as an insulating layer of char quickly forms. The flash of flame across the surface is probably caused by the fracture of the surface layer of cells by thermal shock. This throws small particles away from the surface which then ignite. This rapid action and the heat released is insufficient to cause further reaction. If a larger or more intense flame is used there is enough heat input into the foam to ensure continued decomposition once an initial char has been produced.

Fires are often accompanied by strong air currents which can, if violent enough, lift the char off the burning foam and expose a fresh surface for attack. Bonding of the surface will prevent flash of flame which, although it does not add significantly to the burning of the foam, acts as an excellent source of ignition for any flammable gas mixtures it may encounter. Cladding with a suitable material, besides inhibiting flame spread can also prevent the evolution of the volatiles at the face and ensure that the protective char will not be swept away. The volatile products will still erupt from the edges of clad sheets but they will have been modified, by passage through foam and char, to less easily ignited species.

Toxicity When an organic material burns carbon monoxide is formed and its concentration depends on fire load, oxygen availability and ventilation. In general it is an ever-present and major hazard in fires and is likely to be produced in both the devolatilization and burn-out stages of a fire.

In addition to this hazard emphasis has often been placed on the effect of the elements other than carbon present in the non-traditional materials, eg chlorine in polyvinyl chloride, and fluorine in polytetrafluoroethylene.

In the case of polyurethane foam, among the carbon compounds that have been found in the products of decomposition are: hydrocarbons, aldehydes, alcohols and organic acids[10]. In addition to these attention is focused on the fate of the nitrogen and hydrogen cyanide, amines, isocyanates[8] and oxides of nitrogen[11] have been isolated.

Woolley and Field[12] have shown that rigid and flexible foams behave differently in their release of nitrogen. With rigid foams the nitrogen content is lost by a general, temperature dependent, fragmentation (about 90 per cent loss by 500°C) whereas with flexible foams there is a complete and rapid loss at low temperatures (less than 10 per cent at 200°C, and about 80 per cent at 250°C). Using flexible foams Woolley and co-workers[13] have shown that the amount of hydrogen cyanide produced increased with increasing temperature. Again factors defined by the type of fire and stage of development are evident.

The high toxicity of some phosphorous compounds necessitates some assessment of the fate of phos-

Table IV: Evolution of phosphorus compounds during thermal degradation

Temperature (°C)	Material	Atmosphere		
		N_2	6%O_2-94%N_2	Air
220	1	—	+	+
	2	+	+	+
320	1	+		+
	2	+		+
400	1	+		
	2	+		

Rigid foam (64 kg/m^3)
1 : containing Fyrol 6
2 : 30 parts TCEP in mix
+ : phosphorus present
— : phosphorus absent

phorus-containing fire retardants. While the major part of the phosphorus is retained in the char, and in some cases all of it, there are conditions where volatile phosphorus-containing compounds are produced. Some qualitative results relating to hitherto unidentified organic phosphorus-containing compounds are shown in Table IV[14].

Included for convenience under this heading of toxicity is the smoke formation, a matter of both physiological and psychological importance in fires. It can be seen in Table III [8] that the hazard from smoke is greater at low temperatures and the most offensive material was that without addition of fire retardant. Smoke production when flexible foams undergo flaming and non-flaming combustion and the resultant gas concentrations are shown in Table V[15].

Heating effects with oil contamination Cubes (25mm side) of flexible polyurethane foam without fire retardants were allowed to soak up measured quantities of mineral oil containing no antioxidant. Their temperature was raised to values at which there was evidence of self-heating. For purposes of comparison similarly sized cubes of preformed asbestos lagging were heated and the results obtained are given in Table VI[8].

The total rise and the rate of rise of temperature were both much higher for asbestos lagging. The cellular structure of the polyurethane foam prevents rapid supply of oxygen and removal of oxidation products of the oil. The fibrous nature of the asbestos is conducive to the oxidation owing to the large surface area and the easy gas circulation.

Conclusion

Assessment of the hazards arising from the combustion of polyurethane foams, in common with all other materials, is required so that selection of appropriate materials may be made during design. Various types of polyurethane foams are already available and continuing efforts by the polyurethane foam manufacturers lead to the expectation that further improvements will produce foams that are suitable for use under a wider range of conditions.

References

1. Ferrigno, T. H., *Rigid plastic foams*, 2nd Ed., p. 23 (New York: Rheinhold Publishing Corporation), 1967.
2. Singh, A., Weissbein, L., and Mollica, J. C., *Rubber Age*, 99, 77 (Dec. 1966).
3. Piechota, H., *J. Cell. Plastics*, 1, 351 (1965).
4. Einhorn, I. N., Seader, J. D., Drake, W. O., Mihlfeith, C. M. and Kanikia, M. D., *Polymer Engineering & Science*, 12, (3), 168, (1972).
5. Nicholas, L. and Gmitter, G. T., *J. Cell. Plastics*, 1, (1), 85, (1965).
6. Buist, J. M. and Lowe, A., *Brit. Polym. J.*, 3, 113 (1971).
7. Lawson, D. I., *Fire Research Bull.*, No. 1, "Fire and the atomic bomb", 1954 (London: H.M.S.O.).
8. Boult, M. A., Gamadia, R. K. and Napier, D. H., "Fourth symposium on chemical process hazards with special reference to plant design", at Manchester, April 1971, Institution of Chemical Engineers (in press).
9. Carslaw, H.S. and Jaeger, J. C., *Conduction of heat in solids*, 1957, p. 75 (London: Oxford University Press).
10. Hilado, C. J. in Bruins, P. F. (Ed.), *Polyurethane Technology*, 1969 (New York: Inter-science Publishers Inc.).
11. Bott, R., Firth, J. G. and Jones, T.A., *Brit. Polym. J.*, 1, 203 (1969).
12. Woolley, W. D. W. and Field, P. F., *Fire Research Notes*, 1971, No. 880.
13. Woolley, W. D. W., *Brit. Polym. J.*, 4, (1), 27 (1972).
14. Napier, D. H. and Wong, T. W., *Brit. Polym. J.*, 4, (1), 45 (1972).
15. Gross, D., Loftus, J. J., Lee, T. G. and Gray, V. E., U.S. Dept .of Commerce, National Bureau of Standards, Building Science Series 18, Feb. 1969.

Table V: Smoke and gases produced by burning flexible polyurethane foam

Sample	Specimen Weight	Test	Smoke: Max. value of specific optical density	Smoke: Max. rate of rise of D_s	Smoke: Time to D_s=16	Gas concentrations: CO	HCN	HCl
	g		D_s	(min^{-1})	(min)	ppm	ppm	ppm
15	2·6	F	35	6	1·4	50	2	0
		N	156	9	0·5	50	2	0
128A	4·2	F	262	120	0·2	320	25	150
		N	286	62	0·7	160	2	25
128B	3·5	F	41	15	0·6	150	2	2
		N	300	54	0·7	190	2	2

Flexible polyether foams 15, no additive, density 37 kg/m³.
128A, fire retardant, density 30 kg/m³.
128B, no additive, density 22 kg/m³.

F—flaming combustion.
N—non-flaming combustion.

Table VI: Temperature rise in flexible polyurethane foam with absorbed oil

Material	Oil (ml/cube)	Temperature: Equilibrium (°C)	Rise (°C)	Time (min)	Rate (°C/min)
Asbestos (300 kg/m³)	4	165	114	4	28·5
	5	165	109	5	21·8
	6	163	109	5	21·8
High modulus polyurethane foam (64 kg/m³)	2	157	30	17	1·8
	3	167	31	13	2·4
	4	163	10	65	0·2

THERMAL DEGRADATION OF POLYURETHANE FOAMS

By M. A. BOULT,† R. K. GAMADIA,† and D. H. NAPIER†

SYNOPSIS

In view of the wide industrial usage of polyurethane foams some aspects of their behaviour have been considered under thermally extreme conditions and in a fire emergency.

Foams with and without combustion inhibitors and a foam based on the isocyanurate ring have been examined by heat penetration and weight loss measurements. Analysis of the products of decomposition has established that phosphorus compounds, cyanide, isocyanate and halogenated materials were evolved. Attention was also directed to the surface temperature at which spontaneous ignition occurred (in the range 220° to 400°C) and to the state of the charred residue. The effect upon some of these aspects of atmospheres deficient in oxygen as compared with air have been investigated.

The results obtained indicate some of the hazards liable to arise from these materials, and the degree to which they retain their serviceability under extreme conditions.

Introduction

The rapid growth in the development of plastics has led to their use as an improvement to, or as a substitute for, traditional materials as well as to their use in applications for which traditional materials were not suitable.

The behaviour of traditional materials under both service and emergency conditions is fairly well known except when the range of operating conditions is extended or when experience or research leads to the definition of a new hazard, for example, the long-term effects of blue asbestos on operatives and the toxicology of benzene. A background of experience has not yet been built up for some of the newer materials. It is intended in this paper to draw attention to some aspects of the behaviour of polyurethane foams under both fire emergency and thermally severe service conditions. It is hoped thereby to assist in building up the background of knowledge relating to the behaviour of this material which is now being employed in a wide variety of industries. Some of the important uses include the thermal insulation of plant and pipework at both high and low temperatures, the filling of cavities in walls of buildings both in brickwork and in metal partitioning, and for the major or minor components of furniture. It is also used in clothing and footwear and in packing. It is therefore liable to be in use or on-site in considerable quantities in the chemical and process industries. Aside from these uses it may be noted that it has been used in coal mines as well as in the domestic appliances and automobile industries.

Examination of its behaviour under fire emergency and thermally severe conditions involves considerations of pyrolysis and of combustion in oxygen-deficient atmospheres. In view of the fact that polyurethane foam is somewhat thermally unstable and cannot be classed as a highly resistant organic polymer,[1] extensive thermal damage would be anticipated when temperatures in excess of 250°C are encountered. In order to assess the effect of conditions of pyrolysis and of partial combustion the following have been studied:

(1). Heat penetration rates.

(2). Chemical stability.

(3). Conditions for spontaneous ignition by radiating sources.

(4). Extent of damage to the foam and the structure of the char remaining.

(5). Toxicological properties of products evolved during decomposition of the foam.

Types of Polyurethane Foam

Many formulations have been used to produce a wide range of foams. The first broad classification of these is into flexible and rigid foams. The former is of open-cell structure and is used extensively in furniture; a polyester-based material is used for insulating hot water and low-pressure steam pipes. The latter is of closed-cell structure and such materials are used extensively as thermal and acoustic insulants. There is a range of foams with properties intermediate to the two extremes.

Distinction may be drawn between polyurethane foams on the basis of the raw materials used in their production. They may be based on polyether or polyester with polyol initiator: again tolylene diisocyanate (TDI) or diphenylmethane diisocyanate (MDI) may have been used. Variation may also occur in the blowing agent used although carbon dioxide produced by decomposing isocyanate is usually combined with a halogenated methane. Such variations affect the properties of the foam; for example polyester foams are more flame resistant than polyether-based foams.[2]

†Department of Chemical Engineering and Chemical Technology, Imperial College, Prince Consort Road, London, S.W.7.

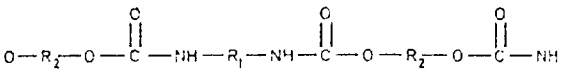

Fig. 1.—*Simplest form of urethane linkage*

A further important division is into those foams that have fire retardant added and those which do not. The former category may be sub-divided into:

(*a*) those with a fire retardant mixed in as a simple additive, *e.g.*, *tris* (chloroethyl) phosphate (TCEP),

(*b*) those in which part of the polyol has been replaced by a phosphorus-containing compound, which becomes incorporated into the chemical structure of the foam. *e.g.*, Firemaster T 23 P (Michigan Chemical Corporation)

$(BrCH_2.CHBr.CH_2O)_3.PO$ 4·4% P

$(H[CH_2.CH_3.CHO]O)_3.PO$ 7% P

Fyrol 6 (Stauffer Chemicals)

$(C_2H_5O)_2\,PO.CH_2N(C_2H_4OH)_2$ 12·6% P

Reference will also be made in this paper to a foam based on MDI which is used to produce the isocyanurate ring with polyols bound in as urethanes; a rigid highly cross-linked foam results.[3]

The simplest form of urethane linkage is shown in Fig. 1 and the isocyanurate ring from MDI is given in Fig. 2.

Heat Penetration Measurements

The investigations relating to heat penetration were performed by subjecting one end of a cylindrical sample of foam, 47 mm dia., to a known intensity of radiation and measuring the axial temperature histories at selected distances from the exposed face. The intensities of radiation used were 4·2 kW/m² (0·1 cal/cm² s) and 21·0 kW/m²; some comparable values from frequently encountered systems are shown in Table I.[4]

TABLE I.—*Radiation Intensities in Some Practical Systems*

	(cal/cm² s)	(kW/m²)
Summer sunshine in England	0·016	(0·672)
Radiation to cause pain in 3 s	0·25	(10·5)
Spontaneous ignition of wood after an extended period	0·7	(29·4)

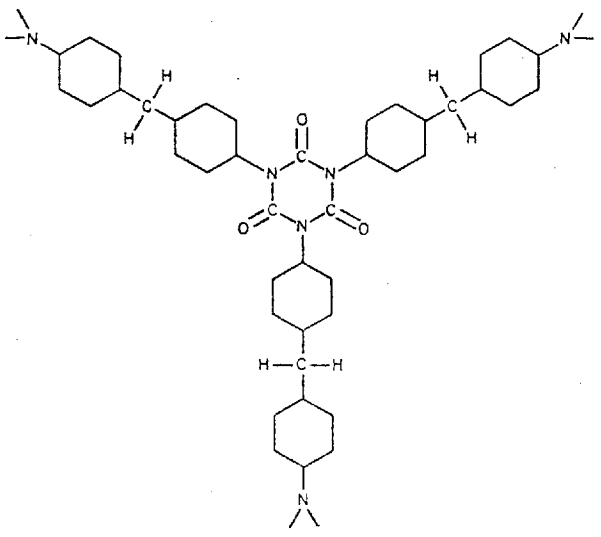

Fig. 2.—*Isocyanurate ring formed from MDI*

Typical temperature histories are shown in Fig. 3. The foams examined were rigid, of nominal density 32 kg/m³ (2 lb ft⁻³). Values of thermal diffusivity were calculated by assuming the system to approximate to a semi-infinite body, subjected to constant radiation;[5] these values and those of some typical building materials are shown in Table II.

TABLE II.—*Values of Thermal Diffusivity of Polyurethane Foams and of some Building Materials*

Material	Thermal Conductivity (W/m °C)	Thermal Diffusivity (m²/s)
(*a*) Polyurethane foam, 20 parts TCEP in mix	$23{\cdot}1\times10^{-3}$	$0{\cdot}81\times10^{-6}$
(*b*) Polyurethane foam		
(*c*) Isocyanurate foam		
(*d*) Polyurethane foam with phosphorylated polyol		
Air	$23{\cdot}9\times10^{-3}$	$18{\cdot}7\times10^{-6}$
Crown glass	$1150{\cdot}0\times10^{-3}$	$0{\cdot}58\times10^{-6}$
Brick	$825{\cdot}0\times10^{-3}$	$0{\cdot}38\times10^{-6}$
Wood (spruce, across grain)	$123{\cdot}0\times10^{-3}$	$0{\cdot}24\times10^{-6}$

The values for polyurethane foams were calculated from the steeply rising part of the curves. Thermocouples were placed at distances behind the exposed face indicated on the curves.

The curves showing heat penetration are of the expected shape but there are certain notable differences between the heating rates in different foams. The heat penetration rate was greater for foam (*a*) containing TCEP than for the foam (*b*) without fire-retardant due to the "fluxing" effect of the additive whereby the cell structure was more readily broken down and heat transfer assisted. It was also observed that a decrease in heat penetration rate occurred in the order (*a*), (*b*), (*d*), (*c*) (as represented in Table II); this correlates with the decreasing cell size of the char.

Surface temperature of the samples, as measured by a shielded thermocouple, was also recorded and that for foam (*b*)—without additive—and foam (*d*)—with phosphorylated polyol—showed a marked decrease after a few minutes. This resulted from the shrinkage of the samples and consequent movement of the exposed face from the thermocouple measuring surface temperature. The fall in temperature recorded on thermocouples close to the surface of foams (*a*), (*b*) and (*d*) was probably due to the internal softening of the foam and to the formation of a layer of char on the thermocouples.

Isocyanurate foam behaved differently from the others as shown by the curves in Fig. 3. The foam did not shrink and charring was more gradual. Cracks were formed in the exposed surface arising from the stresses produced by heating. These resulted in fissures in the material at which decomposition continued thus widening them and aiding the processes of heat penetration.

Heat penetration curves for high modulus and rigid polyurethane foams of nominal density 64 kg/m³ are shown in Fig. 4. The temperature was measured one centimetre behind the exposed face when the samples were exposed to radiation of intensity 21 kW/m² in air and in nitrogen. Curves obtained with rigid foam in both air and nitrogen were similar indicating the controlling influence of the softening and breakdown of the structure of the foam. In respect of heat penetration the behaviour of the foam of high modulus was similar to rigid foam, but the final temperature attained in nitrogen was some 80 degC lower. In comparing the final temperatures attained at 4·2 kW/m² with those in Fig. 4 it is noteworthy that the effect of a five-fold increase in intensity was minimised by the char layer formed at the exposed face; this layer will be discussed later.

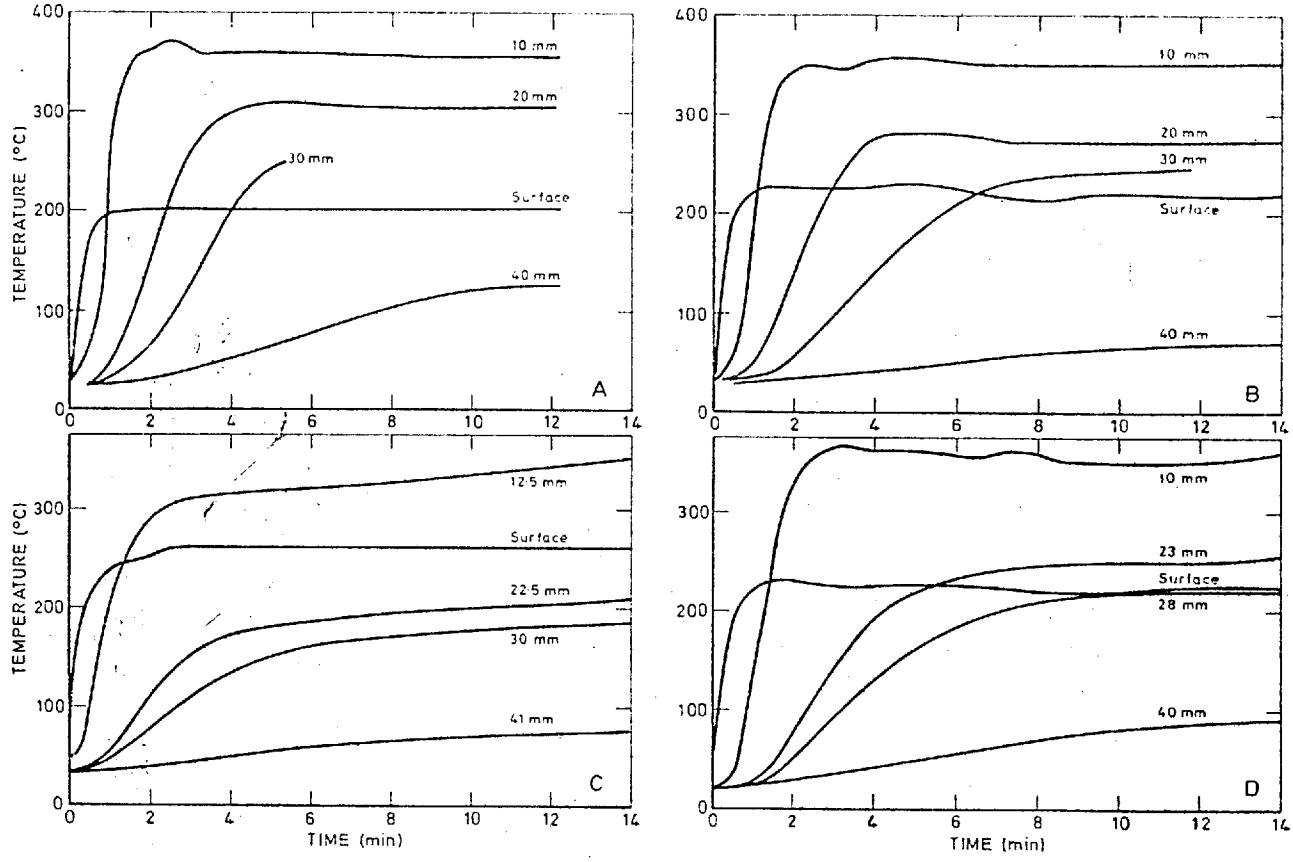

A: Polyurethane foam, 20 parts of TCEP
B: Polyurethane foam, no additive
C: Isocyanurate foam
D: Phosphorylated polyurethane foam (high char)

The foams were all rigid, of a nominal density of 32 kg/m^3, and were subjected to an intensity of 4·2 kW/m^2

Fig. 3.—*Thermal penetration by irradiation. Temperature histories at various depths below heated face*

Curves showing the temperature of a thermocouple inserted into the centre of a small cylinder of foam (height: 40 mm, diameter: 29 mm) which was heated at 300°C are given in Fig. 5; air or nitrogen was passed over the samples at the rates mentioned. The marked difference between the behaviour of the isocyanurate foam and the high modulus foam is of interest. In the case of the former, no strongly exothermic reaction occurred in air whereas for the latter, the sample temperature in air rose rapidly. This divergence in behaviour was observed to commence above about 225°C; when the temperature is raised sufficiently combustion of the isocyanurate results and the sample temperature rises rapidly.

Measurements of Loss of Weight

Thermal damage has been expressed in a number of ways, for example, change in appearance, surface temperature attained, and weight loss. Although it is not a complete index of the performance of a material resulting from the imposition of extreme thermal conditions, loss of weight reflects the alteration in chemical and mechanical properties of the material.

Loss of weight determinations were made by heating samples at fixed temperatures in nitrogen and in air and in atmospheres to which halogenated methanes were added. Losses were recorded at 230, 270, 300, and 330°C, a fresh sample (height: 40 mm, diameter: 22 or 29 mm) being used at each temperature. Some of the results obtained are shown in Table III in which they are expressed as the weight loss after 10 minutes, by which time a steady value had been reached.

When heated in air the rigid and high modulus foams behaved similarly, but when heated in nitrogen the rigid foam lost more weight because of the greater breakdown of the structure of the materials. Furthermore, products of decomposition escape readily from the high modulus foam. Thus they have little effect on subsequent stages of decomposition and on the material yet they decompose as heat penetrates into the sample. The effect on weight loss of incorporation of TCEP almost certainly involves these factors.

The effect of additions of halogenated methane to air or to nitrogen in which polyurethane foams are being heated is not clear. It seems that loss of weight of the foam may be increased probably by chemical attack. On the other hand, considerable reductions in loss of weight were also recorded; examples of both of these are given. These effects in turn varied with the type of halogenated methane used; among other factors it seems likely that the chemical stability and rate of decomposition of the methane derivatives is involved.

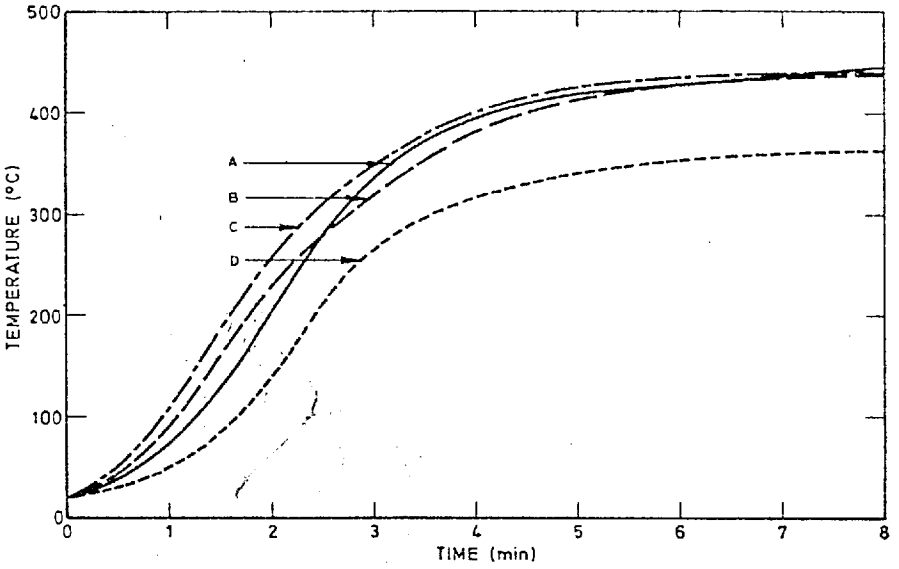

A: High modulus, 64 kg/m³, 0·3 l/min, Air
B: Rigid, 64 kg/m³, 0·3 l/min, Air
C: Rigid, 64 kg/m³, 0·3 l/min, N_2
D: High modulus, 64 kg/m³, 0·3 l/min, N_2

The foams were both without fire retardant additives and were subjected to an intensity of 21 kW/m²

Fig. 4.—*Thermal penetration by irradiation. Temperature histories at one centimetre below heated face of various foams with gas flow past the sample*

From curves similar to those shown in Fig. 6, activation energies have been calulated for the pyrolysis and combustion of cylinders of foam. These may be compared with higher values (165 to 200 kJ/mol) determined by TGA in the same temperature range (discussed Ref. 6). This difference in value may be anticipated in view of the dependence of the weight loss of the heated mass upon the rate of heat penetration. This physical process would be expected to exert a major effect in controlling rate.

The results obtained illustrate that severe thermal damage is to be expected under a wide variety of conditions both in air and in oxygen-deficient atmospheres.

A loss in weight in excess of half that reached in the steady condition at 330°C was usually experienced after heating at 270°C; for example, see the weight loss curves shown in Fig. 6 for high modulus foam heated in air. This was also shown by the isocyanurate foam. This degree of loss is in accord with the temperature range for decomposition of the urethane structure. However, rigid polyurethane foam without the addition of TCEP exhibits a much lower comparable weight loss (about 30%). Breakdown of the internal cellular structure and some softening of this material causes delay and a less easy means of escape for the volatile products of decomposition.

Surface Ignition

Spontaneous ignition of a flammable gas mixture depends on the interrelation of energy, time, and size of energy source. In the experimental arrangement employed in the present investigation an area of foam (0·002 m²) was exposed to thermal radiation of various intensities and the required time to ignition was recorded as well as the temperature near the surface of the sample. This latter value was an estimate of the temperature of the gases evolved rather than that of the surface of the foam. The experiments took place in air but without forced circulation of the air.

The results obtained are given in Table IV. In this table the relationship between rate of energy input and the time for ignition will be noted. Higher temperatures were required to cause ignition of isocyanurate foam and the flame was transitory. The temperatures recorded in this work are considerably lower than those obtained using ASTM 1929-62T, *viz.*, 420 to 450°C.[7] The difference arises

TABLE III.—*Weight Loss of Samples of Polyurethane Foam*

Material	Atmosphere	Loss after 10 minutes (%) 230°C	270°C	300°C	330°C	*E* kJ/mol
High modulus 64 kg/m³	Air	9	30	41	44	79
	Nitrogen	8	15	20	31	59
	Air+0·5% CBM†		33		50	
	Nitrogen+0·5% CBM†		14		25	
Rigid 64 kg/m³	Air				43	67
	Nitrogen	7	12	18	42	59
	Air+0·5% CBM†		10		42	
	Nitrogen+0·5% CBM†		15		33	
Rigid 64 kg/m³ with 30% TCEP	Air	11	26	34	54	75
	Nitrogen	14			48	92
Isocyanurate 48 kg/m³	Air	9	21	25	30	
	Nitrogen	12	21	23	31	

†CBM = Chlorobromomethane

from the fact that in the present arrangement volatile matter was allowed to collect at the irradiated surface, remain hot, and not be cooled by "ignition air". The temperatures recorded in Table IV are in good agreement with that for the decomposition of the urethane structure.

While there is no basis of direct comparison between the work of Wilde and the present results, it appears that the energy intensities required for ignition are of the same order. Wilde draws attention to the rapidity of flame spread on polyurethane foams and the marked improvement recorded with isocyanurate foam when examined by *B.S.* 476 Part I, Section 2.[6]

Qualitative observations were also made of some of the combustion characteristics and these are included in Table IV. Some of these will be considered later.

TABLE IV.—*Surface Ignition Temperatures at Various Radiation Intensities*

Radiation intensity (kW/m²)	Foam	Ignition Time (s)	Ignition Temp. (°C)	Observations
6·3	1	No ignition		Chars have large cavities
	2			
	3			
	4			Considerable shrinkage, even charring.
	5			
8·4	1	5	250	Black sooty smoke. Flame extinguished without irradiation.
	2	4	230	Grey sooty smoke. Some spread of combustion.
	3	4·5	225	Grey sooty smoke.
	4	5	225	Some spread of flame, some shrinkage. Good char.
	5	No ignition		
12·6	1	2·5	250	Combustion penetrated and spread.
	2	3	240	Complete combustion of irradiated area. Extensive spreading.
	3	2	230	Extensive combustion; material softened.
	4	2	240	Flame spread over whole face. Good char.
	5	7·5	400	Small flame, self-extinguished after 20 s.
16·8	1	2·5	250	Complete combustion of irradiated area. Some spread of flame.
	2	1·5	240	Almost complete combustion.
	3	1·5	240	Extensive combustion. Material softened.
	4	<0·5	250	Considerable spread of combustion. Good char.
	5	3·5	380	Small transient flame. Some white smoke.

Rigid Foam 32 kg/m³
1: no additive.
2: 20 parts TCEP in mix.
3: 30 parts TCEP in mix.
4: phosphorylated polyol.
5: isocyanurate, no additive incorporated.

Charred Residue

In many instances it is desirable that in the event of fire the residue of the material affected should maintain its integrity, possess reasonable mechanical strength, and so continue to act as a heat shield. If the char swells and still remains sufficiently strong to withstand the air currents that usually accompany a fire it may offer an added protection to the substrate. In the light of the variety of uses for foamed polyurethane the structure of the char becomes significant, and a description is given here of the effects observed.

When subjected to thermal radiation of intensity 4·2 kW/m² none of the materials under investigation ignited but decomposition occurred and the chars were examined.

Rigid foam without additives (32 kg/m³) yielded, after irradiation for 16 min, a char of cell size 10 mm to a depth of 15 mm from the exposed face followed by char of cell size 7 mm for a further 8 mm and finally 2 mm of discoloured foam. The heated face had receded to a distance of 7 mm from the radiant source but a layer of dense char about half a millimetre thick formed on the surface.

This layer was a characteristic of the charring of all rigid polyurethane foams; it probably arose from shrinkage and from deposition of products from cracked volatile matter as it passed through the hot zone. Rigid foam with 20 parts TCEP produced a similar char but of larger cell size. These chars were mechanically very weak, except for the thin dense char layer. Similar chars were produced from higher density (64 and 128 kg/m³) rigid foam; slight swelling occurred instead of shrinkage. Phosphorylated rigid foam shrank more, but yielded a stronger char of cell size of two millimetres.

High modulus foams shrink slightly on heating but the char, although weak, does not exhibit the softening and breakdown of the foam structure as with rigid foams.

As previously described the isocyanurate foam formed fissures on heating; a char was produced comparable in strength to the original material. Continued heating led to continuation of the decomposition, and a friable, cindery char resulted.

These results were confirmed by the chars produced from the surface ignition work; some of the observations are recorded in Table IV. For example, a block of foam without additives, 30 mm thick, burned completely in the irradiated area to a diaphanous film; spread of flame occurred for about 50 mm along the exposed face. Rigid foams to which TCEP had been added suffered more severe damage with evidence of a greater degree of softening. In contrast to this, when phosphorylated foam was exposed, extensive combustion travelled about 30 mm beyond the irradiated area and flame flashed over the entire surface, but the char did not burn and its mechanical strength was high.

Heating Effects with Oil Contamination

Cubes (side 25 mm) of high modulus polyurethane foam without additives were allowed to take up chosen amounts of mineral oil (without anti-oxidant). Their temperature was raised in an oven to values at which there was evidence of self-heating. These values are given in Table V where the steady oven temperature is designated as the equilibrium value and the rise recorded was that of a thermocouple embedded in the sample.

For purposes of comparison some experiments were carried out with similar-sized cubes of asbestos lagging. When the temperature at which heating commenced was the same for both materials a much larger effect was observed with the asbestos than with the polyurethane foam. Thus in practice oil-contaminated polyurethane foam will offer less hazard than oil-contaminated asbestos in situations were self-heating may occur, unless the service temperature is initially too high to justify the use of polyurethanes. This is due to the relatively rapid consumption of the oxygen enclosed in the foam and the restricted permeability of the material which prevents further supply of oxygen. In addition as the rigidity, *i.e.*, closed-cell character, of the foam is increased,

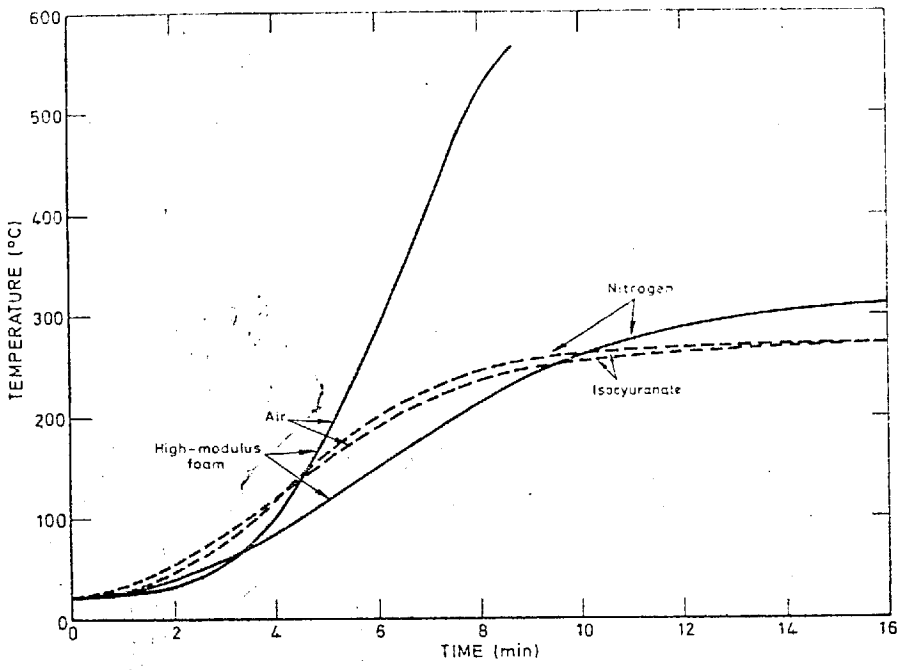

A: Isocyanurate foam, 48 kg/m³, 0·4 l/min, gas
B: High modulus foam, 64 kg/m³, 0·5 l/min, gas
The furnace temperature was 300°C. The sample was a cylinder of height 40 mm and diameter 29 mm

Fig. 5.—*Thermal penetration. Temperature histories at the centre of a sample heated in a furnace with gases passed over the sample*

the hazard is likely to be reduced even further. Addition of a combustion inhibitor to the polyurethane foam might improve this situation still further, particularly if the starting temperature was somewhat higher.

Toxicological Aspects of Thermal Degradation

Examination of the chemical structure of polyurethanes suggests that a variety of materials will be produced when it decomposes. The following have been found among the products of decomposition:[9] hydrocarbons, aldehydes, alcohols, organic acids, oxides of carbon and hydrogen. When combustion inhibitors are added thermal degradation is likely to yield further compounds of less predictable composition.

A few aspects of the toxicological hazards likely to arise during thermal degradation will be discussed here. Firstly, it has frequently been stated that carbon monoxide presents the greatest toxicological hazard during a fire emergency involving cellulosic or plastic materials. Its concentration depends on both the fire load and oxygen availability; alteration of these quantities alters both the quantity and concentration of carbon monoxide produced. These parameters often alter the nature as well as the quantity and concentration of products, thereby rendering a complete assessment of toxic hazards both difficult and protracted. Secondly, generation of smoke presents several hazards, for example, physiological and psychological effects as well as impeding firefighting and rescue operations. Organic materials are certain to produce some carbon monoxide during thermal degradation; in addition attention must be paid to their smoke-forming propensity.

TABLE V.—*Temperature Rise in Polyurethane Foam with Absorbed Oil*

Material	Oil (ml/cube)	Temperature: Equilibrium (°C)	Temperature: Rise (°C)	Time (min.)	Rate (°C/min)
Asbestos	4	165	114	4	28·5
	5	165	109	5	21·8
	6	163	109	5	21·8
High modulus polyurethane foam 64 kg/m³	2	157	30	17	1·8
	3	167	31	13	2·4
	4	163	10	65	0·2

The fate of the phosphorus additives during thermal degradation is a matter of some concern in view of the highly toxic nature of some phosphorus compounds. Some investigations[10] have been made by heating polyurethane foams to which phosphorus additions had been made in various atmospheres and at several temperatures as shown in Table VI. It will be noted that under only one set of the conditions used was phosphorus not emitted. These phosphorus compounds were of low volatility and could be collected in a trap cooled in ice. Infra-red examination of these materials indicated the presence of POC, POC_2H_5, and P=O groupings.

These experiments showed that other toxic materials evolved included: hydrogen cyanide, amines, isocyanate, and halogenated compounds. Both temperature of the foam and the atmosphere in which it was heated determined the concentration and nature of the materials produced.

The results are in agreement with those of Bott, Firth, and Jones[11] who also detected oxides of nitrogen when polyurethane was heated in air to 600° in one case and 750°C in the other.

TABLE VI.—*Evolution of Phosphorus Compounds during Thermal Degradation*

Temperature (°C)	Material	Atmosphere: N_2	Atmosphere: 6%O_2—94%N_2	Atmosphere: Air
220	1	−	+	+
	2	+	+	+
320	1	+		+
	2	+		+
400	1	+		+
	2	+		+

Rigid Foam (64 kg/m³) 1: containing Fyrol 6 2: 30 parts TCEP in mix

+P present
−P absent

TABLE VII.—*Odour Rating of Degradation Products of Polyurethane Foams*

Temperature (°C):	220			320	400
Atmosphere:	N_2	6%O_2—94%N_2	Air	N_2	N_2
Foam					
1	2	2	2	4	4
2	2	2	2	3	4
3	1	1	1	2	3
4	0	1	1	2	3

Odour increasing from 0 (no odour) →1 (just detectable) →2 (definite odour)→3 (strong odour)→4 (overpowering odour)
Foam 1 Rigid polurethane 64 kg/m³, containing Fyrol 6
Foam 2 Rigid polyurethane, 64 kg/m³, containing 30 parts TCEP
Foam 3 Flexible polyurethane 32 kg/m³, without additives
Foam 4 Rigid isocyanurate 32 kg/m³

An attempt[10] was made to allocate to the products from thermal degradation an index of odour as judged by a panel of six persons. The observations are summarised in Table VII. While extremely unpleasant odours present a problem, they are a warning of the presence of the materials mentioned above. This is of undoubted value in alerting to emergency conditions.

Discussion

Detailed analysis of the mechanism of degradation of polyurethane foams has not been attempted here, but it is noteworthy that the heat penetration curves given in Fig. 3 do not exhibit a downward trend in temperature. This results from a combination of the breakdown of the structure of the foam both at the surface and between cells and of exothermic effects. These latter have been mentioned in reporting the results shown in Fig. 5. With some materials the physical factors in heat penetration outweigh the exothermic effects as evidenced by the curves for isocyanurate foam shown in Fig. 3C.

As with all organic materials, polyurethane foam under thermal stress or in fire emergency conditions presents a hazard, that is, there is a fuel supply and a source of carbon monoxide. The degree of hazard varies with the amount of ventilation of the fire and the fire load; elemental composition of the material also plays an important role.

Several highly toxic compounds have been detected among the decomposition products of polyurethane foams and the phosphorus compounds have still to be categorised. However it is likely that the short-term hazard will depend largely on the dilution rate. This is not dissimilar to experience with many traditional materials which also generated highly toxic materials.[12] Often the full toxicological hazard of the decomposition products of a material will only be realised under conditions that seldom occur in practice.

It is however necessary to match the material used to the purpose and mode of use as well as to considerations of location of installation. The toxicological hazard depends not only on oxygen availability but on foam type and on additives incorporated in the foam; these factors are also of importance in several aspects of thermal degradation examined in this paper.

The work of Wilde[8] with tubes and ventilated ducts made from rigid polyurethane foam illustrates the effect of the combustion system on the behaviour of the material. Thus with the former the material exhibited greater flammability than in sheet form due to trapping of the heat in the system and to induced air supply. With the latter the hazards of combustion were found to be increased by the high intensity and rapid spread of combustion.

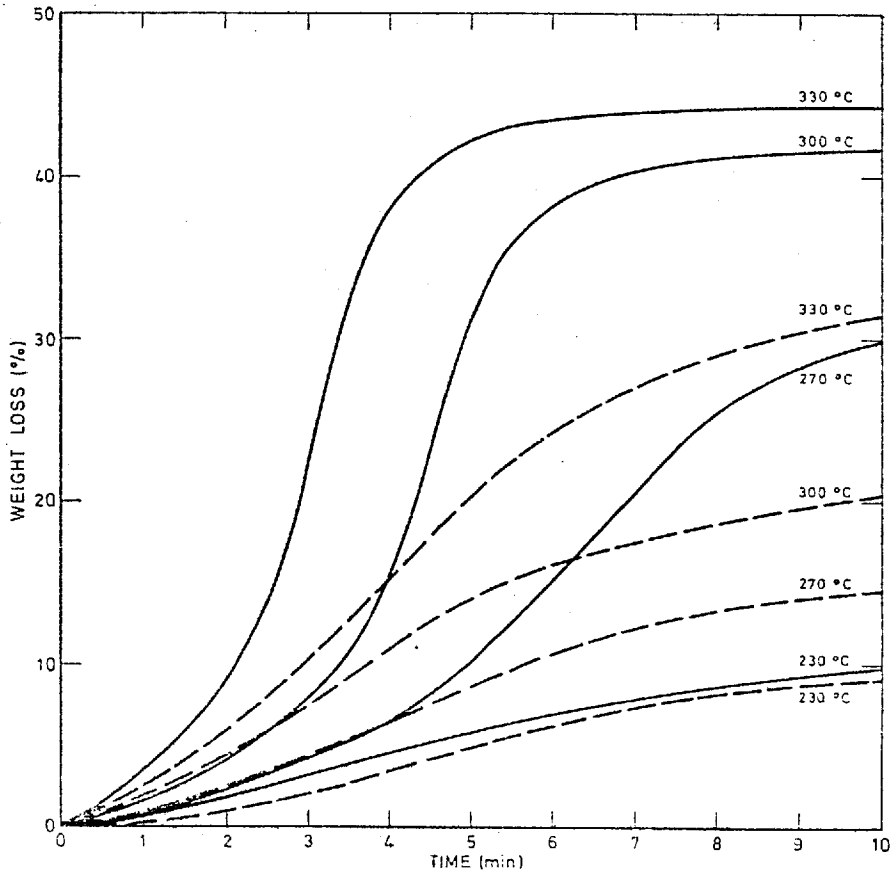

Fig. 6.—*Weight loss measurements. The sample was heated in the furnace at various temperatures with gas flow over the sample and the weight loss was recorded. The results shown are for a high modulus foam of density 64 kg/m³ with a gas flow of three litres per minute*

The work reported above is continuing and other techniques will be brought to bear on the assessment of the behaviour of polyurethane foam in service and in disaster. A longer term aim is to set up a mathematical model based on the experimental work, so that some aspects of the behaviour of polyurethane foams under extreme conditions may be predicted.

Acknowledgments

The authors gratefully acknowledge support of this work initially by the British Aircraft Corporation (for R.K.G.) and subsequently and presently by the British Rigid Urethane Foam Manufacturers Association (for M.A.B.).

References

1 Jones, J. Idris. *Chemistry in Britain*, 1970, **6**, 251.
2 Singh, A., Weissbein, L., and Mollica, J. C. *Rubber Age*, 1966, **99**, Dec. p. 77.
3 Ball, G. W., Haggis, G. A., Hurd, R., and Wood, J. F. *Journal of Cellular Plastics*, 1968, **4**, 248.
4 Lawson, D. I. *Fire Research Bulletin* No. 1 1954 (London: H.M.S.O.).
5 Carlsaw, H. S., and Jaeger, J .C. "*Conduction of Heat in Solids*", 1959, p. 75. (London: Oxford University Press).
6 Tilley, J. N., Nadeau, H. G., Reymore, H. E., Wasceziak, P. H., and Sayigh, A. A. R. *Journal of cellular Plastics*, 1968, **4**, 2.
7 Buist, J. M., Hurd, R., and Stafford, R. L. in Buist, J. M., (Ed.). "*Advances in Polyurethane Technology*", 1968. (London: MacLaren and Sons Ltd.).
8 D. G. Wilde, *Heat. vent. Engr*, 1968, **42**, 283, *Idem*, *Colliery Guard.*, 1968, **216**, 587.
9 Hilado, C. J. in Bruins, P. F. (Ed.). "*Polyurethane Technology*", 1969. (New York: Inter-science Publishers Inc.).
10 Napier, D. H., and Wong, T. W. *British Polymer Journal*, (in press).
11 Bott, R., Firth, J. G., and Jones, T. A. *British Polymer Journal*, 1969, **1**, 203.
12 Rasbash, D. J. in *Conference Supplement* No. 2, Jan. 1967, p. 55. (London: The Plastics Institute).

The manuscript of this paper was received on 30 *November*, 1970.

ADDENDUM.

Page 229, paragraph 2.

The enhancement of the transfer of heat through the foam by the 'refluxing' of TCEP has the advantage of removing heat from the surface, so reducing the temperature there, but this is outweighed by the additional decomposition within the foam caused by the penetration of heat to greater depths.

Paragraphs 4& 7.

Piloted ignition is of major importance in consideration of the hazard of urethane foams as most practical situations include a pilot source of ignition. internal generation of heat within the foam due to secondary curing is eliminated by careful curing of the foam, and there is insufficient oxygen access to afford any degree of heat generating oxidation.

Paragraph 5.

The value of TCEP as a fire retardant additive is its ability to release on heating species capable of forming chlorine radicals which interfere with the flame processes. This is only a temporary effect as the supply of the species is soon depleted.

Page 230, paragraph 2.

The blowing agent is lost from the foam before there is any significant production of volatile matter so there is no advantage taken of its non-combustible nature. It could act as a diluent, and there is some hydrogen chloride produced on heating which could act as a flame retardant.

Paragraph 3.

The sections of the polymer matrix that are most susceptible to thermal damage are where the polyols were extended with propylene oxide as there are flexible ether linkages present.

Thus the first stage of pyrolysis is the elimination of these extensions with production of the volatile fragments indicated by the mass spectrometry results.

Paragraph 4.

For TCEP to be effective it must be released from the foam with the volatile pyrolysis products. The range of 220-260°C for its removal from the foam coincides with the greatest production rate of volatiles, but TCEP tends to distill from the foam more quickly than pyrolysis proceeds, so its advantages are transient. To avoid this problem it would be desirable to include in the foam some material that releases a potential source of chlorine radicals at a controlled rate during the whole time that volatile fragments result from the pyrolysis.

As an additive TCEP has advantages in removing heat from the hot zone and producing flame retardant species with the volatile products. Against these must be weighed its plasticising effct which gives rise to softening of the burning material and a char of reduced size, the increased smoke production and the higher rate of heat penetration. On balance the addition of TCEP appears detrimental to the poly-urethane foam.

Paragraph 5.

The global activation energies determined should be used with care as they represent activity over a wide range of temperature and must incorporate many chemical reactions, the relative predominance and interaction of which are unknown. Even though its analysis is not possible, the activation energy is the best way of representing the weight loss data and provides a means of incorporating the data into a model of behaviour.

Paragraph 8.

The discolouration of the foam at these temperatures indicates that there is an oxidative attack of the foam which could result in the production of peroxy- and hydroperoxy-compounds. These are highly reactive and would form active sites for further degradation as the temperature was raised. Inclusion of a antoxidant would prevent this behaviour.

Page 231, paragraph 2.

By promoting the degradation reactions with carbonaceous products the incorporation of phosphorus by means of a phosphorylated polyol produces a foam that gives a char with superior properties. There is little shrinkage on exposure to elevated temperatures and the resulting char is strong enough to withstand physical damage without complete failure of the insulation. Disadvantages of the phosphorus are the increased smoke production and the presence of organo-phosphorus compounds in the volatile products, but there is less volatile matter produced and hence less fuel for a fire.

Paragraph 4.

The absence of any melting or breakdown of the cellular structure is beneficial as the foam continues to provide insulation against heat transfer even when it has suffered degradation.

Paragraph 8.

The activation energy for the fracture of the urethane group is to be regarded as a global value representing the summation of a variety of simultaneous reactions.

The lower temperature for fracture of urethane bonds in foams with aromatic bases is due to the greater stability of the aryl-NH^{*} radical, a thermodynamic effect. Likewise the additional stability of theisocyanurate ring is due to the

increase in entropy of the structure.

Paragraph 9.

In view of the stability of the isocyanurate ring structure it would appear advantageous to incorporate a catalyst in the urethane foam to promote formation of this structure when the urethane bonds dissociated on heating. As the trimerization is endothermic there will be no heat output to aggrevate the damage.